

University of New Hampshire

## University of New Hampshire Scholars' Repository

---

Doctoral Dissertations

Student Scholarship

---

Spring 2003

### Spatial modeling and visualization of habitat response to hydrologic restoration in New England salt marshes

Raymond Anthony Konisky  
*University of New Hampshire, Durham*

Follow this and additional works at: <https://scholars.unh.edu/dissertation>

---

#### Recommended Citation

Konisky, Raymond Anthony, "Spatial modeling and visualization of habitat response to hydrologic restoration in New England salt marshes" (2003). *Doctoral Dissertations*. 129.  
<https://scholars.unh.edu/dissertation/129>

This Dissertation is brought to you for free and open access by the Student Scholarship at University of New Hampshire Scholars' Repository. It has been accepted for inclusion in Doctoral Dissertations by an authorized administrator of University of New Hampshire Scholars' Repository. For more information, please contact [Scholarly.Communication@unh.edu](mailto:Scholarly.Communication@unh.edu).

## INFORMATION TO USERS

This manuscript has been reproduced from the microfilm master. UMI films the text directly from the original or copy submitted. Thus, some thesis and dissertation copies are in typewriter face, while others may be from any type of computer printer.

**The quality of this reproduction is dependent upon the quality of the copy submitted.** Broken or indistinct print, colored or poor quality illustrations and photographs, print bleedthrough, substandard margins, and improper alignment can adversely affect reproduction.

In the unlikely event that the author did not send UMI a complete manuscript and there are missing pages, these will be noted. Also, if unauthorized copyright material had to be removed, a note will indicate the deletion.

Oversize materials (e.g., maps, drawings, charts) are reproduced by sectioning the original, beginning at the upper left-hand corner and continuing from left to right in equal sections with small overlaps.

ProQuest Information and Learning  
300 North Zeeb Road, Ann Arbor, MI 48106-1346 USA  
800-521-0600

UMI<sup>®</sup>



**SPATIAL MODELING AND VISUALIZATION OF HABITAT RESPONSE TO  
HYDROLOGIC RESTORATION IN NEW ENGLAND SALT MARSHES**

**BY**

**Raymond A. Konisky**

**BS, University of Maine, 1978**

**MBA, Boston University, 1984**

**DISSERTATION**

**Submitted to the University of New Hampshire**

**in Partial Fulfillment of**

**the Requirements for the Degree of**

**Doctor of Philosophy**

**in**

**Earth and Environmental Science**

**May 2003**

UMI Number: 3083734

UMI<sup>®</sup>

---

UMI Microform 3083734

Copyright 2003 by ProQuest Information and Learning Company.  
All rights reserved. This microform edition is protected against  
unauthorized copying under Title 17, United States Code.

---

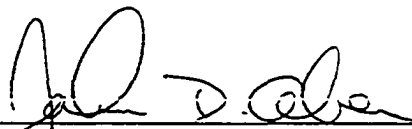
ProQuest Information and Learning Company  
300 North Zeeb Road  
P.O. Box 1346  
Ann Arbor, MI 48106-1346

This dissertation has been examined and approved.



---

Dissertation Director, David M. Burdick, Ph.D.  
Research Associate Professor of Natural Resources



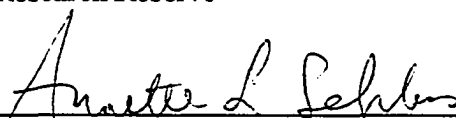
---

John D. Aber, Ph.D.  
Professor of Natural Resources and Earth, Oceans  
and Space



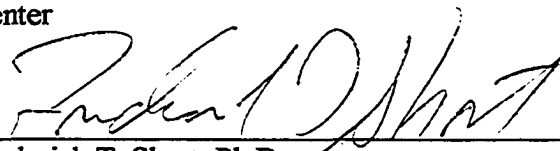
---

Michele Dionne, Ph.D.  
Research Director, Wells National Estuarine  
Research Reserve



---

Annette L. Schloss, Ph.D.  
Research Scientist, Complex Systems Research  
Center



---

Frederick T. Short, Ph.D.  
Research Professor of Natural Resources and  
Marine Sciences

JANUARY 13, 2003

---

Date

## **ACKNOWLEDGEMENTS**

The following people and organizations were instrumental in the development and completion of this dissertation: David M. Burdick provided invaluable leadership and support in his role as Ph.D. Advisor, and his ideas helped frame many aspects of this research project. Committee members John D. Aber, Michele Dionne, Annette S. Schloss, and Frederick T. Short each contributed significantly to the doctoral education process, and to the final form of this manuscript. Roelof M. Boumans assisted with technical aspects of model development. The Cooperative Institute of Coastal and Estuarine Environmental Technology (CICEET) provided funding for this research project. Family and friends played a vital role with constant encouragement and interest, especially Karen, Alexandra, and Brian. In addition, fellow students, researchers, and staff personnel at the Jackson Estuarine Laboratory contributed technical advice, logistics assistance, and ongoing support throughout all phases of the doctoral experience.

## TABLE OF CONTENTS

ACKNOWLEDGEMENTS.....	iii
LIST OF TABLES.....	vi
LIST OF FIGURES.....	viii
ABSTRACT.....	xi
<b>CHAPTER</b>	<b>PAGE</b>
INTRODUCTION	
Problem Statement.....	1
Project Goal and Objectives.....	4
Modeling Approach.....	7
Study Sites.....	10
Dissertation Organization.....	15
I.    AN EXPERIMENT TO DETERMINE PHYSICAL STRESS TOLERANCE AND RELATIVE COMPETITIVE RANKINGS FOR SIX COMMON PLANT SPECIES INHABITING AND INVADING NEW ENGLAND SALT MARSHES	
Experimental Objectives.....	27
Hypotheses of Physical Stress Tolerance.....	31
Hypotheses of Competitive Interactions.....	34
Methods.....	36
Results.....	39
Discussion.....	46
Conclusions.....	61
II.   A BIOMASS PRODUCTION MODEL FOR COMMON PLANT SPECIES OF NEW ENGLAND SALT MARSHES	
Introduction.....	76
Methods.....	80
Results and Discussion.....	86
Conclusions.....	90
III.  A RELATIVE ELEVATION MODEL FOR NEW ENGLAND SALT MARSHES	
Introduction.....	97
Methods.....	102
Results and Discussion.....	110
Conclusions.....	115



<b>IV.</b>	<b>A HYDRAULIC MODEL FOR PREDICTING TIDAL FLOWS IN HYDROLOGICALLY-ALTERED SALT MARSHES</b>	
	Introduction.....	125
	Methods.....	128
	Results and Discussion.....	136
	Conclusions.....	149
<b>V.</b>	<b>A MODEL OF PLANT SUCCESSION FOLLOWING HYDROLOGIC DISTURBANCE IN NEW ENGLAND SALT MARSHES</b>	
	Introduction.....	166
	Model Background.....	170
	Methods.....	174
	Results and Discussion.....	179
	Conclusions.....	187
<b>VI.</b>	<b>SPATIAL MODELING AND VISUALIZATION OF HABITAT RESPONSE TO HYDROLOGIC RESTORATION IN NEW ENGLAND SALT MARSHES</b>	
	Introduction.....	194
	Methods.....	201
	Results and Discussion.....	220
	Conclusions.....	236
	<b>LIST OF REFERENCES.....</b>	<b>265</b>
	<b>APPENDICES</b>	
	Salinity measurements from field transplant experiment.....	279
	Final above and belowground biomass for experimental transplants.....	280

## LIST OF TABLES

	PAGE
I.1 Salt marsh ecosystem functions and values.....	17
I.2 Ecosystem model categories, process components, and input sources.....	18
1.1 Physical characteristics of study gradient locations.....	63
1.2 Survival and final biomass of experimental transplants.....	64
1.3 Biomass of pre-study transplant specimens.....	65
1.4 Relative growth of transplants.....	66
1.5 ANOVA results for transplant relative growth by gradient factors.....	67
1.6 Tolerance factors for plant species by gradient location.....	68
1.7 Competition factors for interspecific combinations.....	69
2.1 Peak standing crop estimates for six common salt marsh plant species.....	91
2.2 Species-specific model parameters for estimating annual plant biomass.....	92
2.3 Model estimates of peak aboveground/belowground biomass.....	93
2.4 Relative sensitivity of biomass model parameters.....	94
3.1 Determinants of salt marsh sedimentation patterns.....	117
3.2 Sedimentation profiles of four study sites.....	118
3.3 Relative sensitivity of elevation model parameters.....	119
4.1 Current hydrologic and elevation parameters values at four study site.....	151
4.2 Relative sensitivity of hydraulic model parameters.....	152
5.1 Relative sensitivity of plant succession model parameters.....	189
6.1 Generalized ecosystem model parameter values, units, and sources.....	239

6.2	Site-specific model parameters for spatial ecosystem model.....	241
6.3	Plant species cover percentages from surveys for study sites.....	242
6.4	Observed and predicted plant cover percentages for study sites.....	243
6.5	Goodness-of-fit matrices for spatial model (individual species).....	244
6.6	Goodness-of-fit matrices for spatial model (aggregate species groups).....	245

## LIST OF FIGURES

	PAGE
I.1	Conditions leading to salt marsh tidal restrictions..... 19
I.2	Conceptual model of salt marsh ecosystem processes.....20
I.3	Hypothesized time scales of salt marsh processes..... 21
I.4	Study site locator map..... 22
I.5	Site map of Oak Knoll Marsh in Rowley, Massachusetts..... 23
I.6	Site map of Little River Marsh in North Hampton, New Hampshire..... 24
I.7	Site map of Mill Brook Marsh in Stratham, New Hampshire..... 25
I.8	Site map of Drakes Island Marsh in Wells, Maine..... 26
1.1	Schematic diagram of transplant experiment design..... 70
1.2	Survival results for transplant species ..... 71
1.3	Final aboveground and belowground biomass results for transplants..... 72
1.4	Relative growth for transplant species..... 73
1.5	Plots of paired competition factors ..... 74
1.6	Comparative growth for interspecific transplant combinations.....75
2.1	Modeled annual biomass curves for common halophyte species..... 95
2.2	Modeled annual biomass curves for common brackish marsh species.....96
3.1	Conceptual model of salt marsh self-maintenance..... 120
3.2	Conceptual model of marsh sediment dynamics..... 121
3.3	Comparison of results from cohort and column sediment models..... 122
3.4	Modeled and measured estimates of elevation change for study sites..... 123

3.5	Estimates of contributions to sediment accretion for study species.....	124
4.1	Conceptual diagram of water level change in salt marshes.....	153
4.2a	Drakes Island Marsh current hydrologic and marsh flooding conditions.....	154
4.2b	Drakes Island Marsh hypsometric curve of marsh elevations.....	155
4.2c	Drakes Island Marsh scenario hydrologic and marsh flooding conditions...	156
4.3a	Little River Marsh current hydrologic and marsh flooding conditions.....	157
4.3b	Little River Marsh hypsometric curve of marsh elevations.....	158
4.3c	Little River Marsh scenario hydrologic and marsh flooding conditions.....	159
4.4a	Mill Brook Marsh current hydrologic and marsh flooding conditions.....	160
4.4b	Mill Brook Marsh hypsometric curve of marsh elevations.....	161
4.4c	Mill Brook Marsh scenario hydrologic and marsh flooding conditions.....	162
4.5a	Oak Knoll Marsh current hydrologic and marsh flooding conditions.....	163
4.5b	Oak Knoll Marsh hypsometric curve of marsh elevations.....	164
4.5c	Oak Knoll Marsh scenario hydrologic and marsh flooding conditions.....	165
5.1	Diagram of succession factors for marsh gradient locations.....	190
5.2	Low elevation plant succession model results.....	191
5.3	Mid elevation plant succession model results.....	192
5.4	High elevation plant succession model results.....	193
6.1	Conceptual schematic diagram of salinity regime assignments.....	246
6.2	Semivariogram analysis of elevation survey results for kriging.....	247
6.3	Comparison of error rates for kriging and linear interpolation analysis.....	248
6.4	Drakes Island base maps for plant cover, elevation, and salinity.....	249

6.5	Little River base maps for plant cover, elevation, and salinity.....	250
6.6	Mill Brook base maps for plant cover, elevation, and salinity.....	251
6.7	Oak Knoll base maps for plant cover, elevation, and salinity.....	252
6.8	Drakes Island validation sequence of plant cover changes 1988-2002.....	253
6.9	Mill Brook validation sequence of plant cover changes 1993-2002.....	254
6.10	Drakes Island validation results for observed and predicted plant cover.....	255
6.11	Mill Brook validation results for observed and predicted plant cover.....	256
6.12	Drakes Island predictions for current and scenario hydrologic conditions...	257
6.13	Little River predictions for current and scenario hydrologic conditions.....	258
6.14	Mill Brook predictions for current and scenario hydrologic conditions.....	259
6.15	Oak Knoll predictions for current and scenario hydrologic conditions.....	260
6.16	Drakes Island visualization of current and scenario hydrologic conditions..	261
6.17	Little River visualization of current and scenario hydrologic conditions.....	262
6.18	Mill Brook visualization of current and scenario hydrologic conditions.....	263
6.19	Oak Knoll visualization of current and scenario hydrologic conditions.....	264

## ABSTRACT

# SPATIAL MODELING AND VISUALIZATION OF HABITAT RESPONSE TO HYDROLOGIC RESTORATION IN NEW ENGLAND SALT MARSHES

by

Raymond A. Konisky

University of New Hampshire, May 2003

Anthropogenic alterations that restrict tidal flows negatively impact 20% of New England salt marshes, but management attempts to restore tides to these sites can be met with unexpected or less than optimal results. Restoration planners may be hindered by a lack of synthesized information regarding important biotic and abiotic factors that determine the distribution of dominant salt marsh plants and invasive species. An ecosystem model was developed to better predict salt marsh habitat response to hydrologic modification as a synthesis of existing models for biomass production, marsh elevation, tidal hydrology, and plant succession. A field experiment was conducted to provide the ecological basis for estimating plant responses to physical stresses and interspecific competition. Six plant species common to New England salt marshes were examined: halophyte species *Spartina alterniflora*, *Spartina patens*, and *Juncus gerardii*, and brackish invasive species *Phragmites australis*, *Typha angustifolia*, and *Lythrum salicaria*.

The model was applied to spatial grids representing marsh area at four salt marsh sites with past or current impacts due to restricted tidal flows. At each site, field data for

model parameterization was acquired according to a regional data-collection protocol. To assess model performance, the spatial distribution of marsh plants was predicted using specifications from past hydrologic and ecological conditions at two sites. Aggregated model predictions of halophyte-dominated and invasive-dominated marsh areas were within 4% of observed totals. The model was then run for each of the four study sites to generate 20-year simulations of plant composition changes resulting from current and possible hydrologic scenarios. Scenarios included changes in culvert shape, dimensions, and placement. Model simulations in response to tidally-restricted conditions predicted gradual replacement of halophytes by brackish invasive species, especially *P. australis*. Simulations involving tidal restoration strongly favored halophyte species. Based on spatial model outputs, realistic visualizations of marsh scenario results were designed and rendered. Use of this technology may provide new ways for resource managers to assess potential restoration outcomes, and to communicate the expected results of marsh improvement projects to non-technical audiences.



## **INTRODUCTION**

### **SPATIAL MODELING AND VISUALIZATION OF HABITAT RESPONSE TO HYDROLOGIC RESTORATION IN NEW ENGLAND SALT MARSHES**

#### **Problem Statement**

Large tracts of New England salt marsh have been altered or destroyed as a direct consequence of agriculture, road and rail building, residential and commercial development, and insect control (Niering and Bowers 1966). Today, as little as 50% of coastal wetlands present before colonial times remain in the New England states of Massachusetts, Maine, and New Hampshire (Cook et al. 1993). Although salt marshes are now protected, negative impacts from roads, bridges, and undersized culverts (see Figure I.1) persist in the form of reduced upstream tidal exchange, a condition commonly known as tidal restriction (Niering and Warren 1980). In New England, tidal restrictions are found in every coastal state, and may affect as much as 20% of remaining salt marsh habitat (Roman et al. 1984, USDA SCS 1994, Neckles and Dionne 2000). Tidal restrictions also occur in other parts of the US, particularly on the west coast (Race 1985,

Beare and Zedler 1987, Simenstad and Thom 1996), but the magnitude of the problem appears to be most acute in New England. A NOAA survey of the Coastal States Organization recently identified estuarine habitat degradation and salt marsh loss, much attributable to tidal restriction, as the highest priority management issue in the Northeast US (Frankic 1999).

Tidal restrictions lead to long-term salt marsh habitat degradation through various pathways and processes. Over time, sediment salinities diminish and salt marsh plant communities convert to brackish and freshwater wetlands dominated by invasive species (Roman et al. 1984, Sinicrope et al. 1990, Burdick et al. 1997). Organics in marsh sediments dry and oxidize, leading to anoxic conditions and poor water quality within marsh creeks and pannes (Portnoy 1991, Portnoy and Giblin 1997). Sedimentation rates diminish and marsh elevations subside, impounding freshwater (Sinicrope et al. 1990, Burdick et al. 1997, Anisfeld et al. 1999, Burdick 2002), and decoupling natural salt marsh sedimentation processes from sea level rise (DeLaune et al. 1983, Boumans and Day 1994). In addition, culverts and dikes create physical barriers that limit access to nursery, refuge, and forage resources for fish (Dionne et al. 1999), disrupting the estuarine food chain and impacting other trophic levels (Reinert and Mello 1995, Kneib 1997, Minello and Webb 1997).

Collectively, the net impacts of tidal restrictions are to reduce or eliminate critical salt marsh ecosystem functions, and ultimately, important societal values that salt marshes provide (see Table I.1, from Short et al. 2000, for a summary of salt marsh

functions and values). Fortunately, some degraded coastal marsh habitats can recover lost functions if the appropriate hydrologic regime is restored (Sinicrope et al. 1990, Roman et al. 1995, Burdick et al. 1997, Burdick et al. 1999, Roman et al. 2002, Warren et al. 2002). As a result, hydrologic restoration of restricted salt marshes is a common management practice today (New Hampshire Office of State Planning 1996, Save the Sound 1998, US Army Corps of Engineers 1999).

Predictive tools, based on well-known hydraulic engineering methods, are now widely available to assess and model the hydrologic aspects of potential salt marsh restoration projects (Roman et al. 1995, US Army Corps of Engineers 1999, Boumans et al. 2002). These programs are calibrated to existing flow conditions and reconfigured with new specifications to model culvert replacement, creation or expansion of tidal creeks, removal of tidal gates, or other hydrologic changes. Based on modeled output, a set of specifications are selected to produce a flood regime that best meets the objectives of the resource managers (i.e., increases tidal exchange and/or alleviates storm flooding, but does not affect cellars, lawns, or wells of residents).

As a result of hydrologic analysis, the new flood regime of a restoration site can be predicted with considerable accuracy. But, it does not necessarily follow that the proposed changes will result in recovery of marsh habitat health or lost biodiversity. In fact, while hydrologic regime is certainly crucial to wetland restoration, it appears that hydrology is only one of many interrelated factors that ultimately determine the success or failure of a wetland restoration project. Zedler (2000), in a review of wetland

restoration progress, pointed out that “it takes far more than water to restore wetlands”, and that it was not possible to anticipate long-term results without also considering a myriad of ecological factors, including plant biology, community succession, and sediment-plant interactions. Inability to account for these complex interactions, even if tidal exchange is adequately restored, may have lead to unintended and less than optimal results for many salt marsh hydrologic restoration projects (Race 1985, Rozsa 1988, Moy and Levin 1990, Frenkel and Moran 1991, Simenstad and Thom 1996). It was therefore proposed that a synthesized model of interrelated salt marsh processes would improve the predictive capability of resource managers faced with salt marsh restoration options.

### **Project Goal and Objectives**

The goal of this project was to integrate a set of critical ecological factors, including biotic and abiotic processes, into a synthesized ecosystem simulation model to predict long-term salt marsh habitat response to hydrologic restoration. A number of important project objectives were identified in order to accomplish this goal, and to make the project as useful as possible for coastal resource managers:

**A. Standard Data Requirements.** The model considered four general categories of interrelated factors: hydrology, coastal geology, plant biology, and plant succession. Simulations of critical processes associated with each of these factors required field data that adequately characterized potential marsh restoration sites. To make the model useful for a wide range of users and locations, an important objective of the project was to use

standardized, commonly-collected field specifications. In support of this objective, model inputs were based on the field collection variables identified by the Programme of Action Coalition for the Gulf of Maine (GPAC) Protocol (Neckles and Dionne 2000). A summary of model categories, key components, and data requirements are listed in Table I.2. As an assessment of model and data collection transferability, project implementation sites included four diverse New England salt marsh locations (see Study Sites).

B. Marsh Plant Ecology. An additional objective of the project was to provide resource managers with synthesized information regarding salt marsh plant species of concern. In undisturbed New England salt marshes, perennial plant species are found in zones of smooth cordgrass (*Spartina alterniflora*), salt hay (*Spartina patens*), and black grass (*Juncus gerardii*), from the seaward to the landward borders of the marsh (Niering and Warren 1980). However, these native species are often replaced by the brackish invasive species common reed (*Phragmites australis*), narrow-leaf cattail (*Typha angustifolia*), and purple loosestrife (*Lythrum salicaria*) when disturbances like tidal restrictions occur (Roman et al. 1984, Sinicrope et al. 1990, Burdick et al. 1997). To gain a better understanding of plant succession dynamics under changing hydrology, a field experiment was conducted to transplant each species across a gradient of tidal flooding and salinity conditions. The experiment was based on the testable hypothesis that physical stress tolerance varied by species, as measured by transplant survival and growth at each gradient location. In addition, transplants were arranged in pair-wise interspecific combinations to assess relative competitive rankings. The experiment

provided species-specific and combination-specific results that formed the predictive basis for plant succession dynamics in response to changing hydrologic conditions.

C. Hydrologic Scenario Assessment. A further objective of the project was to support scenario modeling for marsh hydrologic restoration options. Restoration planners are required to perform “what-if” analysis before initiating construction activities to expand an undersized culvert, add a new culvert, excavate tidal creeks, or alter hydrology in other ways. In support of scenario modeling, a tidal hydraulics component was developed to simulate current flow conditions and potential hydrologic regimes for each considered site. Hydrologic data was used by the ecosystem model as a critical determinant of plant community response to marsh hydrologic restoration.

D. Spatial Technology. A final project objective was to develop and use technology that delivered results in a spatial format. Most models are based on parameters that change over time, but are spatially aggregated (Costanza and Sklar 1985). This approach, however, fails to discern ecologically significant spatial patterns that result from important landscape-level processes, and ignores key interactions between spatial elements (e.g., tidal flooding and plant recruitment). Spatially explicit models therefore provide a more complete and rigorous simulation of critical ecosystem processes (Sklar et al. 1985, Turner et al. 1989). For this project, model outputs included spatial maps and image sequences that animated changes of key outputs (i.e., plant species cover) over time. Spatial animation has now emerged as a software technology with great potential for wetland restoration modeling (Maxwell and Costanza 1997,

Voinov et al. 1998, Voinov et al. 1999). As an extension of the spatial output objective, the project also included the development of photo-realistic visualization video images from spatial model results. Visualizations expand interpretative capabilities for a wide audience of technical and non-technical interests, and offer new communication options for resource managers and stakeholder groups involved in wetland restoration decisions. Collectively, these new spatial technologies are hoped to provide a comprehensive decision-support environment for the assessment of salt marsh conditions and restoration scenarios associated with tidal restriction.

### **Modeling Approach**

As a general technical approach, selected component models of key salt marsh processes were acquired from published sources and reconfigured with New England salt marsh specifications. Existing models leverage current scientific knowledge, and provide a tested and documented foundation for model development. For each component model, specifications were identified for New England salt marsh habitat, based on experimentation and literature searches of parameter values. The models were configured and implemented individually, subjected to a formal sensitivity analysis, and validated with independent data sets as available.

Three process-specific models were selected to simulate the hydrodynamics, plant biomass production, and marsh elevation dynamics of New England salt marshes. The Marsh Response to Hydrological Modification (MRHM) model was developed

specifically to calibrate tidal flow through culvert structures, and to simulate hydrologic restoration scenarios (Boumans et al. 2002). MRHM has been implemented at several New England salt marsh locations, and has been shown to accurately predict upstream tidal range, water discharge, and flood potential. The Generalized Ecosystem Model (GEM) is a process model for plant biomass production and carbon allocation (Fitz et al. 1996). GEM was developed primarily as a wetland ecosystem model, and it has been used to estimate plant production for diverse wetland plant communities, including the Florida Everglades (Voinov et al. 1998), Maryland coastal marshes (Voinov et al. 1999), and New Hampshire eelgrass beds (Short et al. 1998). Simulation of coastal geologic processes controlling marsh sediment formation, including organic and inorganic sediment deposition, accretion, and subsidence, was based on a relative elevation model from Rybczyk et al. (1998). This model has been used to predict elevation response to geomorphologic conditions in a Louisiana coastal wetland, and in the Po River delta of Italy (Day et al. 1999). A fourth component model, for simulating salt marsh plant succession, was developed independently for this project based on the work of J.B. Grace (1987) and Bertness and Ellison (1987).

After individual assessment, component models were linked to form a single synthesized model of salt marsh ecosystem processes. This integrated collection of inputs and commands formed the project *unit model*. For spatial implementation, marsh areas were organized into grids of square cells, and spatial databases were developed to maintain cell-specific values (e.g., coordinate location, plant cover, elevation, flood and salinity regime, sedimentation rate, etc.). The unit model was then run for an individual



cell, or spatially for entire marsh grids (Maxwell and Costanza 1997). When implemented spatially, exchanges between cells were used to simulate plant recruitment from one location in the marsh to another.

A conceptual model of process flows and interdependencies is presented in Figure I.2. As a first step to model processing, a two-week time series of water volume and tidal heights was generated according to selected hydrologic scenario specifications. For each cell, tidal height was compared with elevation to determine the percent time flooded. A composite of all marsh elevations, ordered as a hypsometric curve, was used to produce an estimate of total marsh surface area flooded for each tide. Site-specific measures of substrate salinity and marsh sedimentation rates were used in conjunction with cell elevation and spatial position to estimate salinity regime and sediment deposition. Plant biomass production for each cell was determined by plant species composition and species-specific production rates.

Over the long-term, the accumulation of plant biomass and inorganic sediment deposits, combined with the rate of sea level rise, resulted in net sediment accretion or erosion, and therefore changes in relative elevation. Modeled plant species assemblages responded differentially to physical stresses associated with changes in flood and salinity regime, based on experimentally-derived gradient growth factors. In addition, interspecific plant competition (also based on experimental results) and recruitment from neighboring cells combined with gradient growth factors to influence succession of plant communities. Since changes in species composition affect biomass accumulation, and

therefore sediment accretion, the model included a feedback loop to simulate long-term marsh self-maintenance processes.

Overall ecosystem response to changes in hydrologic conditions was measured in terms of changes to plant species assemblages over time. Since relevant marsh processes occur over a wide range of time scales (see Figure I.3, from Burdick et al. 1997), all model simulations were conducted over extended timeframes. Morgan and Short (2002), studying man-made constructed salt marshes, estimated that these new marsh areas could reach functional levels comparable to native marshes within 5-20 years. It seemed reasonable, then, to assume that existing marshes would adjust to hydrologic alterations within similar timeframes. As a standard approach, all model simulations were run for durations of 20 years.

### Study Sites

Four New England salt marsh sites were selected from coastal and estuarine locations in Massachusetts, New Hampshire, and Maine (Figure I.4). All four marsh sites have a history of impacts from tidal restriction, and therefore represent past or present candidates for hydrologic restoration. The marshes represent a diversity of salt marsh habitat and salinity regimes, including oligohaline (<5 ppt), mesohaline (5-18 ppt) and polyhaline (>18 ppt) marsh conditions (Odum et al. 1984). In addition, the sites are well-known field locations that have been studied for a variety of ecological projects (Kelley

et al. 1995, Burdick et al. 1997, Dionne et al. 1999, Burdick et al. 1999, Burdick et al. 2001, Boumans et al. 2002, Burdick 2002).

Oak Knoll Marsh. Oak Knoll Marsh (Figure I.5) is adjacent to the Massachusetts Audubon Society's Rough Meadows Wildlife Sanctuary, located in Rowley, Massachusetts (42°45'00"N, 70°45'00"E). The 15-hectare study site is an isolated section of back barrier salt marsh formed landward of Plum Island, separated from the extensive Great Marsh of Rowley by Route 1A. Tidal inputs from the Mud Creek, a tributary of the Parker River, flow into the study site through two undersized culverts (north culvert 0.69 m diameter, south culvert 1.03 m diameter) installed under Route 1A ca. 1930. The site has a long history of impacts from agriculture and insect control, and artifacts of its past can be seen today in wooden staddles (staked platforms for salt hay storage) and mosquito-control ditches. A section of marsh seaward from the study site is still harvested annually for salt hay production. Despite the obvious nature of tidal restriction at Oak Knoll, there are no current management plans for hydrologic restoration at the site.

Marsh vegetation at Oak Knoll is dominated by salt marsh species (*Spartina* spp.), but brackish species (*Phragmites australis*, *Lythrum salicaria*, *Typha angustifolia*) and woody plants (*Iva frutescens*, *Juniperus virginiana*) have a substantial and growing presence (Burdick et al. 2001, Boumans et al. 2002). Sediment field elevation stations (Boumans and Day 1994) monitored since 1996 indicate low levels of sediment accretion (~1.5 mm/yr) on the marsh, and possible sediment subsidence (D.M. Burdick, personal

communication). The salinity regime at Oak Knoll is polyhaline near Mud Creek, but measurements from salinity wells located in a *Phragmites australis* stand in the western portion of the marsh indicate mesohaline conditions (Burdick et al. 2001).

Little River Marsh. The Little River Marsh (Figure I.6) is a large back barrier system that covers an expanse of approximately 70 hectares along Route 1A in the towns of Hampton and North Hampton, New Hampshire (42°52'30"N, 70°45'00"E). The natural tidal flow of the marsh has been altered for at least a hundred years, with a series of undersized culverts installed under Route 1A in 1890, 1929, and 1948 (US Army Corps of Engineers 1999). By 1994, New Hampshire coastal resource managers identified Little River as a candidate for hydrologic restoration (USDA SCS 1994). However, the 1948 culvert (1.2 m diameter) was still in place when a >100-year rainfall in October 1996 caused major flooding of the marsh, the roadway, and bordering residential structures. In 1997, a decision was reached by public officials to significantly expand tidal flow capacity under Route 1A. The US Army Corp of Engineers designed a twin 6-by-12 ft box culvert system for Little River, and after several years of hearings and permits, the box culverts were installed and opened to the tides in November 2000.

Vegetation surveys at Little River Marsh indicate that, at the time of hydrologic restoration, the marsh was dominated by brackish species (*Lythrum salicaria*, *Phragmites australis*, and *Typha* spp.), with only sparse patches of salt tolerant species like *Spartina patens* (Burdick 2002). Elevation measurement stations were not installed at Little River until October 2000, but elevation data collected at a nearby reference marsh suggest that

sediment accretion rates will be moderate (~ 4 mm/yr) following hydrologic restoration (Awcomin Marsh downstream, Burdick et al. 1999). The salinity regime of Little River is polyhaline at mid-marsh, but growing season salinities diminish to levels as low as 2 ppt with increasing distance from the tidal source (Burdick 2002).

Mill Brook Marsh Located in Stratham, New Hampshire (43°00'00"N, 70°52'30"E) Mill Brook Marsh (Figure I.7) was formed in a minor fluvial valley near the mouth of the Squamscott River at the southwest corner of the Great Bay. The small 6-hectare marsh follows along Mill Brook, adjacent to the agricultural fields of Stuart Farm. Mill Brook is separated from the Squamscott River by an access road to the farm, and in the mid-1960s a culvert with a flap gate was installed under the road. As a result, the marsh became a freshwater meadow with little or no tidal input. In October 1993, as part of a coordinated private-public restoration effort, the flap gate was removed and a large (2.1 m diameter) arched culvert was installed to recreate the natural tidal flows of the marsh.

At the time of hydrologic restoration, marsh vegetation included *Typha angustifolia*, *Lythrum salicaria*, and remnant patches of salt tolerant species, but salt marsh perennials (*Spartina* spp.) have rebounded strongly since 1993 (Burdick et al. 1999). Elevation stations, installed at the site in 1996, indicate high levels of sediment accretion (~19 mm/yr) following restoration (Burdick et al. 1999). With a location far into the Great Bay Estuary, the salinity regime at Mill Brook Marsh is low polyhaline (~18 ppt) and mesohaline (Burdick et al. 1999).

Drakes Island Marsh Drakes Island Marsh (Figure I.8) is part of the Wells National Estuarine Research Reserve in Wells, Maine (43°15'00"N, 70°30'00"E), formed landward of a barrier beach about 4,000 years ago (Kelley et al. 1995). The study site is a 31-hectare tidal marsh, separated from the larger Webhannet estuary to the south by Drakes Island Road. The marsh has a history of use as a cow pasture, dating from 1848 when a dike was built across the tidal inlet. In the 1920s, the dike was replaced by a culvert and flap gate to accommodate Drakes Island Road, and in the 1950s, the current culvert was installed with a flap gate. Repairs to the culvert over the past 50+ years have led to a current undersized culvert diameter of 1.2 meters. In March 1988, the flap gate broke away and was not replaced, and as a result, partial tidal hydrology was restored. In recent years, the need for solutions to local stormwater management issues has led a public-private coalition to evaluate potential new culvert designs and further hydrologic restoration options for the marsh.

Vegetative cover at Drakes Island continues to be dominated by cattail (*Typha* spp.) in the upper reaches of the marsh, with salt marsh vegetation (*Spartina* spp.) along the creek-banks and in low areas of tidal flooding (Burdick et al. 1999). Marsh elevations appear to be slowly subsiding, with low sediment accretion rates (~ 2.4 mm/yr) observed at field elevation stations since 1996 (Burdick et al. 1999). The marsh soil water salinity regime is polyhaline near the tidal culvert, but mesohaline and oligohaline levels are observed in the cattail zones of the upper marsh (Burdick et al. 1999).

## **Dissertation Organization**

This dissertation is presented in six chapters, following the introductory chapter. In addition, an Appendix containing original field data and a program listing is provided. The dissertation chapters are organized as follows:

**Chapter I. A Field Experiment to Determine Physical Stress Tolerance and Relative Competitive Rankings for Six Common Plant Species Inhabiting and Invading New England Salt Marshes:** This chapter describes a transplant experiment designed to identify the relative tolerance of common New England marsh plants to physical stresses of salt water flooding, and to assess interspecific competitive rankings.

**Chapter II. A Biomass Production Model for Common Plant Species of New England Salt Marshes:** Above and belowground biomass production and annual growth curves are estimated for six common New England salt marsh species.

**Chapter III. A Relative Elevation Model for New England Salt Marshes:** Long term elevation changes are predicted for New England salt marsh locations, based on sedimentation rates, plant biomass production, and sea level rise.

**Chapter IV. A Hydraulic Model for Predicting Tidal Flows in Hydrologically-Altered Salt Marshes:** Tidal flows through culverts and channels are calibrated to current

conditions in four New England salt marshes, and modeled results are used to analyze potential new scenarios for hydrologic changes.

Chapter V. A Model of Plant Succession Following Hydrologic Disturbance in New England Salt Marshes: Community-level changes in plant species composition, following hydrologic disturbance, are predicted using experimental measures of physical stress tolerance and interspecific competitive rankings.

Chapter VI. Spatial Simulation Model and Visualization of Habitat Response to Hydrologic Restoration of New England Salt Marshes: Spatial maps and time-series animations of plant community changes are generated for four New England salt marshes with past or potential hydrologic restoration, including photo-realistic 3-D visualization scenarios.



<b>Functions</b>	<b>Values</b>
Primary production	Support of food webs, fisheries, wildlife
Canopy structure	Habitat, refuge, nursery and settlement for support of fisheries
Organic matter accumulation	Support of food webs, counter sea level rise
Seed production and vegetative expansion	Maintenance of plant communities and biodiversity
Sediment filtration and trapping	Counter sea level rise, improve water quality, and support of fisheries
Epibenthic and benthic production	Support of food webs, fisheries, and wildlife
Nutrient and contaminant filtration	Improve water quality and support of fisheries
Nutrient regeneration and recycling	Support of primary production and fisheries
Organic export	Support of estuarine, offshore food webs, and fisheries
Wave and current energy dampening	Protect upland from erosion and reduce flood-related damage
Self-sustaining ecosystem	Recreation, aesthetics, open space, education, landscape level biodiversity, and historical value

Table I.1. List of important salt marsh ecosystem functions and values to human society (Short et al. 2000).

<b>Process Category</b>	<b>Key Components</b>	<b>Model Input Sources * requires field data</b>
Hydrology	Tidal hydrology Culvert/creek hydraulics Marsh surface flood regime Sediment salinity regime Sea level rise	Local tidal signal * Culvert dimensions * Elevation survey * Salinity well measures * Publications
Geomorphology	Sediment deposition Sediment accretion/subsidence Labile/refractory allocation Decomposition	Marker horizon accretion * Publications Publications Publications
Plant Biology	Biomass production Above/belowground allocation Litter accumulation in soil	Plant cover survey * Field experiment Publications
Plant Succession	Stress tolerance Interspecies competition Recruitment	Field experiment Field experiment Plant cover survey *

Table I.2. General categories, key process components, and model input sources for the integrated salt marsh ecosystem model.



**Figure I.1. Conditions leading to salt marsh tidal restriction: (Top) Road crossing at Oak Knoll Marsh in Rowley, Massachusetts; (Bottom) Tidal culvert at Little River Marsh in North Hampton, New Hampshire before replacement in 2000.**

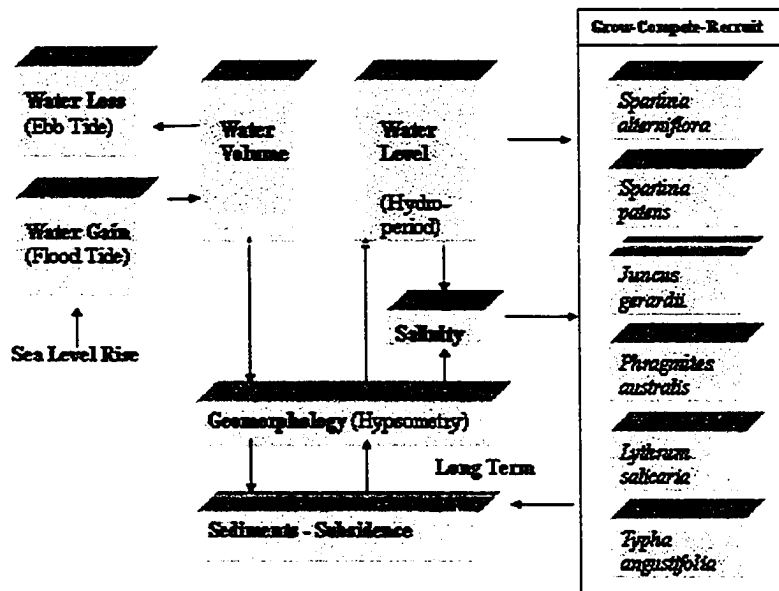


Figure I.2. Conceptual model of key salt marsh ecosystem processes. Tidal cycle determines marsh water volume. Water flow across marsh geomorphologic features (as described by a hypsometric curve) determines local water level, hydroperiod, and influences substrate salinity. Plant species grow in response to physical stress (flooding and salinity), compete for resources, and recruit from neighbors. Net plant production combines with sedimentation and subsidence processes to influence long-term elevation and marsh geomorphology.

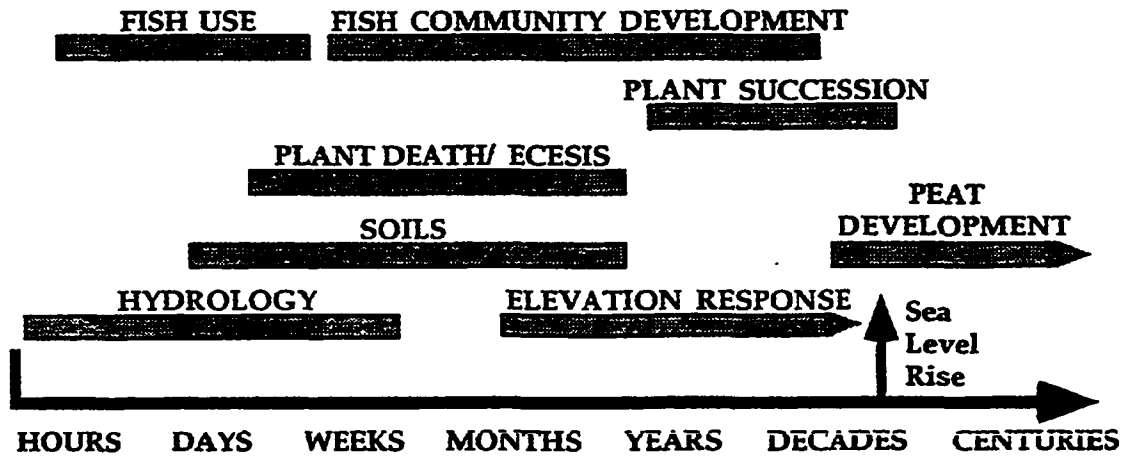


Figure I.3. Hypothesized time scales of processes related to indicators of salt marsh functions (Burdick et al. 1997).

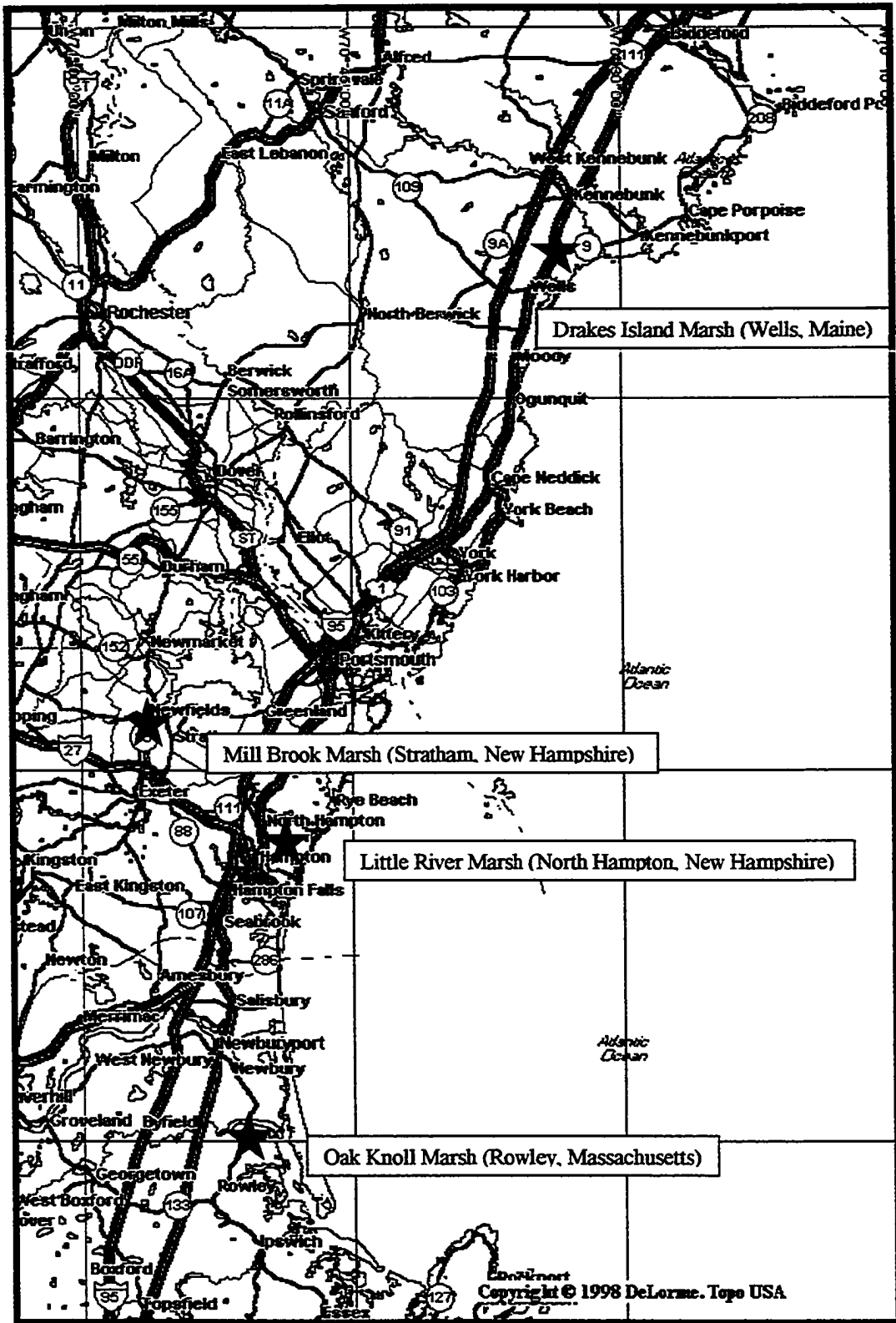


Figure I.4. Locator map for the four study sites.

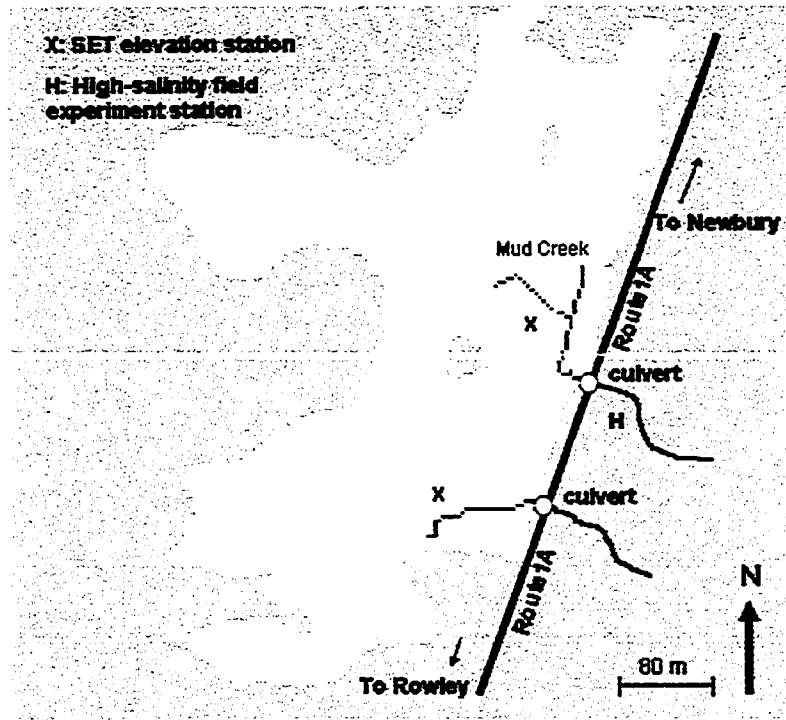


Figure I.5. Site map of Oak Knoll Marsh in Rowley, Massachusetts.

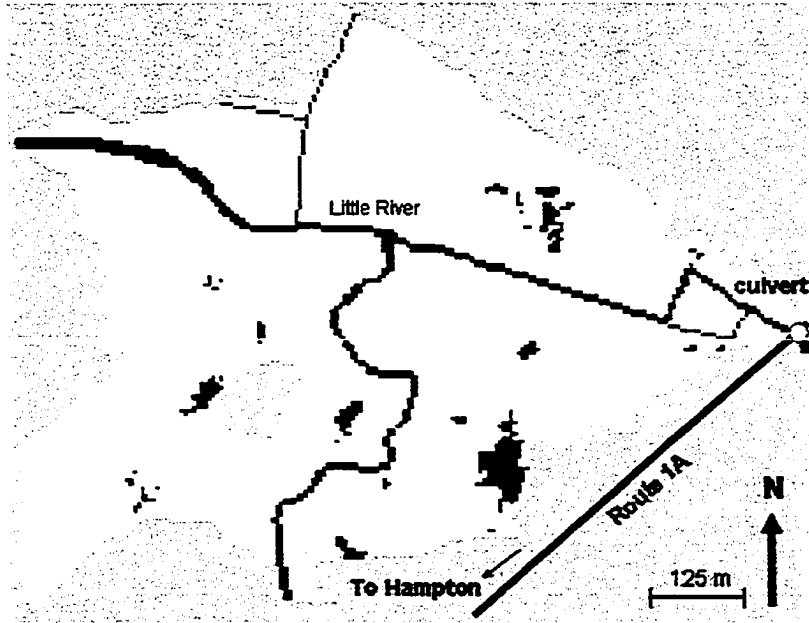


Figure I.6. Site map of Little River Marsh in North Hampton, New Hampshire.



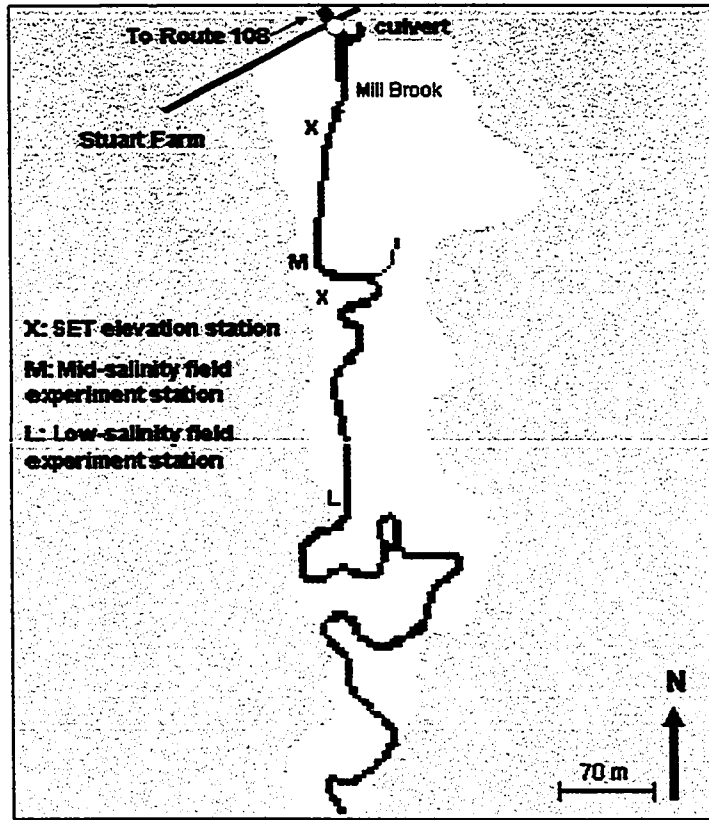


Figure I.7. Site map of Mill Brook Marsh in Stratham, New Hampshire.

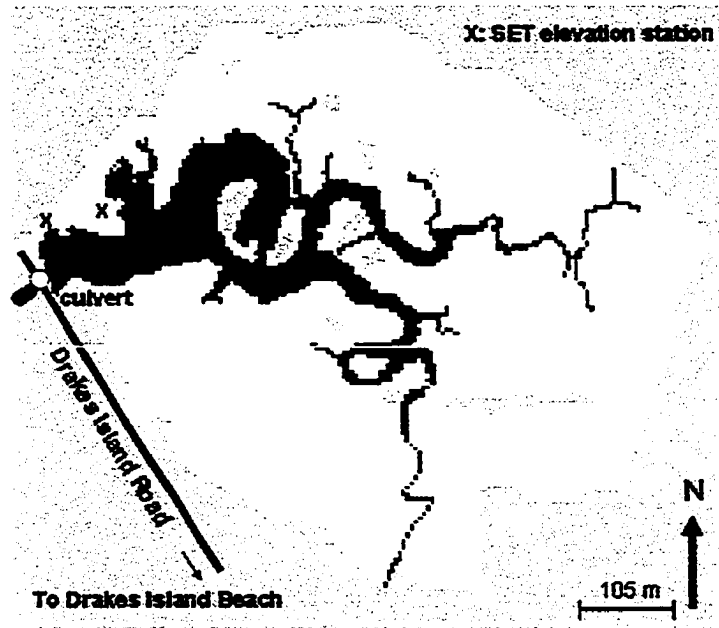


Figure I.8. Site map of Drakes Island Marsh in Wells, Maine.

## **CHAPTER I**

### **AN EXPERIMENT TO DETERMINE PHYSICAL STRESS TOLERANCE AND RELATIVE COMPETITIVE RANKINGS FOR SIX COMMON PLANT SPECIES INHABITING AND INVADING NEW ENGLAND SALT MARSHES**

#### **Experimental Objectives**

Barriers that restrict tides negatively impact many New England salt marshes, and often result in the replacement of native salt marsh plants with brackish invasive species (Sinicrope et al. 1990, Burdick et al. 1997). Resource managers can reintroduce tides at these sites by reducing or removing tidal barriers, a management option known as hydrologic restoration, but these efforts are often met with unexpected or less than optimal results (see Introductory Chapter). Restoration planners would benefit from a synthesized ecosystem model based upon important salt marsh processes. Abiotic and biotic processes, especially those related to tolerance of physical disturbance (i.e., saltwater flooding) and interspecific competition, are key determinants of spatial pattern in marsh plant communities (Bertness and Ellison 1987). Therefore, in order to predict

plant community response to hydrologic restoration, it is essential to obtain detailed knowledge of physical stress tolerance and competitive rankings among dominant salt marsh plant species.

Field observations show that physical stresses associated with saltwater flooding play an important role in the distribution of common salt marsh plants. For example, black grass (*Juncus gerardii*) is commonly found in upland marsh elevations, but not in frequently flooded locations. While observations can be used to determine general distribution zones for *Juncus* and other salt marsh species, only a few experiments have examined the specific effects of saltwater flooding on marsh plants, and these findings apply only to a subset of edaphic conditions and dominant plant species found in northeastern US salt marshes (Bertness and Ellison 1987, Burdick et al. 1989, Bertness 1991b, Hellings and Gallagher 1992).

In New England salt marshes, especially those with altered tidal hydrology, native perennial species such as cordgrass (*Spartina alterniflora*), salt hay (*Spartina patens*), and black grass (*Juncus gerardii*) are often displaced by invasive species like common reed (*Phragmites australis*), narrow-leaf cattail (*Typha angustifolia*), and purple loosestrife (*Lythrum salicaria*) (Roman et al. 1984, Sinicrope et al. 1990, USDA SCS 1994, Burdick et al. 1997, Burdick et al. 1999). An experiment to identify the relative stress tolerance of these six dominant New England salt marsh species, across a wide range of natural conditions, would fill a considerable gap in our knowledge of plant response to changing marsh hydrology. In addition, since competition for resources is

assumed to increase when brackish species invade native marsh vegetation, the relative competitive rankings among these six plant species would provide new information to help predict changes in species assemblages at salt marshes with restricted or restored tidal hydrology.

To address the needs of salt marsh resource managers, an experiment was conducted to transplant six common New England plant species across a natural physical gradient of three tidal flooding and three salinity regimes. A schematic diagram of the three-by-three factorial design is provided in Figure 1.1. Transplanting is a fairly common experimental technique, involving the relocation of established plants into controlled locations. For this study, plants were moved into marsh zones with different flood and salinity regimes to simulate the effects of changing hydrologic conditions on marsh plants in restricted or restored sites. The experiment tracked single-season survival and growth of transplanted shoots across a range of marsh elevations (low: below mean high water, mid: around mean high water, and high: above mean high water) and salinity regimes (low: mesohaline 5-18 ppt, mid: meso-polyhaline 18 ppt, and high: polyhaline >18 ppt, per Odum et al. 1984). At the end of the growing season, live biomass was measured for each species at each of the nine gradient locations to determine the relative species tolerance to physical stress factors.

In addition to stress tolerance, the experiment also measured relative competitive ability among the study species. To create competitive interactions, plant shoots were transplanted into open bottom pots and arranged pair-wise with different species

(interspecific combinations) or with shoots of the same species (intraspecific combinations). This design was based on the theory that, when resources are limited, the best competitor utilizes the limiting resource most efficiently (Tilman 1982, Tilman 1988). In this experiment, the use of small open pots limited expansion space for belowground structures, and since salt marsh sediments are thought to have limited availability of nitrogen (Valiela and Teal 1974), the design was expected to force belowground competition. In addition, close arrangements of transplant shoots in the pots were likely to create shading conditions and aboveground competition for light. Growth comparisons between intra and interspecific combinations were used to test the assumption that competitive interactions had occurred. Also, transplant growth was measured for each participant in interspecific combinations (*Spartina alterniflora*–*Spartina patens*, *Phragmites*–*Juncus*, *Lythrum*–*Typha*, etc.) as a quantitative measure of relative competitive ranking. The experiment was not designed to test significance of differences between these measures, but to provide averaged combination-specific results that could be used as a starting point for assessing relative competitive effects among the important plant species of tidally-restricted salt marshes.

In summary, the field experiment was used to provide species-specific measures of physical stress tolerance across a wide range of marsh conditions, and measures of relative competitive rankings. These measures were used as input parameters for an ecosystem model of plant community response to hydrologic restoration. In addition, experimental results were used to test the underlying hypotheses that physical stress

tolerance and competitive interactions were determinants of marsh plant distribution and growth.

### **Hypotheses of Physical Stress Tolerance**

A general hypothesis of physical stress tolerance for the experiment would state that growth of transplanted individuals would be influenced by physical stress, as determined by the location of the transplants within a gradient of saltwater flooding conditions. Expressed in null form, the hypothesis asserts that transplant growth would not vary across gradient locations. However, dominant salt-tolerant plants of New England salt marshes are known to form into distinct zones along the tidal gradient, with monocultures of *Spartina alterniflora* in the low marsh, *Spartina patens* at mid elevations, and *Juncus* along the landward borders of the marsh (Niering and Warren 1980, Nixon 1982, Bertness and Ellison 1987). Considering these distinct distribution patterns, it was expected that the relocation of plant species into nine gradient elevation and salinity marsh zones would produce very different rates of growth. Since tolerance of saltwater flooding is a key determinant of salt marsh species distribution (Bertness and Ellison 1987, Bertness 1991b), and since salinity stress was present at all study gradient locations, it was reasonable to expect that flood stress (elevation) would be the controlling gradient factor for the salt-tolerant species. Therefore, null and alternate hypotheses of physical stress tolerance for native halophyte species are as follows:

**H<sub>0</sub> *Spartina alterniflora*:** *Spartina alterniflora* growth will be similar across all nine gradient locations.

**H<sub>A</sub> *Spartina alterniflora*:** *Spartina alterniflora* growth will vary by elevation, decreasing from low to high elevation gradient locations.

**H<sub>0</sub> *Spartina patens*:** *Spartina patens* growth will be similar across all nine gradient locations.

**H<sub>A</sub> *Spartina patens*:** *Spartina patens* growth will vary by elevation, decreasing from high to low elevation gradient locations.

**H<sub>0</sub> *Juncus*:** *Juncus* growth will be similar across all nine gradient locations.

**H<sub>A</sub> *Juncus*:** *Juncus* growth will vary by elevation, decreasing from high to low elevation gradient locations.

The distribution patterns of plant species invading tidally-restricted marshes in New England are less well understood, but salinity intolerance has been identified as an important factor for *Typha* (Beare and Zedler 1987), *Lythrum* (Dzierzeski 1991) and *Phragmites* (Hellings and Gallagher 1992, Bart and Hartman 2000, Warren et al. 2001). Evidence of flood intolerance for these species is minimal, although Hellings and Gallagher (1992) found that *Phragmites* growth was lower in soils with high water tables than in well-drained sediments. For this experiment, it was therefore expected that salinity stress would be the controlling gradient factor for the salt-intolerant invasive species. Physical stress hypotheses for the brackish invasive species are as follows:

**H<sub>0</sub> *Phragmites*:** *Phragmites* growth will be similar across all nine gradient locations.



$H_{A \text{ Phragmites}}$ : *Phragmites* growth will vary by salinity regime, decreasing from low to high salinity gradient locations.

$H_{0 \text{ Lythrum}}$ : *Lythrum* growth will be similar across all nine gradient locations.

$H_{A \text{ Lythrum}}$ : *Lythrum* growth will vary by salinity regime, decreasing from low to high salinity gradient locations.

$H_{0 \text{ Typha}}$ : *Typha* growth will be similar across all nine gradient locations.

$H_{A \text{ Typha}}$ : *Typha* growth will vary by salinity regime, decreasing from low to high salinity gradient locations.

To test these hypotheses, a statistical model was developed for each species that analyzed the relationship between growth and physical stress. It was an assumption of this model that the potential effects of interspecific competition were equal across study gradient locations. Some researchers have found that competitive plant interactions become increasingly important as physical stress diminishes (Bertness and Ellison 1987, Pennings and Calloway 1992, Keddy et al. 1994, Huckle et al. 2000, Emery et al. 2001). For the current experiment, this suggested that transplants at gradient locations with lower salinities and higher elevations might be more influenced by competition than transplants at locations with higher salinities and lower elevations. However, with salinity stress present throughout the experimental gradient (mesohaline and polyhaline), potential differences in competitive influence might be lessened. In any case, the species hypotheses for stress tolerance were tested without regard to transplant combination, although the potential influences of competition were useful in explaining some experimental results.

## Hypotheses of Competitive Interactions

A general hypothesis of plant competition for the experiment would state that transplant growth was influenced by competitive interactions, as determined by intraspecific or interspecific pair-wise combinations. Expressed in null form, the hypothesis asserts that transplant growth would not vary between combinations. However, plant competition theory suggests that, since plants occupy niches based on species-specific resource requirements (Tilman 1988), individuals competing for limited resources may experience diminished growth if all competitive participants required the exact same level of resources. If this was true, then intraspecific combinations would have lower growth than interspecific combinations (the selected alternate hypothesis). On the other hand, if interspecific competition was predominantly negative and produced lose-lose interactions (Keddy 1989), intraspecific combinations would experience higher growth. Without a strong indication of expected response, the null hypothesis, as stated below, was selected for statistical analysis. To test the null hypothesis, a one-way ANOVA was run for transplant growth results, with the interspecific and intraspecific grouping as the main effect. Generalized competition hypotheses for the experiment are as follows:

**H<sub>0</sub> competition:** Transplant growth will be similar between intraspecific and interspecific transplant combinations.

**H<sub>A</sub> competition:** Growth of transplants in intraspecific combinations will be different than in interspecific combinations.

For species-level interactions, competitive hierarchies are thought to exist among the native salt-tolerant marsh plants of New England. *Juncus* is usually considered the top competitor, since it dominates the most desirable marsh habitat (i.e., the low-stress upper marsh), followed by *Spartina patens*, and then *Spartina alterniflora*, the low-marsh dominant. In fact, some experimental evidence supports this hypothesized ranking in the high marsh (Bertness and Ellison 1987, Emery et al. 2001). However, since the current experiment was conducted across a gradient of elevation, generalized competitive rankings among halophytes would likely be determined by the best overall tolerator of physical stress conditions. Experimental results of transplant growth for each participant in halophyte-only interspecific combinations were analyzed by graphic analysis to determine relative rankings for salt-tolerant species.

Little is known regarding relative ranks of interspecific competition between the invasive and salt-tolerant species. *Typha*, *Lythrum*, and especially *Phragmites* enjoy notorious reputations as aggressive, monoculture-forming competitors, so it might be expected that these invasive species would out-compete native salt marsh plants in the experiment. But again, since all experimental interactions occurred in salt-stressed locations, it was possible that plant response to salinity stress would mask, or even counter, anticipated competitive interactions. Competitive rankings among the invasive species are also poorly understood, although Keddy et al. (1994) found that *Lythrum* was competitively dominant over *Typha* in freshwater habitats. However, with little corroborating experimental evidence, and the possible confounding influences of physical stress, it was difficult to set specific expectations for halophyte-invasive and invasive-

only competitive interactions. Experimental results of transplant growth for participants in each combination were also analyzed by graphic analysis to determine relative rankings of competitive ability.

### **Methods**

Plant shoots were collected from on-site or nearby sources and transplanted into open-bottom pots (3.2 L food cans with both lids removed) at nine experimental sites. Sites were established in May 2000 at Oak Knoll Marsh (high salinity regime) in Rowley, Massachusetts (42°45'N, 70°45'E), and in May 2001 at Mill Brook Marsh (mid and low salinity regimes) along the Squamscott River in Stratham, New Hampshire (43°00'N, 70°52'E). The Introductory Chapter includes site maps of the Oak Knoll and Mill Brook study locations (Figures 1.5 and 1.7, respectively).

Within each salinity regime, three sites were located in sparsely vegetated areas (presumably disturbed by ice erosion or wrack burial) at high, mid, and low elevations, based observations of surrounding vegetative cover. At Mill Brook Marsh, where areas of disturbance were small and scattered, plots were covered with black plastic sheets two weeks before study start to inhibit growth of existing vegetation. Elevations (NGVD 1929) for each gradient location were determined by rod-and-level survey, and combined with NGVD-adjusted local tide gauge records to compute percent time of tidal inundation. Two replicate plots were established at each site. Within a plot, open pots were forced into the substrate and all existing aboveground biomass was removed with

clippers. PVC pipe wells, with pore-water input holes at depths 5 cm to 20 cm below the marsh surface, were installed at each site to collect interstitial water and to characterize the salinity regime.

In May, individual shoots and root-soil clumps of the study species were taken from nearby areas with saltwater flooding, and transplanted two at a time into the open pots. *Spartina patens* individuals consisted of small groups of 5-7 shoots each. Three additional plant pairs of each species were also collected, separated, dried (65° C) and weighed for estimates of initial aboveground and belowground dry weight biomass. Shoots were randomly assigned to an interspecific or intraspecific pairing (21 total combinations per plot), and transplanted into open pots with a hand-spade. Every two weeks during the growing season, plant heights were measured, non-assigned aboveground biomass was removed with clippers, and well-water salinity was measured with a hand-held refractometer. In mid-September, plants were exhumed, washed, separated, dried, and weighed for final aboveground and belowground biomass.

To determine relative species growth, ending biomass values were standardized to take into account initial plant weights at the Oak Knoll and Mill Brook sites. The standard measure was based on aboveground biomass, rather than below, because of greater potential inaccuracies in separation and measurement of live belowground biomass (Mitsch and Gosselink 1993). The experimental growth metric, relative aboveground biomass growth (RABG), was computed live standing aboveground

biomass (dry-weight) at the end of the experiment, divided by the site-specific estimate of initial live aboveground biomass (dry-weight) at the start of the experiment.

RABG results were used to produce standardized estimates of physical stress tolerance (tolerance factors) and relative competitive rankings (competition factors). These quantifiers were used to parameterize an ecosystem model of plant succession following changes in salt marsh tidal hydrology. Tolerance factors (TF) for each species at each gradient location were calculated as mean species relative growth (RABG) multiplied by survival rate, expressed as a percentage of the maximum species value observed for all nine locations. Competition factors (CF), for each interspecific combination with both participants surviving, were calculated as the overall mean of individual species RABG values versus a competitor, divided by mean species RABG at the location of the competitive pairing.

$$TF_{\text{species at location}} = [\text{RABG}_{\text{species at location}} * \text{Survival}\%_{\text{species at location}}] / TF_{\text{maximum}}$$

$$CF_{\text{species1 vs. species2}} = \text{Mean}[\text{RABG}_{\text{species1 vs. species2}} / \text{RABG}_{\text{species1 location mean}}]$$

Analysis of variance (ANOVA, alpha = .05) was used to detect statistical significance of differences between salinity regimes, and between RABG results for gradient location and competitive groupings. Data were tested for assumptions of parametric testing; RABG values were cube-root transformed to increase homogeneity of variance and normality (Helsel and Hirsch 1997, Underwood 1997); salinity data met the parametric assumptions without transformation. All graphs show untransformed values.

Statistical analyses were conducted with JMP statistical software (SAS Institute 1997). A one-way ANOVA for salinity data was run for polyhaline (HIGH), meso-polyhaline (MID), and mesohaline (LOW) salinity regimes (Student's t-test). To examine the effects of physical stress on RABG, ANOVA was run for salinity regime (SAL) and elevation (ELEV) as main effects, with two-way interactions (SAL\*ELEV), using the Tukey-Kramer HSD test) ANOVA to assess the effects of competitive grouping on RABG was run as a one-way test between interspecific (INTER) and intraspecific (INTRA) combinations (Student's t-test).

## **Results**

### **Site Characteristics**

Salinity and elevation measures showed a gradient of physical conditions, ranging from low salinity–low elevation to high salinity–high elevation locations (Table 1.1). Pooled mean salinity values (mean  $\pm$  standard error) for the low, mid, and high salinity regimes were  $14\pm 1$  ppt,  $18\pm 1$  ppt, and  $23\pm 1$  ppt, respectively, and differences between regimes were all significant (ANOVA: low-mid  $p = .039$ ; mid-high  $p = .002$ ; low-high  $p < .001$ ). Site characteristics for elevation and percent time of tidal inundation fell into discrete ranges. The low elevation locations were  $\leq 1.00$  m NGVD and flooded  $\geq 22\%$  of the time, mid locations were at 1.13-1.21 m NGVD elevation and 11-16% inundated, and high elevation locations were above 1.27 m NGVD and  $\leq 5\%$  inundated (Table 1.1).

## Survival and Growth

Survival. Plant survival was achieved if at least one individual of the assigned transplant pair was found alive in the pot at the conclusion of the experiment. Table 1.2 and Figure 1.2 show the number of surviving transplant pairs ( $n_{\text{initial}}=14$ ) for each species at each of the nine gradient locations. As expected, since study locations were mesohaline or polyhaline, the salt-tolerant species survived at a much higher overall rate than the invasive species (81% versus 46%). *Spartina patens* transplants had the best study survivorship (90%), followed by *Spartina alterniflora* (79%) and *Juncus* (75%). For the invasive species, *Typha* achieved the best survival rate (54%), followed by *Phragmites* (44%). *Lythrum* had the lowest survival of any study species (10%), suggesting poor tolerance of the saline study conditions. *Spartina alterniflora*, *Spartina patens*, and *Phragmites* had at least one surviving transplant pair at each location. Species survival appeared to differ by location (Figure 1.2), suggesting that physical stress was variable and contributed to the mortality of some transplants.

Biomass. At the end of the experiment, total aboveground and belowground live biomass (g dry weight) was measured for each transplant pair assigned to each pot. It was possible for non-transplanted individuals to become established in the pot, either through belowground rhizomes or by seeds. Species not assigned to a pot were clipped bi-weekly, but all individuals of assigned species were left alone and harvested at the end of the study. Species-specific means for gross final aboveground and belowground dry-weight biomass (live transplants only) are presented in Table 1.2 and Figure 1.3. In



addition, results were pooled across all study locations to compute mean aboveground-to-belowground ratios for each species (Table 1.2). Weights of pre-study specimens used to estimate initial biomass are presented in Table 1.3.

Gross final biomass results appeared to be highly variable across species, with *Spartina alterniflora* achieving the largest maximum value of any species for aboveground production (19 g), followed by *Typha* (16 g) and *Phragmites* (9 g). By comparison, the shorter high marsh perennials *Spartina patens* (6 g) and *Juncus* (4 g) produced much lower maximum biomass values. *Spartina alterniflora* also produced five of the highest belowground biomass measures (69 g peak), with *Typha* (33 g), *Lythrum* (29 g) and *Phragmites* (19 g) achieving other top values. In addition, biomass production appeared to be highly variable across the study gradient. *Spartina alterniflora* aboveground biomass varied ten-fold from the high salinity–high elevation location to the mid salinity–low elevation location, and other species followed similar variable patterns. These results, combined with survival data, strongly suggested that species were impacted differentially at gradient locations. In some locations, physical stress levels appeared to produce death, in others, plants survived but grew poorly, and in some cases, plants seemed unaffected by stress (Figure 1.3).

Above-to-belowground ratios identified larger live belowground structures than aboveground for all species. Ratio values ranged from 0.15 (*Lythrum*) to 0.66 (*Phragmites*), and all species except *Phragmites* had more than twice as much live belowground biomass than aboveground. In general, these results indicated the dominant

nature of belowground biomass for hardy perennial species of marshes (Mitsch and Gosselink 1993).

Relative Growth Relative aboveground biomass growth (RABG) provided a standardized experimental metric for comparative analysis of species growth. Mean RABG values for each species at each gradient location, and combined measures by elevation and salinity level are presented in Table 1.4. RABG values of 1 or greater indicated that net growth was achieved at a location, values 0-1 showed that the species survived but lost biomass over the course of the study, and a value of 0 indicated no survival at a location. Species RABG results by location showed that all species experienced significant differential growth across the gradient (Figure 1.4). Therefore, the null hypotheses of physical stress tolerance (similar growth for all locations) were rejected for the study species.

Overall RABG measures were highest for *Spartina alterniflora*, with four gradient location measures of 8 or greater, followed by *Typha* with five-fold or better growth at two locations. *Spartina patens* and *Juncus* shared similar profiles, with relative growth of 3-4 times starting aboveground biomass at their best growth locations. *Spartina alterniflora* was the only study species with net growth (RABG > 1) across all nine gradient locations, indicating the greatest range of tolerance for study conditions. *Spartina patens* and *Phragmites* were the next most successful study species, with net growth at seven out of nine locations. Among the other species, *Typha* grew at five

locations, *Juncus* at four, and *Lythrum* at only two, suggesting that overall tolerance of environmental stresses present in the experiment was relatively low for these species.

Effects of Physical Stress. ANOVA results for relative aboveground biomass growth (RABG) across gradient locations showed that a statistical model with salinity and elevation as main effects, and salinity\*elevation interactions, explained 40%-75% of the variability in species growth (Table 1.5). Whole model results were highly significant ( $p \leq .0001$ ) for all species, except *Lythrum* ( $p = .03$ ). The relative influences of main effects and interactions were variable across the study species. Elevation had the largest effect on growth for the salt tolerant species *Spartina alterniflora*, *Spartina patens*, and *Juncus*. Therefore, alternate hypotheses of physical stress tolerance for halophyte species were accepted. Salinity was the larger of the main effects for the salt-intolerant species *Phragmites*, *Lythrum*, and *Typha*, leading to acceptance of alternate hypotheses of physical stress tolerance for brackish invasive species. Overall, these results supported the ecological concept of elevation and salinity zonation for common plants of the salt marsh.

The interaction of elevation and salinity was the greatest effect for only *Phragmites* (Table 1.5). Surprisingly, *Phragmites* performed well at the high elevation of the low salinity site, but also at the low elevation of the high salinity site (Figure 1.4). In addition, the elevation and salinity interaction term was significant for all species, except for *Lythrum* which survived only at high elevations and therefore could not be tested.

Tolerance factors (TF), a combined measure of relative growth and survival for each species at each gradient location, are presented in Table 1.6. These factors are useful as predictors of species response to changes in edaphic conditions associated with altered tidal hydrology. For each species, tolerance factors identified the optimal study gradient location (TF = 1), locations with survival but reduced growth ( $0 > TF < 1$ ), and locations with no survival (TF = 0). Results showed that *Phragmites*, *Typha*, *Lythrum*, and *Juncus* performed optimally at high elevations, with *Phragmites* and *Typha* best at low salinity, *Lythrum* at mid salinity, and *Juncus* at the high salinity regime. *Spartina patens* preferred mid elevation-high salinity, and *Spartina alterniflora* did best at the low elevation-mid salinity location. For each gradient location, the tolerance factors also identified the species that best tolerated physical stress conditions there (Table 1.6, bold values). *Spartina alterniflora*, with four location values in bold, was the overall best stress tolerator in the study, followed by *Typha* (two locations).

Effects of Competition. One-way ANOVA results were run to detect differences between intraspecific and interspecific competition groups. ANOVA detected no significant differences between the groups ( $r^2/df = .01/318$ , t-test = 1.795,  $p = .07$ ). However, the interspecific group appeared to produce higher relative growth ( $3.06 \pm .26$ , mean  $\pm 1$  SE) than the intraspecific group ( $2.61 \pm .21$ ), indicating that intraspecific competition for resources may have been important.

For each interspecific combination, competition factors (CF) were computed as measures of relative competitive capability (Table 1.7). These factors were useful to

predict plant interactions when species invaded new areas of the salt marsh. Factor values less than one indicated a negative impact by the competitor, values greater than one indicated that the species did better in the presence of the competitor. For example, the *Typha*-on-*Phragmites* factor was 0.59, meaning that *Phragmites* was reduced to 59% of its average relative growth when paired against *Typha*. The *Phragmites*-on-*Typha* factor was 1.29, indicating that *Typha* achieved 129% of its average relative growth in the presence of *Phragmites*.

When related CF values were plotted as single coordinates (e.g., *Phragmites*-*Typha* [0.59, 1.29]), the nature of the competitive relationship between two species can be inferred from the plot quadrant; *lower left*: negative impacts to both species, *upper left*: positive for the competitor, negative for the target species, *upper right*: positive for both species, and *lower right*: positive for the target species, and negative for the competitor. Species plots of pair-wise competition factors are presented in Figure 1.5. Note that coordinate points are absent in cases of interspecific combinations with no mutually surviving participants (*Spartina alterniflora*-*Lythrum* and *Typha*-*Lythrum*).

General inferences of relative competitive capability can be made for each species by comparing the distribution of head-to-head coordinates. Competitors paired with *Spartina alterniflora* all experienced lower growth in its presence, except for *Phragmites*. Transplants paired with *Spartina patens* also showed mostly reduced growth. Conversely, all combinations with *Juncus* produced better than average species growth. Transplants with *Phragmites* showed lower growth for *Spartina alterniflora*, *Juncus*, and

*Lythrum*, but *Typha* was improved. *Lythrum* interspecific pairings only survived with *Spartina patens*, *Phragmites*, and *Juncus*, but these species achieved equal or better than average growth. Results for *Typha* combinations were about average for *Spartina alterniflora*, *Spartina patens*, and *Juncus*, but *Phragmites* growth was reduced in its presence.

## **Discussion**

### **Site Characteristics**

Measures of substrate salinity, elevation, and flooding regime at study locations indicated that the experiment was conducted over a diverse range of salt marsh gradient conditions. The low salinity regime for the study was saltier than anticipated (14 ppt), although the regime was still mesohaline. These results were possibly due to drier than normal rainfall during the study period. Study findings are therefore interpretable for mesohaline and polyhaline estuarine systems, and for marsh elevations from the creek-bank to the upland extent of the tide. This range of coverage appears adequate to represent a wide range of New England salt marsh habitat, including study sites of concern at Little River Marsh in North Hampton, New Hampshire (Burdick 2002) and Drakes Island Marsh in Wells, Maine (Burdick et al. 1997).

### **Effects of Physical Stress**

As noted, native species transplants *Spartina alterniflora*, *Spartina patens*, and *Juncus* survived at nearly twice the rate of invasive species *Phragmites*, *Lythrum*, and *Typha*, likely due to the effects of mesohaline and polyhaline conditions on salt-intolerant species (Beare and Zedler 1987, Hellings and Gallagher 1992, Dzierzeski 1991). However, other factors beyond the control of the experiment may have also impacted survival results, including highly localized differences in soil conditions and species differences in tolerance to physical transplant stress.

In particular, local variability in marsh soil conditions (density, drainage, and substrate salinity) can inhibit salt marsh plant growth (Bertness and Ellison 1987). For the current experiment, two locations (mid and low elevations at the high salinity site) produced surprises in survival results. At the mid elevation location, *Spartina alterniflora* transplants experienced exceptionally high mortality (>70%, Figure 1.2), despite the obvious presence of native cordgrass individuals adjacent to study plots. It was noted during study set-up that sediments in this area appeared to be very dense, and open pots sometimes reached a point of refusal when forced into the sediment. It may be that compacted soils, perhaps with high peat density, differentially prevented cordgrass transplants from establishing here (Bertness 1988). At the low elevation-high salinity location, an opposite effect was observed, as survival was unexpectedly high for *Spartina patens*, *Juncus*, and *Phragmites*. For these species, survival was higher here than at comparable elevations with lower salinities. As a further complication, this site had the highest mean salinity (24 ppt) and most flooding (32% of the time) of any study location (Table 1.1). Although only speculation, it appeared that sediments here may have been

better drained, and therefore less stressful than other low-elevation locations (possibly due to lower sulfide levels, Chambers 1997, Mendelsohn and Morris 2000).

Differential transplant stress tolerance was another potential influence on experimental results. Other salt marsh researchers have used blocks of turf with multiple plants as a basic transplant unit (see Bertness and Ellison 1987, Levine et al. 1998, Emery et al. 2001). In this experiment, plants were excavated and relocated into pots individually, in an attempt to increase competitive interactions. While care was taken to preserve roots and rhizomes, the excavation of individual plants may have damaged these organs. As a result, it may be that the physically smaller species with fine, shallow root structures (*Spartina patens* and *Juncus*) had an advantage over larger species like *Phragmites*, *Typha* and *Lythrum* which had relatively few tap-roots. Future transplant experiments with these larger plant species should probably use small turf plugs (~10 cm diameter) to minimize transplant stress.

Still, since the potential impacts of local soil conditions and transplant stress could not be quantified, it was assumed that observed results of mortality and growth were due substantially to the differences in edaphic factors measured over the course of the experiment (i.e., salinity and flooding). Survival and relative aboveground growth results in response to these physical stress factors are discussed individually for each study species.



*Spartina alterniflora*. Transplants of smooth cordgrass survived and grew across the entire study gradient, with best overall performance at the low elevation site of the mid salinity regime (Table 1.6). *Spartina alterniflora* growth decreased from low marsh to high marsh elevations (RABG of 8.51, 7.88, and 3.11 for low, mid and high elevation, respectively, Table 1.4). This result was unique among study species and suggested that tidal subsidies were critical to *Spartina alterniflora* growth. In fact, McKee and Patrick (1988) summarized cordgrass distribution patterns in eight New England salt marshes, and found that the species was typically limited to the intertidal zone between mean high water and the half-tide line. However, despite observations that *Spartina alterniflora* was not often found in the high marsh, results of this experiment showed that the species was physiologically capable of survival and growth outside of its realized niche in the low marsh, although it may be excluded from high marsh habitats by competition (Bertness and Ellison 1987, Bertness 1991b).

*Spartina alterniflora* growth was also reduced with increasing salinity (RABG of 7.34, 7.03, and 4.24 for low, mid and high salinity, respectively, Table 1.4). This finding agreed with reports of *Spartina alterniflora* growth limits in response to high salinity regimes (Nestler 1977, Webb 1983). In addition, the interaction between salinity and elevation was significant ( $p = .03$ , Table 1.5), indicating the combination of higher salinity and less flooding was a factor in cordgrass growth, possibly an indication of drought stress. Overall, the experiment showed that *Spartina alterniflora* was very well-adapted to mesohaline and polyhaline marshes in New England (Redfield 1972, Niering and Warren 1980, Nixon 1982).

*Spartina patens*. Like cordgrass, salt hay transplants survived at all gradient study locations (Figure 1.2). Top overall performance for *Spartina patens* was achieved at the mid elevation of the high salinity regime, but biomass was lost at the low elevations of the low and mid salinity regimes (Table 1.6). In addition, salt hay growth increased with reduced flooding (RABG of 1.00, 2.43, and 2.44 for low, mid and high elevation locations, respectively, Table 1.4). This finding agreed with reports of *Spartina patens* physical exclusion from the low marsh due to stresses associated with flooding (Burdick et al. 1989, Bertness 1991b). *Spartina patens* growth increased with rising salinity, (RABG of 0.82, 1.47, and 2.98 for low, mid and high salinity, respectively, Table 1.4). *Spartina patens* is known to be well-adapted to salinity stress (Bertness and Ellison 1987, Burdick et al. 1989, Bertness 1991b), but it is unclear how salinity could stimulate growth. For this experiment, it was likely that competition for light was reduced at high salinity locations, due to high mortality (Figure 1.2) and low growth (Figure 1.3) among other species. *Spartina patens*, a relatively short-stemmed species, may have benefited from increased light availability at these locations (Bertness and Ellison 1987, Bertness 1991b), resulting in a highly significant salinity and elevation interaction ( $p < .0001$ , Table 1.5). Experimental results therefore showed that *Spartina patens* was a salt-tolerant species with sensitivity to flood stress, but well-adapted to dominate the mid and high elevations of New England salt marshes (Niering and Warren 1980, Nixon 1982, Bertness 1991b).

*Juncus gerardii*. Transplants of black grass did not survive at the low elevation sites of the low and mid salinity regimes (Figure 1.2), and lost biomass at the low

elevation – high salinity site (Table 1.4). *Juncus* individuals performed best at the high elevation-high salinity gradient location (Table 1.6). Like *Spartina patens*, *Juncus* growth increased with reduced flooding (RABG of 0.97, 1.26, and 1.95 for low, mid and high elevation, respectively) and grew best at the high salinity locations (RABG of 1.36, 0.60, and 2.23 for low, mid and high salinity, respectively, Table 1.4). These results indicated that black grass was highly sensitive to flooding (Bertness and Ellison 1987), although Bertness (1991a) also found that *Juncus* may be limited by salinity stress as well (especially hypersaline conditions above 40 ppt). For this experiment, the improved performance of *Juncus* at high salinity may have been due to reduced competition. Like *Spartina patens*, *Juncus* is a relatively short-stemmed species that appears to be strongly influenced by competition for light (Bertness 1991a). This influence may have also contributed to the significance of the ANOVA interaction term for elevation and salinity ( $p = .02$ , Table 1.5).

*Phragmites australis*. *Phragmites*, along with *Spartina alterniflora* and *Spartina patens*, survived at all study locations (Figure 1.2) and showed surprising tolerance of both salinity and flood stress. As expected, *Phragmites* achieved top overall performance at the high elevation – low salinity gradient location (Table 1.6). However, *Phragmites* growth did not decrease consistently with increased salinity (RABG of 2.17, 1.18, and 1.66 for low, mid and high salinity, respectively, Table 1.4), suggesting that influences besides salinity were important determinants of growth. In fact, other researchers have found that, although salinity stress may limit *Phragmites* distribution in some locations (Hellings and Gallagher 1992, Chambers et al. 1998), the species is also known to

colonize mesohaline (Chambers et al. 1999, Meyerson et al. 2000) and polyhaline salt marshes (Warren et al. 2001, Burdick et al. 2001).

ANOVA results showed that the influence of elevation was not significant for *Phragmites*, ( $p = .26$ , Table 1.5), although growth did increase with reduced flooding (RABG of 1.56, 1.62, and 1.97 for low, mid and high elevation, respectively, Table 1.4). Apparently, there may be some sensitivity to flooding for *Phragmites*, as also suggested by Hellings and Gallagher (1992). However, Warren et al. (2001) reported that *Phragmites* was found along frequently flooded creek-banks in Connecticut, indicating tolerance of flood conditions. The survival results from this experiment also showed that *Phragmites* was capable of survival in areas of frequent flooding (Figure 1.2), although at low growth levels (Figure 1.3). ANOVA results indicated that the *Phragmites* salinity\*elevation interaction was a large effect and appeared to govern *Phragmites* response to physical stress, but additional research may be needed to identify the specific mechanisms involved. Still, overall findings from this experiment indicated that *Phragmites* was capable of survival and growth across the entire range of flood and salinity gradient conditions, suggesting that *Phragmites* is well-adapted to invade most mesohaline and polyhaline salt marshes found along the New England coast (Warren et al. 2001).

*Lythrum salicaria*. Purple loosestrife experienced the highest mortality rate of the six study species, with survival of only 10% of transplants (Figure 1.2). Survivorship was limited to high elevations only, indicating a strong intolerance to saline flood stress.

*Lythrum* is known as a pervasive invader of freshwater wetlands (Whigham et al. 1978), but tolerance to tidal flooding regimes is not well known. Growth of *Lythrum* transplants was best at the low salinity site (Figure 1.3), but survival was best at mid-salinities (Figure 1.2). Results showed that *Lythrum* growth was reduced with increasing salinity (RABG of 2.68, 1.07, and 0.62 for low, mid and high salinity, respectively, Table 1.4), indicating a strong sensitivity to salinity stress. Dzierzeski (1991) also found that purple loosestrife was intolerant of mesohaline and polyhaline marsh conditions, and very high seedling mortality was observed at salinities of 10 ppt or higher.

*Typha angustifolia*. *Typha* transplants survived at seven gradient locations, but survivorship was very low (14%) in the high salinity regimes, and appeared to diminish with increased levels of flooding (Figure 1.2). Like *Phragmites*, top overall performance for *Typha* was achieved at the low salinity - high elevation location (Table 1.6). *Typha* growth was reduced with increased salinity (RABG of 5.77, 1.16, and 0.07 for low, mid and high salinity, respectively, Table 1.4), indicating intolerance to salinity stress. Beare and Zedler (1987), studying *Typha domingensi*, found similar intolerance of salt stress, with growth diminished above 5 ppt and mortality at 25 ppt salinity.

Although *Typha* survival increased with elevation (Table 1.2), growth was best at mid elevation (RABG of 2.79, 4.22, and 2.37 for low, mid and high elevation, respectively, Table 1.4). These results, together with the significance of the salinity and elevation interaction (ANOVA,  $p = .006$ , Table 1.5), suggested that complex interactions of physical stressors, similar to the *Phragmites* response, may also be important for

*Typha*. In general, experimental results compared favorably with reports of narrow-leaf cattail distribution in mid marsh and upland regions of mesohaline and polyhaline salt marshes (Warren et al. 2001, Burdick et al. 1999).

### Competition

Generalized Competition Results of the generalized test between intraspecific and interspecific combinations indicated that relative growth was not significantly different between groups ( $p = .07$ ). The null hypothesis for interspecific competition ( $H_{0\text{competition}}$ ) therefore must be accepted. Although the test lacked significance at  $\alpha = .05$ , growth did appear to be greater for interspecific rather than intraspecific combinations. This suggested that competition for resources among evenly-matched individuals (intraspecific combinations) may have reduced experimental plant growth (Tilman 1988). In addition, it may be that not all interspecific interactions were negative. In fact, Schat (1984) found that some plant interactions, especially those with *Juncus*, provided benefits to other plant species, an effect known as facilitation. In the current experiment, competition factors for *Juncus* and possibly *Typha* suggested that facilitations had occurred (Table 1.7), and if so, these positive interactions might have also contributed to improved growth performance of the interspecific combinations.

To test for the possibility of facilitative effects, relative growth values were isolated for pairings versus each species, and compared with growth results from the remaining pool of interspecific combinations (Figure 1.6). It was expected that relative

growth would be greater for pairings with facilitative species than with other interspecific combinations. In fact, results of these comparisons showed that combinations with *Juncus* (t-test  $p=.04$ ) produced greater growth for the other species. Positive associations among salt marsh plants have been shown to be important in the colonization of disturbed areas. *Juncus* has been found to enhance growth of the marsh elder (*Iva frutescens*) by oxygenating soils, and by reducing substrate salinities through shading (Bertness and Hacker 1994, Bertness and Yeh 1994). In addition, Bertness (1991a) found that shading from spikegrass (*Distichlis spicata*) and *Spartina patens* allowed *Juncus* to colonize disturbed patches. Therefore, facilitative interactions among the study species may have contributed to increased growth of neighbors in some interspecific combinations.

Results from Figure 1.6 also indicated that negative competitive influences were present in the experiment. Growth was lower for plants paired with *Spartina alterniflora* ( $p < .001$ , Figure 1.6), but no other species produced this negative effect. These results suggested that competitive intensity varied with species pairings, or alternatively, that the single-season duration of the study may have been insufficient to produce strong competitive interactions. While the impacts of saltwater flooding on plant mortality and growth can be rapid (Sinicrope et al. 1990, Burdick et al. 1997), competition operates on longer time scales and may require multiple growing seasons to detect significant differences between competing species (Bertness and Ellison 1987, Bertness 1991a, Levine et al. 1998). Nonetheless, it is widely accepted that competition is the most important biotic stress in determining salt marsh community structure (Bertness and Ellison 1987, Pennings and Callaway 1992, Hacker and Bertness 1999, Emery et al.

2001). Results from this experiment also suggested that competition was an important, but variable, influence on plant growth.

Interactions Among Halophytes. Competition factors for each interspecific combination provided the basis for analysis of relative competitive rankings among the study species (Table 1.7 and Figure 1.5). Combinations of *Spartina alterniflora* and *Spartina patens* produced growth results about 20% lower than average for both species, suggesting that competitive interactions were negative but equal. Conversely, the *Spartina patens*-*Juncus* combination was slightly positive for both *Spartina patens* (+4%) and *Juncus* (+14%), although these results also suggested competitive parity. However, the *Spartina alterniflora*-*Juncus* pairing showed an overall competitive advantage for cordgrass, with *Juncus* reduced 30% below average and *Spartina alterniflora* improved by 20%.

These results conflicted with reports from longer term studies that found that *Spartina patens* was competitively inferior to *Juncus*, and that *Spartina alterniflora* was inferior to both species in natural salt marsh settings (Bertness and Ellison 1987, Emery et al. 2001). However, Levine et al. (1998) conducted fertilization experiments with these species and found that the *Spartina alterniflora*<*Spartina patens*<*Juncus* competitive rankings were reversed when nutrient limitations were removed. Emery et al. (2001) found similar results in an additional fertilization experiment, concluding that competitive hierarchies were nutrient-dependent among native New England salt marsh species. Further, Emery et al. determined that competition switched from belowground



to aboveground interactions when resources were abundant. Therefore, *Spartina patens* and *Juncus* may be out-competed by taller *Spartina alterniflora* individuals in high-marsh regions with elevated levels of nutrient runoff and accumulation.

It was possible that the results from the current experiment supported findings from fertilization experiments of Levine et al. (1998) and Emery et al. (2001). The experimental locations at Mill Brook Marsh bordered active agricultural fields, and, although sediment nutrients were not measured, it was likely that some level of fertilizer runoff accumulated here. The site was selected primarily to take advantage of its salinity gradient, and potential impacts of nutrient additions were not considered. It was therefore possible that increased nutrient loads at Mill Brook shifted competition from below to aboveground structures, and contributed to the unexpectedly strong competitive performance of *Spartina alterniflora*. Nutrient enrichment of coastal marshes from rivers and atmospheric deposition appears to be on the rise everywhere in the northeastern US (Jaworski et al. 1997), and increasingly elevated nutrient loads may prevail in many New England salt marshes.

Interactions Between Halophytes and Invasive Species. Even though halophytes were tolerance-advantaged in combinations with the invasive species, this experiment sought to identify relative competitive rankings under natural mesohaline and polyhaline conditions, and not to isolate the differential (and potentially confounding) effects of competition and stress tolerance. In fact, the interactions between physical stress and competition are difficult to separate and poorly understood. Pennings and Callaway

(1992) attempted to determine the relative importance of these factors, and concluded that stress and competitive impacts varied with changing edaphic conditions, but in unpredictable ways. Without salinity as a factor, Keddy et al. (1994), found that competitive rankings for twenty wetland plant species were generally consistent across different flood regimes, suggesting that competitive ability was unchanged across physical stress gradients. Whatever the case, the current experiment attempted to control for differential stress by standardizing head-to-head competitive results at each gradient location (see the Experimental Objectives section). So, despite these limitations and unknown influences, experimental competitive results for halophyte-invasive combinations are presented here to provide some level of insight into key species interactions that are not yet understood.

Competition factors for *Spartina alterniflora*-*Typha* combinations (Table 1.7 and Figure 1.5) indicated that *Spartina alterniflora* achieved slightly better than average growth, but *Typha* growth was diminished (44% lower) compared to its location averages. The relative strength of cordgrass was again somewhat surprising, although *Spartina alterniflora* has been observed to rapidly replace *Typha* when hydrology was restored to tidal-restricted salt marshes (Sinicrope et al. 1990, Burdick et al. 1997, Burdick et al. 1999). It is not known, however, to what extent these cases reflect competitive interactions, or simply *Typha* die-back and subsequent *Spartina alterniflora* colonization of bare regions. In addition, *Typha* can apparently invade *Spartina alterniflora* regions under increasingly oligohaline conditions (Beare and Zedler 1987),

suggesting that physical stress levels may accelerate or reduce relative competitive impacts between these species.

In *Spartina alterniflora-Phragmites* combinations, study results suggested that *Phragmites* was competitively superior to cordgrass. For these pairings, *Phragmites* achieved growth 18% above its averages, while *Spartina alterniflora* growth was 47% lower (the poorest relative performance for cordgrass in any combination). Tolerance factors (Table 1.6) indicated that *Phragmites* was relatively more stress tolerant than *Typha* and *Lythrum*, so if physical stress did influence competitive rankings, improved tolerance for *Phragmites* may have been important. In any case, reports of *Phragmites* invasion in cordgrass stands within mesohaline and polyhaline estuaries are common (Sinicrope et al. 1990, Meyerson et al. 2000, Burdick et al. 2001, Warren et al. 2001) and these findings supported study results of *Phragmites* as a strong head-to-head competitor versus *Spartina alterniflora*.

There were no surviving combinations of *Spartina alterniflora* and *Lythrum*. For computation of competition factors, the *Spartina alterniflora-Lythrum* combination was scored 1-0 in favor of *Spartina alterniflora*, based on a tally of survivorship in *Spartina alterniflora-Lythrum* pairings (a 13-0 advantage for *Spartina alterniflora*).

*Spartina patens*, like cordgrass, also appeared to be a good competitor against *Typha*, achieving 7% higher growth while cattail was reduced to 71% of its average. The *Spartina patens-Phragmites* combination suggested that the two species were evenly

matched. Sinicrope et al. (1990) reported that *Spartina patens* had replaced *Typha* and *Phragmites* in 3% of a Connecticut marsh 10 years after tidal hydrology was restored, also indicating that *Spartina patens* can achieve minor competitive gains against these species. In *Spartina patens*-*Lythrum* combinations, salt hay appeared to be strongly dominant, with 35% improved growth and a 66% reduction in *Lythrum*. Specific reports of *Spartina patens*-*Lythrum* interactions are not known, but remnant populations of salt hay can apparently persist in tidal-restricted salt marshes dominated by purple loosestrife (Burdick et al. 1997), suggesting possible competitive strength versus *Lythrum*.

For *Juncus*-*Phragmites* interactions, *Juncus* growth was reduced (13%), and *Phragmites* growth was substantially higher (51% greater than average). *Juncus* growth was improved slightly in the presence of *Typha* and *Lythrum* (5% and 6%, respectively), but these invasive species were improved considerably (42% and 94%) in combinations with *Juncus*. In the Connecticut marsh restoration reported by Sinicrope et al. (1990), *Juncus* had replaced *Typha* and *Phragmites* in 2% of the marsh, suggesting that *Juncus*, like *Spartina patens*, can be competitive against these species under the right edaphic conditions. Experimental results with *Juncus*, however, are most notable for the improved relative performance of the salt-intolerant species. If *Juncus* is a facilitator of plant growth under stressful marsh conditions (Figure 1.6, Hacker and Bertness 1994, Bertness and Yeh 1994), then it was reasonable to expect that associations with *Juncus* should incrementally benefit the most highly stressed species. In fact, enhanced growth for *Juncus*-invasive pairings (+51%, +94%, and +42% for *Phragmites*, *Lythrum*, and *Typha*, respectively, Table 1.7) did appear to be elevated relative to the positive response

of salt-tolerant species (+14% and +20%, for *Spartina alterniflora* and *Spartina patens*, respectively). These results added further support to the finding that *Juncus* had facilitated growth of neighboring plant species in this study.

Interactions Among Invasive Species. Interspecific combinations among invasive species suffered from high transplant mortality, and therefore competitive results were difficult to interpret or absent. There were only three surviving combinations for *Phragmites-Typha*, one for *Phragmites-Lythrum*, and none for *Typha-Lythrum* (scored 1-0 in favor of *Typha*, based on a 9-0 survivorship advantage). In *Phragmites-Typha* combinations, *Phragmites* relative growth was reduced to 59% of its average, and *Typha* was improved by 29%, suggesting the possibility of a *Typha* competitive advantage. The one surviving *Phragmites-Lythrum* combination was in favor of *Phragmites*. Other reports of relative competitive rankings among these species are unknown, although Keddy et al. (1994) reported that *Lythrum* out-competed *Typha* in freshwater habitats. In general, however, the low counts of surviving experimental combinations for these species severely limited interpretations, and specifics of competitive standings among *Phragmites*, *Typha*, and *Lythrum* remain a clear research opportunity for future studies.

### Conclusions

The experimental transplant of common salt marsh plant species across a natural gradient of salinity regimes and elevations clearly demonstrated that plant species have different tolerances of physical stress associated with saltwater flooding. Species

survival, biomass production, and relative growth all appeared to be strongly influenced by physical factors. In addition, marsh plants varied in response to physical conditions, with halophyte species growth largely controlled by flood levels, and brackish invasive species controlled by salinity regime. Complex interactions between elevation and salinity may have been important determinants of growth for some species (especially *Phragmites*). Interspecific competition also appeared to influence species growth, although these effects were statistically weaker than the impacts of physical stress, and the direction of impact varied with species. Negative competitive effects were found in combinations with *Spartina alterniflora*, but interactions with *Juncus* were facilitative. Relative competitive rankings among the species suggested that *Spartina alterniflora*, *Phragmites*, and *Spartina patens* were the strongest study competitors, although low survival of some other species limited confidence in interpreting competitive results.

Nonetheless, the experiment provided important new clues about how existing communities of salt marsh plants might respond to changes in marsh hydrologic conditions. Species-specific tolerance factors for a range of marsh gradient conditions identified favorable and unfavorable habitat sites for common plant species, and provided a qualitative basis for predicting plant community succession in response to hydrologic changes. Estimates of competitive rankings provided another useful set of metrics to gauge the longer-term effects of competition following an initial hydrologic disturbance. Together, tolerance and competition measures combined to form a valuable new dataset that improved our abilities to understand, simulate, and predict plant community response to hydrologic salt marsh restoration.

	<b>Characteristics</b>		
<b>Site Locations</b>	<b>Mean Substrate Salinity (ppt+SE)</b>	<b>Elevation NGVD(m)</b>	<b>Flooding (% time flooded)</b>
<b>Low Salinity</b>			
Low Elevation	14+2	1.00	22
Mid Elevation	14+2	1.13	13
High Elevation	15+2	1.28	5
<b>Mid Salinity</b>			
Low Elevation	16+2	1.00	22
Mid Elevation	19+2	1.16	11
High Elevation	19+2	1.41	1
<b>High Salinity</b>			
Low Elevation	24+2	0.81	32
Mid Elevation	23+2	1.21	16
High Elevation	21+2	1.51	1

Table 1.1. Physical characteristics of study gradient locations.

Site Locations	<i>Spartina alterniflora</i> Above/Below: .31±.01			<i>Spartina patens</i> Above/Below: .46±.02		
	n	Above	Below	n	Above	Below
<b>Low Salinity</b>						
Low Elevation	12	8.12±1.39	34.77±8.48	7	0.65±.12	2.83±.63
Mid Elevation	14	14.88±2.36	69.19±8.80	14	2.21±.35	7.42±1.29
High Elevation	13	14.54±2.72	45.27±6.20	14	3.46±.40	15.00±1.81
<b>Mid Salinity</b>						
Low Elevation	13	19.04±1.55	61.56±6.41	12	5.73±.48	15.72±1.64
Mid Elevation	14	13.82±1.24	60.71±6.50	14	5.78±.46	15.88±1.53
High Elevation	14	4.11±.42	14.49±1.64	14	6.02±.47	16.41±1.51
<b>High Salinity</b>						
Low Elevation	12	7.60±.81	15.86±1.94	10	2.81±.38	4.35±.45
Mid Elevation	2	2.53±1.51	8.91±5.60	14	4.25±.36	8.49±.69
High Elevation	6	2.11±.81	4.58±1.58	14	2.84±.43	4.46±.85
Site Locations	<i>Juncus gerardii</i> Above/Below: .38±.02			<i>Phragmites australis</i> Above/Below: .65±.06		
	n	Above	Below	n	Above	Below
<b>Low Salinity</b>						
Low Elevation	0			5	3.97±1.37	18.80±.66
Mid Elevation	13	0.79±.13	10.07±.64	8	5.65±.92	18.15±2.34
High Elevation	14	3.86±.73	9.94±2.04	13	8.70±.98	18.28±3.13
<b>Mid Salinity</b>						
Low Elevation	0			6	3.77±.53	7.16±1.81
Mid Elevation	12	0.65±.10	1.40±.15	7	4.86±2.45	10.94±4.02
High Elevation	14	1.40±.16	5.21±.84	6	2.35±.49	4.44±1.35
<b>High Salinity</b>						
Low Elevation	13	0.27±.05	0.76±.14	6	4.06±.81	4.42±1.20
Mid Elevation	14	0.79±.25	2.65±.52	3	2.58±.78	4.78±1.28
High Elevation	14	0.81±.18	2.11±.36	2	1.01±.99	4.94±3.21
Site Locations	<i>Lythrum salicaria</i> Above/Below: .15±.03			<i>Typha angustifolia</i> Above/Below: .33±.03		
	n	Above	Below	n	Above	Below
<b>Low Salinity</b>						
Low Elevation	0			7	8.55±1.78	22.63±3.68
Mid Elevation	0			9	16.04±4.17	32.11±8.74
High Elevation	3	4.56±.85	29.05±4.90	13	11.89±1.57	33.46±8.05
<b>Mid Salinity</b>						
Low Elevation	0			7	3.41±.68	17.63±3.29
Mid Elevation	0			12	3.82±.41	17.40±2.85
High Elevation	8	1.82±.43	13.71±3.04	14	0.90±.14	4.95±.78
<b>High Salinity</b>						
Low Elevation	0			0		
Mid Elevation	0			0		
High Elevation	2	0.29±.02	2.90±.66	6	0.16±.03	1.94±.33

Table 1.2. Surviving number of transplants (n), final aboveground and belowground biomass (mean g dry weight ± SE) and aboveground-to-belowground biomass ratio (mean ± SE) for six study species at elevation and salinity gradient locations.



Species	Low and Mid Salinity Sites			High Salinity Sites		
	n	Above	Below	n	Above	Below
<i>Spartina alterniflora</i>	3	1.73±.02	2.33±.15	3	1.29±.14	1.86±.67
<i>Spartina patens</i>	3	1.98±.08	2.35±.17	3	1.13±.13	1.58±.21
<i>Juncus gerardii</i>	3	1.75±.02	1.82±.06	3	0.29±.09	0.41±.09
<i>Phragmites australis</i>	3	3.16±.17	3.19±.42	3	1.87±.30	0.68±.16
<i>Lythrum salicaria</i>	3	1.70±.02	5.67±1.23	3	0.47±.15	1.63±.39
<i>Typha angustifolia</i>	3	2.14±.03	2.91±.29	3	2.12±.33	2.52±.44

Table 1.3. Number of pairs (n) and initial aboveground and belowground biomass (mean g dry weight ± SE) for pre-study sample specimens by salinity regime location. Aboveground values were used to derive relative aboveground biomass growth (RABG).

	Species					
Gradient Location	<i>Spartina alterniflora</i>	<i>Spartina patens</i>	<i>Juncus gerardii</i>	<i>Phragmites australis</i>	<i>Lythrum salicaria</i>	<i>Typha angustifolia</i>
<b>Low Salinity</b>						
Low Elev	8.41±1.57	0.33±0.06	0	1.26±0.43	0	3.99±0.83
Mid Elev	8.61±1.36	1.12±0.17	0.45±0.07	1.79±0.41	0	7.48±1.94
High Elev	4.70±0.80	1.75±0.20	2.21±0.42	2.76±0.53	2.68±0.50	5.54±0.73
<b>Mid Salinity</b>						
Low Elev	11.01±0.89	0.14±0.03	0	1.19±0.17	0	1.59±0.32
Mid Elev	7.99±0.72	2.41±0.28	0.37±0.06	1.54±0.78	0	1.78±0.19
High Elev	2.37±0.24	3.05±0.24	0.81±0.09	0.75±0.16	1.07±0.25	0.42±0.06
<b>High Salinity</b>						
Low Elev	5.91±0.82	1.50±0.40	0.97±0.18	2.17±0.43	0	0
Mid Elev	1.97±1.18	3.78±0.32	2.77±0.87	1.38±0.41	0	0
High Elev	1.64±0.63	2.52±0.39	2.85±0.64	0.54±0.53	0.62±0.04	0.07±0.02
<b>By Salinity</b>						
Low	7.34±0.70	0.82±0.14	1.36±0.28	2.17±0.23	2.68±0.50	5.77±0.73
Mid	7.03±0.69	1.47±0.23	0.60±0.06	1.18±0.29	1.07±0.25	1.16±0.15
High	4.24±0.70	2.98±0.23	2.23±0.39	1.66±0.32	0.62±0.04	0.07±0.02
<b>By Elevation</b>						
Low	8.51±0.74	1.00±0.24	0.97±0.18	1.56±0.22	0	2.79±0.54
Mid	7.88±0.77	2.43±0.23	1.26±0.36	1.62±0.32	0	4.22±1.03
High	3.11±0.40	2.44±0.19	1.95±0.28	1.97±0.30	1.37±0.28	2.37±0.53

Table 1.4. Species mean relative aboveground biomass growth (RABG) at each gradient location, and for salinity and elevation treatments (mean ± SE).

ANOVA	Species					
	<i>Spartina alterniflora</i>	<i>Spartina patens</i>	<i>Juncus gerardii</i>	<i>Phragmites australis</i>	<i>Lythrum salicaria</i>	<i>Typha angustifolia</i>
Whole Model						
R <sup>2</sup> /df	.52/99	.75/112	.40/93	.40/55	.49/12	.74/67
F ratio	12.4	1.4	9.8	3.9	4.9	29.6
p value	<.0001	<.0001	<.0001	.0001	.03	<.0001
Salinity						
Df	2	2	0	2	2	1
F ratio	11.8	50.7	-	4.0	4.9	79.6
p value	<.0001	<.0001	-	.03	.03	<.0001
Elevation						
Df	2	2	1	2	0	0
F ratio	30.8	64.6	15.9	1.4	-	-
p value	<.0001	<.0001	.0001	.26	-	-
Salinity*elevation						
Df	4	4	2	4	0	2
F ratio	2.8	21.0	4.0	4.8	-	5.6
p value	.03	<.0001	.02	0.002	-	0.006

Table 1.5. Results from two-way ANOVA comparing mean relative aboveground biomass growth (RABG) of study species by salinity, elevation, and salinity\*elevation interaction.

Gradient Location	Species					
	<i>Spartina alterniflora</i>	<i>Spartina patens</i>	<i>Juncus gerardii</i>	<i>Phragmites australis</i>	<i>Lythrum salicaria</i>	<i>Typha angustifolia</i>
Low Salinity						
Low Elevation	<b>0.76</b>	0.04	0.00	0.18	0.00	0.39
Mid Elevation	0.84	0.30	0.15	0.40	0.00	<b>0.93</b>
High Elevation	0.39	0.47	0.79	<b>1.00</b>	0.94	<b>1.00</b>
Mid Salinity						
Low Elevation	<b>1.00</b>	0.72	0.00	0.20	0.00	0.15
Mid Elevation	<b>0.78</b>	0.77	0.11	0.30	0.00	0.30
High Elevation	0.23	0.81	0.29	0.13	<b>1.00</b>	0.08
High Salinity						
Low Elevation	<b>0.49</b>	0.47	0.32	0.36	0.00	0.00
Mid Elevation	0.03	<b>1.00</b>	0.98	0.12	0.00	0.00
High Elevation	0.07	0.67	<b>1.00</b>	0.03	0.14	0.01

Table 1.6. Species tolerance factors (TF) of growth and survival for study gradient locations (bold values identify best species performance for each gradient location).

Competitor	Species					
	<i>Spartina alterniflora</i>	<i>Spartina patens</i>	<i>Juncus gerardii</i>	<i>Phragmites australis</i>	<i>Lythrum salicaria</i>	<i>Typha angustifolia</i>
<i>Spartina alterniflora</i>	—	0.81 (14)	1.20 (14)	0.53 (4)	0.00 (0)	1.08 (9)
<i>Spartina patens</i>	0.80 (14)	—	1.14 (14)	1.02 (6)	1.36 (2)	1.07 (7)
<i>Juncus gerardii</i>	0.70 (11)	1.04 (14)	—	0.87 (7)	1.06 (2)	1.05 (5)
<i>Phragmites australis</i>	1.18 (4)	1.13 (6)	1.51 (7)	—	1.96 (1)	0.59 (3)
<i>Lythrum salicaria</i>	1.00 (0)	0.34 (2)	1.94 (2)	0.63 (1)	—	1.00 (0)
<i>Typha angustifolia</i>	0.56 (8)	0.71 (8)	1.42 (6)	1.29 (3)	0.00 (0)	—

Table 1.7. Competition factors (CF) for interspecific combinations (number of pairings with both participants surviving in parentheses). Row values show the percent of average growth achieved for the species; column values are for the competitor.

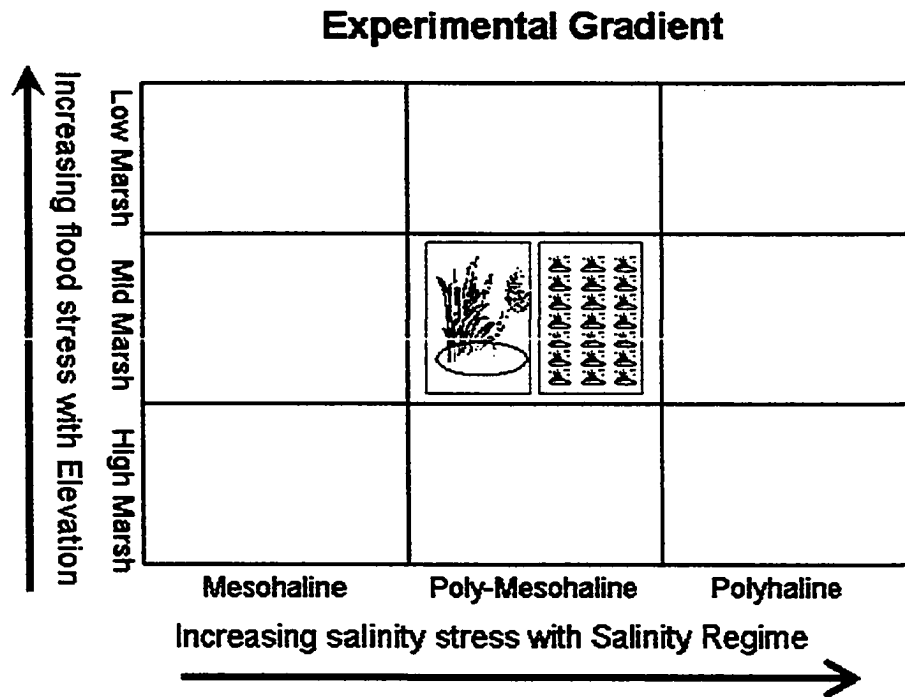


Figure 1.1. Schematic diagram of experimental elevation and salinity gradient locations. Salinity locations were Oak Knoll Marsh for polyhaline (>18 ppt), and Mill Brook Marsh for poly-mesohaline (~18 ppt) and mesohaline (5-18 ppt) regimes. Elevation sites within were in low marsh (tidally flooded > 20% of time), mid marsh (flooded 10–15% of the time) and high marsh (flooded  $\leq$  5% of time). At each gradient location, shoot pairs of six plant species were transplanted into open pot units and assigned to interspecific or intraspecific combinations (twenty-one units per plot with two replicates).

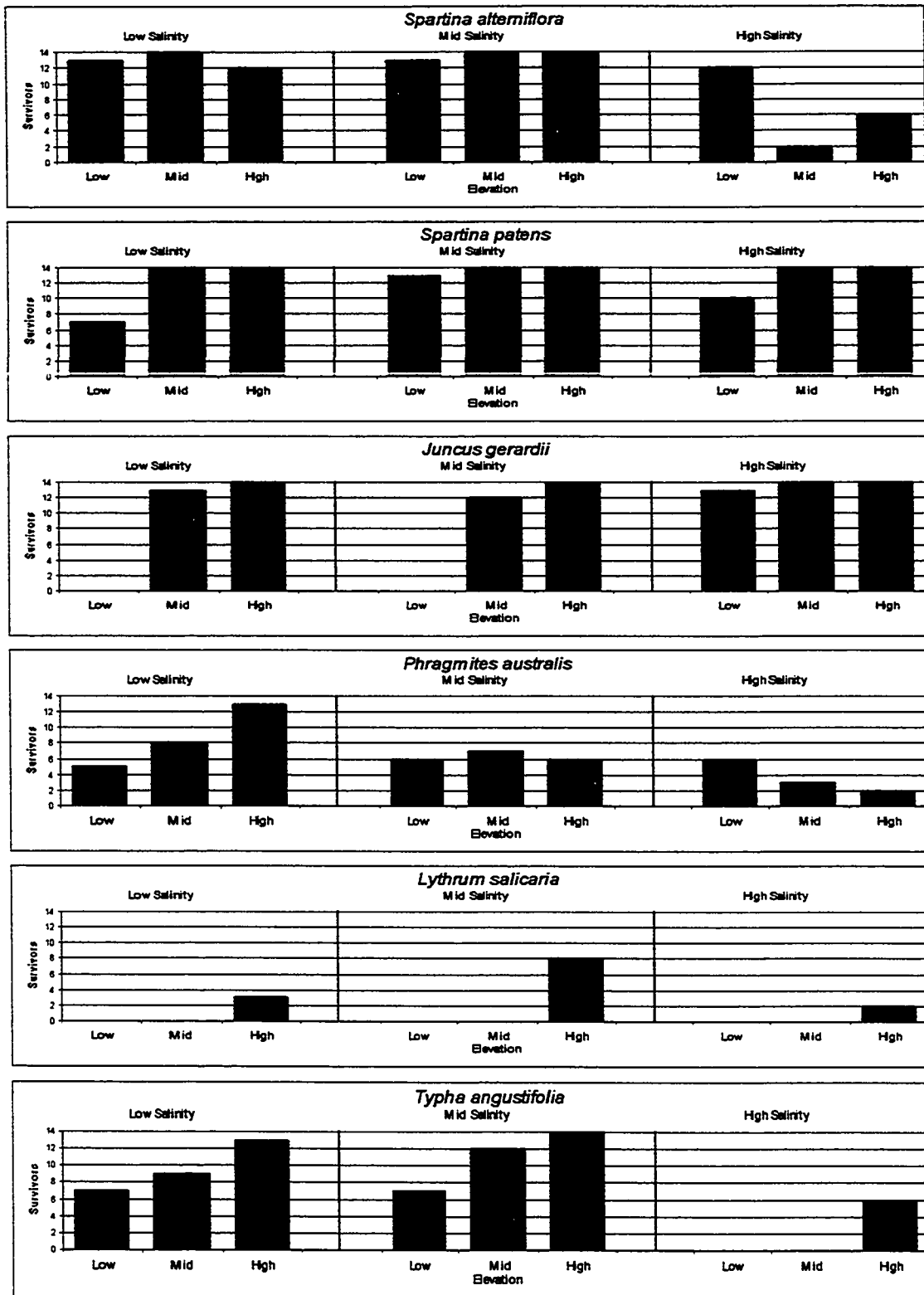


Figure 1.2. Transplant pairs surviving the experiment for six plant species at nine gradient locations (out of 14 initial pairs).

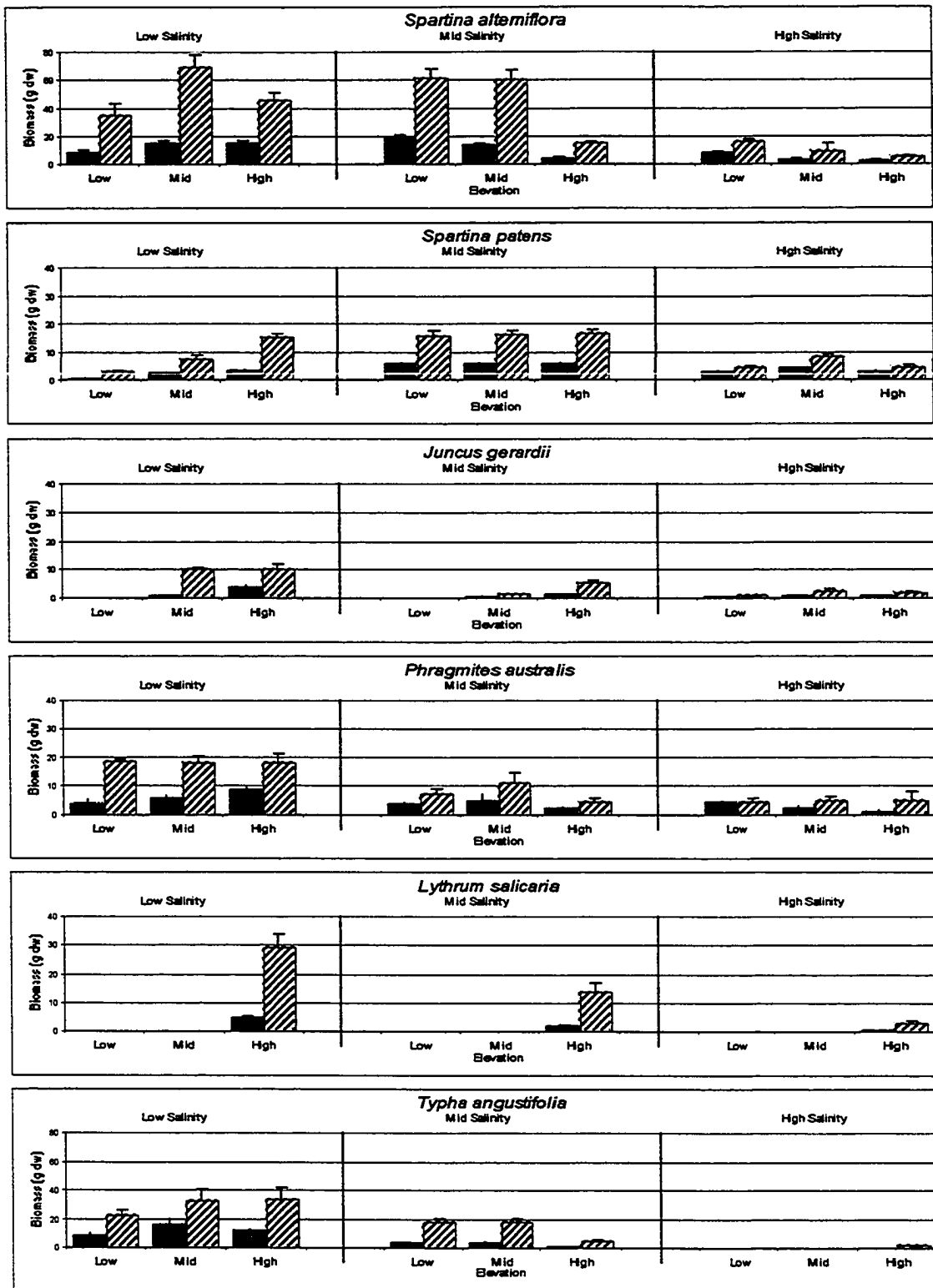


Figure 1.3. Species final aboveground (solid) and belowground (hashed) biomass (mean + SE). Vertical-axis scale 0-80 g for *Spartina alterniflora* and *Typha*, 0-40 g for others.



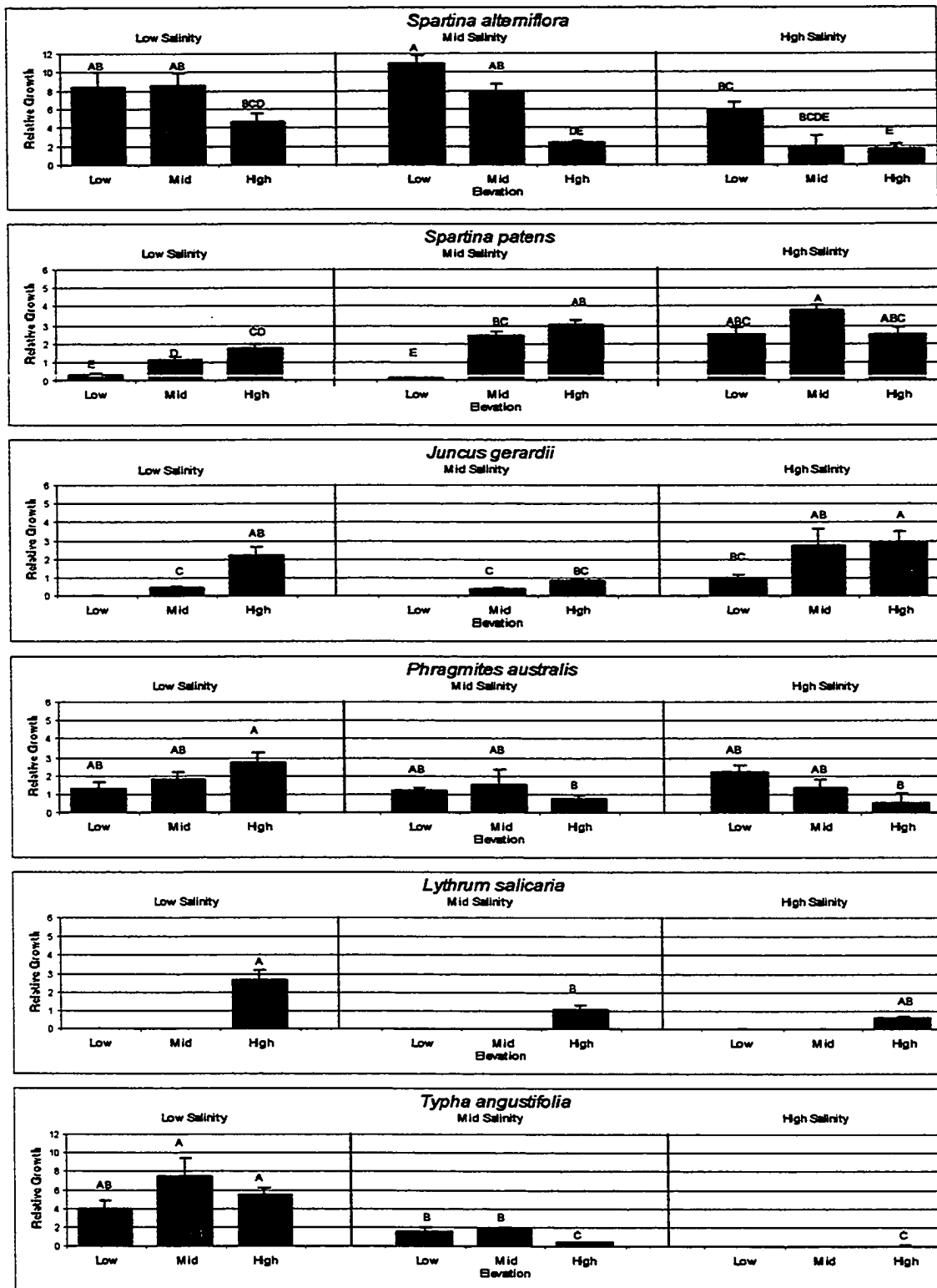


Figure 1.4. Relative aboveground biomass growth (RABG) for species at nine gradient locations (mean + SE). Vertical axis scale 0-12 for *Spartina alterniflora* and *Typha*, 0-6 for others. Bar labels in common were not significantly different ( $p > .05$ ).

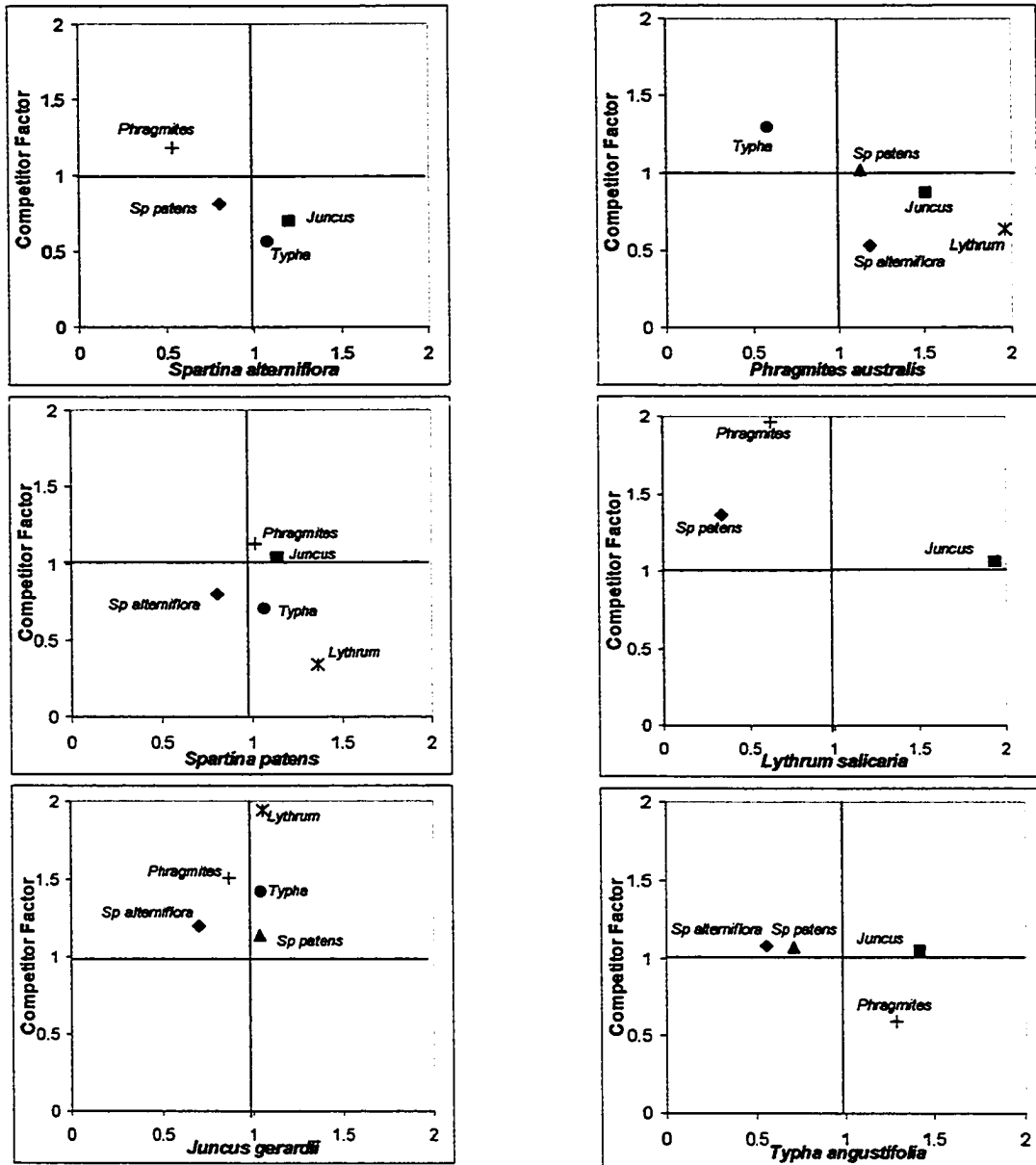


Figure 1.5. Species plots of paired competition factors for interspecific combinations with both participants surviving (x-axis for species; y-axis for labeled competitors).

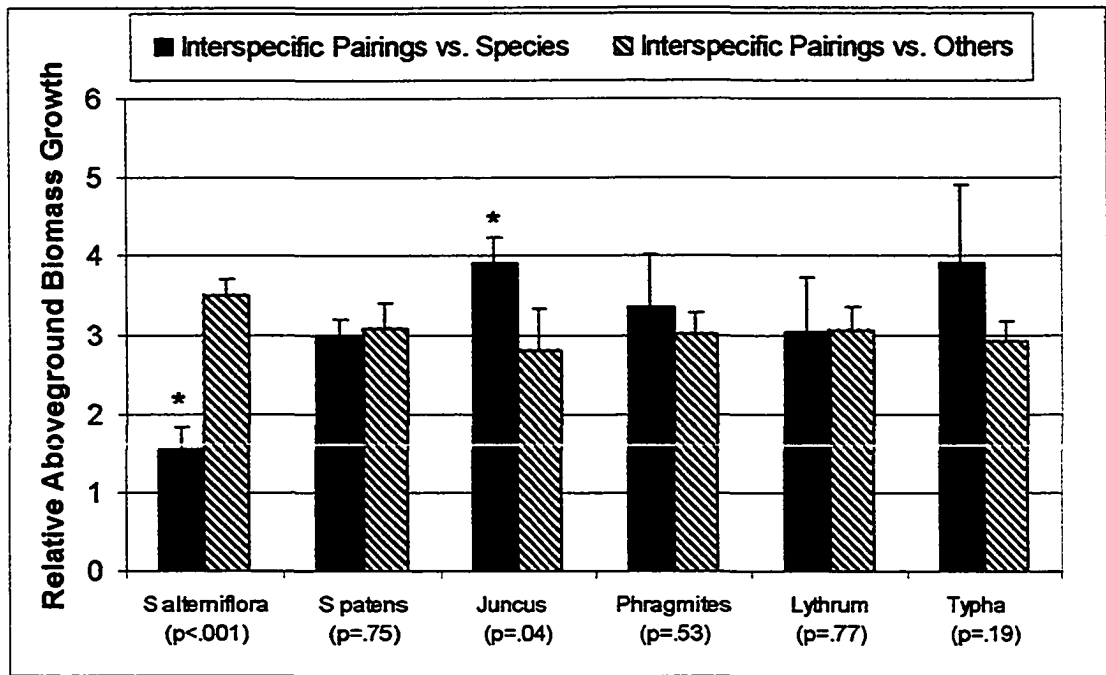


Figure 1.6. Relative growth (mean + SE) for interspecific pairings versus species and versus all others (results from t-test for differences, \* indicates significance at  $\alpha = .05$ ).

## **CHAPTER II**

# **A BIOMASS PRODUCTION MODEL FOR COMMON PLANT SPECIES OF NEW ENGLAND SALT MARSHES**

### **Introduction**

Salt marshes are extensively studied ecosystems that have intrigued researchers since at least the late 1950s. Recently, our understanding of complex salt marsh ecosystem processes has been enhanced by computer-based simulation models. In an effort to build upon this knowledge, the current project synthesizes key elements of existing computer models into a single ecosystem model to predict plant community response to hydrologic restoration of tidal-restricted salt marshes (see Introductory Chapter). The ecosystem model simulates salt marsh processes associated with tidal hydrology, coastal geology, plant biomass production, and plant community succession.

Aboveground and belowground biomass production by salt marsh plants, a critically important salt marsh function, is the focus of this chapter. Biomass from marsh

plants supplies the food web, and largely influences competitive outcomes (Tilman 1988). Furthermore, plant biomass contributes to sediment formation through decomposition (Hatton et al. 1983, Gosselink and Hatton 1984), and by trapping suspended solids in the water column (Stumpf 1983). Sediment formation is of particular interest to the current project, since sediment-building processes directly influence changes in relative marsh elevation and tidal regime. Therefore, a simulation model of annual plant biomass production is an important input component of an ecosystem model that predicts marsh response to changes in tidal hydrologic conditions.

A number of computer models for plant biomass production have already been published. CENTURY (Parton et al. 1993) is a well-known plant production model based on grassland ecology, developed to model soil-plant dynamics for homogeneous terrain-based ecosystems at regional spatial coverage and at long-term temporal scales. FOREST-BGC (Running and Coughlan 1988) is a carbon-allocation model, driven primarily by forest canopy leaf-area index estimates, that considers the impact of water and nutrient limitations on plant production. TEM (Raich et al. 1991, Melillo et al. 1993, McGuire et al. 1997) provides process-based estimates of production and carbon allocation in conjunction with water-balance dynamics. PnET (Aber et al. 1995, Aber et al. 1996) is a process-based terrestrial model that estimates water, carbon, and nitrogen ecosystem balances (gross and net) at a wide range of spatial scales, ranging from forest stands and watersheds, to entire geographic regions. These models are similar in their highly aggregate lumped-parameter approach to water balance dynamics and ecosystem production estimates, and, while this approach is necessary for scaled-up global

scenarios, it is not well suited to the very fine, species-level response scales required for the current project.

The plant production unit model selected for this project is the General Ecosystem Model (GEM) developed by Fitz et al. (1996). GEM is best known as a wetland plant community model, with uses that include a Louisiana cypress swamp (Fitz et al. 1996), the Florida Everglades (Voinov et al. 1998), a Maryland coastal wetland (Voinov et al. 1999), and New Hampshire eelgrass beds (Short et al. 1998). The model has been shown to support spatial implementation (i.e., the exchange of key constituent values between grid cells), and to efficiently process grids with 1000+ cells (Maxwell and Costanza 1997). GEM is also well documented, at least to the extent that model assumptions (equations, relationships and parameters) are explicitly and clearly stated. The original publication (Fitz et al. 1996) described a limited sensitivity analysis and validation of the model, based on comparisons of modeled plant production relative to measured results. GEM also includes component modules for subsurface and nutrient flux processing, but these factors are outside the scope of the current project.

For salt marsh use, this implementation of GEM followed closely the approach taken by Short et al. (1998) for estimation of eelgrass biomass production. An overall rate of gross photosynthesis was specified, and net production was estimated as a function of respiration, mortality, consumption, and physical growth limits (temperature, and in the case of eelgrass, light). To parameterize GEM for salt marsh plants, the rates

of gross photosynthesis, mortality, and consumption were determined by literature review and by model calibration.

Salt marsh plant respiration rates were based on a model developed by Dai and Wiegert (1996) to predict *Spartina alterniflora* biomass production. The Dai and Wiegert model relied on an intensive one-year study of short and tall form salt marsh cordgrass in Georgia to provide specific measurements of *Spartina* above and belowground morphological characteristics. Gross photosynthesis was estimated as a function of photosynthetically active radiation (PAR), leaf surface area, leaf nitrogen content, and air temperature. By comparing gross photosynthesis with measured biomass at monthly intervals, Dai and Wiegert determined the specific rates of respiration for aboveground and belowground cordgrass structures, including growth and maintenance respiration.

For the current project, plant species other than *Spartina alterniflora* also needed to be considered. In New England salt marshes with tidal restrictions, native perennial species such as cordgrass, salt hay (*Spartina patens*), and black grass (*Juncus gerardii*) are often replaced by invasive species like common reed (*Phragmites australis*), narrow-leaf cattail (*Typha angustifolia*), and purple loosestrife (*Lythrum salicaria*) (Burdick et al. 1997). Since these six common species are used to simulate typical New England marsh plant communities, the biomass model is needed to provide estimates of aboveground and belowground plant biomass for each species. To accomplish this, species values of peak aboveground biomass (from literature) and above-to-belowground ratios (from the field

experiment, Chapter I) were used as target parameters to calibrate biomass production results. The calibration process produced species-specific rates for gross photosynthesis and above-to-belowground carbon translocation, and annual biomass curves for aboveground and belowground structures.

## **Methods**

**Approach.** An existing software implementation of the GEM model for eelgrass biomass production (Short et al. 1998) was acquired in the Stella graphic programming format (High Performance Systems, Inc. Hanover, New Hampshire, USA) and re-written into the Microsoft (MS) Visual FoxPro procedural language (Microsoft Corporation, Redmond, Washington, USA). Development of the biomass production model followed this general approach: First, results from the re-written eelgrass model were compared with original model results to ensure that the translation process was complete and accurate. Then, the model was re-specified with salt marsh parameter values and, for each of six salt marsh species, calibrated with iterative model runs until simulated peak above and belowground biomass results agreed with target values. Lastly, the model was subject to a formal sensitivity analysis to assess relative importance of each model parameter.

**Model Structure.** The model used a weekly time-step and operated on a calendar year basis to produce running weekly estimates of plant production. The model generated aboveground and belowground biomass estimates for a hypothetical, single



square meter plot, composed of up to six different common marsh species. Species composition of the cell was specified for *Spartina alterniflora* (*cover\_spa*), *Spartina patens* (*cover\_spp*), *Juncus gerardii* (*cover\_jun*), *Phragmites australis* (*cover\_phr*), *Lythrum salicaria* (*cover\_lyt*), and *Typha angustifolia* (*cover\_typ*). Cover values represented the relative portion of the plot occupied by each species, with the totals of all six species adding up to one. For example, if vegetated cover of a plot was sparse but composed only of *Typha* individuals, *cover\_typ* would equal one and values for the other five species values would be zero. If *Typha* and *Phragmites* were the only species present in a plot and each accounted for an equal area of cover, then *cover\_typ* and *cover\_phr* would both equal 0.5 and the other species values would be zero.

Initial Biomass. Initial aboveground and belowground biomass values were specified for each of the six plant species ( $\text{kgCm}^{-2}$ ). Since the model started all runs in winter (Jan 01), the initial aboveground biomass (*ic\_phb*) value was minimal ( $0.001 \text{ kgCm}^{-2}$ ) at the beginning of each model run. Species-specific initial belowground biomass values (*ic\_nphb\_spp*) were based on the assumption that belowground biomass in early winter was roughly equal to belowground biomass at the end of the growing season. This has been shown to be the case for *Spartina alterniflora* and *Spartina patens* (Gallagher 1983, Gallagher and Howarth 1987), and other perennial marsh species were assumed to follow a similar pattern. Belowground biomass estimates for each species were based on peak aboveground species values from selected published reports, with emphasis on New England mesohaline and polyhaline marshes (Table 2.1). Initial belowground estimates (Table 2.2) were computed from the species ratio of above-to-

belowground biomass (Chapter I), and converted from biomass to carbon with a 40% g-carbon to g-biomass ratio (Gallagher and Plumley 1979). Total initial belowground biomass for the hypothetical marsh plot (*ic\_nphb*) was determined by summing the multiples of species cover values by initial belowground biomass for all six species.

Aboveground Production. Aboveground production was determined by growth, respiration, and mortality rates, with all rates in units of  $\text{kgCm}^{-2}\text{wk}^{-1}$ . Species-specific gross photosynthesis rates (*ph\_mac\_gpp\_spp*) were derived from model calibration and listed in Table 2.2 (see the Species Calibration Points section for details). Photosynthesis was only allowed from early April to mid-November (weeks 14–47) to simulate an average New England growing season. Total gross production for the plot (*ph\_mac\_gpp*) was determined by summing the multiples of species cover values by gross photosynthesis rates for the six species. Total gross production (*gpp\_total*) was the annual total of accumulated weekly gross production. Gross production was reduced by 28% for total aboveground respiration (*phbio\_resp\_rate*), based on the Dai and Wiegert (1996) model for *Spartina alterniflora*, and applied to all six species. It was assumed that respiratory costs associated with seed production were bundled into this aboveground respiration rate. Litterfall (*litterfall*) was triggered on week 42 to simulate the first hard frost in late October. Aboveground biomass (*mac\_ph\_biomass*) was removed by an increasing percentage (4%, 12%, and 24%, respectively) for three weeks following week 42, and then by 40% until year-end to deplete nearly all aboveground biomass. The aboveground mortality rate (*phbio\_mortality*) was 1%, reflecting physical stress due to

drought, salinity, and salt water flooding (Bertness and Ellison 1987), storm-induced wrack burial (Hartman 1988), and herbivory (Teal 1962).

Carbon Translocation To Shoots. Belowground carbon reserves were transferred to emerging shoots and leaves early in the growing season, and replenished later in the year (Gallagher 1983, Hopkinson and Schubauer 1984, Gallagher and Howarth 1987, Lana et al. 1991). The model used exponential functions (Equations 1 and 2), based on Short et al. (1998), to provide a ramp-up of percent carbon reserve use (*translocation*) by aboveground structures in the first six weeks of the growing season (weeks 14-20), followed by reduced use for an additional six weeks (weeks 21-27). The functions were bounded from 0 - 99.5%, with  $x = \text{week} * (52/12)$  to provide point estimates of percent carbon reserves available for aboveground use:

$$C \text{ from reserves}_{\text{weeks 14-20}} = (3.04x^3 - 15.95x^2 + 26.01x - 11.90)/100 \quad (1)$$

$$C \text{ from reserves}_{\text{weeks 21-27}} = (-0.19x^5 + 4.91x^4 - 48.31x^3 + 226.16x^2 - 500.64x + 417.25)/100 \quad (2)$$

Since gross photosynthesis rates and above/below biomass ratios varied by species, model amounts of carbon reserves used by aboveground structures were adjusted by species-specific calibration factors (see Species Calibration Points). Reserve use calibration factors (*trans\_spp*) were multiplied by species cover values to produce a composite reserve use rate (*transrate*). The composite rate was multiplied by total belowground biomass (*mac\_nophh\_biomass*) and percent available reserves to determine weekly amounts of carbon allocated from reserves.

Belowground Production. To replenish reserves, belowground structures received the results of net photosynthesis (gross production less aboveground respiration) during the later stages of the growing season, as gross belowground production (*nph\_mac\_gpp*) (Gallagher 1983, Hopkinson and Schubauer 1984, Gallagher and Howarth 1987, Lana et al. 1991). For three weeks prior to the week 28 seasonal mid-point, an increasing percentage of net photosynthesis (10%, 30%, and 60%, respectively) was moved into reserves. From week 28 until the end of the growing season, all net photosynthesis was stored in belowground structures. Gross belowground production was reduced by belowground respiration for growth (*nphbio\_resp\_rate\_grow*) and maintenance (*nphbio\_resp\_rate\_maint*), at 37% and 1.5% of gross belowground production, respectively, based on Dai and Wiegert (1996). Belowground maintenance respiration was reduced at cold water temperatures. Functions to estimate water temperature (*h2o\_temp*, Eq. 3) and respiration reduction (*mac\_temp\_resp\_lim*, Eq. 4) were based on Short et al. (1998). Total belowground respiration (*nphbio\_resp*) was computed as growth respiration plus maintenance respiration. Belowground mortality (*nphbio\_mort\_rate*) was estimated at 0.5% (based on Garver et al. 1988 for *Typha angustifolia*) to simulate over-wintering mortality of roots and rhizomes.

$$\text{Water Temperature}_{\text{week}} = 15 - 15(\text{COS}((2\pi) * (\text{week} * 7 - 31) / 365)) \quad (3)$$

$$\text{Temperature Response} = (0.0107 * \text{EXP}(0.047 * \text{Water Temperature})) \quad (4)$$

Annual Net Production and Biomass. Total net production (*npp\_total*) was the annual total of accumulated weekly gross production less above and belowground

respiration and mortality. Aboveground biomass (*mac\_ph\_biomass*) was computed as starting aboveground biomass plus gross production and reserve use, less aboveground respiration, litterfall, and mortality. Belowground biomass (*mac\_noph\_biomass*) was calculated as starting belowground biomass plus gross belowground production, less translocation to shoots, belowground respiration and mortality.

Species Calibration Points. Calibration exercises were performed to derive species-specific gross photosynthetic and reserve use rates. For each species, cover values were set to one, initial belowground biomass values were set to the species-specific value (Table 2.2), and the model was run for one year. The resulting annual biomass curves were fit to target values (Table 2.1) for peak aboveground biomass and peak belowground biomass by iterative adjustment of species gross photosynthesis rate (*ph\_mac\_gpp\_spp*) and belowground reserve use rate (*trans\_spp*). Table 2.2 lists results from the calibration exercise. Model calibration was considered complete when both above and belowground simulated peaks were within 5% of the target values for each species.

Sensitivity Analysis. The sensitivity of biomass results to changes in model parameters was determined through a systematic sensitivity analysis. For purposes of this analysis, all species-specific parameters were set to *Spartina alterniflora* values, and accumulated biomass change (net primary production less total mortality) was used as the comparative metric. Non species-specific parameters were varied by  $\pm 5\%$  and  $\pm 20\%$ , and model results were compared with baseline conditions (based on original parameter

values) to assess relative sensitivity of each parameter. Relative sensitivity was calculated as the percent change in accumulated biomass divided by the percent change (either 5% or 20%) in the model parameter (Eq. 5). Higher relative sensitivity values indicated an increased sensitivity to a model parameter. Since simulated biomass production varied over time (for multi-year runs, ending belowground biomass values were not always exactly equal to Table 2.2 initial values), the sensitivity analysis was run for one and twenty year durations to ensure model consistency and long-term stability.

$$\text{Relative sensitivity}_{\text{parameter}} = \% \text{ Change}_{\text{accumulated biomass}} / \% \text{ Change}_{\text{parameter}} \quad (5)$$

## Results and Discussion

Biomass Production. Peak aboveground and belowground biomass model estimates for native and invasive salt marsh species are listed in Table 2.3. Calibration differences between model estimates and target biomass values ranged from 0% for *Juncus* to 5% for *Lythrum*, and the average difference was 2.5%, indicating acceptable overall calibration performance. Model results followed the same patterns of relative biomass rankings as the target values, with largest aboveground biomass estimates for *Typha*, *Phragmites* and *Spartina alterniflora*, and largest belowground estimates for *Lythrum*, *Typha*, and *Spartina alterniflora*. Annual net production ranged from 3125 g/m<sup>2</sup> for *Typha* to 1950 g/m<sup>2</sup> for *Spartina patens* and *Juncus*. Annual turnover rates (net

production/peak aboveground biomass) were estimated between 1.4 (*Juncus*) and 2.1 (*Lythrum*).

Published reports of salt marsh net primary productivity vary widely, making comparisons difficult. Divergent estimates, even for the same species in the same geographic region, can be attributable to differences in local edaphic conditions (salt water flood regime and substrate porosity), plant genotype (short or tall form *Spartina alterniflora*), and the method of estimation (Mitsch and Gosselink 1993). In addition, inter-annual variability in biomass production for salt marsh species has been linked to year-to-year climatic conditions, especially rainfall (Gross et al. 1990). As a result, estimated annual net production for *Spartina alterniflora* in New England has been reported across a wide range of values, from 1600 g m<sup>-2</sup> yr<sup>-1</sup> (Valiela et al. 1976) to 4200 g m<sup>-2</sup> yr<sup>-1</sup> (Ellison et al. 1986). Cordgrass annual turnover rates have been measured at 1.0 – 3.3 (Kaswadji et al. 1990). Model estimates for *Spartina alterniflora*, at 2800 g m<sup>-2</sup> yr<sup>-1</sup> net production, and a 1.8 annual turnover rate, are therefore within the range of values from published sources.

When considering all six species, confidence in model results comes primarily from the calibration fit to observed peak aboveground measures. Aerial biomass is easily measured and commonly reported for most common species. Live belowground biomass, however, is difficult to separate from sediments and dead material (Dai and Wiegert 1996), and relatively few, if any, estimates of total plant production are reported for the majority of salt marsh species. Model results, therefore, are best interpreted in

relative terms. The predicted biomass production rankings for the six species are *Typha* > *Spartina alterniflora* > *Phragmites* > *Lythrum* > *Spartina patens* = *Juncus*, but the differences between highest and lowest production values are only a modest 60%. Even at the low end of the scale, native salt marsh species produce about 2 kg of plant material per square meter, a production rate that ranks salt marsh habitat among the most productive in the world (Mitsch and Gosselink 1993). Still, relative production differences are important for predictions of sediment dynamics. A monotypic marsh plant community dominated by *Typha* or *Phragmites* produces more biomass and contributes more to peat formation than a mix of native halophytic species. Over long time periods, these invasive species may build sediments faster than local sea level rise (Windham and Lathrop 1999), leading to terrestrialization of coastal wetlands and degradation of habitat for plant species dependent upon tidal subsidies for survival.

The biomass model was also used to generate annual curves of above and belowground biomass production for each species. Plots of weekly biomass estimates for native salt marsh species and brackish invasive species are presented as Figures 2.1 and 2.2, respectively. A review of these plots showed that species annual biomass curves produced identical patterns of peak aerial biomass in week 27 and peak belowground biomass in week 47, an artifact of model algorithms for the timing of carbon translocation. Since these curves were based on observations of carbon translocation patterns for cordgrass (Gallagher 1983, Hopkinson and Schubauer 1984, Gallagher and Howarth 1987, Lana et al. 1991), it was possible that seasonal biomass production patterns may differ among the six species. In fact, it is known that *Juncus* reaches peak



aerial biomass about two-three weeks earlier in the growing season than other salt marsh species, a factor thought to contribute to the species relative strong competitive ranking versus *Spartina* spp. (Bertness and Ellison 1987). The extent to which other marsh species diverge from the modeled annual pattern is not known, although it appears that *Typha* (Garver et al. 1988) and *Phragmites* (Bart and Hartman 2000) may achieve maximum aerial biomass somewhat later than in the growing season than the model suggests. In any case, total estimates of aboveground and belowground biomass should be largely unaffected by differences in seasonal timing, and these values were the critical model outputs for subsequent ecosystem simulation use.

Sensitivity Analysis. The relative sensitivity of model parameters for model runs of 1 and 20 years are presented in Table 2.4. Since relative sensitivity was calculated as the percent difference in biomass change divided by percent difference in the parameter, this analysis indicated low overall model sensitivity to any one parameter (all values < 1). In addition, the analysis suggested a fairly consistent balance among model parameters (values ranged from 0.01-0.86). On a relative scale, the model was most sensitive to belowground mortality, aboveground respiration, belowground growth respiration, and above ground mortality, but less sensitive to changes in belowground maintenance respiration and translocation reserve use rates. General model sensitivity to mortality was not surprising, since mortality rates resulted in direct removal of biomass from the system. Except for translocation, parameter sensitivities were diminished from one year to twenty year model runs, presumably due to movement toward a model equilibrium state.

## **Conclusions**

Production of aboveground and belowground plant material is an important contributing factor to the self-maintenance capacity of salt marshes. Since plant species produce biomass at differential rates, estimates of species-specific annual biomass production are critical inputs to a fine-scale salt marsh ecosystem model that considers long-term elevation change. Results presented here showed that a computer model, calibrated to peak aboveground biomass, produced estimates of above and belowground biomass for six common salt marsh species in close agreement with observed values. Annual biomass production curves for each species, while based on *Spartina alterniflora* measures, appeared to reflect general patterns of observed annual growth for most salt marsh species. Model results of species-specific biomass estimates provide the basis for modeling organic material inputs to marsh sediment development. The formation of marsh sediments, and other aspects of marsh elevation change, are discussed and modeled in Chapter III.

Species	Site (salinity regime) and reference	Peak aerial crop (g m <sup>-2</sup> )	Target AG (g m <sup>-2</sup> )	Above Below Ratio	Target BG (g m <sup>-2</sup> )
<i>Spartina alterniflora</i>	Massachusetts (polyhaline) Valiela et al. (1976)	1300			
	Massachusetts (polyhaline) Gallagher and Howarth (1987)	1800	1550	0.314	4900
<i>Spartina patens</i>	Rhode Island (polyhaline) Bertness and Ellison (1987)	1300			
	Louisiana (mesohaline) Burdick et al. (1989)	1200	1250	0.470	2650
<i>Juncus gerardii</i>	Rhode Island (polyhaline) Bertness and Ellison (1987)	1350			
	Rhode Island (polyhaline) Bertness (1991b)	850	1100	0.377	2900
<i>Phragmites australis</i>	Connecticut (mesohaline) Warren et al. (2001)	1300			
	New Jersey (oligohaline) Windham and Lathrop (1999)	1900	1600	0.655	2400
<i>Lythrum salicaria</i>	New Hampshire (mesohaline) Dzierzeski (1991)	400			
	Delaware (oligohaline) Whigham et al. (1978)	1600	1000	0.152	6600
<i>Typha angustifolia</i>	Connecticut (mesohaline) Warren et al. (2001)	1000			
	Texas (oligohaline) Hill (1987)	2600	1800	0.331	5400

Table 2.1. Selected peak live aboveground (AG) standing crop estimates for six common salt marsh plant species chosen to reflect conditions in mid and high salinity New England salt marshes. Average reported values provided target values for calibration of the biomass model. Above-below ratios (Chapter I) were used to determine peak belowground (BG) target value.

<b>Species</b>	<b>Initial Belowground Biomass (kgCm<sup>-2</sup>)</b>	<b>Gross Photosynthesis (kgCm<sup>-2</sup>wk<sup>-1</sup>)</b>	<b>Belowground Reserve Factor (kgCm<sup>-2</sup>wk<sup>-1</sup>)</b>
<i>Spartina alterniflora</i>	1.96	0.061	0.0050
<i>Spartina patens</i>	1.02	0.042	0.0150
<i>Juncus gerardii</i>	1.17	0.042	0.0050
<i>Phragmites australis</i>	0.96	0.048	0.0300
<i>Lythrum salicaria</i>	2.64	0.048	0.0001
<i>Typha angustifolia</i>	2.16	0.068	0.0050

Table 2.2. Species-specific biomass model parameters. Initial belowground biomass determined from published reports and measured above/below ratios. Gross photosynthesis and belowground reserve factors determined from model calibration to fit target peak above and belowground biomass estimates.

<b>Species</b>	<b>Peak Aboveground (kgC m<sup>-2</sup> and g dw m<sup>-2</sup>)</b>	<b>Peak Belowground (kgC m<sup>-2</sup> and g dw m<sup>-2</sup>)</b>	<b>Annual Net Production (g m<sup>-2</sup>yr<sup>-1</sup>)</b>	<b>Annual Turnover (net prod /above peak)</b>
<i>Spartina alterniflora</i>	0.61 / 1525	1.99 / 4975	2800	1.8
<i>Spartina patens</i>	0.48 / 1200	1.06 / 2650	1950	1.6
<i>Juncus gerardii</i>	0.41 / 1025	1.24 / 3100	1950	1.9
<i>Phragmites australis</i>	0.62 / 1550	0.99 / 2475	2225	1.4
<i>Lythrum salicaria</i>	0.42 / 1050	2.49 / 6225	2175	2.1
<i>Typha angustifolia</i>	0.68 / 1770	2.21 / 5525	3125	1.8

Table 2.3. Model estimates of peak aboveground biomass, peak belowground biomass, annual net production, and annual turnover rate for six common salt marsh plant species. Peak biomass values provided in kg-Carbon and g-dry weight equivalents (40% carbon to dry weight ratio).

<b>Parameter</b>	<b>1 yr +5%</b>	<b>1 yr -5%</b>	<b>20 yr +5%</b>	<b>20 yr -5%</b>	<b>1 yr +20%</b>	<b>1 yr -20%</b>	<b>20 yr +20%</b>	<b>20 yr -20%</b>
Aboveground respiration rate	0.772	0.768	0.456	0.456	0.770	0.770	0.456	0.456
Belowground growth respiration rate	0.639	0.634	0.172	0.172	0.636	0.636	0.172	0.172
Belowground maintenance respiration rate	0.061	0.061	0.016	0.017	.061	0.061	0.016	0.017
Aboveground mortality rate	0.263	0.263	0.258	0.261	0.257	0.270	0.253	0.266
Belowground mortality rate	0.832	0.845	0.236	0.239	0.819	0.859	0.201	0.270
Translocation reserve use	0.012	0.012	0.085	0.086	0.012	0.011	0.083	0.087

Table 2.4. Relative sensitivity of biomass change to  $\pm 5\%$  and  $\pm 20\%$  adjustments in parameter values for 1 year and 20 model runs. Relative sensitivity was calculated as % change in biomass divided by % change in parameter.

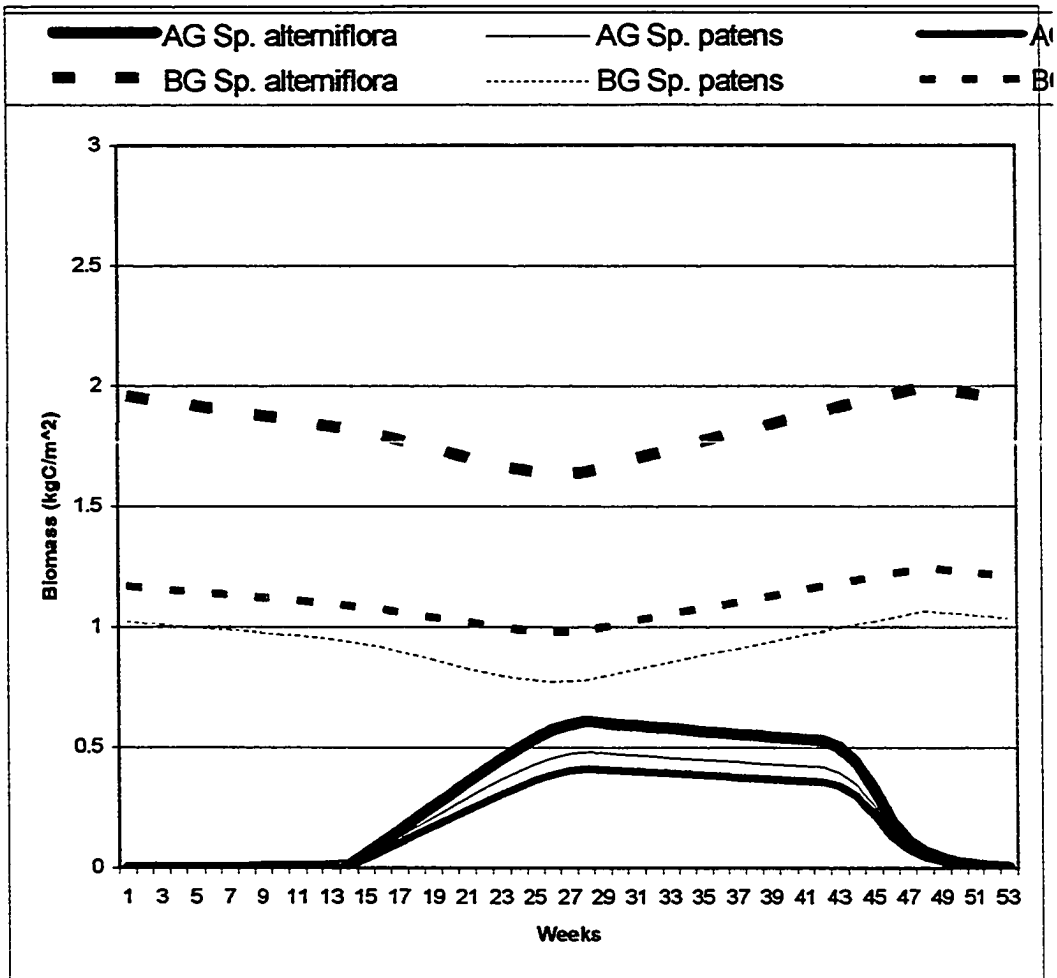


Figure 2.1. Modeled annual aboveground (AG) and belowground (BG) biomass estimates ( $\text{kg C m}^{-2}$ ) for native salt marsh plant species *Spartina alterniflora*, *Spartina patens*, and *Juncus gerardii* (40% carbon to dry weight ratio).

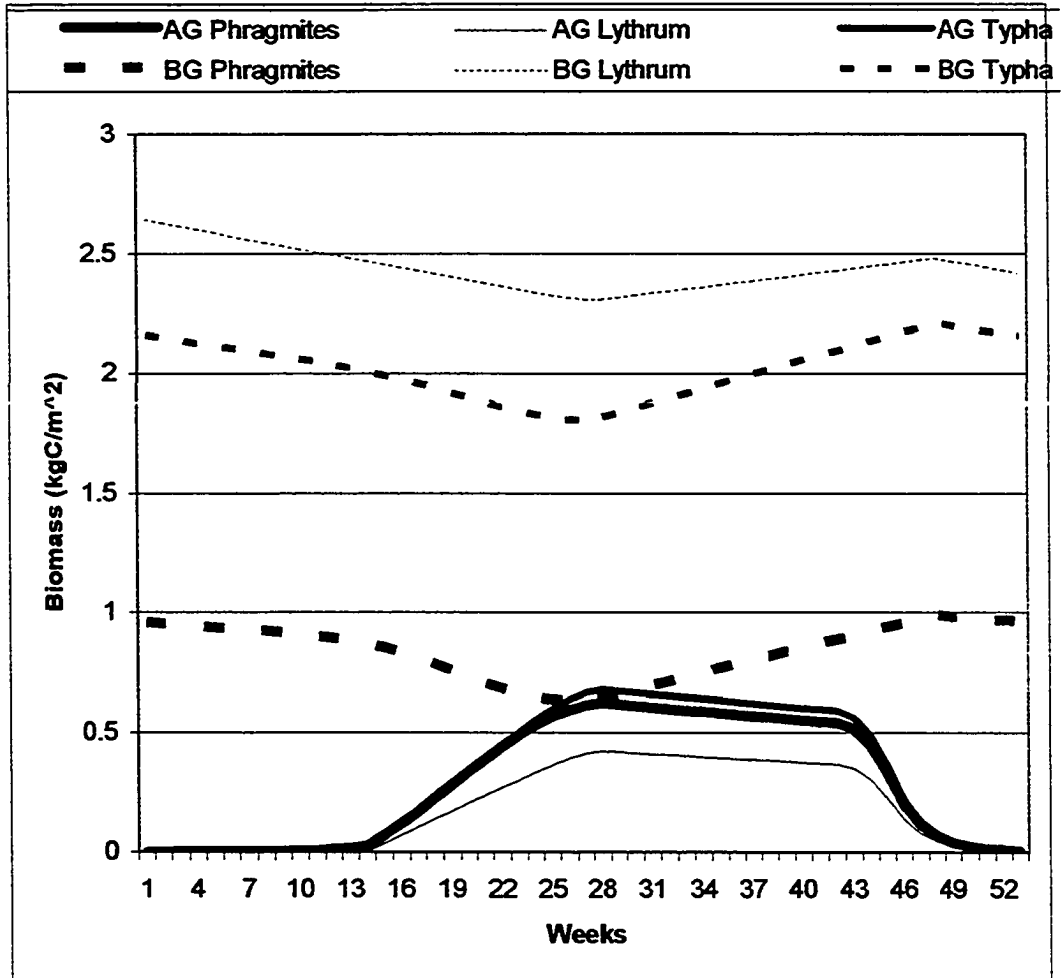


Figure 2.2. Modeled annual aboveground (AG) and belowground (BG) biomass estimates ( $\text{kg C m}^{-2}$ ) for brackish invasive salt marsh plant species *Phragmites australis*, *Lythrum salicaria*, and *Typha angustifolia* (40% carbon to dry weight ratio).



## **CHAPTER III**

### **A RELATIVE ELEVATION MODEL FOR NEW ENGLAND SALT MARSHES**

#### **Introduction**

Salt marshes are often considered flat, featureless expanses of grass, but in fact, subtle differences in elevation are important determinants of salt marsh habitat formation (Niering and Warren 1980). Local microtopography relative to the tidal cycle determines the frequency and duration of tidal inundation, sediment deposition (Stumpf 1983), and the level of physical stress on plant species (Bertness and Ellison 1987). Over the long term, salt marsh plant communities influence local geomorphologic through processes that build elevation, a critical self-maintenance capacity that has allowed salt marsh ecosystems to persist over thousands of years in spite of sea level rise. Redfield (1965) first identified this pattern of habitat migration in tidal marshes, and proposed a simple model of salt marsh elevation change with rising sea level (Figure 3.1).

This chapter describes a computer model that simulated changes in marsh surface elevation as a function of sediment formation processes, plant biomass production, biomass decomposition, and sediment deposition. Estimated marsh surface elevations were compared to sea level and tidal heights to determine the net direction of elevation change, and possible marsh emergence or subsidence. Results of the relative elevation model were used as critical inputs for a synthesized salt marsh ecosystem model, and ultimately for the prediction of plant community response to changes in hydrologic conditions (see Introductory Chapter).

A calibrated model of sediment dynamics in coastal wetlands, developed by Rybczyk et al. (1998), was used as the basis for the salt marsh relative elevation model. In the Rybczyk model, mineral deposits from suspended solids in the water column and organic carbon material from plants were combined to form marsh sediments (Figure 3.2). The marsh surface was modeled as a sediment column composed of eighteen soil cohorts, each with its own composition of minerals, roots, labile organic matter, and refractory organic matter. The height of each cohort was calculated as a function of cohort depth, cohort material composition, decomposition rates for labile and organic matter, and sediment pore space, with cohort heights summed to compute total column height. To estimate relative elevation, the height of the column was reduced by eustatic sea level rise (ESLR) and deep subsurface subsidence. Year-to-year changes in relative elevation were used to determine if marsh surfaces were emerging (net elevation gain) or subsiding (net elevation loss).

In order to implement the Rybczyk model, it was necessary to collect detailed specifications from marsh sediment core analysis. Soils were cored to depths of about 35 cm, separated into eighteen sections (cohorts), and measured for bulk density, pore space, percent organic matter, and percent mineral matter to specify a matrix of input parameters for each cohort. The model was run for the initial cohort matrix with a generalized set of process rates (sedimentation, biomass production, deep burial, etc.) to create a simulated sediment column. Model calibration was used to identify a set of process rates that produced close agreement between simulated and actual sediment column composition. The model was then run with the calibrated rates and cohort specifications to estimate changes in relative elevation for the marsh of interest.

This approach to model implementation, while rigorous for a given marsh site, was calibration-specific and dependent upon extensive soil core collection and analysis. For spatial implementation, tens of thousands of calibration runs would theoretically be needed to pre-process the model for an entire spatial grid. In addition, soil core collection and cohort composition analysis was highly labor-intensive (Rybczyk, personal communication). Since data of this nature are not typically collected at New England marsh sites (Neckles and Dionne 2000), a more generalized, non-calibrated modeling approach was required to meet the objectives of the current project.

To simulate marsh sediment dynamics with a greatly reduced set of input specifications, a generalized model was developed to process the sediment column as a single entity, rather than as a set of individual cohorts. Model focus was narrowed to

sediment accumulation and soil formation, processes that could be parameterized with commonly collected field data. In addition, the calibration and data-intensive processes associated with live root partitioning and soil compaction were handled with a simplifying set of model assumptions. The model was also standardized to simulate sediment accumulation and soil formation within a hypothetical square meter plot of vegetated salt marsh.

Sediments that accumulate on the marsh surface are composed of organic matter, inorganic mineral deposits, and pore space (Hatton et al. 1983, Turner et al. 2000). To parameterize the model, estimates for these sediment components were derived from a variety of sources, including direct field measurement, model output, and literature review. Of the three components, estimation of inorganic deposition was the most problematic, since complex processes like wave transport, particle re-suspension, and channel geomorphology are known to influence sedimentation patterns (see Table 3.1 for a more complete list of factors). Therefore, rather than modeling the sediment deposition process, measurements of sediment accretion were collected directly from marshes of concern. While sediment accretion levels were not part of the core field data standards proposed by Neckles and Dionne (2000), these measures are commonly made using a simple, low-cost field technique of feldspar marker horizons (Cahoon and Turner 1989).

Estimates of organic sediment inputs were determined as a function of plant biomass production (Rybczyk et al. 1998). It was also known that particulate carbon (Chalmers et al. 1985, Yang 1998) and wrack materials (Bertness and Yeh 1994) can be

trapped by aboveground structures and contribute to overall sediment loads, but these influences were not specifically considered in the model. To estimate plant biomass, plant species composition was determined from field survey (Neckles and Dionne 2000). Plant cover values were then used to parameterize a model of plant biomass production (Chapter II), and to determine annual above and belowground net production for the modeled marsh plot. The third sediment component, pore space, was estimated from reported measures of sediment core analysis in the literature. The generalized salt marsh model also required parameter estimates for decomposition rates and component fractions of labile and refractory biomass, which were also obtained from published results.

Based on these parameters, salt marsh sediment dynamics processes were simulated as a single soil column, rather than as a series of cohorts. In the original model, belowground fractional specifications were used to estimate incremental changes in cohort height due to compaction processes and live root partitioning. Since root presence increased elevation and compaction processes reduced elevation (Rybczyk et al. 1998), the net effect of ignoring belowground dynamics would be negligible if the relative impacts of roots and compaction were fairly equal. This simplifying assumption was tested by comparing cohort-based versus column-based model results for a coastal marsh with a complete set of belowground matrix specifications.

To validate the results of the generalized model, the model was run for four New England salt marshes with past or current tidal restrictions and known measures of sediment elevation change (see the Study Sites section in the Introductory Chapter).

These sites all have field stations that included marker horizon plots for measures of sediment accretion rates, and surface elevation tables (SETs) for measures of elevation change (Boumans and Day 1993). For each site, model estimates (using marker horizon data only) were compared with SET measures of elevation change. Since SET devices required specialized equipment for installation and monitoring, data collection for regional marsh assessment might be simplified if the model could predict elevation change based on the low-cost marker horizon techniques. Model estimates of elevation were an important component of an ecosystem model that predicted marsh plant response to changes in hydrologic conditions (see Introductory Chapter).

In addition to validation exercises, the model was run for hypothetical monotypic plots of six common salt marsh plant species (see Chapter II) to identify species-specific organic contributions to marsh sediment accretion rates. These results were used to provide insights into the relative rankings of plant species for building sediments and tracking sea level rise. A formal sensitivity analysis of the model was also conducted to identify relative importance of each parameter in the determination of marsh relative elevation.

## **Methods**

**Approach.** An existing software implementation of the original cohort model was acquired in Stella graphic programming format (High Performance Systems, Inc. Hanover, New Hampshire) and re-written into the Microsoft (MS) Visual FoxPro

procedural language (Microsoft Corporation, Redmond, Washington, USA). The acquired version of the cohort model was specified for use in the coastal wetlands of the Po River delta of Italy (Day et al. 1999). Development of the salt marsh relative elevation model followed this general approach: First, results from the re-written cohort model were compared with original model results to ensure that the translation process was complete and accurate. Next, cohort-based model processes were generalized for single sediment column processing (see Introduction). The column-based model was then run with inputs exactly the same as the cohort model, except for the initial matrix of belowground sediment cohort components. Twenty-year model run comparisons of cohort versus column results were conducted to assess the validity of the generalized approach. The generalized model was then parameterized for New England salt marsh use and run for the site-specific and plant species-specific model scenarios. Lastly, the model was subject to a formal sensitivity analysis to assess relative importance of each model parameter.

Model Structure. The model used a weekly time-step and operated on a calendar year basis to produce running weekly estimates of plant biomass production, plant litter, and sediment deposition. Relative elevation was computed once per year and reported at the end of each calendar year. The simulated marsh sediment column was a hypothetical square meter plot (35 cm deep) composed of six salt marsh species common to New England salt marshes (see Introductory Chapter). Species composition of the plot was specified for smooth cordgrass *Spartina alterniflora* (*cover\_spa*), salt hay *Spartina patens* (*cover\_spp*), black grass *Juncus gerardii* (*cover\_jun*), common reed *Phragmites*

*australis* (*cover\_phr*), purple loosestrife *Lythrum salicaria* (*cover\_lyt*), and narrow-leaf cattail *Typha angustifolia* (*cover\_typ*). Cover values represented the relative proportion of the plot occupied by each species, with the totals of all six species adding up to one.

Global Elevation Parameters. The model used two global rates to determine relative elevation: eustatic sea level rise (*eslr*) and deep subsidence rate (*surate*). Sea level has risen since the last glacial maximum (20,000 years B.P.) and continues to rise today (Peltier 1998). Recent estimates of sea level rise this century, based on tide gauges and altimeter data from satellites, indicated a global mean sea level rise rate of approximately 2 mm/yr and no significant acceleration in rate detectable in the past decade (Nerem 1999). Global warming scenarios, however, have predicted increases in sea level rise by the year 2100 (Gornitz 1995). Recent sea level rise rates from tide gauge data varied by coastal location, with reports of 4.0 mm/yr in Chesapeake Bay (Ward et al. 1998), 2.7 mm/yr at New York City (Donnelly and Bertness 2001), 1.65 mm/yr in Connecticut (Anisfeld et al. 1999), 1.1 mm/yr in New Hampshire, and 2.3 mm/yr in mid-coast Maine (Wood et al. 1989 for New Hampshire and Maine). Based on these reports, mean sea level rise rate for the New England coast was estimated at 1.5 mm/yr (.00002285 mm/wk). Deep subsidence, a function of varying surface loads due to glacial retreat, exacerbates sea level rise and is a major concern in some areas of the US Gulf Coast (Turner 1991). In New England, however, isostatic adjustment appeared to be negligible (<0.5 mm/yr for the southernmost NE coast, Donnelly and Bertness 2001), and therefore deep subsidence was ignored in the model.



Model Inputs. The model separated total deposited marsh sediments into organic and inorganic components. Total organic matter in the plot (*netbio*, kgC/m<sup>2</sup>wk) was estimated as gross weekly biomass production less respiration and non-litterfall mortality (see Chapter II). The inorganic sediment component (*sedinput*, m/m<sup>2</sup>wk) was based on site-specific measures of sediment accretion obtained by field marker horizon (Table 3.2).

Model Parameters. Model parameters included generalized processing rates and fractional percentages associated with sediment constituents. To estimate organic sediment inputs, a net accumulation parameter (*netaccum*) of 20% was applied to total plant biomass (*netbio*), accounting for loss of biomass due to decomposition in the water and air, and direct biomass removal by tides and storms (Chalmers et al. 1985). For simulation of biomass decomposition in the soil, net accumulated plant biomass was fractionalized into aboveground and belowground labile and refractory carbon components. Aboveground biomass was estimated as 80% labile (*llabfrac*), based on an analysis of *Spartina alterniflora* and *Spartina patens* aboveground biomass decomposition in a New England salt marsh (Valiela et al. 1985). For belowground structures, Hemminga and Buth (1991) found that the labile fraction of *Spartina angilca* roots from a Netherlands salt marsh was 20%, and this value was used for the belowground labile fraction (*rlabfrac*) of New England salt marsh plants. Weekly decomposition rates for labile (*klabsurf*) and refractory (*krefr*) components were estimated to be 2% and 0.2%, respectively, also from Valiela et al. (1985). For inorganic

inputs, the mineral volumetric component (*surfmin*) of total sediment accretion (*sedinput*) was estimated as 5% (Gosselink and Hatton 1984, Turner et al. 2000).

Sediment pore space, a highly sensitive model parameter, was specified in the original model for maximum (surface cohort) and minimum (deepest cohort) percentages (93% and 58%, respectively, from Rybczyk et al. 1998). Sediment pore space was combined with organic and inorganic sediment components to compute the volume and height of each cohort. For the generalized salt marsh model, an average value of pore space for the single 35 cm simulated sediment column was estimated at 70%. The average was based on maximum and minimum pore space percentages of 53%-96% respectively, from 10 cm sediment cores collected in four salt marshes in New Hampshire and Maine (Burdick et al. 1999). This dataset was of particular interest since these marshes represented a diversity of hydrologic conditions found in New England (unaltered, tidally-restricted, and hydrologically-restored), and hydrologic conditions are known to influence physical and chemical characteristics of salt marsh sediments (Portnoy and Giblin 1997, Anisfeld et al. 1999).

Sediment Processing. All sediment processing functions were from Rybczyk et al. (1998). Total accumulated organic sediment inputs were fractionalized into aboveground (*litter*) and belowground litter (*rlitter*) components, based on the blended plant species composition above-to-below (*abovebel*) biomass ratio (Equations 1 and 2). Labile fraction of above (*litterin*) and below (*lbin*) litter (Eqs. 3 and 4), and refractory fraction of above (*rlitterin*) and below (*rbbin*) litter (Eqs. 5 and 6) were derived from labile

and refractory ratios. Net labile input to sediment (*labbelow1*, gC/cm<sup>2</sup>wk) was computed as the fraction of above and below labile biomass from litter, less labile decomposition (*klabsurf*) and an annual allowance (at week 30) for deep burial (Eq. 7). Similarly, net refractory input to sediment (*refbelow1*, gC/cm<sup>2</sup>wk) was computed as above and below refractory litter, less refractory decomposition (*krefr*) and deep burial (Eq. 8).

$$\text{Aboveground litter} = (\text{netaccum} * \text{netbio} * .0001 \text{m}^2 / \text{cm}^2 * 1000 \text{g/kg}) * \text{abovebel} \quad (1)$$

$$\text{Belowground litter} = (\text{netaccum} * \text{netbio} * .0001 \text{m}^2 / \text{cm}^2 * 1000 \text{g/kg}) * (1 - \text{abovebel}) \quad (2)$$

$$\text{Aboveground labile} = \text{lfrac} * \text{litter} \quad (3)$$

$$\text{Belowground labile} = \text{rfrac} * \text{rlitter} \quad (4)$$

$$\text{Aboveground refractory} = (1 - \text{lfrac}) * \text{litter} \quad (5)$$

$$\text{Belowground refractory} = (1 - \text{rfrac}) * \text{rlitter} \quad (6)$$

$$\text{Labile Organic Input} = \text{MAX}(0, \text{labbelow} + ((\text{lbin} + \text{litterin}) * .1) - (\text{klabsurf} * (\text{labbelow})) - (\text{IF}(\text{weekcount} = 30, \text{labbelow}, 0))) \quad (7)$$

$$\text{Refractory Organic} = \text{MAX}(0, \text{refbelow1} + ((\text{rbin} + \text{rlitterin}) * .1) - (\text{kref} * (\text{refbelow})) - (\text{IF}(\text{weekcount} = 30, \text{refbelow}, 0))) \quad (8)$$

The mineral contribution to sediment column height (*mincm*, cm/wk) was computed as the mineral component of the total sediment input (Eq. 9). The organic contribution (*orgcm*, cm/wk) was the total organic input (*labbelow1*+*refbelow1*, g dw) with volumetric conversion of 1.14 g dry weight/cm<sup>3</sup> (DeLaune et al. 1983, Eq. 10). The pore space contribution to sediment column height (*porecm*, cm/wk) was computed as mineral plus organic input increased by the column pore space multiplier (Eq. 11).

$$\text{Mineral Contribution} = 100\text{cm/m} * (\text{sedinput} * \text{surfmin}) / 52\text{wk/yr} \quad (9)$$

$$\text{Organic Contribution} = ((\text{labbelow} + \text{refbelow}) * 2.5\text{gdw/gC}) / 1.14\text{gdw/cm}^3 \quad (10)$$

$$\text{Pore space Contribution} = (\text{porespace} / (1 - \text{porespace})) * (\text{mincm} + \text{orgcm}) \quad (11)$$

Elevation of the modeled plot (*cell\_el*, Eq. 12) was computed annually as starting elevation (*cell\_el\_init*) plus total accumulated weekly contributions. Relative elevation (*rel\_el*, Eq. 13) was calculated as plot elevation less sea level rise (*eslr*) and deep subsidence (*surate*).

$$\text{Plot elevation} = \text{cell\_el\_init} + ((\text{mincm}_{\text{total}} + \text{orgcm}_{\text{total}} + \text{porecm}_{\text{total}}) * .01\text{m/cm}) \quad (12)$$

$$\text{Relative elevation} = \text{cell\_el} - (\text{eslr} * 52\text{wk/yr}) - (\text{surate} * 52\text{wk/yr}) \quad (13)$$

Model Exercises. Three modeling exercises were conducted to validate the generalized model, and to make predictions of sediment-building capacity for common salt marsh plant species. All model runs were twenty years in duration. First, the generalized model was configured with specifications from the Po River delta (Day et al. 1999) to compare results with the original cohort model. Next, the model was parameterized with independent data from four New England salt marsh sites (from Burdick et al. 1999) to compare model predictions with estimates from field data. For these validation exercises, the model predicted changes in relative elevation based only on site-specific rates of sediment accretion rates from marker horizon data (Table 3.2). Plant composition of the plot was modeled as 50%-50% *Spartina alterniflora* and

*Spartina patens* to reflect typical plant species composition at the field data collection stations (10 m landward of major creeks). For each site, model predictions were compared with elevation results from SET data (Table 3.2, adjusted for sea level rise) for standard measures of relative elevation. As an additional set of simulations, the model was used to estimate organic contribution to sediment formation for monotypic stands of the six common salt marsh species. To determine the impact of organic inputs only, the model was specified for 100% cover of each plant species, with no inorganic sediment input and no sea level rise.

Sensitivity Analysis. The sensitivity of relative elevation results to changes in model parameters was determined through a systematic sensitivity analysis. For purposes of this analysis, plant species composition of the plot was 50%-50% *Spartina alterniflora* and *Spartina patens*, and the sediment accretion was 4 mm/yr. Model parameters were varied by  $\pm 5\%$  and  $\pm 20\%$ , and model results were compared to baseline conditions (based on original parameter values) to assess relative sensitivity of each parameter. Relative sensitivity was calculated as the percent change in relative elevation change divided by the percent change (either 5% or 20%) in the model parameter (Eq. 14). Higher relative sensitivity values indicated an increased sensitivity to a model parameter. The sensitivity analysis was run for one and twenty year durations to assess model consistency and stability at extended timeframes.

$$\text{Relative sensitivity}_{\text{parameter}} = \% \text{ Change}_{\text{relative elevation}} / \% \text{ Change}_{\text{parameter}} \quad (14)$$

## Results and Discussion

Cohort versus Column Model Comparison. Cohort model calibration for relative elevation change in the Po River delta (Day et al. 1999) produced results indicative of a subsiding coastal marsh. Figure 3.3 shows twenty years of predicted relative elevation change for the marsh, with a cohort model estimation of -4.17 cm net change. The generalized column model, parameterized exactly as the original model except for cohort-level specifications, estimated net change of -3.99 cm for a comparative difference of 4.4%. Close agreement between the models supported the assumption that the net impacts of root expansion and compaction on relative elevation were fairly equal, at least for this particular coastal marsh. Further analysis, however, was required in order to assess the potential applicability of these results to New England salt marsh habitat.

To investigate this issue, model determinants of root expansion and soil compaction processes were identified and analyzed. For cohort processing, root expansion was modeled as a function of litter biomass, with an exponential root distribution function to decrease root presence with sediment depth. Annual litter biomass for the Po River model was 522 g dry weight/m<sup>2</sup>yr. By comparison, modeled litter input for monotypic stands of New England salt marsh species ranged from 758 g dry weight/m<sup>2</sup>yr (*Typha*) to 490 g dry weight/m<sup>2</sup>yr (*Juncus*). A typical 50%-50% mix of *Spartina alterniflora* and *Spartina patens* produced 593 g dry weight/m<sup>2</sup>yr, about 14% more litter than the Po River input. For compaction processes, the key cohort model determinant was pore space, with greater pore space resulting in more elevation loss. Average pore space from the Po River was 60%, less than the pore space value used for

New England salt marshes (70%). By comparison, then, New England salt marshes were modeled with greater organic inputs and a higher percentage of pore space than the Po River wetland. In fact, porosity is known to increase with the proportion of organic matter in marsh sediments (Anisfeld et al. 1999, Turner et al. 2000). Therefore, the coupled processes of root expansion and soil compaction may vary in magnitude with the organic matter fraction, but still demonstrate a canceling effect. An exception may be found in highly oxidized soils associated with some tidal restricted salt marshes, where compaction processes are greatly accelerated due to elevated decay rates of organic matter (Portnoy and Giblin 1997). Nonetheless, this analysis suggested that a column-based model, with generalized parameters, was a viable alternative to the calibration exercises and field measurements required by the original cohort model.

New England Salt Marsh Estimates. The model was parameterized with site-specific sediment accretion rates from four salt marshes to predict annual rates of relative elevation change at each site. Model results were then compared to elevation change from SET measurements, less 1.5 mm/yr sea level rise to estimate relative elevation change (Table 3.2). Figure 3.4 shows modeled and measured SET annual rates of relative elevation change (mm/yr) for each study site. Results indicated that the model estimates of elevation change agreed with the general direction of elevation change from SET measures at each site (positive values indicate emergence, negative values subsidence). However, in all cases, model estimates were diminished in magnitude relative to SET results and relative differences varied from site to site.

At Oak Knoll, the model predicted a slight loss of elevation (-3 mm/yr), about one-third of the annual rate of -1 mm/yr estimated from SET data. Similarly, results from Drakes Island also predicted slight marsh subsidence (-2 mm/yr), although SET estimates there were much higher at -2.9 mm/yr. Both of these marshes currently experience restricted tidal flows due to undersized culverts (Burdick et al. 1999, Boumans et al. 2002), and these results concurred with reports of marsh sediment subsidence relative to sea level in other restricted salt marshes (Portnoy and Giblin 1987, Anisfeld et al. 1999, Burdick et al. 1999).

At Mill Brook, the model and SET estimates both predicted net gains in relative elevation and marsh emergence. The Mill Brook site has a past history of tidal restriction, but an undersized tidal culvert was replaced in 1993 to remove the restriction. As a result of hydrologic restoration, tidal exchange has been greatly increased at Mill Brook (Boumans et al. 2002). Since it was likely that the marsh surface had subsided during tidal restriction, it was expected that the return of tidal flows would result in high levels of sediment accretion (Anisfeld et al. 1999). In fact, sediment accretion at the marsh was measured at 19 mm/yr following restoration, and SET estimates indicated elevation gains of >30 mm/yr (Table 3.2). Model results for Mill Brook also predicted a rise in relative marsh elevation (2.6 mm/yr), but this rate was <10% of the SET estimate.

Model results for the Little River Marsh were based on field data from the nearby reference site at Awcomin Marsh, since the elevation field station at Little River had only been monitored for one field season. Data from Awcomin Marsh suggested that



sediment accretion levels and elevation change at Little River would be moderate to low (4 mm/yr accretion, 0.8 mm/yr elevation change, Table 3.2). The model also predicted a slight positive elevation gain (0.1mm/yr) for the site. However, since the Little River tidal culvert was expanded by more than three-fold flow capacity in late 2000 (see Introductory Chapter), it may be that sediment accretion rates there will follow a similar pattern as Mill Brook and increase significantly.

In general, it appeared that the generalized model predicted the general direction of elevation change, but underestimated the magnitude of the response. Since the elevation model used long-term averaged conditions (biomass production, decomposition, pore space, etc.), and field measurements varied with physical and biotic conditions, it may be that the model missed short-term but important changes in sediment dynamics. For example, the estimated increase in relative elevation at Mill Brook was 17 mm/yr greater than the measured contribution from sediment accretion (Table 3.2), suggesting that a surge in belowground plant growth may have occurred to account for this increase in elevation (Burdick et al. 1999). In addition, the 19 mm/yr measured rate of sediment accretion at Mill Brook appeared to reflect a temporary flush of creek sediments and not a sustained level of sediment deposition (Anisfeld et al. 1999). At Drakes Island and Oak Knoll, SET estimates of accelerated subsidence may be due to elevated organic decomposition rates, possibly associated with year-to-year increases in temperature or low soil moisture (Valiela et al. 1985). However, despite the potential influences of short-term phenomena on specific marsh sites, overall marsh emergence or

subsidence was correctly modeled using averaged rates and a minimal set of parameters, even if estimates were not entirely consistent with results based on SET data.

Plant Species Predictions. Figure 3.5 shows the results of model scenarios for species-specific estimates of organic contribution to sediment accretion. Modeled organic accretion, based on species biomass production, ranged from 0.72 mm/yr for *Juncus* to 1.15 mm/yr for *Typha*. The results indicated that invasive species, especially *Typha* and *Phragmites*, build sediments faster than native high marsh species like *Spartina patens* and *Juncus*, and may possibly out-compete these species by reducing flood levels over the long term (Windham and Lathrop 1999).

In addition, results from the species model scenarios can be considered in light of projected future sea level rise. Assuming that organic and inorganic contributions to vertical accretion are roughly equivalent (Anisfeld et al. 1999, Turner et al. 2000), the model estimated average long-term vertical accretion rate of 2.1 mm/yr for low marsh habitat dominated by *Spartina alterniflora*. This value compared favorably with long-term salt marsh accretion rates of 1.1-5.9 mm/yr for Connecticut (Anisfeld et al. 1999), and 2.0-4.9 mm/yr for Rhode Island (Donnelly and Bertness 2001), based on isotopic dating of deep sediment cores. These results suggested that rapid sea level rise in excess of 2 mm/yr (Gornitz 1995), especially without increases in sediment loads, may inundate coastal marshes and convert high marsh habitat to low marsh (Donnelly and Bertness 2001).

**Sensitivity Analysis.** The relative sensitivity of model parameters for model runs of 1 and 20 years are presented in Table 3.3, with relative sensitivity calculated as the percent difference in relative elevation change divided by percent difference in the parameter. This analysis indicated that pore space was the most sensitive model parameter (Rybczyk et al. 1998). Pore space sensitivity resulted from model use as a multiplicative factor for computation of sediment column height (Eq. 11). The next most sensitive parameter was the rate of sea level rise, since this rate was directly applied to plot elevation (Eq. 13). In addition, the model was sensitive to changes in the inorganic (mineral fraction) and organic (net production accumulation) input rates. These rates controlled the relative contribution of inorganic and organic inputs to sediment formation. Processing rates for above and belowground carbon components were generally minor influences on elevation results. Parameter sensitivities were diminished from one year to twenty year model runs, presumably due to movement toward a model equilibrium state.

### **Conclusions**

The elevation of New England salt marsh habitat changes constantly in response to physical and biotic factors. A model that considers these factors can be used to estimate long-term relative elevation change and marsh habitat response. A generalized relative elevation model for New England salt marsh habitat, based on sediment dynamic relationships specified in a calibrated model, produced elevation results in agreement with the calibrated model. The model was implemented for four New England salt marshes with diverse hydrologic conditions, and produced results consistent with field

measures for long-term direction of elevation change. The magnitude of predicted elevation change, however, was in all cases less than estimates from field measures, possibly due to model reliance on general-case parameters that missed short-term extremes in physical and biotic conditions. Despite this lack of precision (compared to surface elevation table measurements), the generalized model appeared adequate to predict overall emergence or subsidence of New England salt marsh habitat. In addition, the model identified relative rankings of elevation-building capacity, and flooding risk associated with potential sea level rise, for common marsh plant species.

<b>Factor</b>	<b>Impact</b>
Relative elevation change (from deep subsidence, sea level rise, accretion and subsidence)	Higher elevations are inundated less frequently and receive lower sediment supplements
Tidal regime	Frequent and long lasting tidal inundation often results in higher sedimentation rates
Sediment source	Presence of significant river-borne or near shore inorganic sources increases sedimentation rates
Relative distance from open water	Sediment settling reduces suspension with increasing distance from open water
Sediment particle size, density, and organic/inorganic mix	Larger, heavier inorganic particles have lower settling velocities and deposit closer to sediment source
Ground cover	Plant stems reduce water flow and turbulence, increasing sediments
Tidal water velocity and channel turbulence	Faster water and more turbulence re-suspends particles, often leading to sedimentation across larger spatial areas
Wind direction and velocity	Winds create wave action and turbulence, especially during storms, causing sediment re-suspension and redistribution of sediments
Erosion	Ice erosion remove plants and reintroduce sediments to the water column
Tidal channel geomorphology	Meandering processes, and associated changes in channel depth, width, and velocity, add to inorganic sediment loads
Anthropogenic effects	Causeways can limit sediment loads; filling, dredging and some agricultural practices increase re-suspension and sedimentation

Table 3.1. Determinants of salt marsh sedimentation patterns.

<b>Study Site</b>	<b>Sediment Accretion (mm yr<sup>-1</sup> ± SE)</b>	<b>Elevation Change (mm yr<sup>-1</sup> ± SE)</b>	<b>Relative Elevation Change (mm yr<sup>-1</sup>)</b>
Oak Knoll Marsh	1.61±0.17	0.50±0.06	-1.00
Little River Marsh*	4.26±1.83	2.30±5.40	0.80
Mill Brook Marsh	19.02±1.81	36.00±10.00	34.50
Drakes Island Marsh	2.38±0.34	-1.40±0.20	-2.90

Table 3.2. Sediment elevation measures for the four study sites. Oak Knoll data from unpublished sources, all others from Burdick et al. (1999). Sediment accretion data used marker horizon techniques (Cahoon and Turner 1989); elevation change data used SET measures (surface elevation tables, Boumans and Day 1993). Relative elevation values are computed as elevation change less sea level rise (1.5 mm/yr). \*Little River data from Awcomin Marsh downstream reference marsh (Burdick et al. 1999).

<b>Parameter</b>	<b>1 yr +5%</b>	<b>1 yr -5%</b>	<b>20 yr +5%</b>	<b>20 yr -5%</b>	<b>1 yr +20%</b>	<b>1 yr -20%</b>	<b>20 yr +20%</b>	<b>20 yr -20%</b>
Eustatic sea level rise	16.50	16.36	15.20	15.23	16.45	16.41	15.22	15.22
Belowground labile fraction	0.15	0.15	0.14	0.14	0.15	0.15	0.14	0.14
Aboveground labile fraction	0.39	0.37	0.36	0.36	0.39	0.39	0.36	0.36
Decomposition rate labile	0.55	0.53	0.49	0.50	0.52	0.54	0.48	0.51
Decomposition rate refractory	0.09	0.09	0.08	0.08	0.09	0.09	0.08	0.08
Column pore space	46.05	36.43	42.85	33.89	76.26	27.73	70.96	25.81
Mineral fraction	7.78	7.78	7.20	7.20	7.78	7.78	7.20	7.20
Net production accumulation	9.64	9.66	9.02	9.02	9.65	9.65	9.02	9.02

Table 3.3. Relative sensitivity of estimated elevation change to  $\pm 5\%$  and  $\pm 20\%$  adjustments in model parameters at 1 year and 20 year durations. Relative sensitivity is calculated as % change in relative elevation divided by % change in parameter.

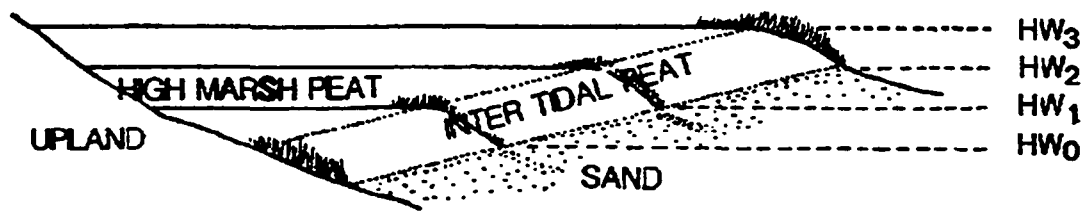


Figure 3.1. Conceptual model of salt marsh self-maintenance, showing migration of salt marsh as high water boundary increases from HW<sub>0</sub> to HW<sub>3</sub> (from Redfield 1965).



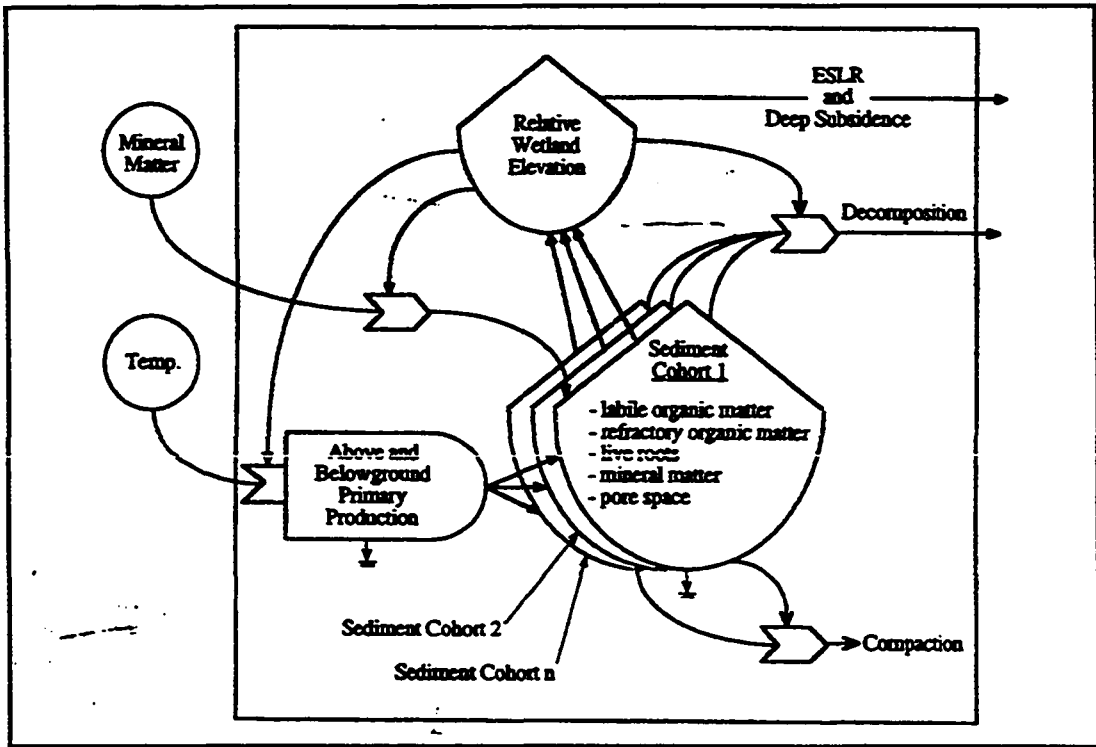


Figure 3.2. Conceptual model of sediment dynamics (Rybczyk et al. 1998), based on eighteen sediment cohort levels.

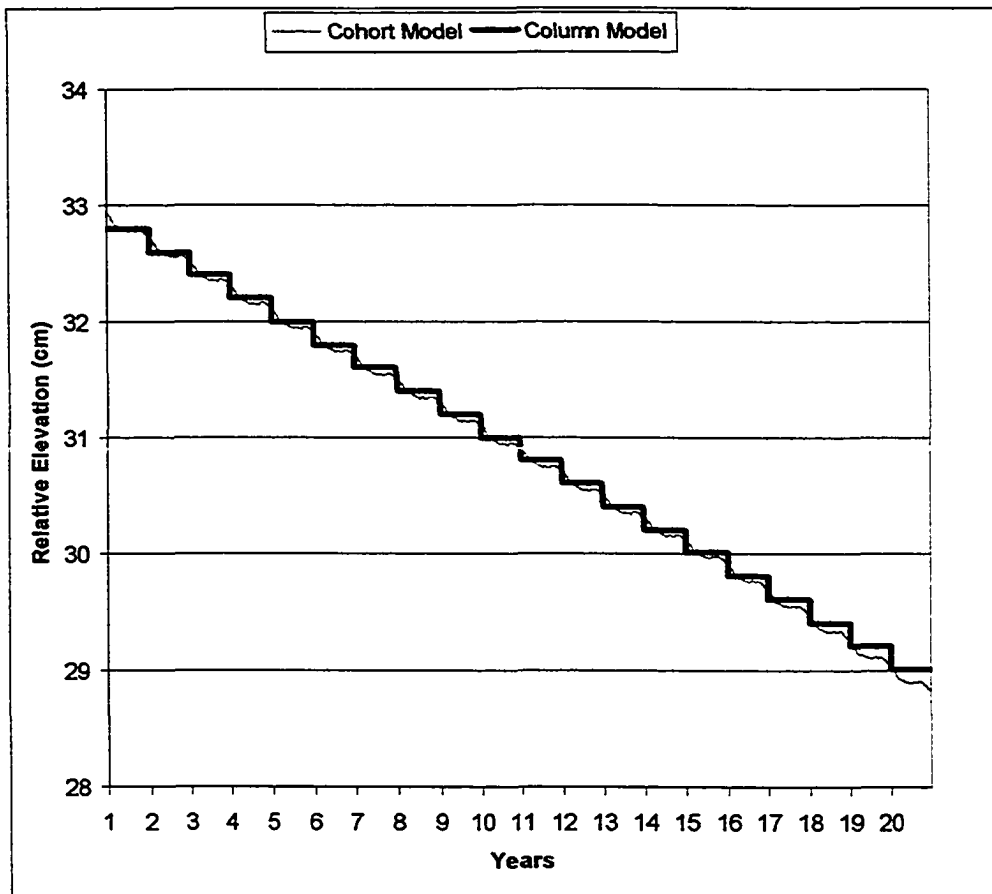


Figure 3.3. Results of model comparison between calibrated cohort model (Rybczyk et al. 1998) and generalized column model. Model specifications are from the Po River delta (Day et al. 1999). Chart shows differences between modeled elevation changes over twenty years.

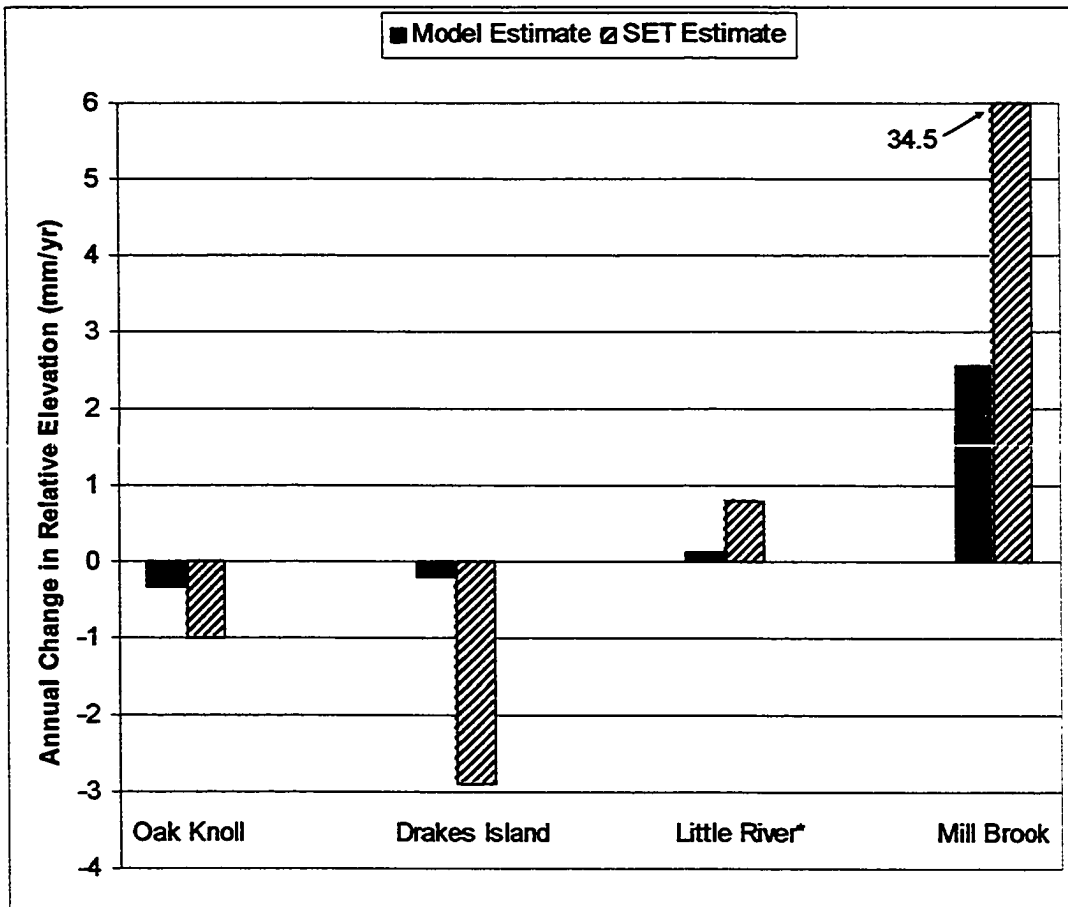


Figure 3.4. Comparison of changes in relative elevation from model estimates and surface elevation table (SET) measures at four New England salt marsh locations (\* Little River estimates based on measures from Awcomin Marsh downstream reference marsh, Burdick et al. 1999).

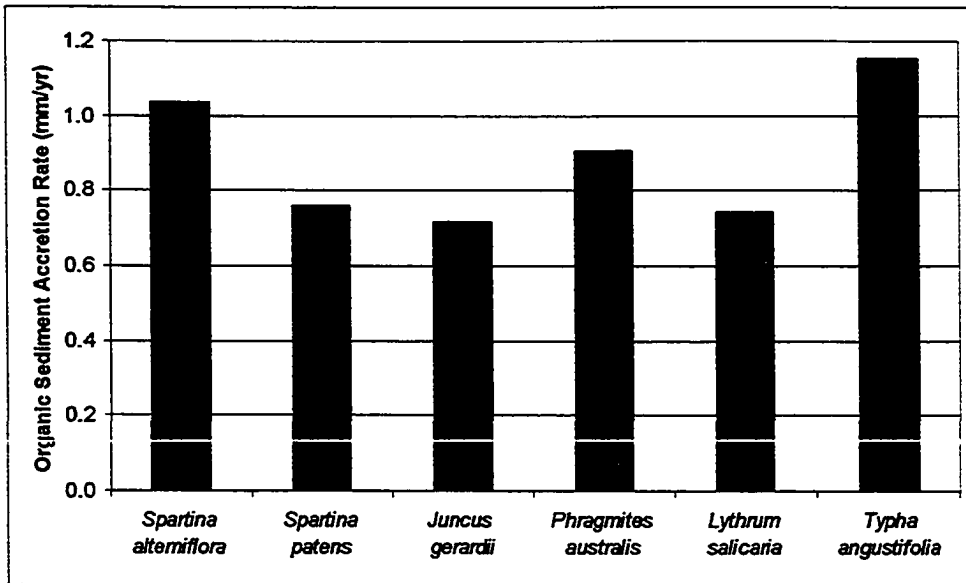


Figure 3.5. Modeled estimates of relative organic contribution to sediment accretion for monocultures of six common New England salt marsh plant species (inorganic sediment inputs and sea level rise excluded). Results are partly based on species annual biomass production (Chapter II).

## **CHAPTER IV**

### **A HYDRAULIC MODEL FOR PREDICTING TIDAL FLOWS IN HYDROLOGICALLY-ALTERED SALT MARSHES**

#### **Introduction**

Roads, bridges, dredge-spoil berms, and culverts often become barriers to natural tidal flows in salt marshes, and these tidal restrictions negatively affect as much as 20% of remaining salt marsh habitat in New England (Roman et al. 1984, USDA SCS 1994, Neckles and Dionne 2000). Over time, salt marshes with tidal restrictions may experience reduced plant biodiversity (Roman et al. 1984, Sinicrope et al. 1990, Burdick et al. 1997), degraded water quality (Portnoy 1991, Portnoy and Giblin 1997), diminished ability to keep pace with sea level rise (DeLaune et al. 1983, Boumans and Day 1994), and disrupted food webs for fish and birds (Dionne et al. 1999, Reinert and Mello 1995). Fortunately, these damaged habitats can recover lost functions if the appropriate hydrologic regime is restored (Sinicrope et al. 1990, Burdick et al. 1997, Roman et al. 2002, Warren et al. 2002), and as a result, hydrologic restoration of restricted salt

marshes is a common management practice today (New Hampshire Office of State Planning 1996, Save the Sound 1998, US Army Corps of Engineers 1999).

Planning and implementing an optimal hydrologic regime for a coastal ecosystem is not a trivial task, however, and goes beyond a simple accounting of water in and water out with the tides. Engineering options for modifying tidal flow need to consider the specific impacts of culvert and creek design on public safety, project costs, and property protection. In terms of ecological considerations, potential new flood regimes need to be understood in terms of tidal heights, frequency of flooding, and duration of flooding (Burdick et al. 1997), and therefore require a site-specific knowledge of tidal signal, culvert and creek dimensions, and marsh elevations. When tides are reintroduced to an altered salt marsh, failure to accurately account for these physical factors can lead to open mud flats from too much flooding (Race 1985, Rozsa 1995, Williams and Orr 2002), or unplanned brackish and upland habitats from too little flooding (Moy and Levin 1991, Burdick et al. 1997). Therefore, a model that considers these hydrologic factors and predicts salt marsh flood regime would be beneficial to coastal resource managers as a decision-support tool.

This chapter describes a hydraulic model for hydrologically-altered salt marshes, based on the Marsh Response to Hydrological Modification calibrated model (MRHM) developed by Boumans et al. (2002). MRHM predicted upstream water level and water volume flow through tidal culverts, based on measured records of downstream tidal signal and culvert pipe dimensions, and calibrated parameters (Figure 4.1). In addition,

the model used a profile of surface elevations for each marsh, known as a hypsometric curve, to estimate the area of a marsh flooded by each tide. For this project, the MRHM model was expanded to consider other common inflow culvert and channel structures found in New England, including box culverts, and open channel flows. Further, new calibration parameters were added to MRHM for better performance across a wider range of tidal-restriction conditions.

The expanded MRHM model was used at four New England salt marshes with current or past tidal restrictions (see Introductory Chapter, Study Sites). The salt marshes at Little River (North Hampton, New Hampshire) and Mill Brook (Stratham, New Hampshire) were hydrologically restored in the past ten years, after many years of tidal restrictions. At Drakes Island (Wells, Maine) and Oak Knoll (Rowley, Massachusetts), long-term tidal restrictions persist today due to undersized culverts beneath roadways. For each of these sites, hydrodynamic model implementations were developed based on specifications and data sources collected in the field. Model requirements for field data were based on the recommendations of a regional protocol for standardized data collection in coastal marshes along the Gulf of Maine (GPAC, Neckles and Dionne 2000), to meet an important project objective for transferability.

The general approach for use of this model was to calibrate predictions of upstream tidal heights to observed conditions, and then to use the calibrated model as the basis for conducting hydrologic scenario analysis. In particular, marshes with current tidal restrictions were modeled with hypothetical new culvert designs to simulate

hydrologic restoration, and marshes with restored hydrology were modeled with the dimensions of past undersized culverts. Results from this exercise provided new information about the restoration capacity of restricted marshes, and a basis for comparison for those marshes improved by hydrologic restoration. In addition, model results were evaluated with published reports of hydrologic conditions at each marsh to assess relative performance of the model under diverse situations, and to gauge the usefulness of the model as a general purpose decision-support tool. The hydraulic model was also used as a component of an integrated salt marsh ecosystem model that predicted plant community response to changes in tidal hydrology (see Introductory Chapter, Figure I.2).

### **Methods**

**Model Approach.** An existing software implementation of the MRHM model (Boumans et al. 2002) was acquired in the Stella graphic programming format (High Performance Systems, Inc. Hanover, New Hampshire) and re-written into the Microsoft (MS) Visual FoxPro procedural language (Microsoft Corporation, Redmond, Washington, USA). Development of the hydraulic model followed this general approach: First, results from the re-written model were compared with original MRHM model results to ensure that the translation process was complete and accurate. Then, for each of the four salt marsh study sites, the model was specified with the dimensions of the local tidal culvert or culverts, and estimates of tidal heights upstream of the culvert were generated based on the measured downstream tidal signal. As with the original



MRHM model, freshwater inputs of surface and groundwater were not considered. For each model run, estimates of upstream tidal heights were correlated with measures from the upstream gauge. Model parameters were iteratively adjusted until the highest coefficient of determination ( $r^2$ ) was achieved, at which point model calibration was considered complete. The  $r^2$  values were derived by comparing time-series of water levels generated by the model and observed water levels (Boumans et al. 2002). Lastly, the model was subjected to a formal sensitivity analysis to assess the relative importance of each model calibration parameter.

Model Structure. The model used a 6-minute time step over a complete two-week tidal cycle to estimate total water volume ( $m^3$ ), water height (m NGVD), and area flooded (%) for the upstream portion of each study site. Model inputs were downstream tidal signal, culvert dimensions, and a summary of marsh survey elevations. Results were saved to a hydrologic-scenario table of upstream water heights for each time step (3360 total estimates).

Marsh Surveys. For each site, marsh elevations were sampled with rod-and-level survey equipment along random transects. Five or six transects were identified perpendicular to the main creek, each one at a random distance along a creek centerline determined from aerial photographs. Transects ran from upland edge to upland edge, as determined by vegetation and slope. For each transect, between 7 and 48 elevation points were measured at 15-meter intervals. In addition to elevation, percent species cover was recorded for each plant species found in a 0.50  $m^2$  quadrat at the survey point, and

locations of major plant zones were noted on field maps. Since the random transects included creeks, survey results could be used to plot the relationship between elevation and total marsh area at each site (hypsothetic curve, Neckles and Dionne 2000). Elevation points were adjusted to NGVD (1929) by including an NGVD benchmark in the survey at each site. Existing NGVD benchmarks were available at Drakes Island and Mill Brook, but not Oak Knoll, Little River, and Awcomin Marsh (Little River downstream reference site), so temporary benchmarks were established at these locations by closed-circuit elevation survey from the nearest known benchmark.

Tidal Cycle. At Drakes Island and Mill Brook, pressure-transducer devices (YSI, at 15-minute data intervals) were used to record water levels on both sides of the tidal culvert (4/23/96-5/6/96 at Drakes Island, 4/22/98-5/8/98 at Mill Brook, Boumans et al. 2002). For the Little River site, a sonic datalogger mounted on a metal platform (Infinilog, at 6-minute data intervals) was used to record water levels upstream of the culvert from 10/24/01-11/13/01. Since a datalogger could not be safely deployed downstream of the culvert (open ocean), the Little River downstream signal was based on an Infinilog datalogger record collected at nearby Awcomin Creek over the same time period. At Oak Knoll, Infinilog dataloggers were used upstream and downstream of the Mud Creek (north) culvert from 11/14/01-11/28/01. Datalogger records were downloaded to an IBM PC laptop and imported into MS FoxPro table format for analysis and standardization. Water levels were examined to select a complete two-week record of values with a minimum of out-of-range values (an intermittent condition apparently caused by accumulation of wrack around the sensor). Out-of-range values in the selected

dataset were estimated by linear interpolation from the nearest known data points. For Drakes Island and Mill Brook, values were converted from 15-minute to 6-minute intervals by linear interpolation. Tidal heights were adjusted to NGVD by a site-specific datum correction factor determined from the marsh elevation survey.

Inflow Channel Dimensions. The model considered three types of inflow channels: open creeks, pipe (barrel) culverts, and box culverts. At each site, culverts or creeks were measured to determine physical dimensions (e.g., length and diameter, with open creek bottoms assumed to be semi-circular in cross section). In addition, elevations were surveyed for culvert invert elevation (culvert bottom), and estimates of creek bottom and marsh surface at the upstream culvert entrance. The culvert and tidal creek dimensions for each study location are presented in Table 4.1.

Flow Estimates. The model was configured with current culvert and creek dimensions for each site, and run through a two-week cycle of downstream tidal heights to generate estimates of baseline upstream water flows. Results for water discharge, based on hydraulic equations with English measures (cubic ft/sec), required metric conversion prior to output at 6-minute time step intervals. Water level at the start of the model run was estimated as the elevation of the creek bottom (*creek\_el*) plus a calibrated initial water level (*wlevel\_init*, Equation 1). Hydraulic head was computed as the absolute value of the difference between upstream and downstream water level (Eq. 2), and the direction of tidal flow was determined as +1 for inflow into the marsh, or -1 for outflow to the open ocean (Eq. 3), based on Boumans et al. (2002).

$$\text{Water Level}_{\text{initial}} = \text{creek\_el} + \text{wlevel\_init} \quad (1)$$

$$\text{Head} = \text{ABS}(\text{Water Level}_{\text{upstream}} - \text{Water Level}_{\text{downstream}}) / .3048 \text{ ft/m} \quad (2)$$

$$\text{Direction} = ((\text{Water Level}_{\text{downstream}} - \text{Water Level}_{\text{upstream}}) / .3048 \text{ ft/m}) / \text{Head} \quad (3)$$

For each inflow channel, the model computed water discharge based on running estimates of hydraulic head and channel-specific discharge formulae. Flows were combined for multiple culverts as a model assumption of hydrologic connectivity. The open creek discharge formula was based on an estimate of creek diameter (Eq. 4, Chanson 1999). For culvert flows, the hydraulics formulae used different surface roughness factors for concrete (0.012) and corrugated metal (0.024), depending on the culvert material (*kutters*, from Simon 1976). Barrel culvert discharge was estimated using culvert diameter and length (Eq. 5, Simon 1976), and box culvert discharge used width and height (Eq. 6, Chanson 1999).

$$\text{Discharge}_{\text{creek}} = (.432 * \text{SQRT}(32.2) * \text{Head}^{1.9}) / (\text{culdiam}^{.4} * \text{culdiam}) * 3600 \text{ sec/hr} \quad (4)$$

$$\text{Discharge}_{\text{barrel}} = 10 * \text{SQRT}(\text{Head} / (((2.5204 + 1.2) / \text{culdiam}^{.4}) + ((466.18 * \text{kutter}^2) * \text{cullen}) / (\text{culdiam}^{16/3})))) * 3600 \text{ sec/hr} \quad (5)$$

$$\text{Discharge}_{\text{box}} = (\text{culwidth} * \text{culheight} * \text{SQRT}(2 * 32.2) * (\text{Head} / 1.5)) * 3600 \text{ sec/hr} \quad (6)$$

Discharge estimates were maximum values, based on the assumption of culverts or creeks flowing full (Simon 1976, Chanson 1999). These values were re-adjusted with calibration to reflect observed measures during partial flow conditions. A calibrated

upstream conductivity factor (*upcond*) was used to simulate reduced inflows when the upstream creek was not filled on the incoming tide, and when the upstream creek bank was overtopped at the peak of incoming tides (Eq. 7). Water flow for each inlet was computed as discharge reduced by the calibration factor, except when water height was below the culvert invert elevation (*thresh*) or if a flap gate (*flap*, 0=off, 1=on) was in place (Eq. 8, Boumans et al. 2002).

$$\text{Conductivity Factor} = \text{IF}((\text{Water Level}_{\text{upstream}} > \text{marshel AND Direction} < 0) \text{ OR } (\text{Water Level}_{\text{upstream}} < \text{marshel AND Direction} > 0), 1, \text{upcond}) \quad (7)$$

$$\text{Flow} = \text{upcond} * \text{IF}(\text{thresh} \geq \text{MAX}(\text{Water Level}_{\text{downstream}}, \text{Water Level}_{\text{upstream}}), 0, \text{IF}(\text{flap} > 0, \text{MIN}(0, \text{Direction} * \text{Discharge} * .028317 * .1\text{hr}/6 \text{ min}), (\text{Direction} * \text{Discharge} * .028317 * .1\text{hr}/6 \text{ min}))) \quad (8)$$

Water Level Estimates. Upstream water level was estimated by adding flows for each tidal inlet, and adjusting results with model calibration factors. To simulate observed conditions of upstream water retention (impoundment), a flooding effect parameter (*floodeffect*) was used with an exponential function to increase upstream water volume during the build-up of spring tides (Eq. 9). This calibration result was multiplied by the sum of volumetric flow through one or more channels to generate incremental upstream water gain (Eq. 10). An additional calibration factor was used to simulate a similar condition associated with spring tides, when upstream water levels lagged behind the downstream signal. To model this response, upstream flows were reduced as a

function of total flows (Eq. 11), based on a comparison of hydraulic head and a calibrated threshold level (*headthresh*). Water volume was computed as the sum of incoming flows for one or more channels, plus or minus any adjustments for water gain or water loss (Eq. 12). Lastly, upstream water level was computed as water volume multiplied by a calibrated geomorphologic factor (*creek\_sl*) that served as a generalized estimate of creek slope in the upstream terrain (Roman et al. 1995, Boumans et al. 2002).

$$\text{Flood Effect} = \text{EXP}((\text{Water Level}_{\text{upstream}} - \text{marshel})/\text{marshel}) \quad (9)$$

$$\text{Water Gain} = \text{floodeffect} * (\sum \text{Flow}_{\text{channel1-2}}) \quad (10)$$

$$\text{Water Loss} = \text{IF}(\text{Head} < \text{headthresh}, 1, 0) * (\sum \text{Flow}_{\text{channel1-2}}) \quad (11)$$

$$\text{Water Volume} = (\sum \text{Flow}_{\text{channel1-2}} + \text{Water Gain} - \text{Water Loss}) * .1 \text{ hr}/6 \text{ min} \quad (12)$$

$$\text{Water Level} = \text{Water Volume} * \text{creek\_sl} \quad (13)$$

Area Flooded Estimates. Upstream water levels were compared with marsh elevation survey results to estimate the area of marsh surface flooded at each point in the tidal cycle. Composite estimates of area flooded were used to determine the frequency and duration of flooding (hydrologic regime) for each study location. To compute area flooded, marsh elevation points from random transect surveys at each location were sorted from high to low values. The total number of points was divided by 100 to determine the percent of the survey represented by each point, and each sorted point was ranked for cumulative percentage (point ranking\*percent). Since the survey was a random sampling, the cumulative percentage associated with each elevation point was assumed to represent the portion of the marsh at that elevation. The result of this

exercise, a table of related elevations and percentages known as a hypsometric curve, was used to determine the percentage of the marsh flooded for any specified upstream water level. At each time step, the model performed a table-lookup with water level as the matching key, returning the percent of total marsh area flooded from the hypsometric data. It should be noted that this simulation approach assumed that water was instantaneously distributed across the entire upstream marsh surface with each change in water level. In reality, flooding is slowed by friction with marsh sediment surfaces and vegetation (Stumpf 1983), and natural variations in marsh geomorphology cause irregularities in flood patterns (Wood et al. 1989, Gardner et al. 2002). However, flood scenarios based on hypsometry are thought to provide reasonable estimates of marsh hydroperiod (with a minimum of field survey work) and this approach has been accepted as a regional standard for assessment of marsh flood regime in the Gulf of Maine (Neckles and Dionne 2000).

Model Scenarios. For each study location, the site-calibrated model was used to generate hydrologic scenarios for baseline (current) conditions, and for hypothetical conditions associated with altered hydrology. Marsh locations with existing tidal restrictions (Drakes Island and Oak Knoll) were modeled with various culvert expansion scenarios to simulate the potential impacts of tidal restoration on marsh hydrology. Based on these scenario results, specific recommendations for hydrologic changes were made for these restricted study sites. Marsh locations with restored tidal hydrology (Mill Brook and Little River) were modeled with culvert specifications from before hydrologic restoration to simulate potential impacts of long-term continued tidal restriction.

**Sensitivity Analysis.** The sensitivity of predicted upstream water level to changes in calibration parameter values was determined through a systematic sensitivity analysis. For purposes of this analysis, the model was configured with the downstream signal and baseline calibration values of Little River Marsh (a site that used all four of the primary model calibration parameters). Model calibration parameters were varied by  $\pm 5\%$  and  $\pm 20\%$ , and new upstream water levels were generated. The analysis compared original (baseline) peak upstream water level with new values of peak upstream water level to assess relative sensitivity of each calibration parameter. Relative sensitivity was calculated as the percent change in peak upstream water level divided by the percent change (either 5% or 20%) in the model parameter (Eq. 14). Higher relative sensitivity values indicated an increased sensitivity to a model calibration parameter.

$$\text{Relative sensitivity}_{\text{parameter}} = \% \text{ Change}_{\text{peak upstream water level}} / \text{Change}_{\text{parameter}} \quad (14)$$

## **Results and Discussion**

Model results for current hydrologic conditions at each of the four study sites were presented as two-week tidal hydrographs of water elevations from the observed record downstream of the culvert (downstream record), the observed record upstream of the culvert (upstream record), and the predicted upstream water elevation record (upstream model). For each site, the coefficient of determination ( $r^2$ ) between observed and predicted upstream water levels was used as the standard measure of model



performance. Marsh elevation results were presented as hypsometric curves for each study site. Observed upstream water levels were used together with the hypsometric curve to show the percent of marsh area flooded over the two-week tidal cycle. In addition to current hydrologic conditions, model scenarios were developed for each study site to predict tidal hydrology associated with site-specific changes of inflow structures.

Drakes Island Marsh Current Conditions. Tidal hydrographs for Drakes Island Marsh (Figure 4.2a upper chart) clearly showed the restricted nature of upstream tidal hydrology at the site due to the undersized 0.91 m (3 ft) culvert. For all tides, the upstream response was diminished in comparison with the downstream signal, with lower peaks and higher troughs. During spring tides (Days 9 to 13), the downstream record showed a tidal range of 2 meters, but the upstream tidal range was only about 1/6 of the downstream signal (~ 35 cm). Impoundment of tidal waters at the site was obvious, with a minimum of 1 meter of water in the upstream channel at all times. The area of marsh flooded (Figure 4.2a lower chart) showed that impounded water covered from 17 – 30% of the marsh at low tide, with the height of impounded water increased with tidal range during building spring tides. In addition, flooded marsh area reached a peak of only 85% during spring tides, indicating that 15% of the marsh would not be flooded during a typical tidal cycle. The hypsometric curve for Drakes Island (Figure 4.2b) revealed three tiers of surface elevation. The lowest 20% of the marsh surface (0.7 to 1.0 m NGVD) was the impounded area around the culvert, an additional 15% was creek-bank and low marsh area (1.0 to 1.45 m NGVD), and the remaining 65% of the surface was high marsh at 1.45 m NGVD or higher.

The calibrated model produced results in agreement with the upstream record (Figure 4.2a upper chart), although  $r^2$  of 0.92 for Drakes Island was the lowest value of the four study sites. The divergence between model and observed was most evident during spring tides (Days 9 to 13). For these tides, the model predicted a steeper rise in water level on the incoming tide and higher levels of impoundment than observed. A close examination of the upstream record indicated that observed upstream tidal heights were not always correlated with downstream tidal heights, and in fact, it appeared that upstream water levels experienced a delayed response to the highest tides. This effect was best seen around Day 11 (Figure 4.2a upper chart) when a 2.00 m downstream high tide produced a 1.47 m upstream water level, but the following 2.38 m high tide produced only a 1.44 m upstream water level. It appeared that increased upstream impoundment with building tides prevented downstream water from flowing into the marsh. In addition, the restricted upstream channel has been subject to stormwater flooding (ATTAR Engineering 1996), a factor not considered in this model. At Day 5, the upstream water levels increased by 5 cm although downstream tidal heights were receding, possibly a response to precipitation. In fact, National Climate Data Center rainfall records from Portland, Maine (approximately 30 miles north) indicated that a total of 0.8 inches of rain fell on Days 1, 2, and 3 (April 23-25 1996). Therefore, model agreement with upstream water levels may have been reduced at Drakes Island due to rainfall runoff, and possibly in connection with impoundment conditions that greatly reduced channel outflow during spring tides.

Drakes Island Hydrologic Scenarios. The persistence of brackish plant species and subsidence of marsh surface elevations (Burdick et al. 1999, Boumans et al. 2002), as well as stormwater flooding (ATTAR Engineering 1996), indicated that Drakes Island Marsh was a good candidate for hydrologic restoration. However, residential encroachment around the periphery of the marsh raised concerns that increased tidal flows might increase the potential for flooding (see Introductory Chapter, Study Sites). Therefore, the model was configured with two hydrologic scenarios that did not consider full tidal restoration of the site: Option\_1 simulated the installation of a second culvert adjacent to the original one, with an identical diameter of 0.91 m (3 ft) but 50 cm lower in elevation and with a flap gate to prevent tidal inflows; Option\_2 modeled the installation of a second culvert also 0.91 m in diameter and 50 cm lower in elevation, but without a flap gate. Simulations for these scenarios and comparisons with current conditions are presented in Figure 4.2c.

Scenario hydrographs (Figure 4.2c upper chart) showed that impoundment would be reduced with both options, but only Option\_2 produced tidal heights higher than current upstream conditions (peak heights were 1.58, 1.54, and 1.74 m NGVD for current conditions, Option\_1, and Option\_2, respectively). Reduction in impoundment during spring tides was best with the tide-gate option (Option\_1), with low water levels at 1.33, 1.01, and 1.21 m NGVD for current conditions, Option\_1, and Option\_2, respectively, at the height of the spring tide cycle (Day 13, Figure 4.2c upper chart). However, both scenario options reduced impoundment, with identical minimum low water levels of 0.89 m NGVD (compared with 0.95 m NGVD under current conditions).

Area of marsh flooded (Figure 4.2c lower chart) indicated that the tide gate for Option\_1 would reduce marsh flooding, with only the four highest tides flooding 50% or more of the marsh surface and a maximum of 63% of the marsh area flooded. This was a substantial reduction in flooding compared to current conditions, with ten of the highest tides flooding 50% or more of the marsh and a peak of 85% area flooded. The non-gated scenario, however, would greatly improve tidal exchange in the marsh, with 2/3 of the high tides (18 per two-week tidal cycle) flooding most of the marsh, and flood coverage for 97% of the marsh area. Since this configuration also reduced impoundment, Option\_2 would be recommended as the best management option of the two scenarios. This analysis, however, did not consider the potential impacts of stormwater flooding at the site, a factor outside the current scope of the model. Based on results found here and the ATTAR Engineering Report (1996), marsh response to stormwater should be examined closely before proceeding with hydrologic changes at Drakes Island.

Little River Current Conditions. Hydrographs for the Little River Marsh (Figure 4.3a upper chart) indicated that the recent installation of twin 1.83 m by 3.66 m (6 by 12 ft) box culverts at the site successfully restored natural tidal flows to the marsh (see Introductory Chapter, Study Sites). Upstream tides were closely aligned with the downstream signal, and achieved heights within ~15 cm of downstream high tides. On the ebb tide, residual water in the creek was about 20 cm deep, although as much as 50 cm of water stayed in the creek during the spring tide cycle (Days 0 to 4, Figure 4.3a upper chart). Marsh area flooded showed that 90% or more of the marsh surface was inundated on spring tides (about six tides per two-week tidal cycle), but most high tides

barely flooded above the creek banks (Figure 4.3a lower chart). Figure 4.3b showed that this was due to the steepness of the creek banks at the site (0 to 1.2 m NGVD) and the mostly flat topography of the marsh surface (90% of the marsh at 1.4 to 2.0 m NGVD). As a result, most of the marsh surface was either totally inundated or totally dry, depending on the height of the high tide.

The model-observed coefficient of determination for Little River was 0.97, indicating strong agreement between the upstream record and the model predictions (Figure 4.3a upper chart). Tidal peak estimates were within 3 cm of observed heights for all high tides except at Day 1 when the model was 20 cm low. Model low water estimates were also close to observed levels, but the model consistently predicted faster drainage on the ebb flows, especially during spring tides (Days 0 to 4, Figure 4.3a upper chart). This was likely due to the large expanse of tidal marsh at Little River Marsh (70 ha), a surface that clearly required a long time to drain after inundation by spring tides. The model attempted to simulate this condition with the flood effect calibration parameter (notice the slower drainage predictions during spring tides), but the very large marsh drainage area apparently caused more water to flow into the creek during the ebb tides than could be predicted by the model as formulated. In the past, the Little River Marsh was known to impound stormwater during rainfall events, a major impetus for the culvert expansion project (US Army Corps of Engineers 1999, Burdick 2002). It appeared, however, that this condition was improved with the new box culverts. During data collection at Little River, a single day 0.8-inch rainfall was recorded in the region (National Climate Data Center station at Portland, Maine, approximately 50 miles from

the site). However, observed upstream water levels showed little additional water on that date (Day 6 Figure 4.3a upper chart). In general terms, except for the timing of drainage after high tides, the calibrated model produced excellent results for the Little River Marsh.

Little River Hydrologic Scenarios. Little River Marsh was hydrologically restored in November 2000, therefore model simulations were used to examine the historic conditions of tidal restriction at the site. This type of analysis was used to provide a basis of comparison between past and current conditions, and as an assessment tool to measure the benefits of hydrologic restoration (i.e., “what-if” no changes were made). To configure this scenario, the model used the dimensions of the pre-restoration culvert (1.22 m diameter culvert pipe at 0.24 m NGVD invert elevation, US Army Corps of Engineers 1999). Scenario results are presented in Figure 4.3c.

The model indicated that past hydrologic conditions at Little River were severely restrictive of tidal flows, with peak tidal heights of only 1.32 m NGVD, and tidal ranges limited to 15–40 cm between ebb and flood tide (Figure 4.3c upper chart). These results were generally in agreement with the pre-restoration hydrologic studies conducted at the site that recorded low upstream tidal ranges (~50 cm by the US Army Corp of Engineers 1999, 20 to 66 cm by Burdick 2002). In addition, considerable impoundment of tidal water was predicted, with about 50 cm of retained water in the tidal creek at all times. Burdick (2002) recorded minimum low tide water levels of about 20 cm during neap tides, thus the predicted level of impounded water appeared to be overestimated by about

30 cm. However, the channel was dredged as part of the restoration effort, likely accounting for some of these differences since model predictions were based on calibrated results from current (dredged) conditions. In addition, increased water velocity through the channel following restoration had probably scoured sediments from the creek bottom (Williams et al. 2002) and produced areas of pooling at low tide.

The predicted area of marsh flooding (Figure 4.3c lower chart) suggested that pre-restoration spring tides only flooded about 10% of the total marsh area (7 ha) during the highest spring tides. Burdick (2002) reported that high tides rarely flooded the marsh surface, although rainfall events (especially in conjunction with spring tides) were capable of flooding most of the marsh. Overall, results from this scenario concurred with published reports that pre-2000 Little River Marsh was severely restricted in tidal flooding, and an excellent candidate for hydrologic restoration.

Mill Brook Current Conditions. Results for Mill Brook Marsh indicated that the project to expand the tidal culvert to 1.83 m (6 ft) in diameter had successfully returned natural tidal flows to the marsh. Tidal hydrographs for Mill Brook showed that upstream tidal heights typically reached downstream levels (maximum difference of 13 cm on Day 7, Figure 4.4a upper chart). Upstream drainage on the ebb tide was also closely matched with downstream results, indicating that impoundment was not an issue at Mill Brook following restoration. The area of marsh flooded during high tides showed a strong diurnal pattern throughout the tidal cycle (Figure 4.4a lower chart) and achieved 90% flooding during spring tides (Days 1 to 5). Hypsometry of Mill Brook indicated that the

tidal creek had steep banks (-0.5 to 1.0 m NGVD, Figure 4.4b), but the majority of the marsh surface was along a gradual slope from 1.0 to 1.6 m NGVD, until a sharp elevation break at the upland edge. The gradual slope in elevation accounted for the incremental changes in flooded area with the tidal cycle at Mill Brook (as opposed to the flat surface at Little River which was basically all flooded or all dry).

Model results for Mill Brook indicate strong performance of the calibrated model ( $r^2 = 0.97$ ). High tide peaks were very closely related, with differences less than 1 cm (Figure 4.4a, upper chart). However, the model consistently overestimated the amount of water left in the tidal creek on the ebb tide, by about 13 cm. Measures of creek water depths taken at low tide during the elevation survey in 2001 showed that about 25 cm of water were always in the creek (data not shown), suggesting that flow conditions have continued to change since the tidal signal was measured in 1998. Like Little River, it appeared that increased current velocity following culvert expansion had eroded the creek bottom and allowed more water to pool around the culvert entrance at low tide. In addition, Burdick et al. (1999) reported that sediments were deposited on the marsh at a very high rate between 1996 and 1998 (1.9 cm/yr). Evidence of channel erosion and sediment redistribution appeared similar to the geomorphic responses of hydrologically restored tidal marshes along the US west coast. Simenstad and Thom (1996), at the Gog-Le-Hi-Te estuarine site in Washington state, found extensive accretion of inorganic sediments on the marsh immediately following introduction of tides, with fine sediments moved from the marsh surface into tidal channels during later years. Williams and Orr (2002) also found that sediment re-suspension and deposition followed tidal restoration in



San Francisco Bay marshes, and concluded that these geomorphic processes were critical determinants of habitat development and re-vegetation for tidal mudflats. Since post restoration changes in channel morphology (as suspected at Mill Brook and Little River) can influence long-term marsh tidal prism and sediment formation, hydrogeomorphology would appear to be another important consideration for planners of tidal restoration projects (Simenstad and Thom 1996, Williams et al. 2002).

Mill Brook Hydrologic Scenarios. A hydrologic scenario for Mill Brook was configured with pre-restoration conditions to provide a basis for assessing changes due to hydrologic restoration at the site, similar to the scenario provided for Little River. This model run, however, simulated the use of a tidal flap gate at Mill Brook (Burdick et al. 1997), which prevented tides from flowing onto the marsh surface. Scenario results for pre-restoration Mill Brook water levels and tidal flooding are presented in Figure 4.4c.

Model simulations from pre-restoration showed no upstream tidal signal, with the model preventing all tides from flowing through the culvert (Figure 4.4c upper chart). Burdick et al. (1997 and 1999), however, reported that remnant populations of halophyte plant species were found near the culvert prior to 1993, suggesting that some tidal flows were passing through the flap gate. Since specifications for tide gate flows were not available, the model assumed that the marsh was completely shut off from tidal sources. Area of marsh flooded (Figure 4.4c lower chart) predicted that only a few centimeters of water would cover the creek bottom. Upstream flooding at the site prior to restoration has not been documented, although floods following snow melt were observed in early

spring (D. Burdick, personal communication). In any case, the model predicted a complete elimination of tidal flows at Mill Brook before the tide gate was removed in 1993.

Oak Knoll Current Conditions. Tidal hydrographs for Oak Knoll Marsh in Rowley, Massachusetts (Figure 4.5a upper chart), showed that the upstream tidal range was reduced in comparison with downstream levels due to undersized culverts of 0.61 m (24 in) in the north and 1.03 m (40 in) in the south. Upstream tidal heights were as much as 50 cm less than downstream heights during spring tides (Days 0 to 4), although this difference was reduced to ~10 cm at neap tides. Water was not severely impounded upstream, however, and creeks were generally drained on the ebb tide except for the highest spring tides. The area of tidal flooding was 90% or more during the four highest spring tides, although a large area of the marsh surface (>90%) remained above water for more than 2/3 of high tides (Figure 4.5a lower chart). The hypsometric curve at Oak Knoll (Figure 4.5b) indicated that the marsh contained few creeks (~5% of the marsh from 0 to 1 m NGVD) and a large portion of the marsh was very flat (1 to 1.3 m NGVD). Also, Boumans et al. (2002) found that the upstream high marsh was 16 cm lower than downstream high marsh, suggesting that the Oak Knoll marsh surface was subsided in response to long term tidal restriction at the site (DeLaune et al. 1983, Boumans and Day 1994, Chapter III).

Calibrated model estimates for upstream water heights strongly agreed ( $r^2 = 0.97$ ) with the upstream measures at Oak Knoll. Differences between model and observed

results were most evident at the tidal peaks (Figure 4.5a upper chart). During the highest of the spring tides (Days 0 to 4), the model overestimated the peak heights by ~10 cm. As the tidal cycle diminished, the model underestimated peak heights by a similar amount. These inconsistencies were most likely due to the presence of two separate culverts at the site (~100 m apart, Introductory Chapter, Figure I.5), which may have invalidated the model assumption of hydrologic connectivity among all inflows. The model pooled together flows from both culverts, but comparative upstream water levels were recorded only at the north culvert (see Methods). To achieve an optimal  $r^2$ , model peak flows were calibrated to an average set of tidal conditions that were representative of most tides but missed the extremes of the tidal cycle. Despite these differences, the model appeared to capture the nature of the tidal restriction at Oak Knoll, and provided an adequate basis for scenario modeling.

Oak Knoll Hydrologic Scenarios. Habitat degradation associated with tidal restriction at Oak Knoll was indicated by expansion of brackish plant species and reduction in substrate salinities (Burdick et al. 2001), and by subsidence of marsh surface elevations (Boumans et al. 2002, Chapter III). To assess potential hydrologic improvements in the marsh, the model was configured with two hydrologic restoration scenarios: Option\_1 simulated expansion of the north culvert diameter to 1.22 m (4 ft); Option\_2 modeled expansion of both north and south culvert pipes to the approximate width of the tidal creeks, 1.52 m (5 ft). Simulations for these scenarios and comparisons with current conditions are presented in Figure 4.5c.

Scenario hydrographs (Figure 4.5c upper chart) showed that upstream tidal heights would be increased with both options, especially during spring tides (Days 0 to 4). Peak tidal heights were 1.27, 1.32, and 1.39 m NGVD for current conditions, Option\_1, and Option\_2, respectively. In addition, no water was retained in the creeks on the ebb tide, even for spring tides. The area of marsh flooded (Figure 4.5c lower chart) was increased with both options, with 90% or more of the marsh flooded by five (Option\_2) or six (Option\_1) high tides, a modest increase from four tides under current conditions. However, both scenarios added substantially (5% to 20% increases) to the percent of area flooding during spring tides. The scenario for expansion of both culverts (Option\_2) also increased area flooding for several non-spring tides (Days 5 to 8). Based on these results, hydrologic restoration appeared to be a good management option for improving salt marsh habitat at Oak Knoll. Since increases in peak flooding during spring tides were similar for both scenarios, the lower-cost option (Option\_1, expansion of the north culvert only) appeared to be a reasonable management recommendation for potential restoration work at the site.

Sensitivity Analysis. The results of model sensitivity analysis for calibration parameters are presented in Table 4.2. Since relative sensitivity was calculated as the percent difference in peak upstream water level divided by percent difference in parameter value (5% to 20%), this analysis indicated low overall model sensitivity to any one calibration parameter (all values < 1). In addition, the analysis suggested a fairly consistent balance among model parameters, with maximum sensitivity values ranging from 0.195 to 0.336. On a relative scale, the model was slightly more sensitive to peak

tide head threshold than the other calibration parameters. This parameter adjusted upstream water volume during spring tides, and therefore would have a direct effect on the sensitivity metric, peak upstream water level. Overall, however, results from this analysis indicated that the calibration parameters were useful to fine-tune the model, but model output was largely determined by site-specific inputs from field data sources (i.e., downstream signal, culvert dimensions, and marsh elevations).

### Conclusions

Tidal hydrology is of critical importance in salt marshes, and marshes with restricted tidal flows are often characterized by lost or degraded natural habitat. Since restoration of tidal hydrology can lead to habitat recovery, management options for tidally-restricted salt marsh sites include hydrologic alteration of tidal culverts and channels. A calibrated model was used to simulate current flow conditions and marsh flooding over a two-week tidal cycle, at four New England salt marshes with past or present tidal restrictions. The model used recorded measurements of the downstream tidal signal, culvert dimensions, and elevation survey results as inputs, and a set of calibration parameters were used to fine-tune the model for each location. Calibrated model results for upstream tidal heights were compared with recorded upstream measurements to assess model performance. At three sites, the predicted-observed  $r^2$  was 0.97, and 0.92 was achieved at the other site (Drakes Island). Differences between predictions and observations were likely due to model limitations in handling extreme impounding conditions and stormwater runoff (Drakes Island), and conditions that may

have invalidated the model assumption of hydrologic connectivity (Oak Knoll). In general, however, the calibrated model produced estimates in strong agreement with observations across a range of marsh hydrologic conditions.

Based on the calibrated upstream model, inflow conditions were manipulated in a series of hydrologic scenarios to assess the potential impacts of altered tidal hydrology for each site. Tidal restoration sites (Little River and Mill Brook) were configured with culvert dimensions prior to restoration, and the model generated upstream results with greatly diminished (Little River) or non-existent (Mill Brook) tidal water levels and marsh flooding, as appropriate for each site. At the tidally-restricted sites (Drakes Island and Oak Knoll), restoration scenarios were conducted for each site based on practical considerations of site-specific hydrologic options. For both sites, the model identified restoration scenarios that improved tidal exchange, reduced impoundment, and increased marsh flooding. These results suggested that the model would be beneficial as a decision-support tool for coastal resource managers considering multiple options for hydrologic restoration of degraded marshes. In addition, model projections of flood regime could be used, together with salinity regime, to produce estimates of salt marsh gradient conditions that are critical determinants of plant community structure.

	<b>Parameter Name</b>	<b>Drakes Island</b>	<b>Little River</b>	<b>Mill Brook</b>	<b>Oak Knoll</b>
<b>Marsh Parameters</b>					
Creek elevation at culvert (m)	creek_el	0.870	0.041	-0.280	-0.450
Marsh elevation at culvert (m)	marsh_el	1.580	1.500	1.20	1.000
Calibrated creek slope	creek_sl	.00020	.00006	.00060	.00012
Calibrated initial water level (m)	wlevel_init	0.20	1.00	0.45	0.00
Calibrated flood effect (m)	floodeffect	0.00	1.60	0.00	0.00
Calibrated peak threshold reduction	headthresh	0.00	0.52	0.40	1.00
<b>Culvert 1 Parameters</b>					
Type	cultype_1	Barrel	Box	Barrel	Barrel
Diameter (ft)	culdiam_1	3.00	N/A	6.00	2.00
Width (ft)	culwidth_1	N/A	6.00	N/A	N/A
Height (ft)	culheight_1	N/A	12.00	N/A	N/A
Length (ft)	cullen_1	63.00	252.00	60.00	70.90
Invert elevation (m)	thresh_1	0.947	0.250	-0.400	-0.428
Kutters roughness coefficient	kutter_1	0.024	0.012	0.024	0.012
Flap gate	flap_1	0	0	0	0
Calibrated upstream conductivity	upcond_1	0.32	1.00	0.32	0.80
<b>Culvert 2 Parameters</b>					
Type	cultype_1	N/A	Box	N/A	Barrel
Diameter (ft)	culdiam_2	N/A	N/A	N/A	3.38
Width (ft)	culwidth_2	N/A	6.00	N/A	N/A
Height (ft)	culheight_2	N/A	12.00	N/A	N/A
Length (ft)	cullen_2	N/A	252.00	N/A	70.90
Invert elevation (m)	thresh_2	N/A	0.250	N/A	-0.428
Kutters roughness coefficient	kutter_2	N/A	0.012	N/A	0.024
Flap gate	flap_2	N/A	0	N/A	0
Calibrated upstream conductivity	upcond_2	N/A	1.00	N/A	1.00

Table 4.1. Hydrologic and elevation parameter values for current conditions at study sites.

<b>Calibration Parameter</b>	<b>+5%</b>	<b>-5%</b>	<b>+20%</b>	<b>-20%</b>
Creek slope	0.005	0.195	0.051	0.149
Upstream conductivity	0.113	0.238	0.001	0.019
Flood effect	0.007	0.001	0.216	0.027
Peak tide head threshold	0.190	0.007	0.203	0.336

Table 4.2. Relative sensitivity of peak upstream water level to  $\pm 5\%$  and  $\pm 20\%$  adjustments in baseline calibration parameter values. Relative sensitivity was calculated as % change in model-observed peak upstream water level divided by % change in parameter.



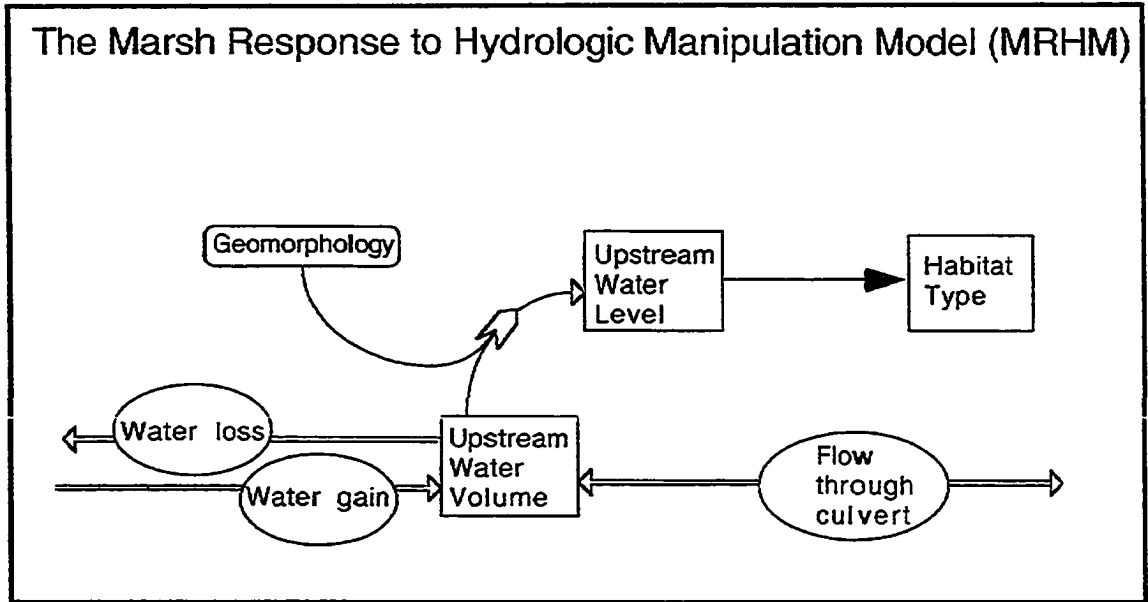


Figure 4.1. Conceptual diagram of water level change in salt marshes, including marshes with tidal restrictions, from Boumans et al. (2002).

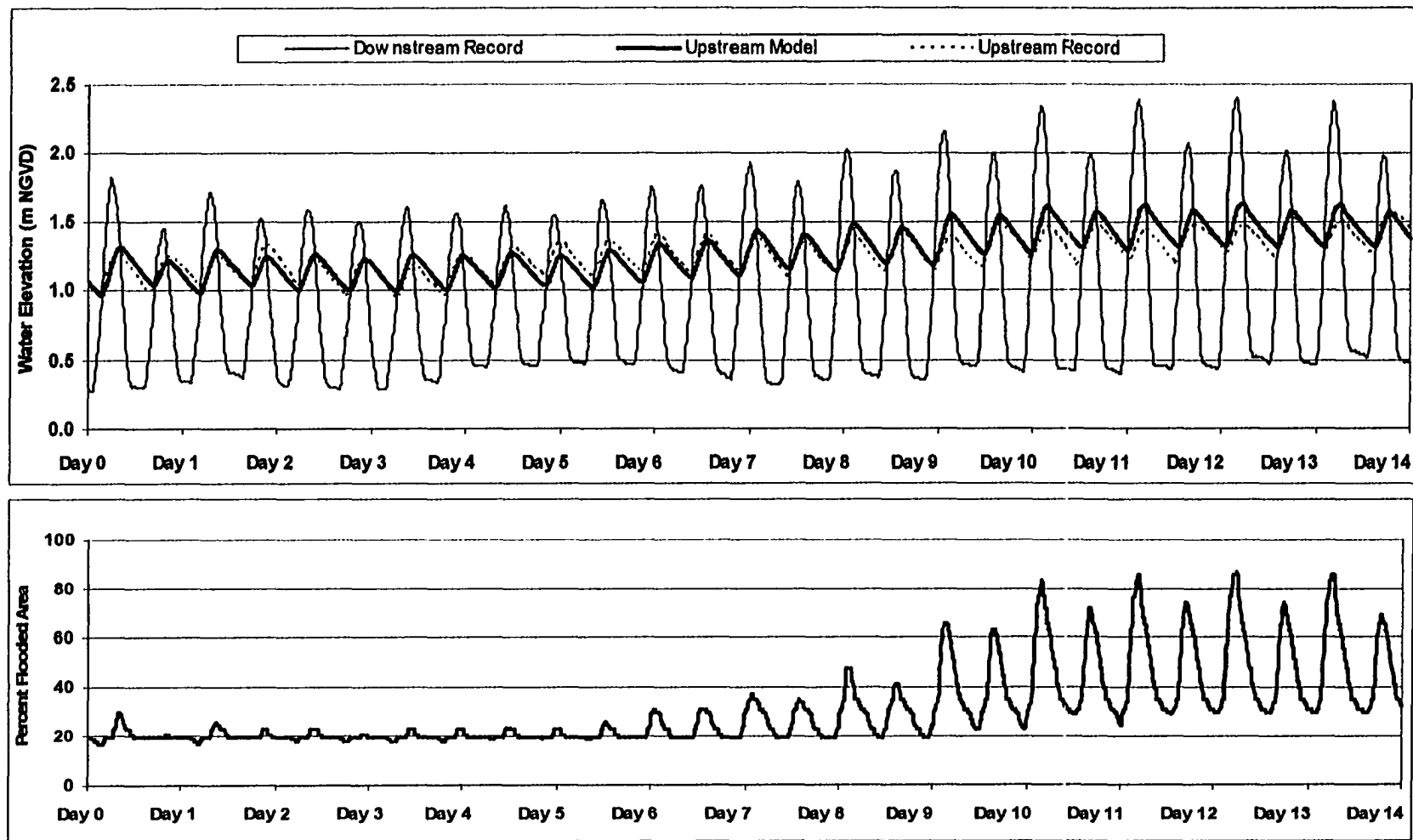


Figure 4.2a. Drakes Island current hydrologic conditions for 14-day tidal cycle; Upper chart: tidal hydrograph of water elevations (m NGVD) for downstream record, upstream model, and upstream record; Lower chart: tidal flooding of marsh area.

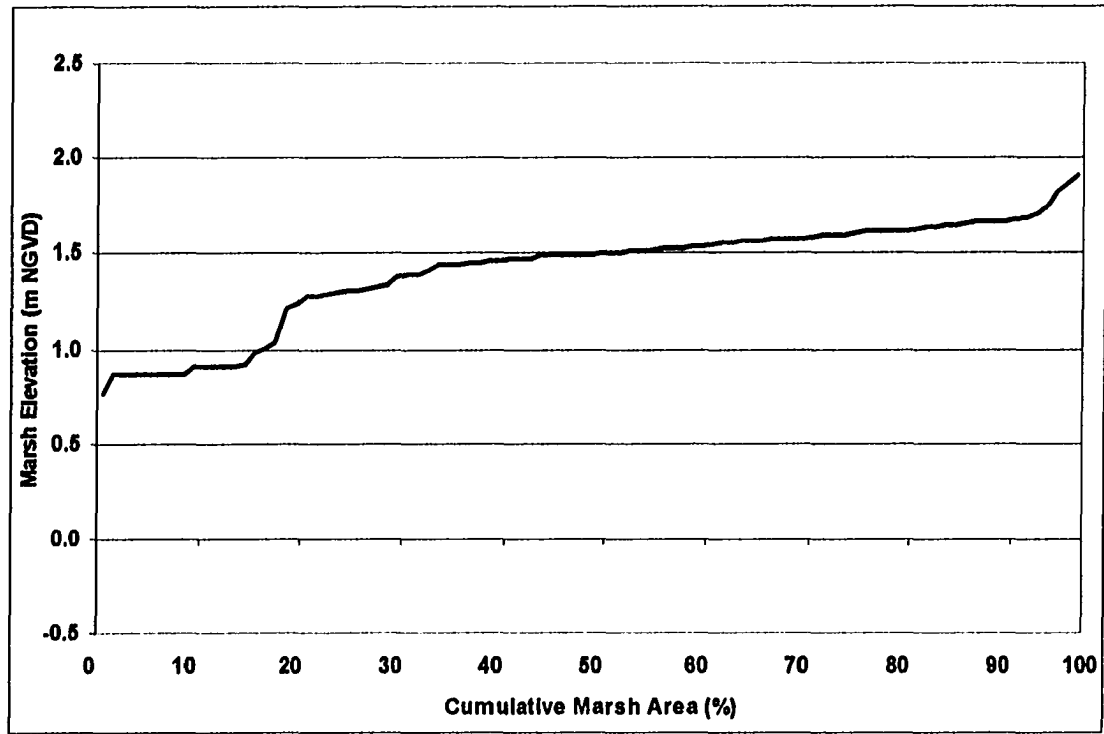


Figure 4.2b. Drakes Island hypsometric curve, showing cumulative marsh area (%) by elevation (m NGVD).

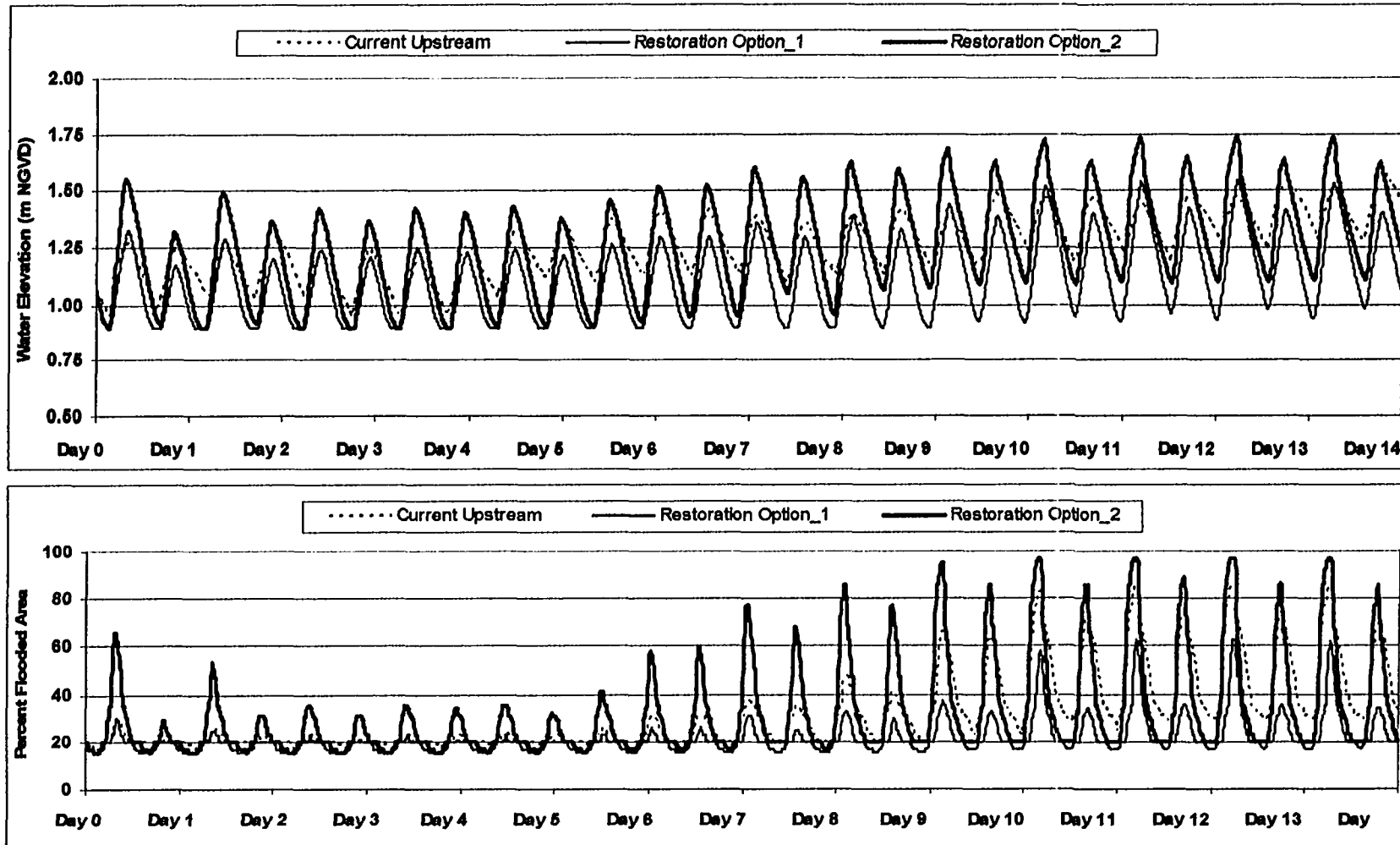


Figure 4.2c. Drakes Island restoration scenarios (Option\_1 added 0.91 culvert 50 cm below current w/flap gate, Option\_2 added 0.91 culvert 50 cm below current w/out flap gate). Upper chart: Upstream water levels; Lower chart: Area of marsh flooded.

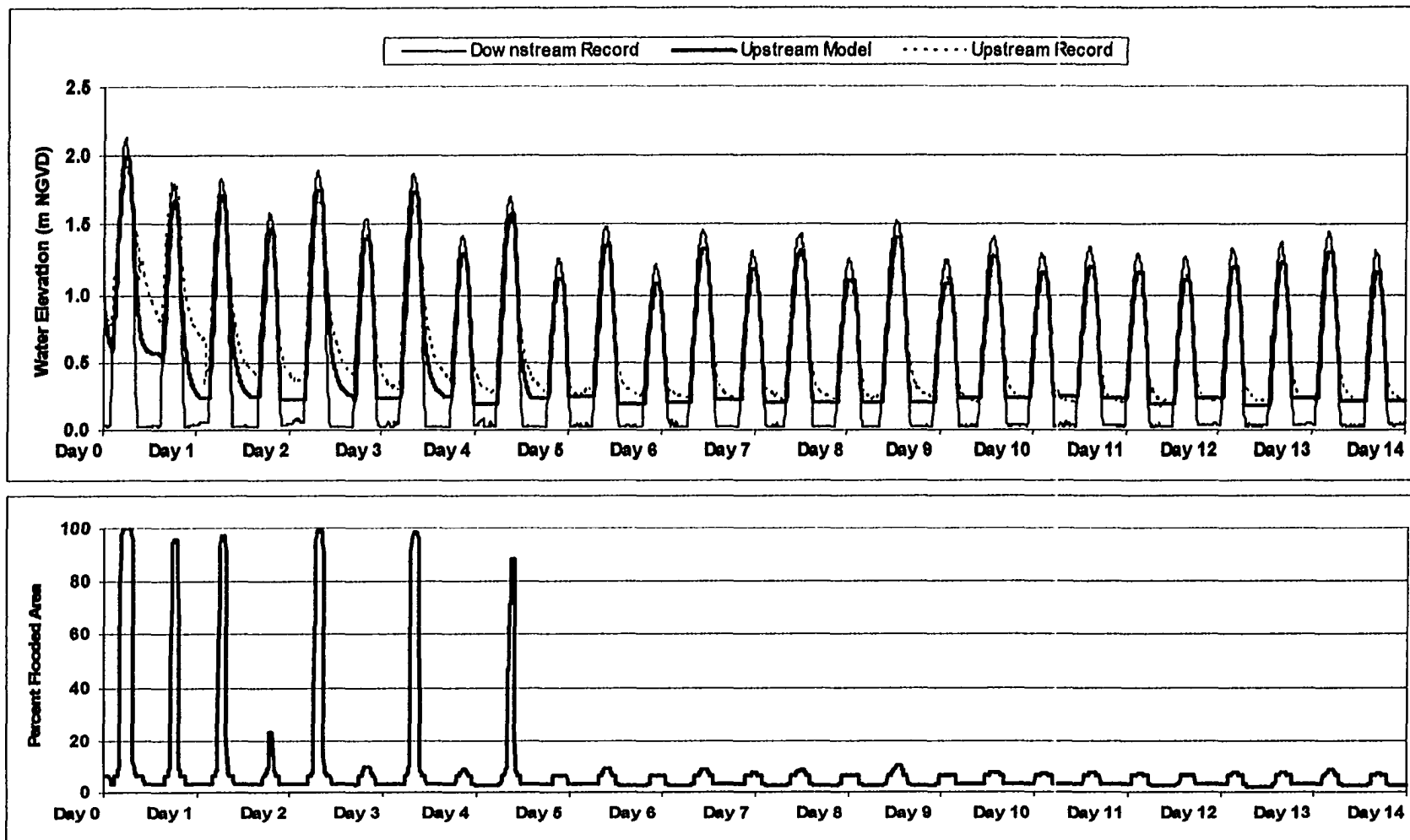


Figure 4.3a. Little River current hydrologic conditions for 14-day tidal cycle; Upper chart: tidal hydrograph of water elevations (m NGVD) for downstream record, upstream model, and upstream record; Lower chart: tidal flooding of marsh area.

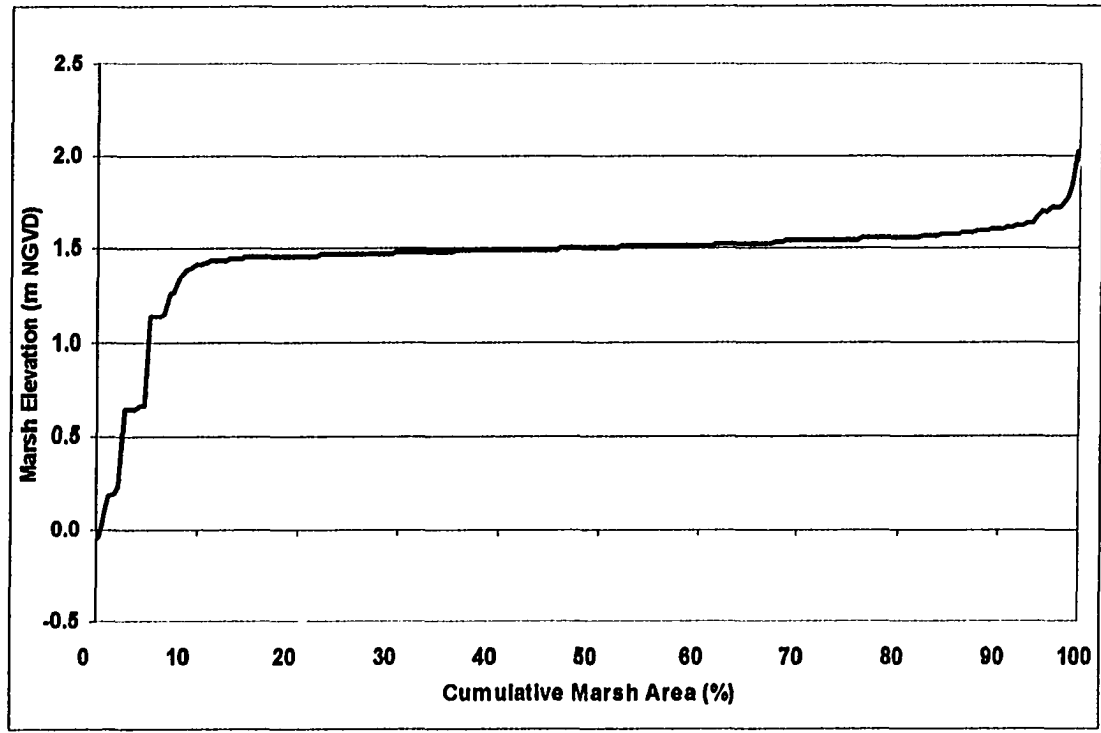


Figure 4.3b. Little River hypsometric curve, showing cumulative marsh area (%) by elevation (m NGVD).

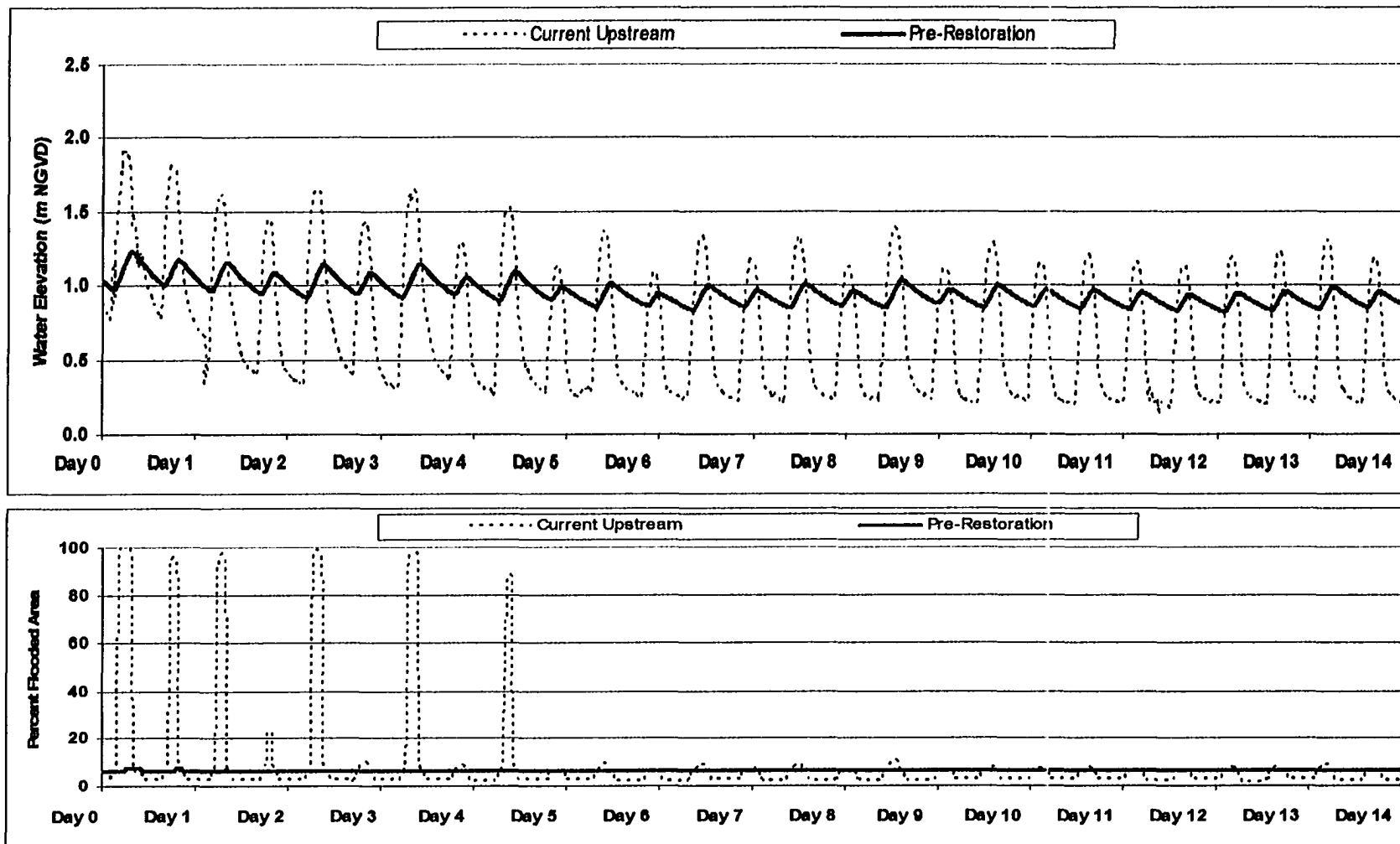


Figure 4.3c. Little River hydrologic scenario for pre-restoration conditions (1.22 m diameter culvert at 0.24 m NGVD invert elevation). Upper chart: Upstream water levels; Lower chart: Area of marsh flooded.

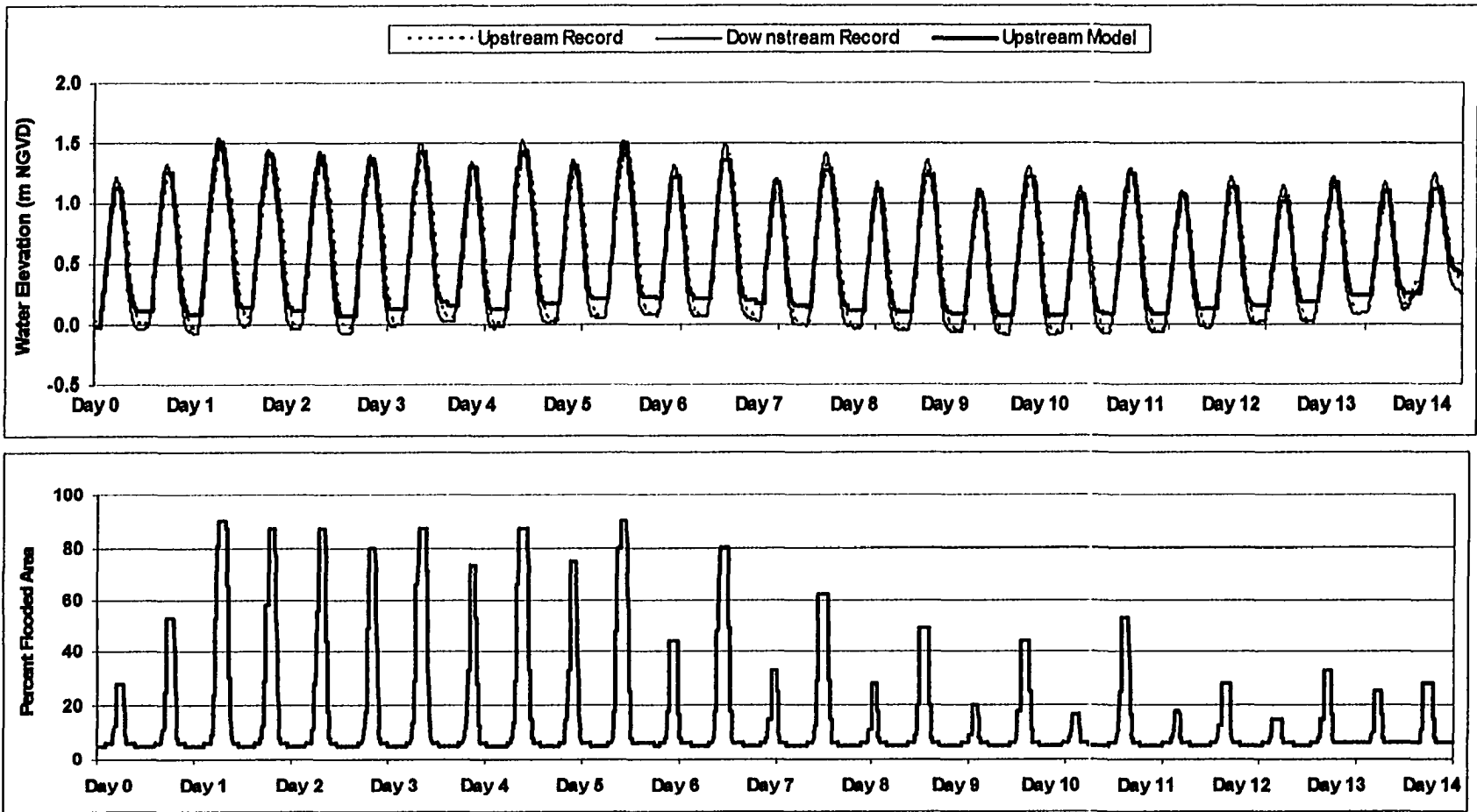


Figure 4.4a. Mill Brook current hydrologic conditions for 14-day tidal cycle; Upper chart: tidal hydrograph of water elevations (m NGVD) for upstream record, downstream record and upstream model; Lower chart: tidal flooding of marsh area.



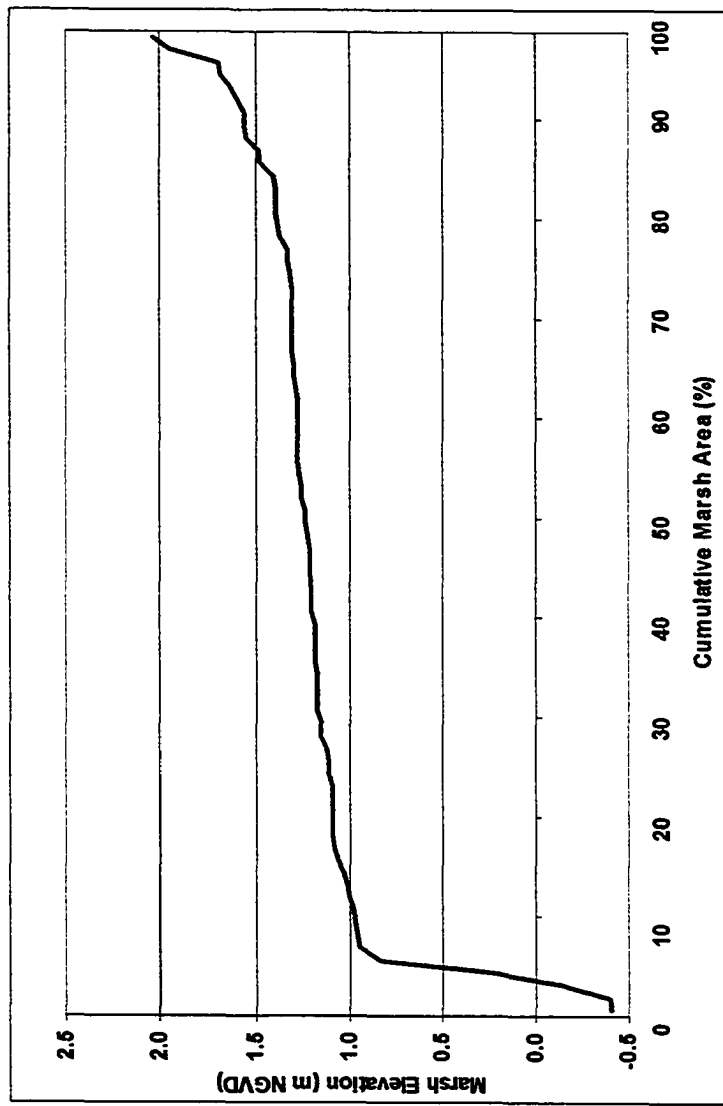


Figure 4.4b. Mill Brook hypsometric curve, showing cumulative marsh area (%) by elevation (m NGVD).

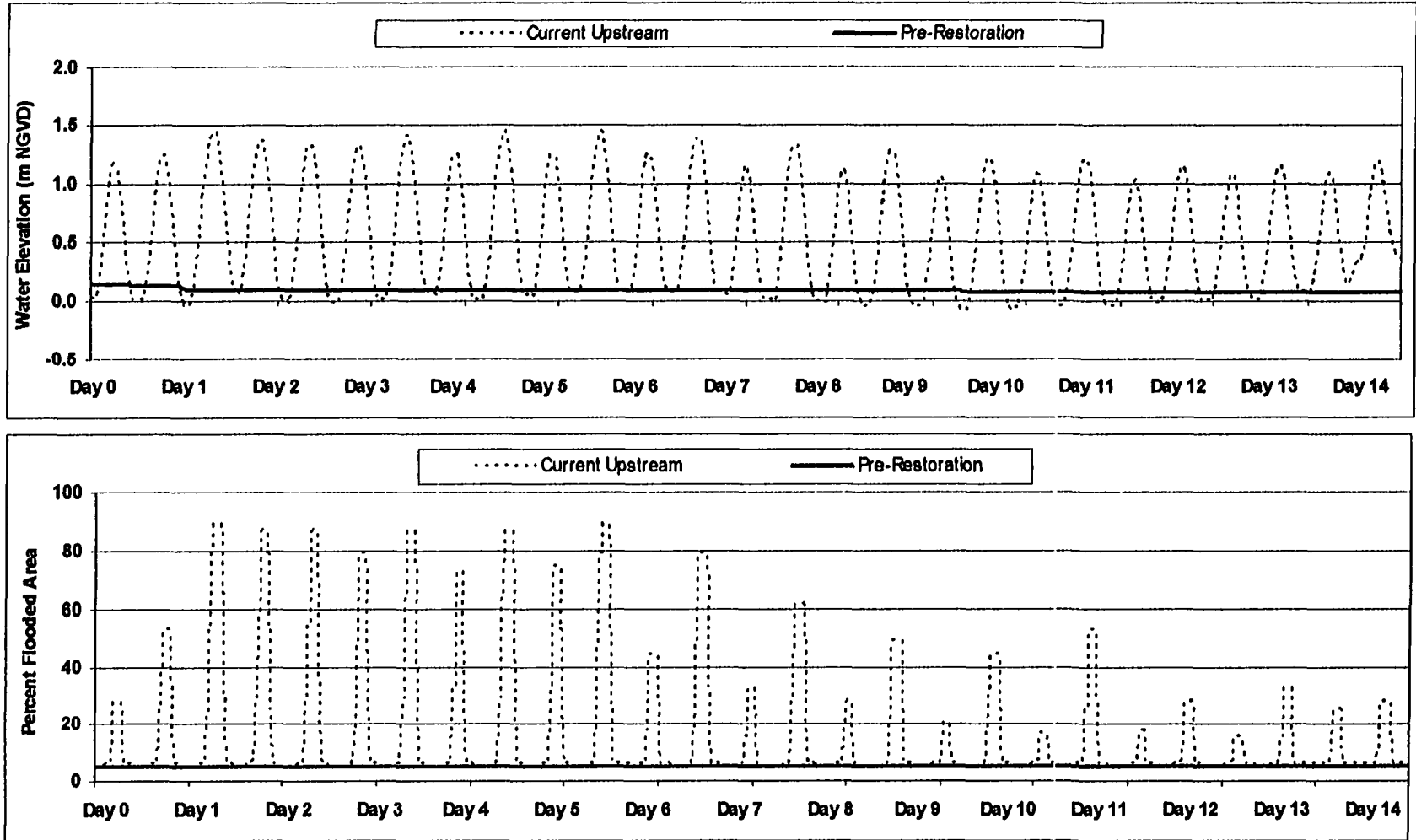


Figure 4.4c. Mill Brook hydrologic scenario for pre-restoration conditions (0.91 m diameter culvert with flap gate to prevent tidal inflow). Upper chart: Upstream water levels; Lower chart: Area of marsh flooded.

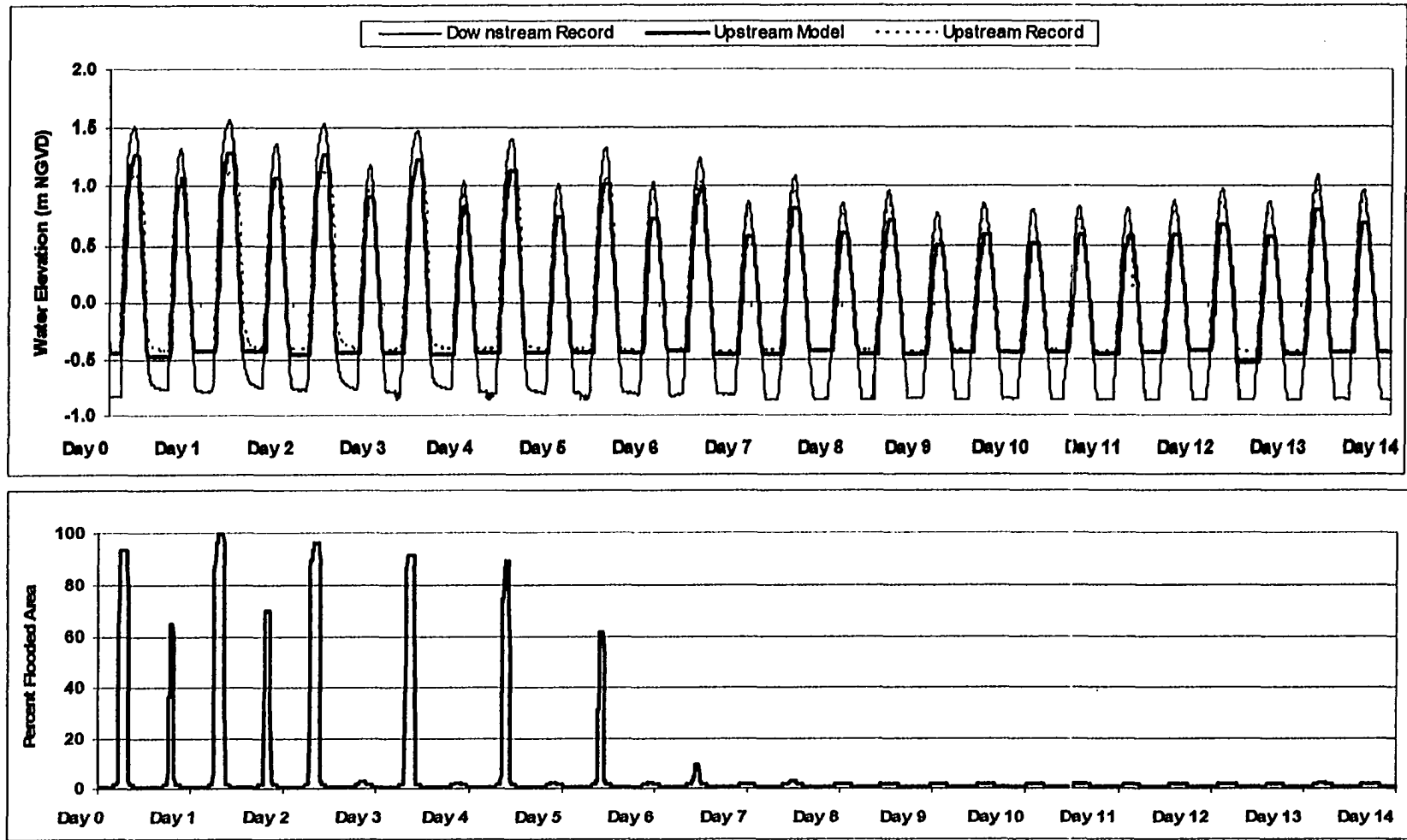


Figure 4.5a. Oak Knoll current hydrologic conditions for 14-day tidal cycle; Upper chart: tidal hydrograph of water elevations (m NGVD) for upstream record, downstream record and upstream model; Lower chart: tidal flooding of marsh area.

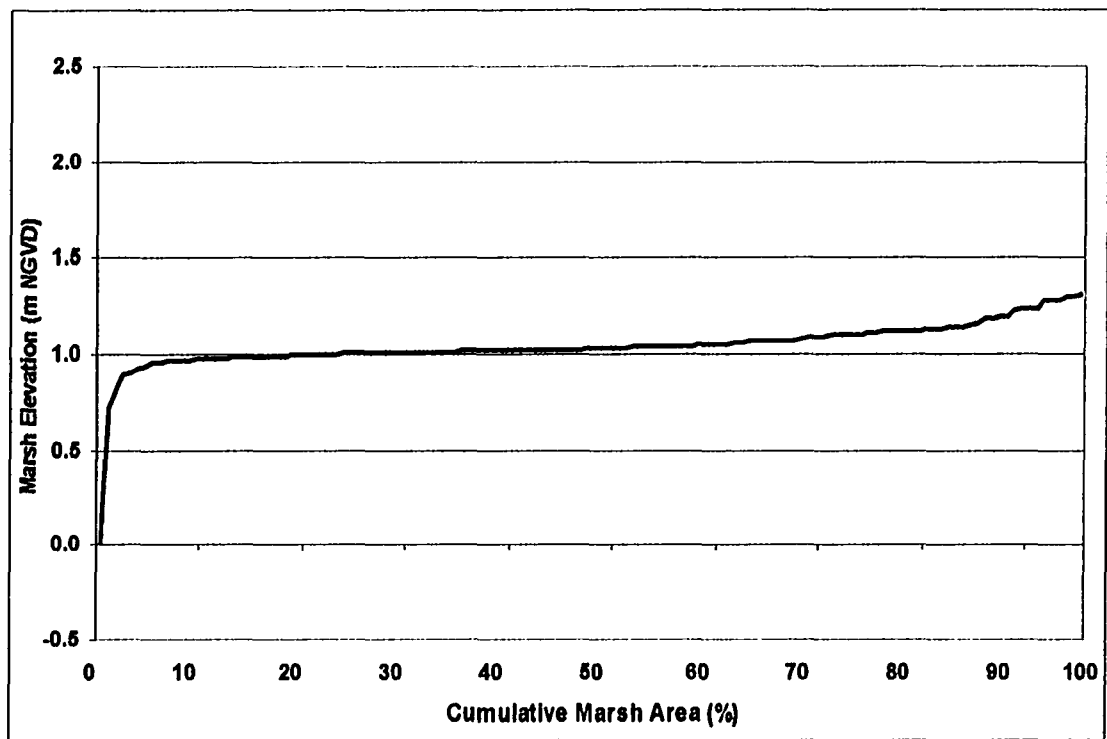


Figure 4.5b. Oak Knoll hypsometric curve, showing cumulative marsh area (%) by elevation (m NGVD).

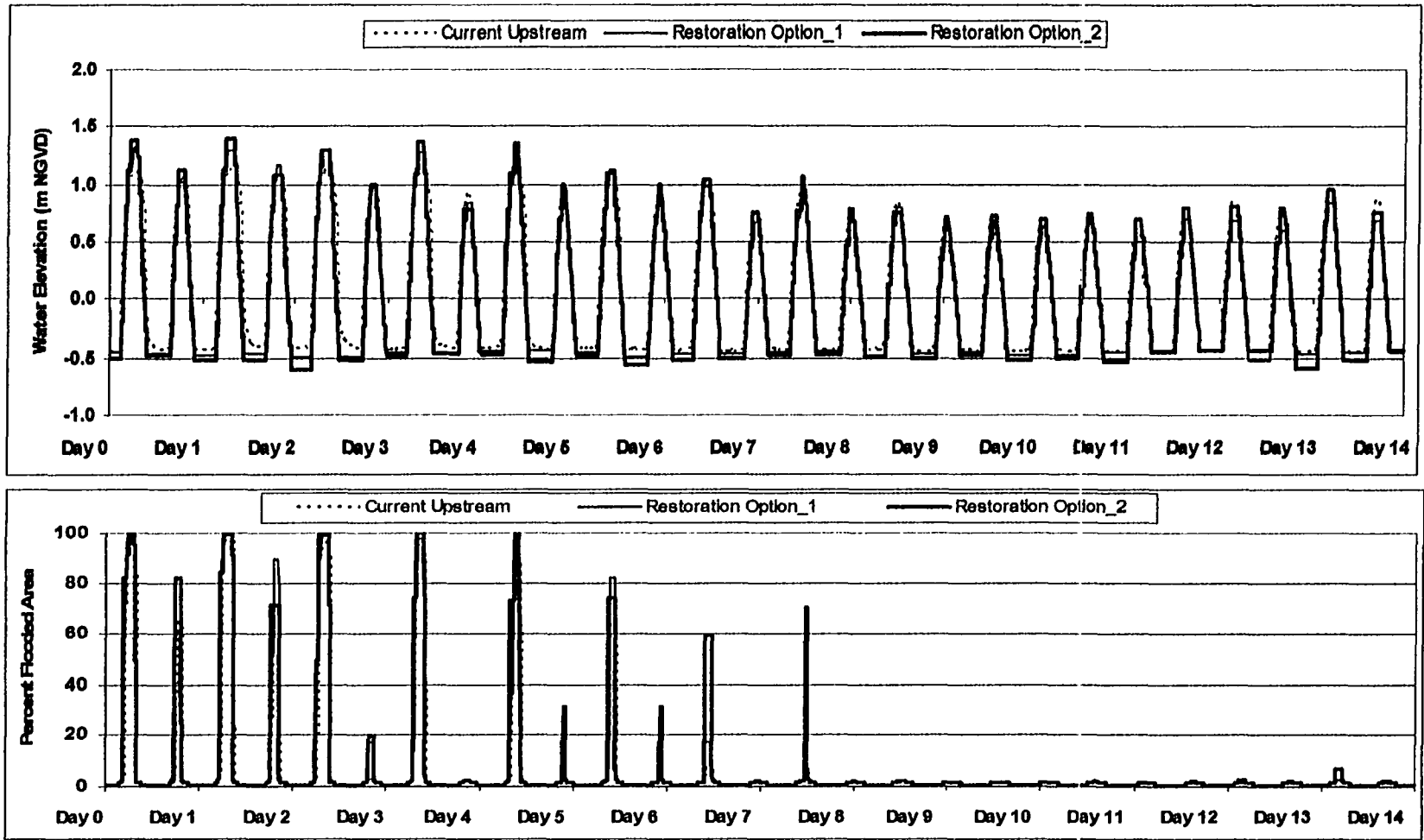


Figure 4.5c. Oak Knoll hydrologic restoration scenarios. Option\_1: expand north culvert to 1.22 m diameter; Option\_2: expand north and south culverts to 1.52 m diameter. Upper chart: Upstream water levels; Lower chart: Area of marsh flooded.

## **CHAPTER V**

### **A MODEL OF PLANT SUCCESSION FOLLOWING HYDROLOGIC DISTURBANCE IN NEW ENGLAND SALT MARSHES**

#### **Introduction**

Anthropogenic alterations that restrict tidal flows negatively impact many New England salt marshes, and attempts to restore tides to these sites are often met with unexpected or less than optimal results (see Introductory Chapter). Restoration planners may be hindered by a lack of synthesized information regarding important salt marsh factors that control the response of marsh plant species to hydrologic changes. These factors include physical processes like marsh sediment dynamics (Chapter III) and tidal hydrology (Chapter IV), but also biotic processes such as plant biomass production (Chapter II), stress tolerance, and plant competition. This chapter describes a computer model that simulates the response of common salt marsh plant communities to physical stress and interspecific competition. The model is an important component of an

integrated ecosystem model that predicts changes to plant community species composition in response to hydrologic modification.

In New England, native marsh halophytes like cordgrass (*Spartina alterniflora*), salt hay (*Spartina patens*) and black grass (*Juncus gerardii*) are often replaced by the invasive species common reed (*Phragmites australis*), purple loosestrife (*Lythrum salicaria*) and narrow-leaf cattail (*Typha angustifolia*) as tidally-restricted salt marshes convert to less-saline habitats (Roman et al. 1984, Sinicrope et al. 1990, Burdick et al. 1997). However, reintroduction of tidal flows to brackish marsh sites can reverse plant species replacement, causing die-back of invasive species and promoting increased cover of salt-tolerant plants (Roman et al. 1984, Sinicrope et al. 1990, Burdick et al. 1997, Streever and Genders 1997, Roman et al. 2002, Warren et al. 2002). In either case, the alteration of marsh tidal hydrology is a disturbance event that leads to changes in community composition with respect to these six important plant species. To predict plant community response to changing hydrologic conditions, a detailed species-level understanding of plant succession dynamics must first be acquired.

Plant succession, the directional change of species composition over time, is a long-held concept and a fundamental ecological principle, dating back to two opposing views from the early part of last century: F.C. Clements' "organismic" concept of plant communities as a single entity of interdependent units, and H.A. Gleason's "individualistic" concept of communities as loose associations of species (Richardson 1980). But despite nearly a century of scientific attention, the relative importance of

processes that influence and control plant succession remain a topic of considerable debate. Of the potential factors that may influence species compositional change over time, differences in plant life-history strategies (growth and reproductive characteristics) have long been recognized as key determinants (Connell and Slayter 1977). Grime (1979) developed a theory of succession based on a grouping of species with similar life-history strategies, and proposed that changes in species composition follow a progression from ruderal colonizers, to competitors, to stress tolerators. Tilman (1982, 1988), however, theorized that competition was always present, and, as resource availability shifted with stages of succession, relative allocations to above or belowground structures favored different species at different times. Huston (1979) pointed out that physical disturbance was the trigger mechanism that reset resource conditions and enabled the entire process.

Computers have long been used to simulate plant succession. In fact, some of the earliest uses of computer technology in the field of ecology were probabilistic models of forest succession (Shugart et al. 1973, Horn 1975, Shugart and West 1976). In 1977, Zieman and Odum developed a computer model of salt marsh plant succession for areas of dredge spoil, based on correlative measures of *Spartina alterniflora* growth as a function of physical factors (Mitsch and Gosselink 1993). Sklar et al. (1985) constructed a spatial model of coastal wetland succession that switched between broad categories of habitat type (from upland to open water) with annual fluxes in freshwater inputs and sediment loads. Recently, Boumans et al. (2002) modeled marsh zones upstream of tidal culverts and plant response to hydrologic modification as a reflection of downstream



plant communities at similar elevations. These models, however, failed to consider the specific impacts of disturbance and succession on plant communities, and the individual response of plant species to changes in physical stress and competitive conditions. Therefore, to meet the objectives of the current project (i.e., a spatially-explicit model of plant community change, see Introductory Chapter), a fine-scale, species-driven approach to succession modeling was needed.

In New England salt marshes, experimental evidence strongly suggests that both life-history strategies and species interactions dictate the presence or absence of plant species assemblages, and changes in species composition over time. Bertness and Ellison (1987), in a landmark study, found that New England salt marsh plant species were excluded from areas by physical stress or competition, and concluded that physical stress tolerance and interspecific competition were the key determinants of spatial vegetation patterns. Further investigations have shown that not all salt marsh plant species interactions are negative, and that positive interactions (facilitations) may also be very important following disturbance (Bertness 1991a, Bertness and Hacker 1994, Bertness and Yeh 1994). In addition, marsh species recruitment from neighboring plants through clonal expansion (Brewer et al. 1998, Chambers et al. 1999) and seed dispersal (Rand 2000) can also influence patterns of distribution. Other potential factors, such as herbivory, disease, and allelopathy, have shown little evidence of major roles (although Silliman and Zieman 2001 found that *Spartina alterniflora* consumption by periwinkles may have been important in a Georgia marsh). It appears, then, that New England salt marsh plant succession is primarily a function of three factors: physical stress tolerance,

species interactions, and recruitment potential. These three factors were combined to model salt marsh plant succession following hydrologic disturbance.

### **Model Background**

To develop a fine-scale succession model, relative measures of physical stress tolerance, competitive ranking, and recruitment potential were derived for six dominant plant species common to healthy and impacted New England salt marshes. Species-specific measures of physical stress tolerance and relative competitive rankings were determined in a transplant experiment conducted across a gradient of salt marsh salinity and elevation conditions (see Chapter I). Recruitment potential was based on plant species composition in neighboring plots. To simulate hydrologic disturbance, a hypothetical marsh plot was assigned to one of nine marsh gradient locations for flood and salinity regime (Figure 5.1), according to a series of model scenarios. For example, to simulate the impacts of restored salt water flooding to low-lying marsh zones, the scenario would call for a low elevation and high salinity plot location. Similarly, a plot assignment of high elevation and low salinity would be used to model the impacts of tidal restriction at a location adjacent to the upland edge. Within a plot, the model tracked the percent of marsh area occupied by each of the six plant species. Changes in species composition percentages over time were used as the model metric for quantifying plant succession.

For each species in the hypothetical plot, the model estimated the specific tolerance of physical stress conditions and the likelihood that the species would continue to exist at the gradient location. To simulate the likelihood of persistence at a gradient location, a portion of each species cover value was determined to be “at-risk” for replacement by another plant species. If a species had demonstrated poor survival and growth at the location, the model designated a high percentage of species cover to the at-risk pool (up to 100% if no survival was measured). For a species that did well at the location, only a minimal percentage (5%) of cover was assigned to the at-risk pool. With this scheme, a species that performed well at a gradient location was highly resistant to replacement, based on the preemptive advantage of established wetland plants identified by Grace (1987).

Species performance at each gradient location was determined by a relative tolerance factor, derived from a field experiment (Chapter I). Tolerance factors were standardized values, ranging from 0 to 1, that reflected species growth and survival at a gradient location (0=no survival, 1=best growth and survival among all locations, Table 1.6). These factors produced an array of best-performance locations distributed across the study gradient, with only one plant scoring best for most gradient locations. The one exception was the low salinity - high elevation location, which was best for both *Typha* and *Phragmites*. Therefore, algorithms developed using these tolerance factors were used to control the distribution of plant species across a matrix of marsh gradient locations, with only minor adjustments needed to break the *Typha-Phragmites* tie (see Special Handling for Low Salinity-High Elevation Location, Methods).

The model simulated succession by allocating the at-risk pool to all of the plant species present in the plot. For each species, the likelihood of receiving an allocation from the at-risk pool was based on three succession factors: stress tolerance of plot conditions, competitive ranking versus other species in the plot, and the species composition of neighboring plots. As described, stress tolerance was quantified by tolerance factors (Table 1.5). Like tolerance factors, competitive rankings among the species were identified by a set of combination-specific competition factors, based on the results of a field experiment (Chapter I). Interspecific arrangements of plant species were analyzed to determine, for each combination, reduction in growth (competition factor < 1) or improved growth (competition factor > 1) in the presence of a competitor. Differences in competition factors for each species combination were used to allocate from the at-risk pool. In addition, the species composition of neighboring marsh plots was used as a measure of recruitment. If neighboring plots were, for example, dominated by *Phragmites*, a portion of the at-risk plot area would be allocated to common reed as a simulation of clonal expansion and seed dispersal. In this manner, the three succession factors (tolerance, competition, and recruitment) were combined to predict changes in species composition for each modeling scenario that was considered.

Within the processing logic of the model, the relative importance of the three succession factors was varied by gradient location, based on the concept that the relative importance of physical stress tolerance and competition changes with salt marsh environmental conditions. Bertness and Ellison (1987) found that physical tolerance of

flood and salinity was most important in the high-stress areas of low marsh, but interspecific competition was the key determinant of species presence in the low-stress areas adjacent to uplands. Since 1987, subsequent experiments in the salt marsh have supported these general findings (Bertness 1991a, Pennings and Callaway 1992, Levine et al. 1998, Brewer et al. 1998, Dormann et al. 2000, Van Der Wal et al. 2000, Emery et al. 2001). To simulate this observed response, the model used a weighting scheme to adjust the relative importance of stress tolerance and competition depending upon the overall stress level at each gradient location. Tolerance factors were favored over competition at the three highest stress locations (80% - 10%), competition factors were favored over tolerance at the three lowest stress locations (80% - 10%), and the factors were weighted equally at the three mid-stress locations (45%-45%, Figure 5.1). Since most of the literature identified stress tolerance and competition as the key determinants, recruitment was deemed less influential and weighted consistently across the gradient at 10%.

As a result of this succession modeling scheme, plant species assemblages changed over time in response to shifts in hydrologic conditions. Multiple modeling scenarios were used to predict changes to plant species assemblages under simulated hydrologic conditions associated with tidal restriction (reduced salinities and tidal inundation) and tidal restoration (increased salinities and tidal inundation). In addition, a sensitivity analysis was conducted to assess relative sensitivity of model predictions to changes in factor weights.

## Methods

Model Structure. The model program was developed in the Microsoft (MS) Visual FoxPro software environment (Microsoft Corporation, Redmond, Washington, USA), with all model specifications, parameters, and procedures included in a single program file. The model used a weekly time-step and operated on a calendar year basis (Jan-Dec) to produce annual estimates of plant species cover for a hypothetical marsh plot. All model runs were twenty years in duration.

Model Inputs. Species cover values for *Spartina alterniflora* (*cover\_spa*), *Spartina patens* (*cover\_spp*), *Juncus gerardii* (*cover\_jun*), *Phragmites australis* (*cover\_phr*), *Lythrum salicaria* (*cover\_lyt*), and *Typha angustifolia* (*cover\_typ*) were assigned for each modeling scenario. Cover values represented the relative portion of the plot occupied by each species, with the totals of all six species adding up to one. The simulated plot was also assigned to a salinity regime and an elevation relative to the tidal cycle (according to the model scenario requirements), to determine the location of the plot within the marsh gradient of salinity and flood regimes.

Delimiters of Marsh Gradient Locations. The model considered nine gradient locations, from low to high marsh elevations, and from mesohaline to polyhaline salinity regimes (Figure 5.1). Gradient delimiters were based on literature review and specific measures of flooding and salinity at experimental locations (Table 1.1). Assignment of flood regime was determined from plot elevation relative to the tidal cycle as follows:

low elevations were below mean high water, mid elevations were between mean high water and an elevation that was flooded by no more than 15% of the tides, and high elevations were above this 15% tidal flooding elevation. Use of mean high water as the low marsh delimiter was based on many field observations of this elevation as the general boundary between *Spartina alterniflora* and *Spartina patens* plant zones (Niering and Warren 1980, Bertness and Ellison 1987, McKee and Patrick 1988, Bertness 1991b, Bertness 1992).

Delineation of an elevation to separate mid from high marsh, however, was not readily available from known sources. Instead, a useful delimiter of high marsh boundary was inferred from published reports of marsh vegetation borders and tidal heights. In New England salt marshes, high marsh areas are often include tracts of black grass (Niering and Warren 1980). Bertness and Ellison (1987) measured tidal heights at the low boundary of the black grass (*Juncus gerardii*) zone in a Rhode Island marsh, and found that 15% of tides flooded this area. These results were consistent with an earlier analysis of the *Spartina alterniflora*-*Juncus roemerianus* border from US Gulf Coast salt marshes (13% of tides flood, Eleuterius and Eleuterius 1979). In addition, Warren et al. (2001) analyzed tidal flood levels of *Phragmites* stands in Connecticut, and found that a vegetation break occurred at the 15% tidal flooding elevation, with *Phragmites* significantly reduced and *Typha* more common at the highest marsh elevations. It appears, then, that an elevation flooded by 15% or fewer high tides may be ecologically significant for salt marsh plants of concern in New England. This elevation was used by

the model to delineate the landward extent of the mid marsh, and plots with elevations above this line were considered upper marsh.

To assign salinity regime, three categories of salinity levels were modeled: low (mesohaline 5-14 ppt), mid (meso-polyhaline 14-18 ppt) and high (polyhaline >18 ppt). Specific salinity ranges for each category were based on readings taken during the growing season from salinity wells at experimental locations (Table 1.1); mesohaline and polyhaline categories were based on Odum et al. (1984). Growing season salinity levels were specifically assigned for each model scenario.

Plant Succession. Model processing logic for plant succession was based on plant cover values, gradient location, species-specific tolerance factors, interspecific competition factors, and species composition of neighboring plots. The first step in the succession modeling process was to determine the at-risk pool for each species ( $atrisk_{species}$  Equation 1), computed as the percent cover of the species multiplied by 1 minus the tolerance factor (TF) for the species at the gradient location (Table 1.6, with a minimum of 5% to simulate random disturbance).

The next step allocated the at-risk pool to species present in the plot. Re-allocation from recruitment was based on species cover of neighboring plots, which, for these (non-spatial) scenarios, was assigned to the same species cover values as the plot. The at-risk pool for each species in the plot was multiplied by the neighbor cover values and summed across species, with the product multiplied by the recruitment weighting



factor (*recruit\_wf*) to determine recruitment re-allocations (Eq. 2). Next, all interspecific combinations in the plot were analyzed to compute pair-wise reallocations. For each pairing, re-allocation was computed as the difference in species competition factors (CF, Table 1.7) multiplied by the product of the at-risk pool and the competition weight factor at the location (*comp\_wf*), plus the difference in tolerance factors (TF, Table 1.6) multiplied by the product of the at-risk pool and the tolerance weight factor at the location (*tol\_wf*, Eq. 3). Pair-wise reallocation amounts were standardized by the relative cover percentage of each species so as not to exceed the total percentage of occupied area in the plot. Cover values for each species in the plot were then adjusted according to the standardized re-allocation values for each species combination present in the plot. The model computed plant succession changes once per year, at week 30.

$$\text{At-risk}_{\text{species } i-j} = \text{cover}_{\text{species } i-j} * \text{MAX}(.05, (1 - \text{TF}_{\text{species } i-j \text{ at location}})) \quad (1)$$

$$\text{Recruit re-allocation}_{\text{species } i-j} = \text{recruit\_wf} * \sum(\text{at-risk}_{\text{species } i-j} * \text{neighbor cover}_{\text{species } i-j}) \quad (2)$$

$$\text{Pair-wise reallocation}_{\text{species } i \text{ from } j} = ((\text{CF}_{\text{species } i \text{ on } j} - \text{CF}_{\text{species } j \text{ on } i}) * \text{At-risk}_{\text{species } i-j} * \text{comp\_wf}_{\text{location}}) + ((\text{TF}_{\text{species } i \text{ at location}} - \text{TF}_{\text{species } j \text{ at location}}) * \text{At-risk}_{\text{species } i-j} * \text{tol\_wf}_{\text{location}}) \quad (3)$$

Special Handling for *Typha* and *Phragmites*. As noted earlier, best-performance gradient locations for the study plants were unique by species, except for *Typha* and *Phragmites*. Since the two species achieved top performance at the low salinity – high elevation location (Table 1.1), special handling was needed to break the stalemate and to provide each species with a relative advantage under certain conditions within the gradient location. Advantages were based on the delineation of two high elevation sub-

zones: below the elevation of the highest tide measured (regular, but infrequent tidal flooding), and above the highest tide measured (the greatest spring high tides and storm-related flooding). In the regularly-flooded sub-zone, *Phragmites* was given an advantage over *Typha*. This advantage was based on the findings of Warren et al. (2001), who determined that *Phragmites* was much more likely to occur in salt marsh locations with infrequent but regular tidal flooding (even if *Typha* was present). Further, *Typha* was considered relatively less tolerant of salt water flooding (Beare and Zedler 1987) than *Phragmites*. Since the modeled low salinity regime was mesohaline (5-18 ppt, Chapter I), regular flooding of mesohaline tidal water would likely inhibit *Typha* growth and survival along the seaward borders of the high marsh. To simulate this advantage, the *Typha* tolerance factor was reduced from 1 to 0.5 in regions of the high marsh with elevations below the maximum extent of regular tides, with the *Phragmites* tolerance factor left unchanged.

Model Scenarios. Modeling scenarios were conducted to simulate the impacts of changing hydrologic conditions (i.e., tidal restoration or tidal restriction) on marsh plant community composition. This was done by simply varying the marsh gradient location: higher salinities and tidal flood levels simulated hydrologic conditions associated with tidal restoration; lower salinities and tidal flooding reflected conditions in marshes with tidal restrictions. A hypothetical plant community was used to initialize each scenario, with the six study species each at 16.7% cover. Ten scenarios were modeled: one for the low-salinity high elevation gradient location at an elevation above the extent of regular tidal flooding (favoring *Typha*), another for the low-salinity high elevation location at an

elevation receiving between 15% and 0% of regular tidal flooding (favoring *Phragmites*), and eight scenarios for each of the remaining elevation and salinity gradient locations.

Sensitivity Analysis. The sensitivity of plant species cover to changes in weights of model succession factors (recruitment, competition, and physical stress tolerance) was determined through a systematic sensitivity analysis. For purposes of this analysis, the model was configured for the low salinity-low elevation gradient location, with all species equally distributed (16.7% species cover). The comparative model result was plant species cover of *Spartina alterniflora*. Model weights were varied by  $\pm 5\%$  and  $\pm 20\%$ , and model results were compared with baseline conditions (based on original weights) to assess relative sensitivity of each parameter. Relative sensitivity was calculated as the percent change in plant species cover divided by the percent change (either 5% or 20%) in the model weight (Eq. 4). Higher relative sensitivity values indicated an increased sensitivity to a model succession factor. Since plant cover varied over time, the sensitivity analysis was run for one and twenty year durations to ensure model consistency and long-term stability.

$$\text{Relative sensitivity}_{\text{succession factor}} = \% \text{ Change}_{\text{plant species cover}} / \% \text{ Change}_{\text{succession weight factor}} \quad (4)$$

## Results and Discussion

Model scenario results are presented and discussed in groups arranged by marsh gradient location for elevation (low, mid, and high). Within each elevation group, figures

are provided for the low, mid, and high salinity regimes. All figures are annotated with four-letter codes to designate salinity and elevation gradient locations (e.g., LSLE = low salinity – low elevation; HSHE = high salinity – high elevation, etc.).

Low Elevation Scenarios. Model succession scenarios are presented in Figure 5.2 for hypothetical marsh plots in the three salinity regimes at low elevations (i.e., below mean high tide). These high-flood scenarios were used to simulate plant community response to reintroduction of tidal flows in low-lying areas of subsided marshes. Model predictions indicated that, for all three salinity regimes, *Spartina alterniflora* would quickly emerge as the dominant plant species and maintain plot control for the 20-year duration of the model run. At low and mid salinity, cordgrass achieved greater than 90% cover by year 20, with primary subordinate species *Typha* at low salinity and *Spartina patens* at mid salinity (Figure 5.2, LSLE and MSLE, respectively). At the highest salinity level, *Spartina alterniflora* dominance appeared to be more challenged, with only a 50% - 38% advantage over *Spartina patens* at year 20 (HSLE, Figure 5.2). Also at this location, *Phragmites* retained 11% plot cover at year 20, the only species besides *Spartina alterniflora* and *Spartina patens* to maintain more than 2% cover at low elevations.

Model predictions for low elevation scenarios were a direct result of species-specific physical stress tolerance rankings, reflecting overall best performance for *Spartina alterniflora* under high-flood conditions (Table 1.6), and also that plant succession at low marsh elevations was influenced mostly by stress tolerance (Figure 5.1,

based on Bertness and Ellison 1987). Model outcomes favoring cordgrass were consistent with many field observations of *Spartina alterniflora* dominance at elevations below mean high tide in mesohaline and polyhaline salt marshes (Niering and Warren 1980, McKee and Patrick 1988, Bertness 1991b, Bertness 1992). The relative strength of *Spartina patens* was somewhat surprising, since the species is generally thought to be flood intolerant (Niering and Warren 1980, Bertness 1992), although occasional patches of salt hay are sometimes observed in the field at elevations below mean high tide (Bertness and Ellison 1987). For the model, results were based on the unexpectedly strong growth and survival performance of *Spartina patens* at the polyhaline low marsh location in the field experiment (Chapter I, Table 1.6). Predictions for *Juncus*, the other halophyte study species, indicated low succession potential at low elevations. Weak results for *Juncus* at this location were expected for a plant species typically found in the higher elevations of salt marsh habitat (Niering and Warren 1980, Bertness and Ellison 1987, Bertness and Yeh 1994).

The relatively poor performance of *Phragmites*, *Lythrum*, and *Typha* at low elevations was also expected. Tolerance factors derived from flood-stressed locations of the field experiment were generally low for these species, especially *Lythrum* and *Typha* (Table 1.6). Field reports also indicated that *Lythrum* (Whigham et al. 1978) and *Typha* (Warren et al. 2001) were rarely found along creek banks in mesohaline and polyhaline marsh sites. However, Warren et al. (2001) observed *Phragmites* expansion in low-marsh areas, suggesting that common reed may be a better stress tolerator than other brackish invasive species. In fact, rapid die-back of *Typha* and *Lythrum* was reported

when tidal flows were reintroduced to low-lying areas of restricted marshes (Sinicrope et al. 1990, Burdick et al. 1997), but *Phragmites* stands may persist (although in stunted forms) for years following tidal restoration (Sinicrope et al. 1990, Roman et al. 2002). In general, however, low-marsh replacement of brackish invasive species by *Spartina alterniflora* and *Spartina patens*, as suggested by the model, was an expected plant community response to reintroduction of tidal flooding (Sinicrope et al. 1990, Burdick et al. 1997, Burdick et al. 1999, Roman et al. 2002, Warren et al. 2002).

Mid Elevation Scenarios. Predictions for model scenarios at mid elevations, between the elevation of mean high tide and 15% tidal flooding, are presented in Figure 5.3. These scenarios were useful to show plant response to intermediate hydrologic conditions along a transitional gradient from tidal restoration (high flooding) and tidal restriction (low flooding). Model predictions of dominant plant species for these scenarios varied by salinity regime, with *Spartina patens* performing best at the mid and high salinity locations (MSME and HSME, respectively), and *Typha* at low salinity (LSME). *Spartina alterniflora* was diminished from its dominant levels at lower elevations, but still performed well enough to maintain 20% and 40% cover in the understory at low and mid salinity (LSME and MSME, respectively). At the high salinity location, *Juncus* performance was greatly improved from the low elevation location (HSLE Figure 5.2) and was second only to *Spartina patens* (44% to 56%, respectively, HSME Figure 5.3).

The relative strength of *Spartina patens* at higher-salinity mid-marsh elevations was consistent with many field observations of salt hay distribution in New England (Niering and Warren 1980, Bertness and Ellison 1987, Bertness 1991a, Bertness 1991b), and suggested that *Spartina patens* would out-perform brackish invasive species at these elevations under conditions where high-salinity tidal flooding was reintroduced (Sinicrope et al. 1990, Burdick et al. 1997, Roman et al. 2002). However, the overall mix of dominant halophyte and brackish invasive species at mid elevations (as opposed to *Spartina alterniflora* dominance at all low elevations) suggested an important shift in marsh edaphic conditions, and therefore plant community composition, with reduced flooding. In terms of the model, changes in elevation triggered the use of a new set of tolerance factors (mid-elevation factors, Table 1.6), and also a transition in determinants of succession from tolerance-based to more competition-based control (Figure 5.1, with competition factors listed in Table 1.7). The result of this shift was especially evident at the low salinity locations: *Spartina alterniflora* beat *Typha* at low elevation (96% to 3%, respectively LSLE Figure 5.2) but dominance was reversed at mid elevation (*Typha* 72% to *Spartina alterniflora* 19%, LSME Figure 5.3). In fact, field reports appeared to support this prediction, with strong indications that *Typha* distribution in mesohaline and polyhaline marshes is typically limited to elevations above mean high water (Sinicrope et al. 1990, Warren et al. 2001). These findings, together with model results, suggested that multiple stresses associated with the combination of flooding and salinity may interact in complex ways to exclude relatively stress-intolerant species (i.e., *Typha*) from certain regions of the salt marsh gradient (Beare and Zedler 1987, Pennings and Callaway 1992, Warren et al. 2002).

High Elevation Scenarios. Model scenarios for high elevation marsh habitat (elevations above the 15% tidal flood level) are presented in Figure 5.4. Scenarios at the low salinity regime simulated plant community response to tidal restriction, with higher salinity scenarios simulating non-impacted salt marsh conditions. At mid and high salinity, marsh halophyte species were predicted to dominate, with *Spartina patens* at mid salinity and *Juncus* at high salinity (MSHE and HSHE respectively, Figure 5.4). Best-performing subordinate species for these higher salinity scenarios varied, with *Lythrum* achieving 20% cover at mid salinity and *Spartina patens* reaching 30% at high salinity. However, for upland-edge marsh regions at low salinity, the model predicted dominance of the salt-intolerant species. At elevations above the extent of regular tidal flooding, *Phragmites* and *Typha* both performed well, with *Typha* eventually dominating (LSHEa, Figure 5.4). At upland-edge regions with infrequent but regular tidal flooding, *Phragmites* was predicted to be the dominant species (LSHEb, Figure 5.4). This scenario showed the impact of model adjustments designed specifically to favor *Phragmites* over *Typha* in this elevation sub-zone of the high marsh.

Overall model results for low-flood scenarios indicated that changes in salinity regimes were the most important determinants of species dominance. This was expected, since stress due to flooding was low or absent in these locations, and therefore salinity was the sole source of physical stress. Because competition was thought to be a stronger determinant of species composition than physical tolerance in these low-stress regions (Bertness and Ellison 1987, Pennings and Callaway 1992, Streever and Genders 1997,



Emery et al. 2001), competition factors were used to control plant succession here (Figure 5.1).

Model predictions of *Spartina patens* and *Juncus* dominance at the mid and high salinity areas of the high marsh were in line with field observations of known species distribution in pristine New England salt marshes (Niering and Warren 1990, Bertness and Ellison 1987). In addition, these halophytes are known to replace brackish plant species in impacted marsh sites restored to high salinity regimes, although the modeled rate of species replacement appeared to be slower in the high marsh than in the low marsh. As an indicator of this delayed response, *Spartina alterniflora* achieved 90% dominance in 20 years at low elevation (Figure 5.2, LSLE and MSLE), but the dominant halophyte species at high elevations only reached 65% cover in 20 years (Figure 5.4, MSHE and HSHE). The persistence of brackish species in less-flooded areas has been noted in the field, even at high salinities (Sinicrope et al. 1990, Burdick et al. 1997, Warren et al. 2002), suggesting that species composition changes due to competition may be slower than changes associated with physical stress in these systems.

At the low salinity regime, model predictions clearly favored brackish species *Typha* and *Phragmites* over the halophytes. These predictions were consistent with observations of long-term brackish species replacement of halophytes in tidally restricted salt marshes (Roman et al. 1984, Chambers et al. 1999, Windham and Lathrop 1999, Burdick et al. 2001, Burdick et al. 2002, Roman et al. 2002, Warren et al. 2002). Notably, succession scenarios did not identify a gradient location of dominance for

*Lythrum*. Model results for *Lythrum* were a reflection of poor overall species growth, survival, and competitive performance in the field experiment (Chapter I), likely associated with low species tolerance of mesohaline and polyhaline salinity levels (Dzierzeski 1991). Purple loosestrife, however, was observed in regions of high marsh at three of the tidal-restricted study sites (Little River, Mill Brook, and Oak Knoll, Introductory Chapter), indicating that the succession model was somewhat lacking in predictions of *Lythrum* capability for some areas within the salt marsh gradient. It may be that zones of very low salinity exist in some areas, possibly due to the intrusion of groundwater (Gardner et al. 2002). At best, the model suggested that *Lythrum* would persist if already entrenched along the upper elevations of mesohaline marshes, perhaps in regions isolated from competitive dominant species like *Phragmites* and *Spartina patens*. In any case, even though model results were clearly explained by field experiment measures, it appeared that the model was generally underestimating *Lythrum* potential in some of the lower salinity regions of salt marsh habitat.

Sensitivity Analysis. The relative sensitivity of parameters for model runs of 1 and 20 years is presented in Table 5.1. Since relative sensitivity was calculated as the percent difference in species cover divided by percent difference in succession parameter weight, this analysis indicated low overall model sensitivity to any one succession parameter (all values < 1). In addition, the analysis suggested a fairly consistent balance among model parameters (values ranged from 0.01-0.37). On a relative scale, the model was most sensitive to tolerance and competition weights and less sensitive to changes in the recruitment rate. These sensitivity results were expected, since the model recruitment

rate was kept constant at 10%, while the tolerance and competition weights varied between 10% and 80%. All parameter weight sensitivities increased from one year to twenty year model runs, but since overall sensitivity was low, these increases were negligible and did not indicate model instability at extended timeframes.

### Conclusions

Human alterations to tidal hydrology of salt marshes result in directional changes in plant species composition over time. Hydrologic conditions that restrict natural tidal flows, and the reintroduction of tides to restricted sites, are disturbances that trigger plant succession changes. For New England salt marshes, the most important processes that control plant succession are physical stress tolerance, interspecific competition, and recruitment from neighboring plants. A model of plant succession for common species of New England salt marshes was developed to predict the response of plant communities to hydrologic conditions based on the influences of these three processes. The model was parameterized with species-specific stress tolerance factors, and combination-specific competition factors derived from a field experiment that measured growth and survival across a physical gradient of flood and salinity regimes. Model results supported the findings that, for marshes with tidal restriction, salt marsh halophytes are replaced by brackish invasive species, and further, that these brackish species will persist under restricted-flow conditions. However, when the model simulated the reintroduction of tidal flows, brackish species were succeeded by salt-tolerant plants native to salt marsh habitats, and, especially in the low marsh, these changes were sometimes rapid. Model

predictions appeared to follow observed changes across a range of marsh gradient conditions, from mesohaline to polyhaline salinities, and from creek-bank to the upland border. As a result, this succession model was expected to provide valuable estimates of plant species composition change in response to hydrologic modification of salt marsh habitats.

<b>Parameter</b>	<b>1 yr +5%</b>	<b>1 yr -5%</b>	<b>20 yr +5%</b>	<b>20 yr -5%</b>	<b>1 yr +20%</b>	<b>1 yr -20%</b>	<b>20 yr +20%</b>	<b>20 yr -20%</b>
<b>Recruitment weight</b>	.061	.061	.042	.042	.031	.031	.010	.010
<b>Tolerance weight</b>	.061	.123	.333	.374	.031	.123	.317	.120
<b>Competition weight</b>	.061	.123	.333	.374	.031	.123	.317	.120

Table 5.1. Relative sensitivity of species cover values to  $\pm 5\%$  and  $\pm 20\%$  adjustments in parameter values for 1 year and 20 year model runs. Relative sensitivity was calculated as % change in species cover divided by % change in model parameter weight.

### Salt Marsh Gradient Locations

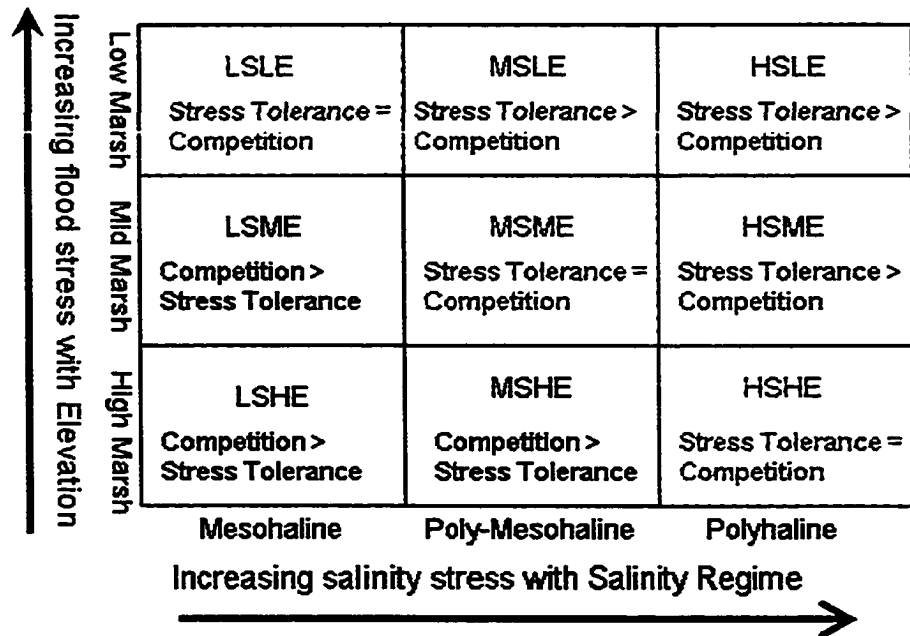


Figure 5.1. Diagram of succession factors for salt marsh gradient locations. Gradient location codes identify salinity (LS: low salinity, MS: mid salinity, HS: high salinity) and flood regime (LE: low elevation, ME: mid elevation, HE: high elevation), from field experiment (Chapter I). Shading indicates locations with similar physical stress levels. Relative influence of stress tolerance and competition assignments for plant succession model based on Bertness and Ellison (1987).

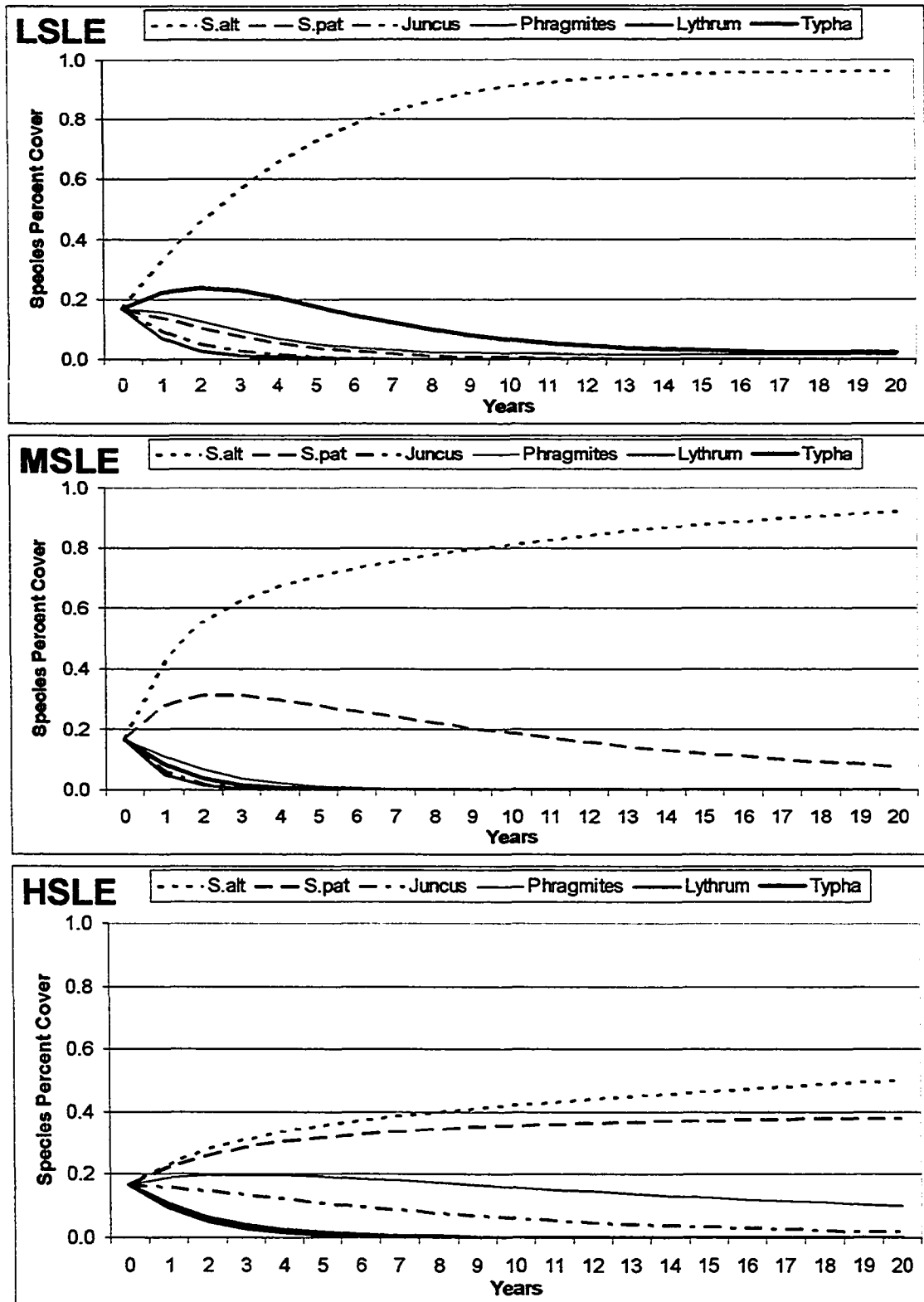


Figure 5.2. Low elevation (LE) plant succession model scenarios for three salinity regimes (LS: low, MS: mid, HS: high).

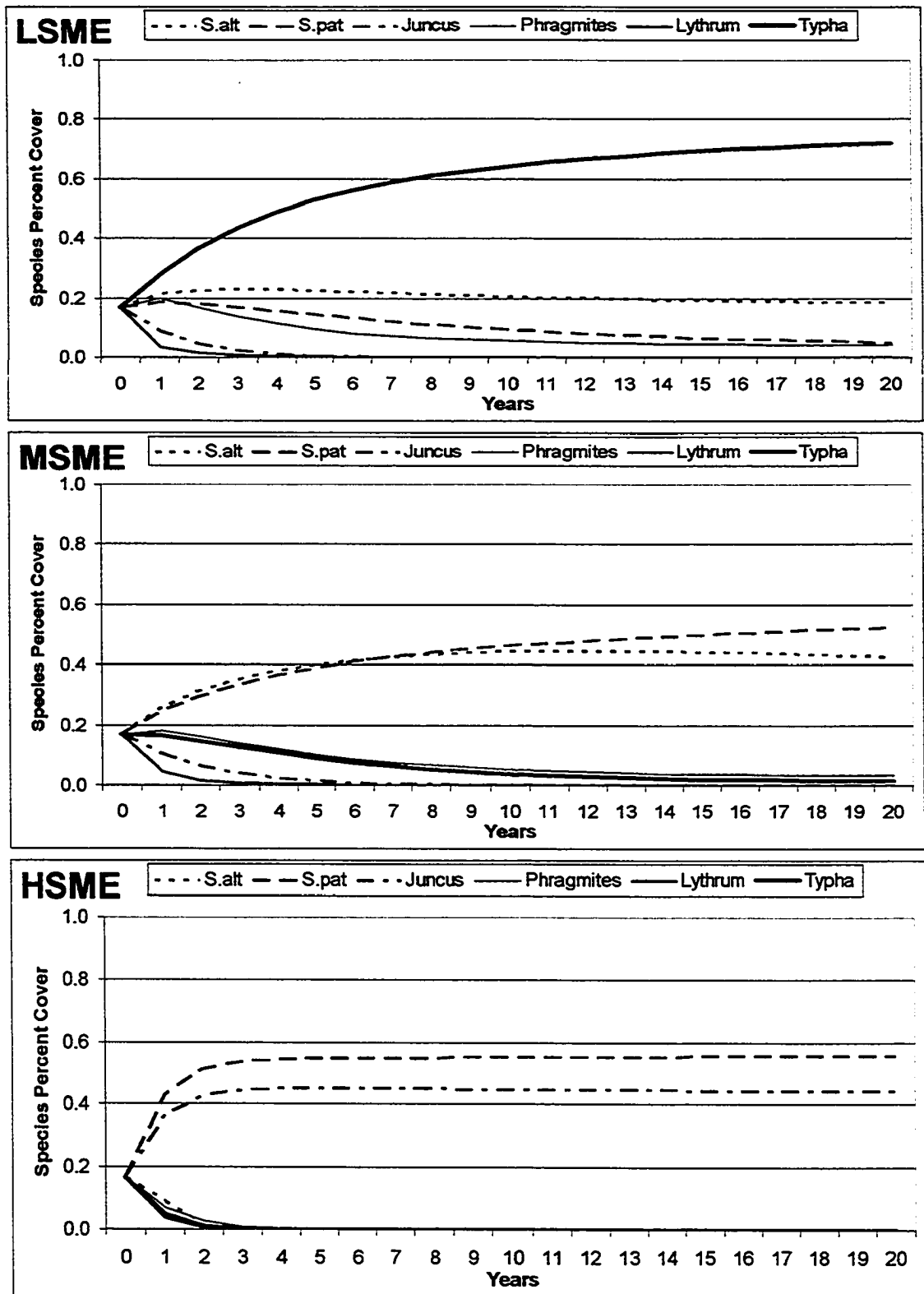


Figure 5.3. Mid elevation (ME) plant succession model scenarios for three salinity regimes (LS: low, MS: mid, HS: high).



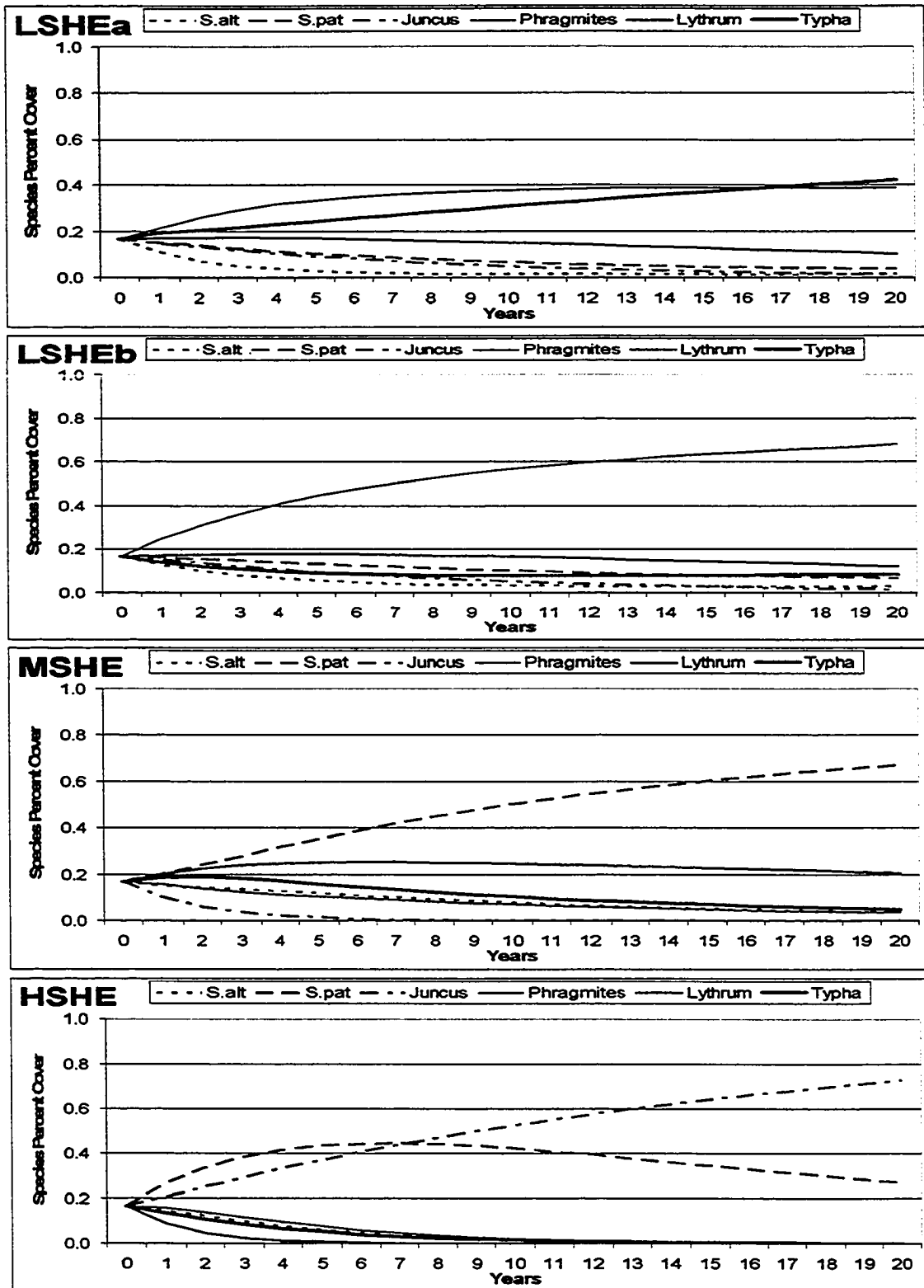


Figure 5.4. High elevation plant succession model scenarios for three salinity regimes (LS: low, MS: mid, HS: high). LSHEa is at an elevation above extent of regular tidal flooding; LSHEb is at an elevation between 15% and 0% of regular tidal flooding.

## **CHAPTER VI**

# **SPATIAL MODELING AND VISUALIZATION OF HABITAT RESPONSE TO HYDROLOGIC RESTORATION IN NEW ENGLAND SALT MARSHES**

### **Introduction**

Today, as little as 50% of coastal wetlands present before colonial times remain in the New England states of Massachusetts, Maine, and New Hampshire (Cook et al. 1993). An estimated 20% of this salt marsh habitat is negatively impacted by roads and culverts that form barriers to natural tidal flows, a condition commonly known as tidal restriction (Roman et al. 1984, USDA SCS 1994, Neckles and Dionne 2000). Salt marshes with tidal restrictions may experience reduced plant biodiversity (Roman et al. 1984, Sinicrope et al. 1990, Burdick et al. 1997), degraded water quality (Portnoy 1991, Portnoy and Giblin 1997), diminished ability to keep pace with sea level rise (DeLaune et al. 1983, Boumans and Day 1994), and disrupted food webs for fish and birds (Dionne et al. 1999, Reinert and Mello 1995). Fortunately, these marshes can recover lost functions if the appropriate hydrologic regime is restored (Sinicrope et al. 1990, Roman et al. 1995,

Burdick et al. 1997, Boumans et al. 2002, Roman et al. 2002, Warren et al. 2002), and as a result, hydrologic restoration of restricted salt marshes is a common management practice today (New Hampshire Office of State Planning 1996, Save the Sound 1998, US Army Corps of Engineers 1999, Warren et al. 2002). However, lack of synthesized information regarding important salt marsh processes, including plant biology, community succession, and sediment-plant interactions, may lead to unintended and less than optimal results for many salt marsh hydrologic restoration projects (Race 1985, Moy and Levin 1990, Sinicrope et al. 1990, Frenkel and Moran 1991, Rozsa 1995, Simenstad and Thom 1996, Zedler 2000, Warren et al. 2002, Williams and Orr 2002).

In order to improve the predictive capability of resource managers faced with salt marsh restoration options, a synthesized computer model of interrelated salt marsh processes was developed. Past efforts with computer modeling have advanced our understanding and ability to predict salt marsh succession (i.e., the directional change of plant species composition over time). In 1977, Zieman and Odum developed a correlative model to predict salt marsh plant succession in areas of dredge spoil (Mitsch and Gosselink 1993), and Sklar et al. (1985) constructed an early spatial model that tracked physical processes associated with habitat succession in coastal wetlands. To specifically address the needs of restoration planners, Roman et al. (1995) developed a hydrologic model that simulated changes in tidal regime for a tidally restricted New England salt marsh. Boumans et al. (2002) advanced this approach with a model that estimated flood regime, but also connected hydrologic change to plant community succession through comparisons of observed plant distributions at similar relative

elevations. None of these models, however, considered the specific impacts of hydrologic disturbance on individual plant species' tolerance of physical stress and competitive ability, factors recognized as the key determinants of spatial vegetation patterns in New England salt marshes (Bertness and Ellison 1987). Vegetation of disturbed salt marshes is an especially important concern for resource managers attempting to restore native halophyte communities to areas dominated by brackish marsh plants. Therefore, species-specific knowledge of marsh plant successional attributes, coupled with a fine-scale model applied over a spatial domain, should provide a novel and valuable simulation tool for coastal resource managers considering hydrologic restoration.

This chapter describes a project that integrated diverse ecological factors, including biotic and abiotic processes, into a synthesized ecosystem model. The specific goal of the project was to develop, test, and use this synthesized model as a predictor of long-term salt marsh habitat response to hydrologic restoration. A conceptual diagram of the ecosystem model components and processes is provided in Figure I.2 (Introductory Chapter). As a first step, the model estimated water volume for marsh areas upstream of tidal barriers, based on two-week measures of tidal heights and physical dimensions of the tidal inflow channel or culvert. Tidal water volume estimates were combined with site-specific factors of marsh geomorphology (including a composite of marsh elevations ordered as a hypsometric curve) to predict local water depths, hydroperiod, and general salinity level. Flooding and salinity regimes were used as the primary determinants of plant succession processes, which considered physical stress tolerance, competitive

ability, and recruitment potential to predict changes in plant species composition. Further, plant species composition determined the rate of plant biomass and litter production, which combined with inorganic deposits to form new marsh sediments. In this manner, the ecosystem model included a feedback loop among biotic and abiotic marsh components that influenced the long-term self-maintenance capacity of salt marsh habitat in relation to rising sea level.

Beyond the specific predictions of the ecosystem model, major project objectives were four-fold. First, standardized, widely available field specifications were chosen as inputs to make the model more easily transferable to potential restoration sites. Second, important ecological datasets that identified physical stress tolerance and competitive rankings among important salt marsh plant species were provided by a field experiment. Third, new software tools for design and assessment of hydrologic restoration scenarios were developed, tested, and refined. Finally, advanced spatial technologies were employed to provide rigorous fine-scale simulations of salt marsh ecosystem functions, and to develop assessment tools for management. Spatial models and outcomes are the focus of this chapter, including the development, validation, use, and evaluation of spatial simulations and visualizations for tidal restoration of New England salt marshes.

Four project sites were selected for study because of past or present hydrologic conditions of tidal restriction (see Introductory Chapter, Study Sites). Drakes Island (Wells, Maine) and Oak Knoll (Rowley, Massachusetts) are sites with continued tidal restriction due to undersized culverts. Little River (North Hampton, New Hampshire)

and Mill Brook (Stratham, New Hampshire) are marsh locations with past tidal restrictions and restored hydrology. Collectively, these sites provided a diversity of marsh conditions and habitat types that added depth to the range of evaluated conditions for model use. In addition, Drakes Island and Mill Brook represented sites with past hydrologic modifications that were the subject of prior research, and therefore useful as test sites for validating spatial results.

At each site, the model considered six dominant plant species of the salt marsh. In New England salt marshes, native perennial species occur in monotypic zones of cordgrass (*Spartina alterniflora*), salt hay (*Spartina patens*), and black grass (*Juncus gerardii*) (Niering and Warren 1980). Where tidal restrictions are present, these native plants are often replaced by invasive species like common reed (*Phragmites australis*), narrow-leaf cattail (*Typha angustifolia*), and purple loosestrife (*Lythrum salicaria*) (Sinicrope et al. 1990, Roman et al. 1995, Burdick et al. 1997, Roman et al. 2002, Warren et al. 2002).

An underpinning of the simulation model was the concept that salt marshes exist across a physical gradient of elevation and salinity conditions (Niering and Warren 1980, Odum et al. 1984). Subtle differences in gradient conditions are known to favor or to disadvantage a plant species based on relative tolerance of stressful physical conditions and the changing influence of competitive interactions (Bertness and Ellison 1987). Since these conditions change when tidal hydrology is modified, a detailed understanding of changes to gradient regimes was central to the prediction of plant response. To

simulate the marsh gradient, observed elevation and salinity regimes were subdivided into nine different zones (high-mid-low elevation regimes by high-mid-low salinity regimes). The assignment of gradient location to a specific marsh plot was a critical modeling function. To assign salinity regime, the model considered the salinity of the tidal inflow, the plot elevation, and the location of the plot in relation to the tidal source, the upland, and the nearest creek. Elevation regime assignments were based on flood conditions (a combination of tidal signal and plot elevation). The common element for these key assignments was elevation, arguably the most important of all model descriptors. In an effort to obtain the best, high-resolution (sub-decimeter accuracy) estimates of elevation, the model included statistical subroutines to estimate elevation of non-sampled marsh area based on kriging algorithms.

Since model components required arrays of spatial information, specialized database structures were developed to store relevant information for each site. The elemental model processing unit was the *cell*, a square plot of fixed dimensions and known relative spatial coordinates [x,y] that, when combined on a grid, described the entire surface area of a study site. Spatial databases were constructed for each site with one observation per cell. The first set of observations in a spatial database contained information about the baseline, or current conditions for each cell (elevation, salinity regime, plant cover, etc.). Baseline information was based on field survey data collected at the site and mathematical techniques that provided parameter estimates for every cell in a marsh grid. For each year in the model run, the program created an additional annual entry for each cell. The standard timeframe for model simulation was twenty years, a

duration that appeared to reasonably approach the observed timescale over which many important marsh functional processes occur (Morgan and Short 2002).

For modeling exercises, a first set of tasks involved the validation of model performance for spatial and aggregated simulation results. Prediction of a dominant plant species for each cell was the primary output of the model. At the Drakes Island and Mill Brook sites, marsh conditions were simulated at the time of past hydrologic modification (based on published records). Comparisons of observed-versus-predicted plant cover from these validation exercises provided a rigorous set of metrics with which to assess spatial and composite model predictive performance. Validation exercises were conducted in addition to formal sensitivity analysis at the process component level of the model (biomass processes based on Fitz et al. 1996, Chapter II; relative elevation processes based on Rybczyk et al. 1998, Chapter III; hydrologic processes based on Boumans et al. 2002, Chapter IV; and plant succession processes based on Grace 1987, and Bertness and Ellison 1987, Chapter V).

Following validation exercises, the model was used to predict anticipated changes in plant cover for each site over the next twenty years. These simulations were based on current marsh hydrologic conditions. In addition, scenario simulations were conducted based on hypothetical hydrologic conditions selected for each site (see Chapter IV). For Drakes Island and Oak Knoll, the scenarios considered hydrologic restoration of tidal flows associated with culvert expansion. At Little River and Mill Brook (sites with recently restored tidal flows) scenarios were selected to simulate the past regimes of



restricted tides. Output from model simulations were analyzed for ecological impacts associated with changes in marsh plant cover, and rendered as time-sequence animations. In addition, spatial model output was transferred to a 3-dimensional imaging package for the construction of high-level (non-technical) visualizations of marsh scenario results.

## **Methods**

**General Approach and Processing.** An integrated salt marsh ecosystem model program was developed in the Microsoft (MS) Visual FoxPro software environment (Microsoft Corporation, Redmond, Washington, USA), as a synthesis of process models for biomass production, relative elevation, and plant succession. The model used four sources of inputs: 1) generalized model parameters, 2) scenario-specific upstream tidal record, 3) site-specific model parameters and 4) a spatial database containing cell-specific information for each study site.

All standard model runs were 20 years in duration, except for certain validation exercises. Model processing proceeded according to the following procedures in a loop of specified duration: First, a marsh cell was selected from a site spatial database, and baseline (year 0) information about the cell was provided (elevation, salinity, cover type, plant species composition, etc.). Only cells with cover types for marsh plant vegetation or bare area were processed. Next, the model determined the gradient location for the cell based on elevation, salinity, tidal heights, and spatial distances from tidal sources and open water (see Assignment of Elevation Regime and Assignment of Salinity Regime

sections). The model also determined the sedimentation rate for the cell at this time (see Estimation of Sedimentation Rate).

With an estimated cell gradient location, the model cycled through a 52-week annual processing loop. First, annual above and belowground biomass for the cell was computed according to the specifications of the biomass production process model (Chapter II). Biomass results were then passed to the relative elevation process model to determine any changes in cell elevation (Chapter III). Next, the model estimated any changes in plant species composition based on the plant succession process model (Chapter V). The spatial implementation of the plant succession model also included a function for computing aggregate species composition of neighboring cells as a measure of recruitment potential (see Estimation of Neighbor Species Composition). At the conclusion of the 52-week loop, the model created a new entry in the spatial database for the cell (year  $0+x$ , where  $x$  was the year of the annual loop). The model then repeated the process for the next cell in the spatial database (ordered sequentially by coordinate location, from [1,1] to [200,200]), and repeated the annual loop until the specified total number of years were reached.

Generalized Model Parameters. Model parameters that were used for all cells, sites, and scenarios are identified in Table 6.1. These parameters included values that controlled model processing for determination of plant biomass (Chapter II), relative elevation (Chapter III), and plant species succession (Chapter V). Species-specific measurements of physical stress tolerance and combination-specific measures of

interspecific competitive capability are provided in Tables 1.6 and 1.7, respectively (from Chapter I).

Scenario-Specific Upstream Tidal Record. The model used a two-week table of upstream tidal heights (m NGVD at 6 minute intervals) in the determination of flood regime, salinity regime, and sedimentation rate for each spatial cell. For each site, the table contained two sets of records: current upstream tidal heights from automated data collection in the field, and scenario upstream tidal heights as estimated by the tidal hydraulics model (Chapter IV). Model scenarios varied by site. For the tidal-restricted sites of Drakes Island and Oak Knoll, the scenarios predicted new water levels based on expanded culvert designs (Chapter IV, Figures 4.2c and 4.5c, respectively). For restoration sites Little River and Mill Brook, the scenarios estimated upstream water levels in the marsh if historic tidal restrictions were still present (Chapter IV, Figures 4.3c and 4.4c, respectively).

Site-Specific Model Parameters. Parameters of required model inputs for each study site location are listed in Table 6.2. Area parameters identified the cell size for site spatial grids, total number of cells, and total marsh area. Elevation parameters identified the elevation of mean high water, the elevation that was flooded by only 15% of high tides (a high marsh delimiter), and the maximum tidal height for current and scenario upstream conditions. In addition, site values for an average elevation of upland edge and creek bottom were required. Elevation parameters were primarily used as delimiters for determination of cell flood regime. The model also required two site-specific measures

to estimate cell salinity regime; maximum distance from the tidal inflow culvert to the furthest extent of the marsh, and the salinity level (high, mid, or low) of the incoming tidal flow (see Assignment of Cell Salinity Regime in this section). Lastly, an average site measure of sediment accretion at field elevation stations (Chapter III, Table 3.2) were provided to estimate marsh surface sedimentation rates for each cell.

Spatial Baseline Map Development. For each study site, mapping techniques were used to construct spatially-explicit cell grids that described cover type (marsh plant, upland, or water), elevation, and salinity regime. Map development was based on aerial photographs (standard 3.75-minute digital orthophoto quadrangles from the U.S. Geologic Survey). For the Little River site, a geographic information system (GIS) cover map from the New Hampshire Office of State Planning was used in addition to the orthophoto. Photos were scanned, and a section of the photo that included the marsh site was expanded to a full page and printed. This page was further expanded by about 1-to-4 using a copy machine, pages were edge-matched, and the marsh outline was delineated by differences in appearance between upland and marsh vegetation. The final image was overlaid on a drafting worksheet separated into 40,000 2 mm x 2 mm cells (a total grid of 200 rows by 200 columns). The orientation of the grid image was always placed north-to-south along the column axis; scale was determined by comparing image dimensions to known distances in the field (typically, culvert length). The resulting grid image was used to identify the upland boundary of the marsh, including roadways and upland islands within the marsh, and flooded areas of tidal creeks, deep ditches, and salt marsh pannes.

Baseline maps were developed by drawing marsh transects and plant community zones on the grid image from field notes taken during the elevation survey (see Chapter V, Marsh Elevation Surveys, Methods). To delineate transect lines, the main creek centerline was established on the grid and transects were drawn perpendicular to the centerline at randomly chosen intervals. Transect starting locations were located on the grid, and survey points were numbered from start to finish at the map scale interval that represented 15 m on the ground. The dominant plant community type (species with the highest percent cover) for each survey point was recorded on the grid by color-coding the cell with an ink marker. Individual cells were expanded to entire zoned regions of dominant plant communities based on field notes, and produced a complete color-coded grid of cover types for each marsh. A total of nine cover types were used; six for specific plant community types, and one each for non-vegetated marsh, upland, and constantly submerged cell areas.

Translation of paper-based grid images to computer-based databases was accomplished using drafting tools and custom software. Grid images were secured to an 18' x 24' drafting table with a moveable T-bar guide. Row by row, images were 'scanned' by moving the T-bar guide to the row and recording the cover type, start column, and end column for blocks of cells with the same cover. Results were entered into custom software that generated one record in a database for each grid cell (40,000 total cells per site, although some cells represented bordering uplands). Each cell was identified by a row and column coordinate and coded with cover type. For cells that also occurred on elevation survey points, the observed elevation (adjusted to m NGVD) was

added to the cell record. In this manner, a spatial database was developed for each study site that identified the baseline cover type for each cell in the marsh grid, and the known elevation of survey points. Procedures used to assign percent cover for each plant species, elevation for non-sampled locations, and flood and salinity regimes are described in the following sections.

Estimates of Initial Species Cover. The baseline mapping procedure resulted in a cover type for each vegetated cell (indicating the dominant species) but the model required numerical estimates of individual species percentages for predictions of plant species composition changes. Results from the marsh vegetation survey (Chapter IV, Methods) were used to derive these estimates. Since the field survey recorded actual species or bare ground percent cover, and the model required the relative portion of the plot occupied for each species, survey data required standardization prior to model use. For plots with 5% or more vegetated cover, bare ground cover was allocated to each of the six species found in the sample quadrat according to the observed proportions of species percent cover. Samples with less than 5% vegetated cover were coded as bare ground. In addition, if a sample quadrat had less than 5% study species, and trees, shrubs, or other upland plants were present, the plot was coded as upland.

Percent cover for several common non-study plant species found in the surveys were added to study species based on observed plant associations. *Salicornia europaea* (glasswort), a succulent annual halophyte, is typically found in disturbed areas or bare patches of New England low marsh and high marsh habitat (Niering and Warren 1980).

Ellison (1987) studied the distribution of *Salicornia europaea*, and found that it was most common beneath the canopy of short-form *Spartina alterniflora*, therefore glasswort percent cover was assigned to *Spartina alterniflora*. *Distichlis spicata* (spikegrass), another halophytic colonizer, is often found in disturbed areas of high marsh. Reports indicated that, although spikegrass was common in both *Spartina patens* and *Juncus gerardii* zones, the species was most often found in the wetter (lower-elevation) areas of the high marsh typically associated with *Spartina patens* (Niering and Warren 1980, Bertness and Ellison 1987). Therefore, occurrences of *Distichlis* from the field surveys were added to *Spartina patens* cover percentages. Lastly, *Spartina pectinata* and *Scirpus* spp. were frequently observed in the brackish marsh regions of study sites. These species are often associated with stands of *Typha angustifolia* and sometimes *Phragmites australis* (Burdick et al. 1999, Warren et al. 2001). For this model, observations of *Spartina pectinata* and *Scirpus* spp. were assigned to *Typha*. Occurrences of other species were noted in the field, but ignored in the computation of species cover percentages.

Species cover values were used to construct average species assemblages for each cover type at a site. This was done by grouping samples according to dominant plant species, and computing the mean cover of all six species within the group. These averages were then applied to all of the cells for that site sharing a common cover type. For example, if *Juncus*-dominated samples for a site were evenly split between 80-20% and 60-40% *Juncus-Spartina patens* cover percentages, then all *Juncus* cells were assigned to 70% *Juncus* and 30% *Spartina patens*. Initial species cover proportions for

each site, grouped by dominant plant association, are presented in Table 6.3. The mean cover percentages for the dominant species ranged from 60% (*Juncus*) to 90% (*Typha*), with an overall mean of 77%, indicated that all of the six study species were capable of dominating marsh regions and forming exclusive stands in New England salt marshes (Niering and Warren 1980, Dzierzeski 1991, Bertness 1992, Warren et al. 2001). The added contributions of associated plant species cover to the six study species were generally minimal (< 2%). Exceptions were 13% *Spartina pectinata* added to *Typha* at Drakes Island, 10% *Distichlis spicata* added to *Spartina patens* at Oak Knoll, 6% *Scirpus* spp. added to *Typha* at Mill Brook, and 5% *Salicornia europaea* added to *Spartina alterniflora* at the Little River study site (data not shown).

Estimates of Elevation. Survey point sampling represented only a small fraction of the total grid cells in a marsh, but all cells required a measure of elevation to determine flood regime. For this project, the statistical technique known as ordinary kriging (Isaaks and Srivastava 1989) was used to estimate elevations for non-sampled cells. Kriging, a method that produced statistically optimal estimates for unobserved locations using a small but spatially-explicit sample, has been shown to be a robust estimation technique for geospatial estuarine applications (Little et al. 1997, Porter et al. 1997). The technique was based on a statistical analysis of differences between observed values at varying distances (spatial continuity), and assumed that autocorrelation between points depends only on distance. To use an example from the current project, elevation at one salt marsh location was likely to be very similar to the elevation at another point only one meter away (unless a creek or ditch was encountered). But it would be expected that this



similarity would decrease with distance from the first location, up until a point where all elevation similarities were simply random. The identification of this maximum distance, and a function that estimated changes in autocorrelation over distance, was developed through the process of semivariogram analysis, a mandatory first step in the use of kriging techniques.

Semivariogram analysis was based on a plot of differences between point elevations as a function of distance between survey points. The statistical measure for differences between point elevations was the moment of inertia (half of the squared difference between elevation point values, Isaaks and Srivastava 1989). The analysis combined survey elevation points from all four marsh sites. The key statistical measure from the semivariogram, the range, was computed as the distance at which 95% of the maximum difference between points (a value known as the sill) was observed. Semivariogram results were then compared with estimates from basic statistical functions to select a transition model for kriging algorithm use. Three common functions were evaluated for this project: spherical, exponential, and Gaussian (Isaaks and Srivastava 1989). Estimates from these functions were compared with observed results, and least-squares analysis was performed to find the model with the best fit.

Ordinary kriging algorithms were developed in a separate software program (see Program Listing 1) according to the specifications provided by Isaaks and Srivastava (1989). Computer instructions for matrix inversion were based on Ayers (1962). For this project, kriging algorithms used the three nearest known elevation points to estimate an

unknown value (a search function found the three nearest survey points based on cell coordinates and cell size). If the upland edge was found to be nearer than any of the three survey points, the upland edge elevation (*uplandel*, Table 6.2) was used as one of the three kriging points (replacing the furthest survey point). The kriging utility produced elevation estimates for each marsh cell that was not coded as upland or water area.

To assess the accuracy of elevation estimates, kriging was used to generate estimates for each known survey point. PRESS statistics were computed as the measure of error for each estimate (prediction sum of squares, Equation 1, Little et al. 1997). PRESS results from kriging were also compared with results from an exercise using linear interpolation to estimate elevation of known points (a simple average of the elevation measured before and after each point along the transect). For this exercise, estimates were not made for the first and last points of each transect, or when one of the nearest survey points was located in a creek or ditch.

$$\text{PRESS} = \sum_{\text{point } i-j} (\text{Observed Elevation}_{\text{point } i-j} - \text{Estimated Elevation}_{\text{point } i-j})^2 \quad (1)$$

Assignment of Flood Regime. The model determined the flood regime (low marsh, mid marsh, or high marsh) for each cell by comparing the elevation of the cell to site and scenario-specific water elevation delimiters identifying mean high water and high marsh elevations (*mhwater* and *hiwater*, respectively, Table 6.2). Model use of these delimiters was based on reports of ecological significance at these relative elevations for common salt marsh plant species (see Chapter V, Delimiters of Marsh Gradient Locations). Specific elevation values were identified from an analysis of tidal

heights in a complete two-week tidal cycle of current conditions, and a selected hydrologic scenario for each site (Chapter IV). Mean high water was the average of all high water elevations in the tidal cycle record, and cell elevations below this level were assigned to the low elevation regime. The high marsh elevation began at the height of the 4<sup>th</sup> highest high tide in the tidal cycle record (flooded by 15% of 27 high tides in two-weeks). Cell elevations between mean high water and the high marsh elevation (inclusive) were assigned to the mid elevation regime. Cells with elevations above the high marsh line were assigned to the high elevation regime.

Assignment of Salinity Regime. Model determination of cell salinity regime was based on five factors: cell elevation, maximum high water elevation, creek salinity at the tidal source, relative location of cell between the nearest open water and upland, and relative location of cell between the nearest tidal source (culvert or creek mouth) and upland. These factors were processed by a salinity submodel to assign a low, mid, or high salinity regime to each cell. These regimes generally corresponded to levels of mean substrate salinity measured during the field experiment described in Chapter I (low: mesohaline 5-18 ppt, mid: meso-polyhaline 18 ppt, and high: polyhaline >18 ppt, per Odum et al. 1984). Site-specific field data required to parameterize the salinity submodel (elevation, tidal signal, substrate salinity at the tidal source) were based on regional data collection standards (Neckles and Dionne 2000), supplemented with scale measurements from USGS orthophotos and spatial grid computation.

Under field conditions, observed marsh substrate salinity levels have been related to a number of physical and biotic factors, among them marsh proximity to open ocean (Odum et al. 1984, Warren et al. 2001), distance from tidal creek (Pearlstone 1993, Gardner et al. 2002), marsh plant shading (Bertness 1991a), rainfall and evapotranspiration (Gardner et al. 2002), and soil hydraulic properties (Harvey et al. 1987). In fact, it seems the more we know about the spatial distribution of salt marsh salinity levels, the more difficult it becomes to develop a predictive model (see Gardner et al. 2002 for a discussion of observed salinity anomalies). However, two generalities can be stated with some confidence. First, overall marsh salinity levels are diminished with increased distance away from the open-ocean source. Many estuarine researchers attribute this effect to the upstream dilution of intruding tidal saltwater (Odum et al. 1984, Pearlstone et al. 1993, Warren et al. 2001, Gardner et al. 2002). Second, within a marsh system, salinity levels are generally reduced with movement away from the tidal creek toward the upland edge, likely due to interactions of relative elevation, substrate hydraulics, tidal signal, and the tidal pressure wave (Harvey et al. 1987, Pearlstone et al. 1993, Gardner et al. 2002). So, a spatial scheme that considered the distances from tidal sources and creeks, combined with relative elevation, should be able to capture the essence of general shifts between broad (but ecologically-important) salinity regimes.

In concept, salinity model processing created a matrix of salinity subzones within each marsh spatial grid. These subzones were delineated by modeled breakpoints that grouped collections of cells with common spatial properties (i.e., closeness to open water and tidal source). Two sets of delimiters were used. First, the model computed the

distance from a cell to the tidal source, and divided this distance by the site maximum distance from the tidal source as a relative measure of closeness to the tidal source (0-1, *sdist*). Next, the model determined the distance from the cell to the nearest open water and divided this value by the distance to the nearest upland edge as a relative measure of closeness to tidal water (0-1, *wdist*). Cell values were then grouped into three equal sized categories for relative distance from source ( $S1:sdist > .67$ ,  $S2:.67 > sdist > .33$ , and  $S3:sdist < .33$ ) and for relative distance from water ( $W1:wdist > .67$ ,  $W2:.67 > wdist > .33$ , and  $W3:wdist < .33$ ). As a result, each marsh was separated into nine subzones: high salinity cells were S3 and W3, S3 and W2, or S2 and W3; mid salinity cells were S3 and W1, S2 and W2, or S1 and W3; and low salinity cells were S2 and W1, S1 and W2, or S1 and W1 (Figure 6.2). An exception to this scheme was made for cells with elevations above the maximum high water mark for the marsh (*maxwater*, Table 6.2), in which case the cell salinity was always low. This accounted for the occurrence of high marsh vegetation in high elevation islands near the tidal source for some marsh sites (notably, Drakes Island and Oak Knoll). In addition, if the salinity of the incoming tidal water (*salinity*, Table 6.2) was mid or low (not the case for any study site), the model would shift the salinity regime to a reduced level, as appropriate.

Estimates of Cell Sedimentation Rate. For each cell, the model estimated the sedimentation rate based on three factors: cell elevation, upstream tidal heights, and site-specific sediment accretion rates. Estimates were based on Stumpf (1983), who found that sedimentation on a marsh surface was a function of the settling of suspended solids, and therefore the highest rates were on the levees that formed along tidal creeks. Further,

Stumpf determined that the rate of deposition diminished from creek bank to high marsh as the water-borne particles settled out, but this was more a function of tidal flooding than distance from the creek. In particular, it was found that the level of tidal inundation accounted for the observed levels of sedimentation at mid and high marsh locations. Stumpf attributed this phenomenon to storm-flooding events and regular tides. Other researchers have also found that flood level was an important determinant of sedimentation patterns (Ward et al. 1998, Anisfeld et al. 1999), although there are many other complex physical and biotic factors that present serious challenges to modelers (see Chapter III, Table 3.1).

For the study sites of this project, average sediment accretion rates were measured at field elevation stations located near (10 m) main creeks at each site, according to the regional data collection protocol (Neckles and Dionne 2000). These values (*sedmax*, Table 6.2) were therefore considered the maximum sedimentation rates for each site. To simulate the distribution of sediments across the marsh surface, the model compared the elevation of each cell to the upstream tidal record (see Chapter IV) and computed the percent of time the cell was flooded by the tide. Since the model considered only flooding from typical (non-storm) tides, the percent of time flooded for each cell was used to estimate a reduction in sediment accretion from the measured maximum value at the creek bank. An analysis of tidal inundation levels recorded during the field experiment (Chapter I, Table 1.1) showed that the study mid-marsh areas were flooded 13-16% of the time by tides. Therefore, flood levels above 16% inundation were considered representative of the low marsh conditions at field elevation stations (10 m

from creek). Cells with 16% or higher flood inundation were assigned to the maximum sedimentation rate; cells with flooding less than 16% received a reduced fraction of maximum sediments according to percent of time flooded (Eq. 2). Estimates of sediment deposition were used as inputs to the relative elevation processing model (Chapter II).

$$\text{Sediment Input} = \text{sedmax} * (1 - (\text{MAX}(0, 16 - \text{Flood Percent} / 16))) \quad (2)$$

Estimation of Neighbor Species Composition. Modeled processes associated with plant succession required an estimate of neighboring plant species composition as a measure of recruitment potential (Chapter V). The model estimated neighbor composition once per annual cycle, at week 30. To compute these estimates, the model first located all neighbor cells in the spatial grid (cells sharing a border, with a total of up to eight). The model then averaged the percent cover values for the six study species across all neighbor cells to compute an aggregate profile of neighbor species composition. Neighbor species composition was stored to the spatial database, and used in conjunction with a recruitment weight factor to compute the portion of plant succession change attributable to recruitment (Chapter V).

Model Validation. The spatial model was first used to establish performance benchmarks associated with model validation. The validation sites, Mill Brook and Drakes Island, were chosen as the two study sites with the longest record of observation following hydrologic modifications (9 to 14 years ago, respectively, see Study Sites, Introductory Chapter). To initialize validation conditions, the spatial databases for these

sites were configured with estimates of marsh plant cover just prior to hydrologic restorations, based on Burdick et al. (1999). This report, however, was very limited in terms of specific plant cover and spatial distribution. At Drakes Island, a two-sample survey (2 m<sup>2</sup>) was conducted in 1988, the year of known hydrologic modification at the site (unplanned removal of the tide gate). The survey indicated that the marsh was dominated by *Typha* spp. but no spatial information was recorded. Therefore, a pre-modification cover map was created for Drakes Island with each cell configured identically with 50% cover for *Typha*, and 10% cover for each for the other five species. At Mill Brook, a six-sample survey (6 m<sup>2</sup>) conducted in 1993, the year of planned tidal restoration, indicated that that marsh was dominated by mixed zones of *Lythrum salicaria*, *Typha* spp. and *Phragmites australis*, with remnant populations of *Spartina patens* and *Juncus gerardii*. A rough spatial map of Mill Brook was constructed that delineated these plant zones (D. Burdick, personal communication) and like Drakes Island, the dominant species in each zone was assigned 50% cover with the other five species receiving 10%.

In addition to plant cover, model validation runs required estimates of cell elevation prior to hydrologic modification. If current elevations were used, the model would incorrectly estimate elevations when new sediments and organic matter were applied, resulting in differences in elevation that might alter assignment of cell gradient location. Therefore, starting cell elevations for validation exercises were estimated as the current elevation plus or minus an adjustment factor. Adjustment factors were generated for each cell by running the model for the number of years since hydrologic modification



(9 years for Mill Brook, 14 years for Drakes Island), and computing the net differences between modeled values and current cell elevations. As a result, cell elevations for the last year of validation runs (the current year) closely agreed with estimates based on recent survey results.

Validation model runs produced spatial databases that contained, for each marsh cell, one baseline record (year 0) and multiple prediction records (years 1-9 for Mill Brook, 1-14 for Drakes Island). Individual species results were analyzed, and a cell cover type was assigned to the species with the greatest cover value. For each year in the model run, annual spatial cover maps for each site were generated using an output utility that assigned different colors to cover types. An image of each map was copied into a standard image edit utility (Microsoft Photo Editor, Microsoft Corporation, Redmond, Washington, USA), and output into JPG file format. A complete series of annual images were then compiled with a shareware utility (Platypus Animator, C Point Pty, Ltd., Queensland, Australia) into AVI animation file format for playback as a time-sequence video.

To quantify the performance of the spatial model, plant cover results from the final year of the validation model runs were compared against current conditions. A utility program read through the validation database cell-by-cell and compared predicted cover type with the observed cover type from the same-coordinate cell in the baseline database. A summary matrix was generated that showed observed versus predicted cell counts for each species at each site.

Two separate performance metrics were used to assess the model goodness-of-fit, based on Turner et al. (1989). To measure spatial error, an address goodness-of-fit metric (address error) was computed for each species by expressing the number of cells with matching (predicted = observed, Model Match) species cover type as a percentage of the total number of observed cells (Survey Total), subtracted from 100% (Eq. 3). To measure non-spatial accuracy, a composite goodness-of-fit metric (composite error) was computed for each species by expressing the total number of predicted cells (Model Total) as a percentage of the total number of observed cells (Survey Total), subtracted from 100% and reported as an absolute value (Eq. 4). Site measures of accuracy and composite error were computed as the average error of all species, weighted by the relative percent of each species observed at the site. Error results were also combined for both sites to compute overall model performance metrics. Since restoration managers are mostly concerned with recovery of natural plant communities, the six study species were grouped as native halophytes (*Spartina alterniflora*, *Spartina patens*, and *Juncus*) and brackish invasive species (*Phragmites*, *Lythrum*, and *Typha*) for an additional analysis of model error rates.

$$\text{Address Error}_{\text{species}} = 100 - (100 * (\text{Model Match}_{\text{species}} / \text{Survey Total}_{\text{species}})) \quad (3)$$

$$\text{Composite Error}_{\text{species}} = \text{ABS}(100 - (100 * (\text{Model Total}_{\text{species}} / \text{Survey Total}_{\text{species}}))) \quad (4)$$

Model Scenarios. For each study site, the model was run for twenty years configured with current hydrologic conditions and baseline spatial maps (elevation and salinity). For Drakes Island and Oak Knoll, the model predicted changes in species composition with continued tidal restriction (note that, even though Drakes Island was partially restored in 1988, it was still considered a tidally restricted site). For Little River and Mill Brook, the simulations showed the impacts predicted from tidal restoration. In addition to current conditions, site-specific hydrologic scenarios were used for a second set of twenty year model runs. At Drakes Island and Oak Knoll, hydrologic scenarios were selected from an analysis of tidal restoration options (Chapter IV). Simulations showed the predicted impact on plant species composition if these restoration scenarios were implemented. At Little River and Mill Brook, model scenarios were used to show the predicted distribution of marsh plants if past tidal restrictions had remained in place. As with the validation model runs, spatial output for each year of each model run was saved in image format, and compiled as part of a scenario animation file.

3-D Visualization. A software visualization tool, World Construction Set (WCS, 3DNature, Inc., Arvada, Colorado, USA), was used to render realistic animated images of marsh sites under current and hydrologic scenario conditions. Development of visualization images was based on the generation of a fine-scale digital elevation map (DEM) for each study site. To generate these maps, a software utility was built to scan an entire marsh grid of current cell elevations and to output the grid as a single ASCII array of elevation values (200 rows by 200 columns). The ASCII array file was then imported into the WCS software to create a digital elevation map for each study site.

From this starting point, standard features of the WCS program were used to assign images of marsh vegetation types to regions of similar elevation, and to manipulate other factors such as lighting, perspective, aspect, and texture. In this manner, a composite image of each salt marsh was designed. An additional feature of WCS allowed for the specification of a maximum water elevations and timing sequences to simulate tidal flooding. Maximum water levels for current conditions and hydrologic scenarios (Table 6.2) were used as WCS parameters to generate images of tidal flooding for each study site. Lastly, these images were used to generate animation files (AVI format) for time-sequence visualizations of different hydrologic scenarios.

### **Results and Discussion**

Spatial model and visualization output represented highly aggregated model results, based on many layers of internal model parameters and estimates. For purposes of clarity, results are presented in a stepwise approach that builds layer-by-layer toward the final model outcomes. Therefore, results were organized into sections that described model output in the following order: 1) cell estimates for elevation, 2) baseline site maps of plant cover, elevation, and salinity (current conditions), 3) plant cover site maps from validation exercises, 4) plant cover site maps for current and hypothetical hydrologic conditions at extended timeframes (+20 years), and 5) site visualization images of restored conditions (current or hypothetical).

Estimates of Cell Elevation. Semivariogram analysis, conducted prior to kriging estimation for cell elevations, generated a plot of point-to-point differences in marsh survey elevations over distance (Figure 6.2). The plot showed that differences between survey elevations increased with distance between points, until an asymptote was reached at a distance of about 45 meters between points (three intervals of 15 meters from the field survey). This 45 m distance was computed as the semivariogram range, the distance at 95% of the asymptote value (0.065, estimated from Figure 6.2). Interpretation of the graph meant that, along a transect survey, there was correlation between two consecutive points (15 meters apart), but this correlation was reduced with distance until, at 45 meters or more between points, all correlation was due to random effects. The diagram showed that, even at 15 meters, about 2/3 of the maximum error was reached (0.041 at 15 m to 0.065 beyond 45 m). These findings were based on a sample size of only four marsh systems, but if other regional salt marshes exhibit similar elevation profiles, the analysis implied that elevation surveys conducted for purposes of estimating spatial grid elevations should use transects no more than 90 m apart. This would ensure that all non-sampled points were 45 m or less from known elevation points. A check of transect spacing for the current project indicated that, on average, survey transects were 85 m apart (data not shown), a distance that fell just within the limits of this new guidance.

Three transition models were tested for fit with observed results: spherical, exponential, and Gaussian. Sum of the squared differences between model predictions and the observed results were 0.00020, 0.00006, and 0.00011 for the spherical, exponential, and Gaussian models, respectively. The exponential model achieved the

best fit (least difference) and was therefore selected for kriging use. The expression for the exponential function (Eq. 6) was taken from Isaaks and Srivastava (1989).

$$\text{Difference in Elevation} = 1 - \text{EXP}(3 * \text{Distance to Nearest Survey Point} / \text{Range}) \quad (6)$$

An analysis of kriging error with the PRESS statistic (prediction sum of square, Little et al. 1997) was based on the comparison of kriging and linear interpolation estimates for known survey points. Results of the mean PRESS statistic for each of the four study sites are provided in Figure 6.3. In three of the four sites, the kriging error was less than the error from linear interpolation (and about the same at Little River). Error reduction was 5% at Mill Brook, 18% at Drakes Island, and 22% at Oak Knoll, suggesting that kriging was an improved estimation method over simple interpolation methods. Figure 6.3 also indicated that elevation estimates were more prone to error at Drakes Island, and less so at Little River. This result agreed with observations of high variability in elevation at Drakes Island (many upland islands) and low variability at Little River (large flat expanses). The relative steepness at the center of the hypsometric curve at Drakes Island (Chapter IV, Figure 4.2b, from 20 – 80% of the marsh surface) was another indication of elevation varying across much of the marsh area. Overall, results from the PRESS analysis indicated that kriging produced reasonable elevation estimates and improvements over simpler interpolation methods.

Initial Spatial Database and Base Maps. Using estimates of elevation and other factors (see the Methods section for specific rules), the model examined each cell in each

spatial database to assign flood and salinity regime categories. In addition, cell cover type was assigned from data recorded during the grid design process. Three separate cover maps were then generated for each site: cover type (six plant species, water, upland, or bare ground), salinity regime (high, mid, and low) and flood regime (high marsh, mid marsh, or low marsh). A species-by-species summary of baseline plant cover at each site was also provided (Table 6.4, current conditions).

Initial maps for Drakes Island are presented in Figure 6.4. The cover map showed the distribution of *Spartina alterniflora* and *Spartina patens* around the impounded tidal creek, surrounded by primarily *Typha* toward the uplands. *Typha* was the dominant plant species at the site by a wide margin (58% cover, Table 6.4). In addition, several large but distinct colonies of *Phragmites* were observed. An interesting feature of Drakes Island, the hilly islands of upland plant species, was evident throughout the marsh. The salinity map clearly showed the distribution of high salinity cells clustered near the inlet of the tidal creek (left edge of map), with diminished salinity moving toward the upland and away from the creek entrance. The elevation map indicated the asymmetric variability of elevation at the site, and in particular, the many regions of low-lying areas scattered across the marsh surface. Close examination of the elevation map also revealed somewhat linear patterns of elevation estimates that were artifacts of the kriging algorithms.

Baseline spatial maps for Little River are presented in Figure 6.5. The cover map indicated the distribution of halophyte species along the creek banks and toward the tidal

source (right edge of map), but in general, the recently-restored site was still dominated by brackish species. *Lythrum*, *Phragmites*, and especially *Typha* accounted for 56% of the current marsh cover, but *Spartina patens* presence was considerable as well (Table 6.4). Little River also contained a number of large pannes throughout the marsh, more so than the other study sites. The salinity map showed that a high percent of marsh area was near enough to a creek and low enough in elevation to be assigned to high salinity levels, although large tracts of the marsh were also low salinity (left side of map, away from tidal source). These assignments seemed to reflect the vegetative cover of the map, with *Typha* and *Lythrum* found in peripheral areas, and *Spartina alterniflora* and *Spartina patens* in the marsh flats and around the pannes. The elevation map showed that a majority of the marsh was mid elevation (above mean high water but flooded by at least 15% of tides), suggesting that Little River might respond very well to the recent hydrologic restoration project. As with the Drakes Island map, intermittent linear patterns of elevation were likely artifacts of kriging, and probably not representative of actual elevations.

Figure 6.6 showed the base maps for Mill Brook. Plant cover at Mill Brook appeared to align well with the outline of the tidal creek, with *Spartina alterniflora* and *Spartina patens* accounting for nearly half (49%, Table 6.4) of the total plant cover. Several patches of *Phragmites* were also evident, but *Typha* was the most prevalent species (42%, Table 6.4) and occupied large tracts of the marsh toward the uplands and away from the tidal source (culvert at top edge of the map). The salinity and elevation maps for Mill Brook showed excellent agreement, with low elevations and high salinities



along the creek toward the source, a middle region between creek and uplands, and low salinities at the upland borders.

Maps for Oak Knoll are presented in Figure 6.7. The cover maps showed a linear pattern of *Spartina alterniflora* along the creeks and large ditches, and large tracts of *Spartina alterniflora* and *Spartina patens* in the marsh flats. These two species combined for 69% of the total marsh cover (Table 6.4), the most of any study site. The marsh also contained substantial areas of *Phragmites* (~20% of the marsh), and several patches of *Lythrum* and *Typha*. The modeled salinity regime appeared to follow closely with the outline of the main creeks and ditches. In addition, the elevation map revealed very little low elevation terrain (below mean high water) at Oak Knoll.

Model Validation. Field specifications from the Drakes Island and Mill Brook sites provided independent datasets for the assessment of model performance. At Drakes Island, the model was configured for pre-1988 marsh conditions (prior to the inadvertent removal of the tide gate) and run for 14 years until the present. A time sequence of model predictions for marsh plant cover is presented in Figure 6.8. Initial plant cover in 1988 was entirely *Typha*, but large tracts of the marsh surface were predicted to be dominated by *Spartina alterniflora* and *Spartina patens* within two years. It is important to note that the model selected a cover type based on relative plant cover, so if marsh areas were sparse following hydrologic disturbance, emerging vegetation would provide sufficient individuals to trigger a shift in plant cover type. Modeled timing of plant succession at Drakes Island following tidal restoration generally agreed with published

reports of single-season die-back of invasive species like *Typha* and *Phragmites* in low and mid marsh areas, and re-colonization by halophyte species (Roman et al. 1984, Sinicrope et al. 1990, Burdick et al. 1997, Roman et al. 2002, Warren et al. 2002). Following the dramatic changes associated with the disturbance event, the model predicted only gradual differences in plant cover for the remaining years of the model run.

Time sequence model simulations for Mill Brook (Figure 6.9) produced spatial patterns of plant succession similar to those predicted at Drakes Island. By 1995 (two years following hydrologic restoration), *Spartina alterniflora* and *Spartina patens* had replaced *Lythrum* and *Typha* in low-lying areas near the tidal creek. However, species replacement in high marsh locations appeared to be a slow process even though the tidal restriction at Mill Brook was completely removed. This result suggested that plant habitat response to hydrologic restoration may follow different trajectories of recovery between low marsh and high marsh locations (Warren et al. 2002). If physical stress becomes less of a determinant of plant succession in the high marsh and competition becomes more important (Bertness and Ellison 1987), then differences in low marsh and high marsh habitat recovery rates following hydrologic restoration may be attributable to the fundamental shifts between primary succession (rapid response to disturbance) and secondary succession (slow response to competition), as hypothesized by Tilman (1982, 1988).

Analysis of validation results were conducted to provide a quantified measure of model performance. Plant cover for the last year of the validation model runs, percent cover for each species, and current conditions are shown for the Drakes Island and Mill Brook sites (Figures 6.10 and 6.11, respectively). The model produced reasonably good agreement between predicted and observed total species composition (figure pie charts), however, the spatial agreement for cell-by-cell cover was highly variable.

To quantify model agreement with observed conditions, spatial results were analyzed and error metrics computed (Tables 6.5 and 6.6). Address error was a measure of cell-by-cell spatial agreement between observed and predicted plant cover for each species. At Drakes Island, address error ranged from a low of 21% (*Typha*) to a high of 100% (*Juncus*). Since error computations were highly sensitive to the number of observed cells for each species, the least common species typically produced the highest margin of error. To correct for this bias, a weighted average of address error was generated for each site (Table 6.5, underlined value in Address Error). The 39% error at Drakes Island indicated that, on average, the model picked the wrong species in 39 out of each 100 cells (61% accuracy). For Mill Brook, address error ranged from a low of 27% for *Spartina alterniflora* to a high of 100% (*Juncus* and *Lythrum*), with a weighted average error of 55%.

When results from both sites were combined, the overall weighted average for address error was 46%, a reasonable result considering the very limited spatial information available for initial pre-restoration configurations. In addition, the

assignment of initial plant cover values at 50% for dominant and 10% for all other species provided a big advantage to the dominant species that was (mathematically) difficult to overcome. Still, despite the long odds of picking a single correct species out of six from a nebulous starting point, the model managed to get it right more than half the time (54%). For individual species, combined spatial results were best for *Typha* (28% error), but this was expected since *Typha* was the most common dominant species at the start of the model runs at both sites, and, as noted, this species was awarded a five-to-one advantage in initial cover over other species. Overall results for *Spartina alterniflora* and *Spartina patens* were good (49% and 68% error, respectively), although the model was a poor predictor of *Phragmites* spatial distribution (only 4% correct). *Phragmites* results were likely associated with the species' patch-like colonization pattern in marshes, rather than in predictable zonal pattern by elevation or salinity (Warren et al. 2001, Chapter I).

Address errors for aggregated halophyte and brackish species groups showed improved results relative to individual species totals, with error rates ranging from 19% to 35%, and average errors of 23% and 30% for Drakes Island and Mill Brook, respectively (Table 6.6). For the sites combined, the weighted average of address error was 25%, indicating that 3 out of 4 spatial cells were correctly predicted as either halophyte or brackish species.

Composite error was a measure of model performance in predicting the total number of species cells for each site. Since the model could select more cells for a species than was observed and these values were percentages of observed counts, the

measure was unbounded. At Drakes Island, the composite error ranged from a low of 2% for *Typha* to a high of >1000% for *Juncus* (Table 6.5). Like address error, these values were sensitive to the number of total cells observed. Even though the model predicted that *Juncus* would occupy 470 marsh cells (<1% of total marsh area at Drakes Island), the error computation used a basis of only 16 cells. Overall composite error at Drakes Island was 11%, meaning that the model, on average, deviated from observed species counts by 11% (high or low) at the site. At Mill Brook, species composite error ranged from a low of 20% for *Juncus* to >1000% for *Lythrum*, with an average site composite error of 42% (Table 6.5). This error was nearly four times the rate at Drakes Island, a somewhat perplexing result. The Mill Brook site had the advantage of a slightly more detailed initial plant cover map than Drakes Island, but this obviously did not contribute to better model performance for the site. Model error at Mill Brook was largely a result of predicted *Lythrum* occurrence along the upland edges of the marsh (~10% of total marsh area, Figure 6.11), a hold-over from the initial cover map. However, *Lythrum* is almost entirely absent from the marsh today, calling into question the accuracy of the initial distribution map, or model performance with regard to this species.

Combined model results for individual species counts showed that overall composite error was 12%. This weighted average was obviously more influenced by Drakes Island results than Mill Brook, since Drakes Island had about twice as many total vegetated cells (Table 6.5). Composite species error rates were excellent for *Spartina alterniflora* (3%), *Spartina patens* (4%), and *Typha* (8%), but poor for *Juncus* and especially *Lythrum* (Table 6.5). Results for *Juncus* and *Lythrum* were, at least in part,

attributable to low overall species counts. *Phragmites* error was intermediate (20%), and the model was conservative in predictions of cover (predicted cover was less than observed, Table 6.5). The better model performance for predicting species aggregate counts was expected, given the difficulties inherent in predicting exact spatial results from very limited initial data.

Composite error for aggregated halophyte and brackish species groups, like the address error results, showed improvements from individual species rates. Composite error ranged from 1% to 10%, with average errors of 1% and 9% for Drakes Island and Mill Brook, respectively (Table 6.6). For the sites combined, the aggregated composite error was 4%, indicating an average model accuracy of 96% in predicting the total halophyte or brackish species area in a marsh following hydrologic disturbance. Aggregate estimates of general plant cover in response to hydrologic restoration has considerable value for management, since halophyte and brackish species cover appears to be the most common metric for monitoring and assessing impacted salt marshes (Neckles and Dionne 2000). Therefore, validation results strongly suggested that the model was capable of generating useful and accurate predictions of changes in salt marsh plant species composition following hydrologic modification.

Model Scenarios. Twenty-year model runs were conducted to predict changes in plant species composition under current hydrologic conditions at the four study sites. In addition, hydrologic scenarios were used to predict marsh habitat changes associated with specific hydrologic modifications at each site. Simulation results for Drakes Island are

presented in Figure 6.12 and Table 6.4. Under current conditions of tidal restriction, the model predicted that halophyte species would be slowly replaced by brackish species, with the combined cover of *Spartina alterniflora* and *Spartina patens* reduced from 38% to 28% of marsh area, and combined cover of *Phragmites* and *Typha* increased from 62% to 71% of the marsh (Table 6.4). The increase in brackish species was due entirely to a four-fold increase in *Phragmites* cover. These results were consistent with observed reports of brackish species replacement of halophytes in tidally restricted salt marshes (Roman et al. 1984, Sinicrope et al. 1990, Burdick et al. 1997, Burdick et al. 1999). However, if a second 0.91 m (3 ft) culvert was added at an elevation 50 cm below the current culvert, the increase in tidal flow would double *Spartina alterniflora* cover from current levels, reduce *Typha*, and hold *Phragmites* in check (although *Spartina patens* habitat would be somewhat reduced, Table 6.4, Figure 6.12). These hydrologic restoration predictions were also in line with field observations, in this case recolonization of halophytes and diminished vigor of brackish species (Sinicrope et al. 1990, Burdick et al. 1997, Burdick et al. 1999, Roman et al. 2002, Warren et al. 2002). Therefore, if management objectives were to control or reduce brackish plant species and increase overall cover of native salt marsh species, these results indicated that addition of a second culvert would be an effective strategy.

For Little River, model scenario summaries are presented in Figure 6.13 and Table 6.4. Model projections of the recently expanded tidal hydrology at Little River indicated that the restoration project would lead to significant changes in plant cover. Marsh regions of *Spartina alterniflora*, *Spartina patens*, and *Juncus* were all predicted to

expand, to a combined total of 72% of the marsh surface area (Table 6.4). At the same time, cover percentages for the brackish species were all reduced, with *Lythrum* virtually eliminated from the marsh. Model results appeared to be in agreement with the conclusions of a pre-restoration study at Little River that predicted rapid retreat of brackish species and expansion of *Spartina patens* and other halophytes in response to hydrologic change (Burdick et al. 2002). These predictions were in stark contrast to results from the scenario of continued tidal restriction at Little River (Figure 6.13). Under this scenario, brackish species would dominate 93% of the marsh area, with *Phragmites* eventually becoming the principal plant species (56% cover, Table 6.4).

Model simulations conducted for Mill Brook indicated that the site had stabilized after almost ten years since hydrologic restoration (Figure 6.14 and Table 6.4). *Spartina alterniflora* and *Spartina patens* cover was predicted to slowly increase and dominate most of the marsh surface in twenty years (from 49% to 65%, Table 6.4). The model estimated that *Phragmites* cover would also continue to expand, although by only 3%. However, *Typha* was expected to lose significant amounts of cover, especially along the creek banks (Figure 6.14). On balance, these adjustments appeared to reflect fairly stable habitat conditions in the marsh, especially in relation to the dramatic changes reported to have occurred there from 1993 to 1996 (Burdick et al. 1997, Burdick et al. 1999). The scenario for return to pre-restoration conditions at the site indicated that, like Little River, these conditions would directly lead to the replacement of halophytes by *Typha* and especially *Phragmites* (54% cover, Table 6.4).



Spatial model results for Oak Knoll, a site with current tidal restrictions, are provided in Figure 6.15 and Table 6.4. With the undersized tidal culverts remaining in place for the next twenty years, the model projected that *Phragmites* cover would nearly double (Table 6.4) and invade much current *Spartina alterniflora* habitat (Figure 6.15). In addition, an increase in *Typha* cover was predicted along the upland edges of the marsh. Burdick et al. (2001) reported that *Phragmites* cover was expanding at Oak Knoll, however, the predicted loss of *Spartina alterniflora* habitat was somewhat puzzling. This prediction appeared to be driven by elevation estimates for the site (Figure 6.7), which indicated that very little of the site was at an elevation below mean high water. Therefore, most of the marsh regions currently covered by *Spartina alterniflora* were considered by the model to be mid marsh. Since this was not the preferred habitat of *Spartina alterniflora* (McKee and Patrick 1988, Chapter I), the model considered cordgrass at a disadvantage at Oak Knoll. In fact, *Spartina alterniflora* individuals observed at the site were typically short-form, stunted, and growing in mixed communities with *Spartina patens* (Boumans et al. 2002), affirming model estimates that much cordgrass at the site was in less-preferred gradient locations for the species. Further predictions of the model indicated that current stands of *Lythrum* would be replaced by *Phragmites* and *Typha* in future years if no changes were made at the site (Figure 6.15). The predicted eradication of *Lythrum*, similar to the pre-restoration scenario at Little River, conflicted with observations of long-term persistence of the species at these sites and indicated that the model may be underestimating *Lythrum* performance in high marsh areas where it is already well-established.

Model results for the hydrologic restoration scenario at Oak Knoll (expansion of the north culvert from 0.61 to 1.22 m), predicted that *Spartina patens* would expand to dominate the marsh and replace *Spartina alterniflora* and *Phragmites* (reduced by about half), especially near tidal creeks (Figure 6.15, Table 6.4). *Typha* would become the dominant species along the upland marsh borders. These results, especially the predicted increase in *Spartina patens* and the decrease in *Spartina alterniflora* cover, again appeared to be related to the scarcity of low elevation habitat at the site. In addition, the hydrologic restoration scenario only increased peak tidal heights by about 5 cm (although the frequency of flooding during spring tides was increased 5-20%, Chapter IV), and this small increase was apparently not enough to trigger a shift in current *Spartina alterniflora* zones from mid marsh to low marsh gradient locations. As a result, the model predicted continued halophyte dominance at the site (59%, Table 6.4), but with *Spartina patens* replacing *Spartina alterniflora* across most of the marsh area. This prediction mirrored the observed presence of *Spartina patens* throughout the surrounding environs of the Rough Meadows Sanctuary, a region well-known for its salt hay production (Burdick et al. 2001, Boumans et al. 2002). Therefore, the model indicated that hydrologic restoration at the site was a viable management option, especially if restoration objectives were to control the spread of *Phragmites* and to return the Oak Knoll marsh to its original state before tidal restriction.

Visualizations. Visualization image sequences for the four study sites were created with World Construction Set (3DNature, Inc.), based on translation of elevation estimates from the spatial databases into a standard DEM (digital elevation model)

format. Selected still images from these sequences are presented in Figures 6.16 to 6.19. At Drakes Island (Figure 6.16), the visualization showed an aerial view of the marsh, looking north from the culvert at Drakes Island Road. Images were developed for flood tides during the spring tide cycle under current conditions (upper image) and restoration scenarios (lower image). For Little River (Figure 6.17), images showed a slightly elevated view of the marsh as seen along the centerline of the main creek (due west) from above the culvert. The images projected spring tide flooding under current conditions (upper image), and for a similar tide under prior restricted conditions. Visualization scenes for Mill Brook were from above the expanded culvert, looking south, with the agricultural fields visible on the right side of the image (Figure 6.18). The scenes showed a current spring tide flood (upper image) and an empty creek to simulate conditions with the historic tide gate. For Oak Knoll, images were rendered for close-ups of the north creek, looking west from the culvert, to visualize differences in peak flood tides under current and restored conditions (Figure 6.19).

When viewed as animations, these images provided a new way to envision hydrologic changes for an impacted salt marsh system. Visualizations are particularly beneficial for people most connected and familiar with a marsh site (i.e., local residents), since the images are designed to show easily recognizable marsh topographic features, with changes only in plant cover and tidal flooding. In particular, these images can be used to assure residents that proposed hydrologic changes will not impact their property, especially during the maximum extent of tidal flooding. Visualizations of expected habitat change also show that proposed changes to the marsh are often subtle, and that

aesthetics will be preserved in the future. For these reasons, it is expected that visualization technology will be useful for coastal managers as an important new communications tool in the process of consensus-building among local and regional resource stakeholders.

### **Conclusions**

The spatial simulation model developed for this project was composed of four separate processing models for plant biomass production, marsh relative elevation, hydrodynamics, and plant succession. These models were based on published sources, and each component was independently implemented and validated. The integration of these process components into a single synthesized model brought together results from many years of field observations, theoretical studies, and experimentation in the area of salt marsh research. Outcomes from specific model exercises suggested that, in particular, marsh elevation was the most important determinant of model predictive ability. In support of this finding, kriging statistical estimation methods were used, based on field survey measures, to provide fine-scale spatial elevation maps. Kriging estimates were found to improve accuracy over simple interpolation techniques. The spatial elevation maps were used as the modeling basis for the assignment of marsh gradient location (flooding and salinity regime), and spatial schemes were devised that produced coherent assignments of gradient regime in comparison with observed vegetation cover.

Spatial model results analyzed for two independent validation sites determined that the average error for total marsh area of individual plant species was 12%, and this rate was lowered to 4% when results were grouped as halophytes and brackish invasive species. Model outputs should therefore be valuable for restoration planners seeking to predict marsh habitat changes in response to proposed hydrologic changes. The model was used to make long-term predictions of plant species composition change at four New England salt marsh sites (including the two validation sites) with past or current tidal restrictions. When configured with existing hydrologic specifications, model results appeared to reflect conditions of species stability or change appropriate for the history of hydrologic modifications at each site. The model was also used to simulate hydrologic restoration at tidally restricted marsh sites, based on scenarios likely to be proposed by resource managers. In these cases, model predictions were consistent with plant community responses observed at marshes with studied restoration activities. Lastly, realistic visualizations of marsh flooding under different scenarios were produced to explore new ways for managers to assess potential restoration outcomes, and as a communications tool aimed at informing (and reassuring) stakeholders faced with changes to a local natural resource.

In the final analysis, the real value of these technologies will be determined by those people directly involved in identifying, planning, and implementing hydrologic improvements in degraded New England salt marshes. We now have years of experience in designing and monitoring these projects, but results to date have suggested that there is still much to learn. Warren et al. (2002), in a summary of Connecticut tidal

restoration projects over the past twenty years, stated “The final form and function of [such] tidally restored wetlands *cannot be forecast in detail* [emphasis added] but will reflect biological, chemical, and physical changes associated with historical degradation of ecosystem functions and structures interacting with the restored tidal hydrology”. Maybe so. But the uncertainties and complexities inherent in these endeavors should *not* discourage us from working toward highly-specific predictions of salt marsh response, especially when those predictions are based on synthesized knowledge derived in large part from the teams of researchers cited within these chapters. It is certain, however, that new tools based on advanced technologies will continue to advance the science, and perhaps the politics, of wetland restoration.

Parameter	Name	Value and Unit	Source
<b>Relative Elevation</b>			
Root labile fraction	rlabfrac	0.2 unitless	Hemminga and Buth 1991
Leaf labile fraction	llabfrac	0.8 unitless	Valiela et al. 1985
Surface labile decomposition rate	klabsurf	0.2 week <sup>-1</sup>	Valiela et al. 1985
Surface refractory decomposition rate	rlabsurf	0.002 week <sup>-1</sup>	Valiela et al. 1985
Surface mineral volume fraction	surfmin	0.05 unitless	Turner et al. 2000
Net biomass accumulation fraction	netaccum	0.2 unitless	Chalmers et al. 1985
Pore space fraction	porespace	0.7 unitless	Burdick et al. 1999
Sea level rise rate	eslr	1.5 mm year <sup>-1</sup>	Wood et al. 1989
<b>Biomass Production</b>			
Initial above biomass	ic_phb	0.001 kgC m <sup>-2</sup>	Minimum value
Shoot respiration rate	phbio_resp_rate	0.28 week <sup>-1</sup>	Dai and Wiegert 1996
Root growth respiration rate	nphbio_resp_rate_grow	0.37 week <sup>-1</sup>	Dai and Wiegert 1996
Root maintenance respiration rate	nphbio_resp_rate_maint	0.015 week <sup>-1</sup>	Dai and Wiegert 1996
Root mortality rate	nphbio_mort_rate	0.005 week <sup>-1</sup>	Garver et al. 1988
Shoot mortality rate	phbio_mort_rate	0.01 week <sup>-1</sup>	Bertness and Ellison 1987; Hartman 1988; Teal 1962
Week of peak aerial biomass	peakweek	week 28	Gallagher 1983; Gallagher and Howarth 1987
Week of initial litterfall	litterweek	week 45	Calibrated
<i>S. alterniflora</i> initial roots	ic_nphb_spa	1.96 kgC m <sup>-2</sup>	Calibrated
<i>S. alterniflora</i> maximum gross photosynthesis rate	mac_pp_rate_spa	0.061 kgC m <sup>-2</sup> wk <sup>-1</sup>	Calibrated
<i>S. alterniflora</i> translocation rate	trans_spa	0.005 kgC m <sup>-2</sup> wk <sup>-1</sup>	Calibrated
<i>S. alterniflora</i> shoots:roots	abovebel_spa	0.314 unitless	Chapter I
<i>S. patens</i> initial roots	ic_nphb_spp	1.02 kgC m <sup>-2</sup>	Calibrated
<i>S. patens</i> maximum gross photosynthesis rate	mac_pp_rate_spp	0.042 kgC m <sup>-2</sup> wk <sup>-1</sup>	Calibrated
<i>S. patens</i> translocation rate	trans_spp	0.015 kgC m <sup>-2</sup> wk <sup>-1</sup>	Calibrated
<i>S. patens</i> shoots:roots	abovebel_spp	0.470 unitless	Chapter I

Table 6.1. Generalized ecosystem model parameter values, units, and sources.

Parameter	Name	Value and Unit	Source
<i>Juncus</i> initial roots	ic_nphb_jun	1.17 kgC m <sup>-2</sup>	Calibrated
<i>Juncus</i> maximum gross photosynthesis rate	mac_pp_rate_jun	0.042 kgC m <sup>-2</sup> wk <sup>-1</sup>	Calibrated
<i>Juncus</i> translocation rate	trans_jun	0.005 kgC m <sup>-2</sup> wk <sup>-1</sup>	Calibrated
<i>Juncus</i> shoots:roots	abovebel_jun	0.377 unitless	Chapter I
<i>Phragmites</i> initial roots	ic_nphb_phr	0.96 kgC m <sup>-2</sup>	Calibrated
<i>Phragmites</i> maximum gross photosynthesis rate	mac_pp_rate_phr	0.048 kgC m <sup>-2</sup> wk <sup>-1</sup>	Calibrated
<i>Phragmites</i> translocation rate	trans_phr	0.030 kgC m <sup>-2</sup> wk <sup>-1</sup>	Calibrated
<i>Phragmites</i> shoots:roots	abovebel_phr	0.655 unitless	Chapter I
<i>Lythrum</i> initial roots	ic_nphb_lyt	2.64 kgC m <sup>-2</sup>	Calibrated
<i>Lythrum</i> maximum gross photosynthesis rate	mac_pp_rate_lyt	0.048 kgC m <sup>-2</sup> wk <sup>-1</sup>	Calibrated
<i>Lythrum</i> translocation rate	trans_lyt	0.0001 kgC m <sup>-2</sup> wk <sup>-1</sup>	Calibrated
<i>Lythrum</i> shoots:roots	abovebel_lyt	0.152 unitless	Chapter I
<i>Typha</i> initial roots	ic_nphb_typ	2.16 kgC m <sup>-2</sup>	Calibrated
<i>Typha</i> maximum gross photosynthesis rate	mac_pp_rate_typ	0.068 kgC m <sup>-2</sup> wk <sup>-1</sup>	Calibrated
<i>Typha</i> translocation rate	trans_typ	0.005 kgC m <sup>-2</sup> wk <sup>-1</sup>	Calibrated
<i>Typha</i> roots:shoots	abovebel_typ	0.331 unitless	Chapter I
<b>Plant Succession</b>			
Tolerance weight	tfactor	0.1-0.8 unitless	Based on gradient location; Bertness and Ellison 1987
Competition weight	cfactor	0.1-0.8 unitless	Based on gradient location; Bertness and Ellison 1987
Recruitment weight	rfactor	0.1 unitless	Chapter V
Species stress tolerance at gradient locations	tf_gradient_species	0-1 unitless	Chapter I, Table 1.6
Competitive effect of species 1 on species 2	cf_species1_species2	unitless	Chapter I, Table 1.7

Table 6.1 (continued). Generalized ecosystem model parameter values, units, and sources.



	<b>Parameter Name</b>	<b>Drakes Island</b>	<b>Little River</b>	<b>Mill Brook</b>	<b>Oak Knoll</b>
<b>Marsh Area</b>					
Cell size (m <sup>2</sup> )	cellsize	19.36	25.81	7.84	12.96
Total number of cells	celltotal	16,022	16,996	7,271	11,622
Total marsh area (m <sup>2</sup> )	totalarea	310,186	438,606	57,005	150,621
<b>Elevation (m NGVD)</b>					
Current mean high water	mhwater	1.381	1.315	1.245	0.885
Scenario mean high water	mhwater	1.535	1.068	0.010	0.873
Current high marsh	hiwater	1.487	1.612	1.420	1.105
Scenario high marsh	hiwater	1.720	1.687	1.693	1.228
Current maximum high water	maxwater	1.577	1.920	1.459	1.128
Scenario maximum high water	maxwater	1.740	1.318	0.010	1.318
Upland edge	uplandel	1.748	1.687	1.693	1.228
Creek bottom	creekel	0.910	0.000	0.400	0.016
<b>Salinity Regime</b>					
Maximum distance to culvert (m)	sdist	750	1060	550	450
Salinity of tidal inflow	salinity	high	high	high	high
<b>Sediment Accretion (mm/yr)</b>					
	sedmax	2.38	4.26	19.02	1.61

Table 6.2. Site-specific parameters for the four study sites. Hydrologic scenarios are culvert expansion for Drakes Island (additional 0.91 culvert 50 cm lower) and Oak Knoll (north culvert increased to 1.22 m diameter); pre-restoration conditions for Little River (1.22 m culvert) and Mill Brook (0.91 m culvert with tidal flap gate).

Initial species cover proportions (dominant species in bold)	Drakes Island	Little River	Mill Brook	Oak Knoll
<i>Spartina alterniflora</i>	<b>.807</b>	<b>.772</b>	<b>.873</b>	<b>.718</b>
<i>Spartina patens</i>	.121	.139	.030	.277
<i>Juncus</i>	.001	.007	.000	.000
<i>Phragmites</i>	.037	.018	.000	.005
<i>Lythrum</i>	.001	.001	.000	.000
<i>Typha</i>	.033	.063	.097	.000
<i>Spartina alterniflora</i>	.129	.081	.170	.142
<i>Spartina patens</i>	<b>.796</b>	<b>.869</b>	<b>.778</b>	<b>.796</b>
<i>Juncus</i>	.015	.029	.000	.036
<i>Phragmites</i>	.001	.016	.000	.023
<i>Lythrum</i>	.001	.001	.000	.002
<i>Typha</i>	.058	.004	.052	.001
<i>Spartina alterniflora</i>	.235	.050	.000	.060
<i>Spartina patens</i>	.342	.230	.000	.297
<i>Juncus</i>	<b>.362</b>	<b>.714</b>	<b>.714</b>	<b>.627</b>
<i>Phragmites</i>	.001	.004	.000	.016
<i>Lythrum</i>	.001	.001	.000	.000
<i>Typha</i>	.059	.001	.286	.000
<i>Spartina alterniflora</i>	.001	.034	.027	.000
<i>Spartina patens</i>	.028	.119	.075	.227
<i>Juncus</i>	.001	.032	.000	.000
<i>Phragmites</i>	<b>.968</b>	<b>.813</b>	<b>.721</b>	<b>.773</b>
<i>Lythrum</i>	.001	.001	.000	.000
<i>Typha</i>	.001	.001	.177	.000
<i>Spartina alterniflora</i>	.001	.001	.000	.000
<i>Spartina patens</i>	.286	.286	.214	.214
<i>Juncus</i>	.001	.001	.000	.000
<i>Phragmites</i>	.001	.001	.000	.000
<i>Lythrum</i>	<b>.568</b>	<b>.568</b>	<b>.786</b>	<b>.786</b>
<i>Typha</i>	.143	.143	.000	.000
<i>Spartina alterniflora</i>	.053	.096	.028	.028
<i>Spartina patens</i>	.020	.007	.069	.069
<i>Juncus</i>	.001	.001	.000	.000
<i>Phragmites</i>	.001	.005	.009	.009
<i>Lythrum</i>	.001	.001	.000	.000
<i>Typha</i>	<b>.924</b>	<b>.890</b>	<b>.894</b>	<b>.894</b>

Table 6.3. Vegetation survey results of mean percentages of species cover for dominant plant associations (bold values). Species percentages for each site were used as baseline (initial) values of spatial cells for twenty-year model simulations.

	<i>S. alterniflora</i>	<i>S. patens</i>	<i>Juncus</i>	<i>Phragmites</i>	<i>Lythrum</i>	<i>Typha</i>	Bare Area
<b>Drakes Island</b>							
Current conditions	21	17	0	4	0	58	0
Current (predicted)	17	12	0	18	0	57	0
Current (+20 years)	16	12	0	18	0	53	0
Restored (+20 years)	45	7	0	9	0	39	0
<b>Little River</b>							
Current conditions	7	35	2	14	6	37	0
Current (+20 years)	12	57	3	7	0	22	0
Restricted (+20 years)	1	4	2	56	0	37	0
<b>Mill Brook</b>							
Current conditions	27	22	2	8	0	42	0
Current (predicted)	38	16	1	4	10	31	0
Current (+20 years)	31	34	0	11	0	24	0
Restricted (+20 years)	1	1	0	54	0	44	0
<b>Oak Knoll</b>							
Current conditions	23	46	5	20	3	2	1
Current (+20 years)	2	45	4	35	0	14	0
Restored (+20 years)	2	57	2	11	0	29	0

Table 6.4. Summary of observed and predicted marsh cover percentages for four study sites. Percentages consider only vegetated and bare areas (submerged areas excluded). Drakes Island and Mill Brook sites include results of validation model runs for prediction of current cover.

	<i>S. alterniflora</i>	<i>S. patens</i>	<i>Juncus</i>	<i>Phragmites</i>	<i>Lythrum</i>	<i>Typha</i>	Model Total	Composite Error
<b>Drakes Island</b>								
<i>S. alterniflora</i>	<b>1055</b>	415	6	72	0	668	2216	21
<i>S. patens</i>	807	<b>957</b>	8	272	0	459	2503	10
<i>Juncus</i>	232	148	<b>0</b>	24	0	66	470	2838
<i>Phragmites</i>	12	76	0	<b>8</b>	0	472	568	18
<i>Lythrum</i>	0	0	0	0	<b>0</b>	0	0	-
<i>Typha</i>	711	681	2	107	0	<b>6158</b>	7659	2
Survey Total	2817	2277	16	483	0	7823	13416	<u>11</u>
Address Error	63	48	100	98	-	21	<u>39</u>	
<b>Mill Brook</b>								
<i>S. alterniflora</i>	<b>1275</b>	697	28	88	0	377	2465	41
<i>S. patens</i>	179	<b>238</b>	40	123	0	445	1025	28
<i>Juncus</i>	3	5	<b>0</b>	1	0	89	98	20
<i>Phragmites</i>	9	72	3	<b>30</b>	0	121	235	55
<i>Lythrum</i>	141	107	16	133	<b>0</b>	266	663	33050
<i>Typha</i>	142	295	36	151	0	<b>1423</b>	2049	25
Survey Total	1749	1414	123	526	2	2721	6535	<u>42</u>
Address Error	27	83	100	94	100	47	<u>55</u>	
<b>Sites Combined</b>								
<i>S. alterniflora</i>	<b>2330</b>	1112	34	160	0	1045	4681	3
<i>S. patens</i>	986	<b>1195</b>	48	395	0	904	3528	4
<i>Juncus</i>	235	153	<b>0</b>	25	0	155	568	309
<i>Phragmites</i>	21	148	3	<b>38</b>	0	593	803	20
<i>Lythrum</i>	141	107	16	133	<b>0</b>	266	663	33050
<i>Typha</i>	853	976	38	258	2	<b>7581</b>	9708	8
Survey Total	4566	3691	139	1009	2	10544	19951	<u>12</u>
Address Error	49	68	100	96	100	28	<u>46</u>	

Table 6.5. Matrices of address and composite goodness-of-fit for validation sites at Drakes Island, Mill Brook, and the two sites combined. Bold values show cell counts with species address agreement. Underlined values are weighted average of percent error for address and composite goodness-of-fit.

	Halophyte Species	Brackish Species	Model Total	Composite Error
<b>Drakes Island</b>				
Halophyte Species	<b>3628</b>	1561	5189	2
Brackish Species	1482	<b>6745</b>	8227	1
Survey Total	5110	8306	13416	<u>1</u>
Address Error	29	19	<u>23</u>	
<b>Mill Brook</b>				
Halophyte Species	<b>2465</b>	1123	3588	8
Brackish Species	821	<b>2126</b>	2947	10
Survey Total	3286	3249	6535	<u>9</u>
Address Error	25	35	<u>30</u>	
<b>Sites Combined</b>				
Halophyte Species	<b>6093</b>	2684	8777	5
Brackish Species	2303	<b>8871</b>	11174	3
Survey Total	8396	11555	19951	<u>4</u>
Address Error	27	23	<u>25</u>	

Table 6.6. Aggregated matrices (halophyte and brackish species) of address and composite goodness-of-fit for validation sites at Drakes Island, Mill Brook, and the two sites combined. Bold values show cell counts with group address agreement. Underlined values are weighted average of percent error for address and composite goodness-of-fit.

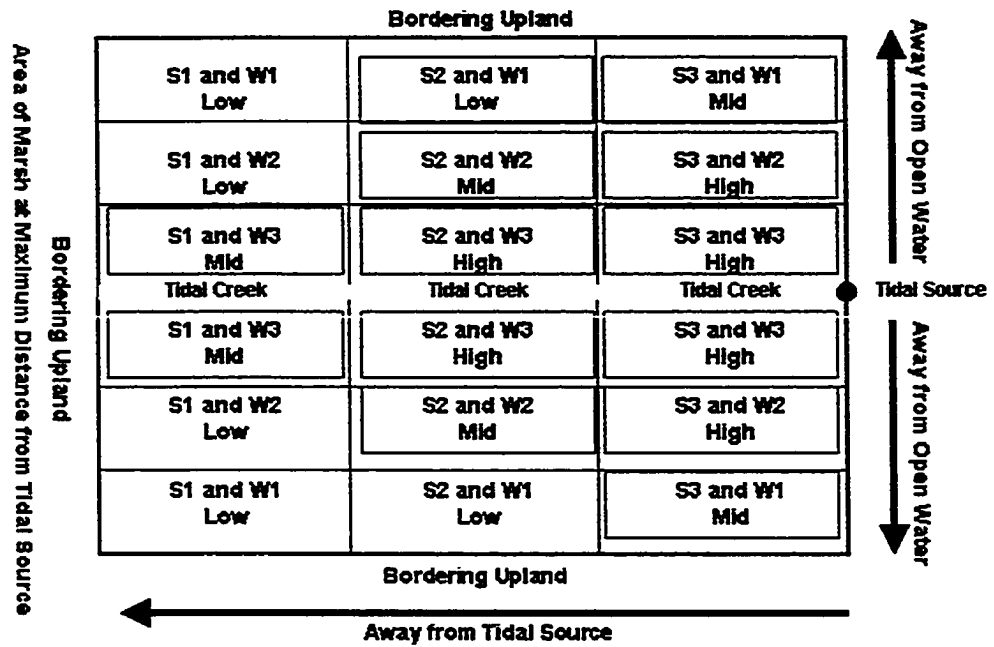


Figure 6.1. Conceptual schematic of salinity regime assignment. Marsh areas are zoned on two axes: distance from tidal source (S3, S2, and S1, from nearest to source to furthest from source), and distance from tidal creek water (W3, W2, and W1, from nearest to creek to furthest from creek). Salinity regime assignments (High, Mid, and Low) based on zone combinations, as indicated. Shading indicates relative salinity strength from high to low.

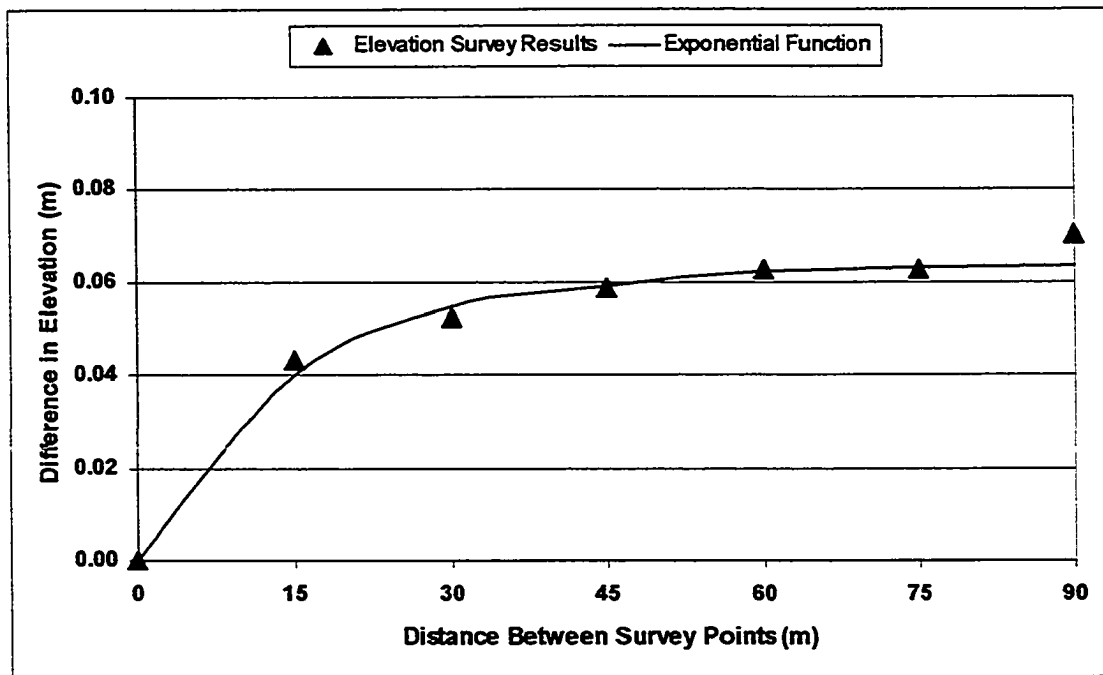


Figure 6.2. Semivariogram analysis showing how difference in marsh elevation (half of the squared difference between points) varied with increasing distance between points, for all study sites combined. Curve shown is the best fitting function (exponential) used for kriging algorithms.

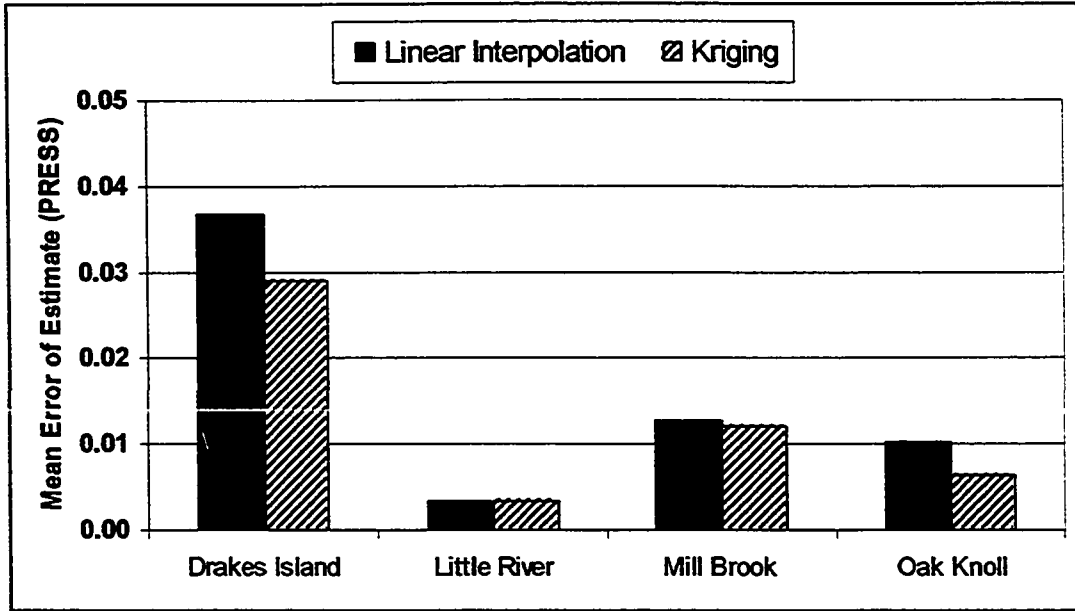


Figure 6.3. Comparison of mean errors (PRESS is the prediction sum of squares) between estimation methods using kriging and linear interpolation for known survey elevation points at four study sites.



# Drakes Island

## Base Maps

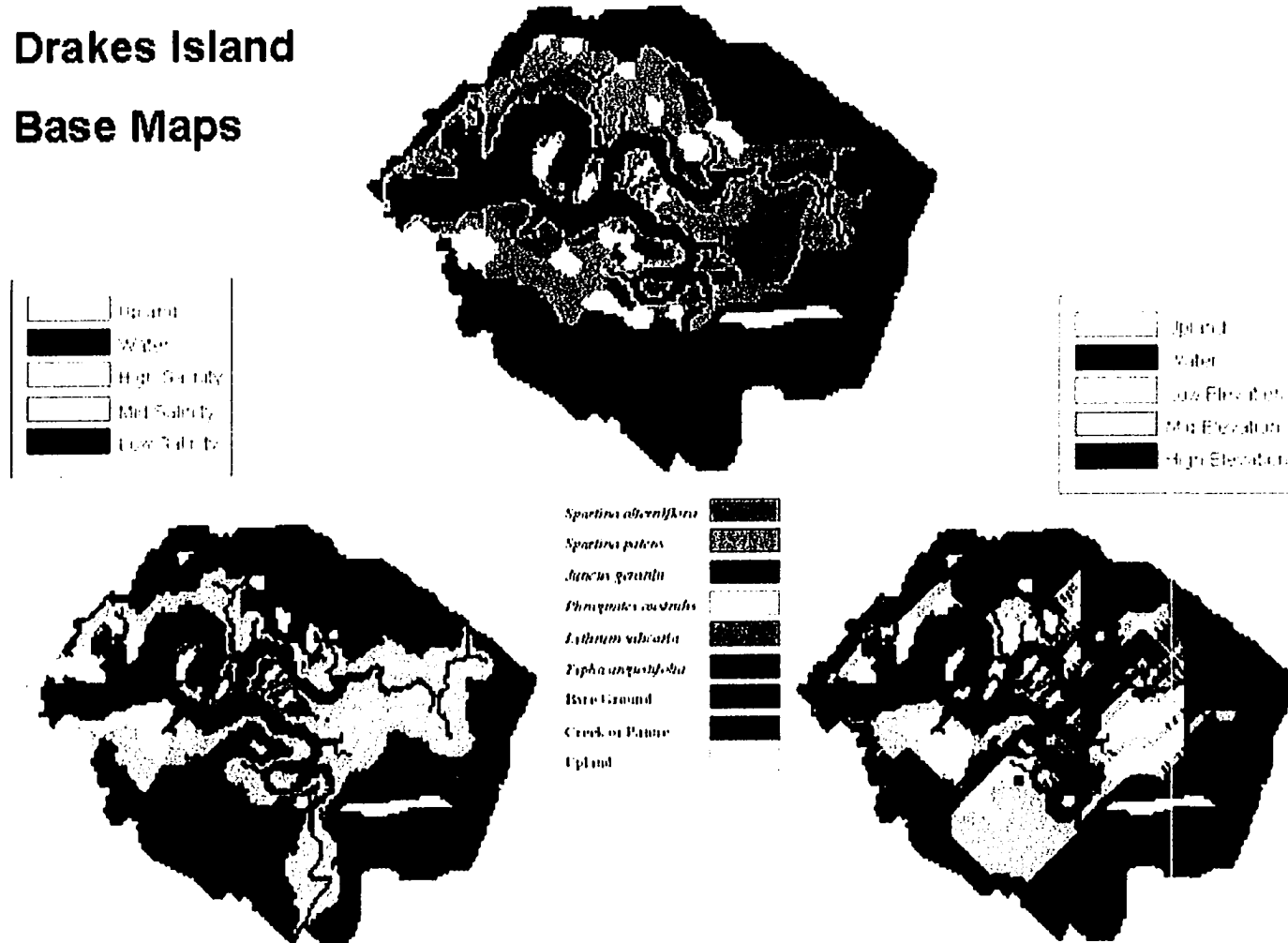


Figure 6.4. Base maps for Drakes Island in 2002. Top: Plant Cover; Lower Left: Salinity; Lower Right: Elevation

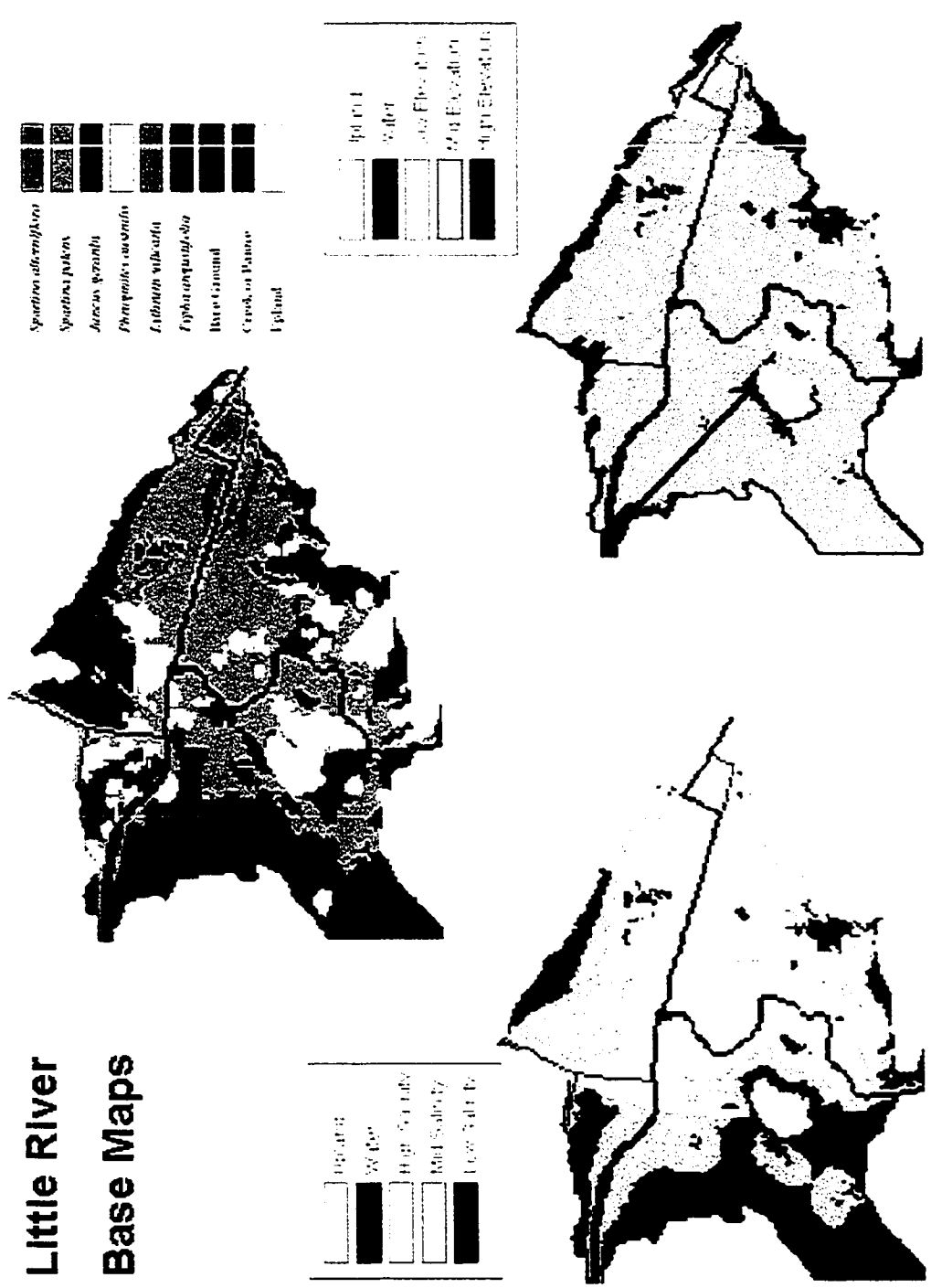


Figure 6.5. Base maps for Little River in 2002. Top: Plant Cover; Lower Left: Salinity; Lower Right: Elevation

# Mill Brook Base Maps

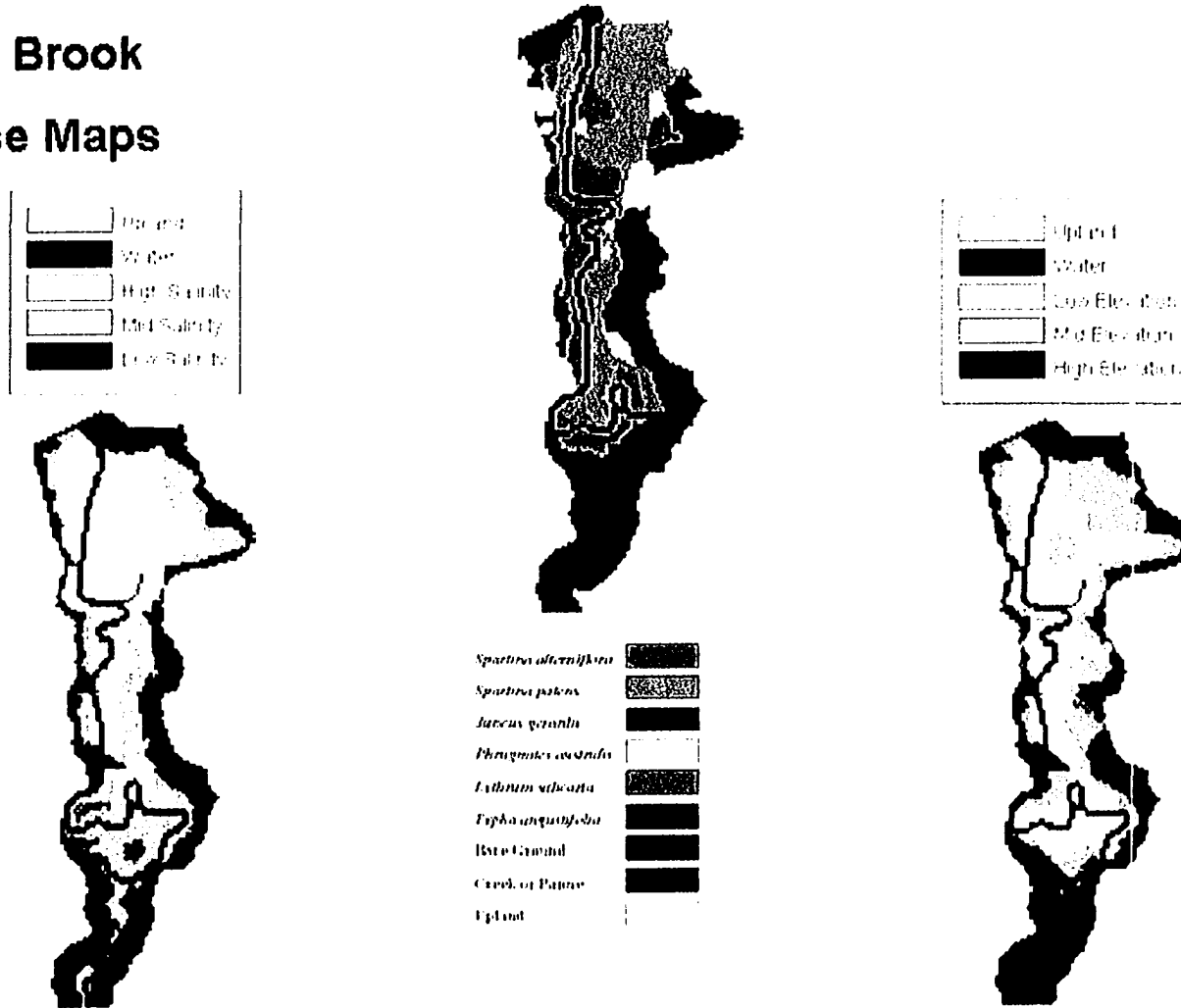


Figure 6.6. Base maps for Mill Brook in 2002. Top: Plant Cover; Lower Left: Salinity; Lower Right: Elevation

# Oak Knoll

## Base Maps

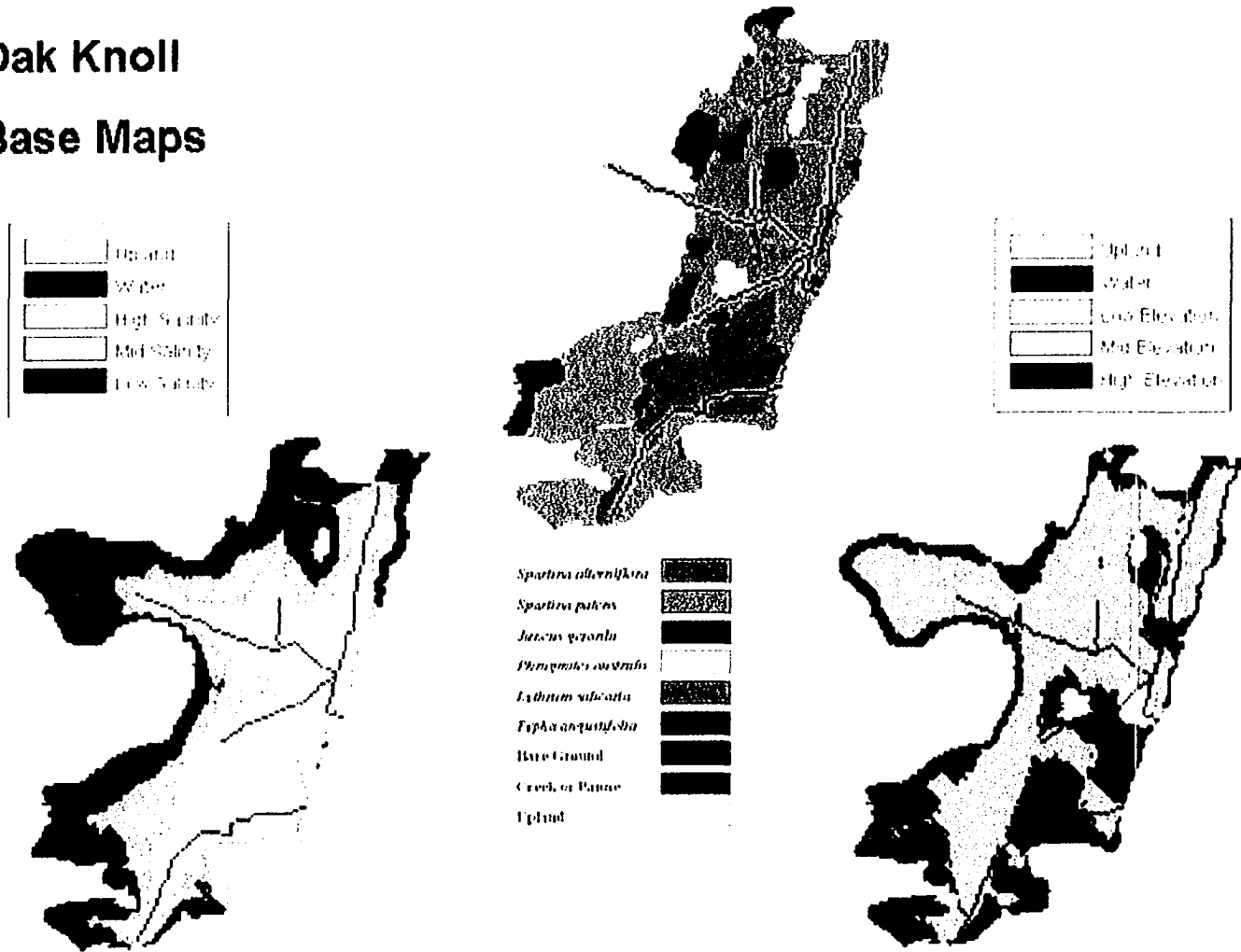


Figure 6.7. Base maps for Oak Knoll in 2002. Top: Plant Cover; Lower Left: Salinity; Lower Right: Elevation

# Drakes Island

## Validation Sequence 1988-2002

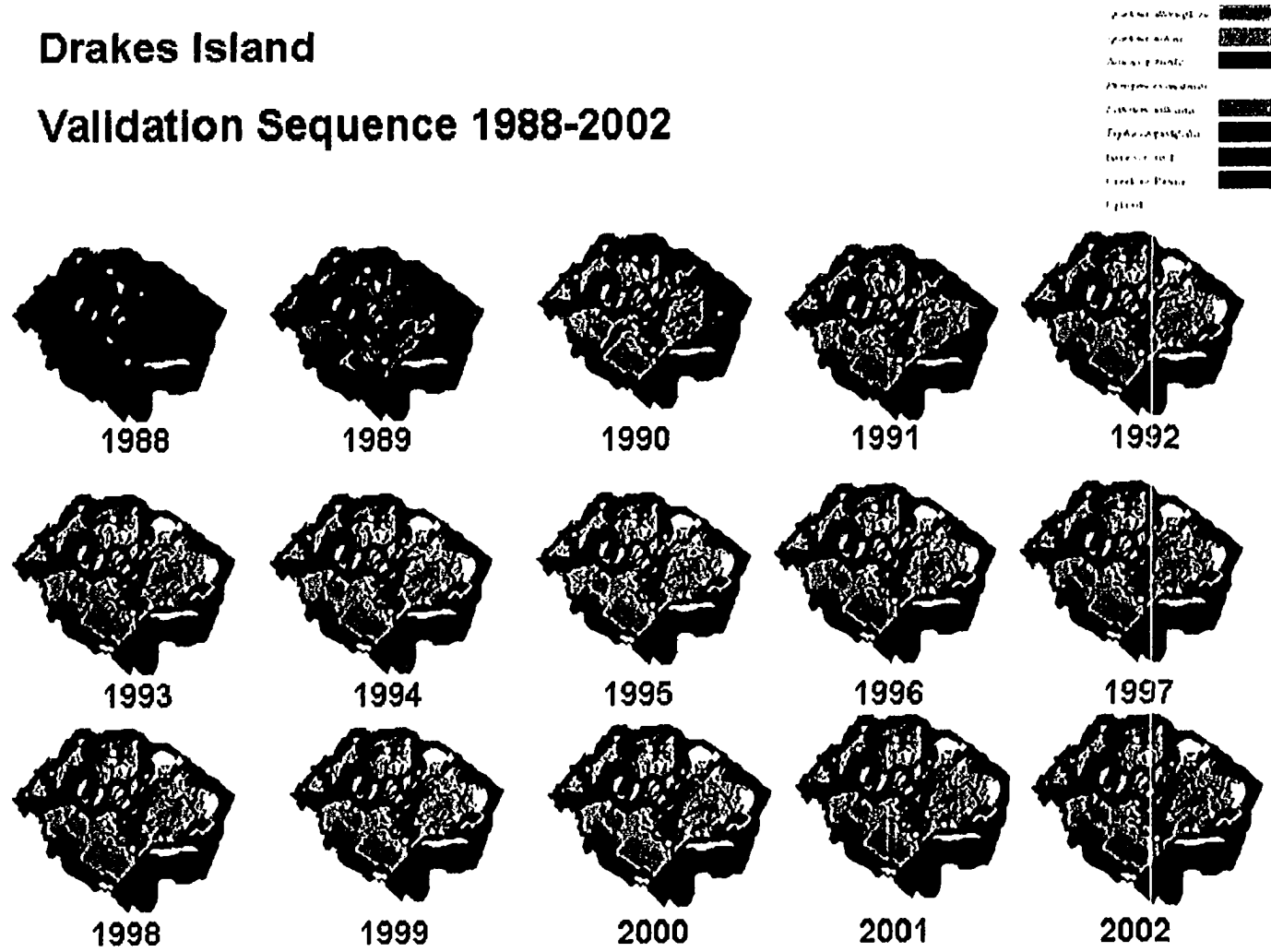


Figure 6.8. Drakes Island validation sequence (1988-2002) showing predicted changes associated with partial hydrologic restoration.

## Mill Brook Validation Sequence 1993-2002

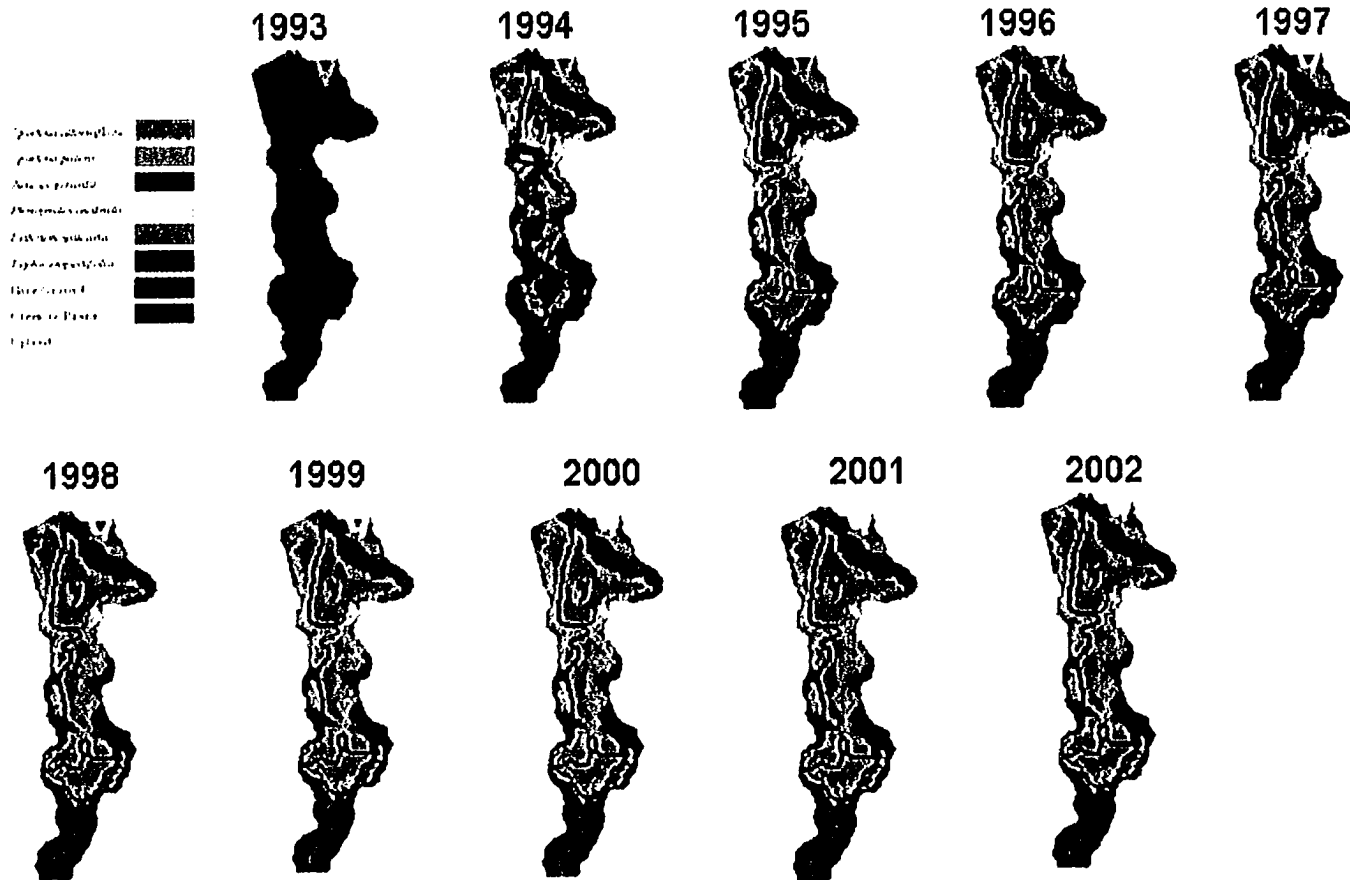


Figure 6.9. Mill Brook validation sequence from 1993-2002 showing predicted changes associated with full hydrologic restoration.

## Drakes Island Validation

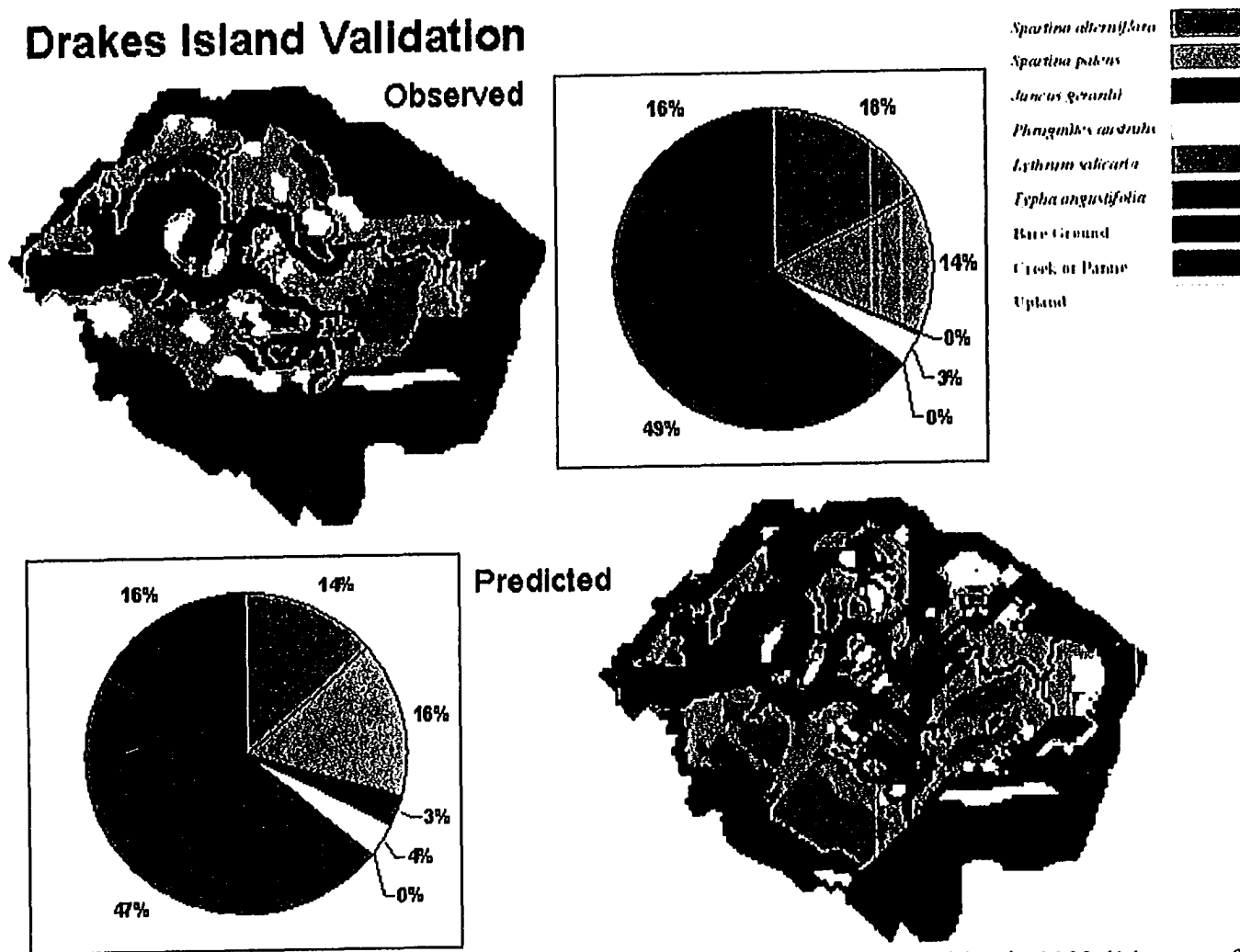


Figure 6.10. Drakes Island results for observed and predicted plant species composition in 2002 (14 years after partial restoration).

# Mill Brook Validation

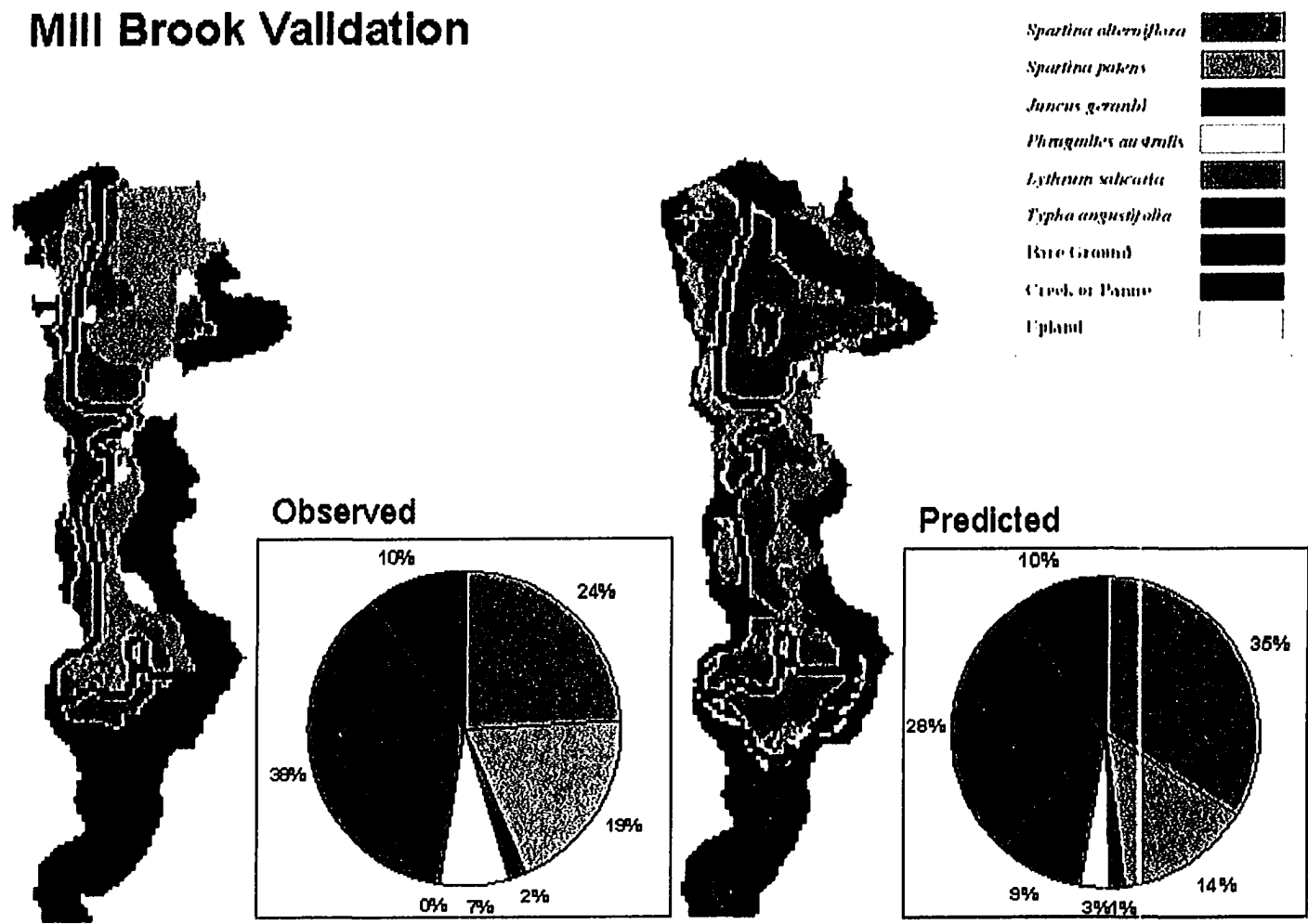


Figure 6.11. Mill Brook results for observed and predicted plant species composition in 2002 (9 years after full restoration).



# Drakes Island

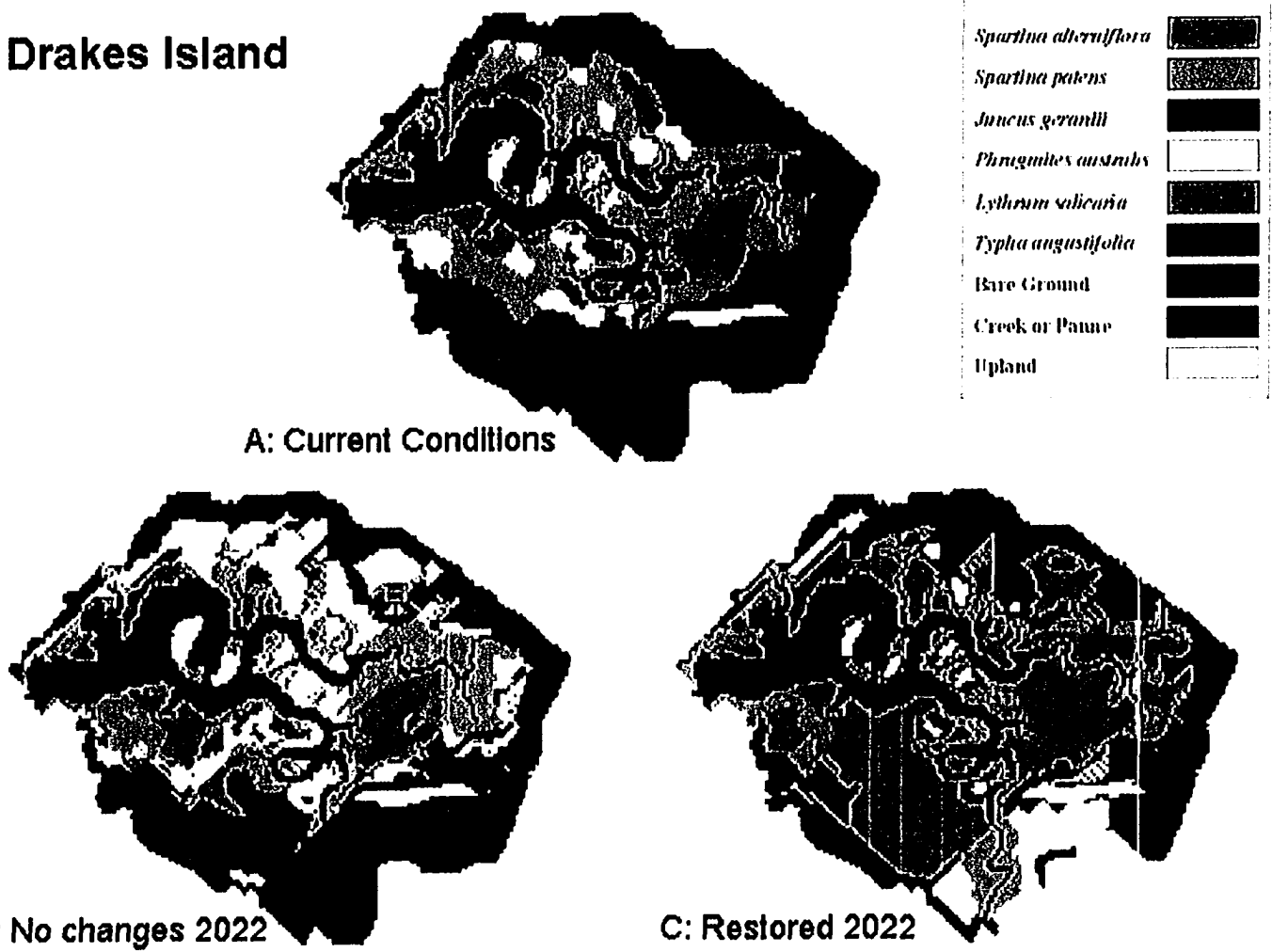
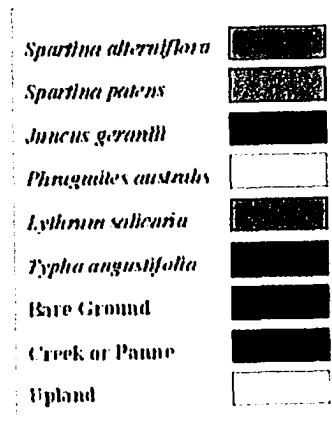
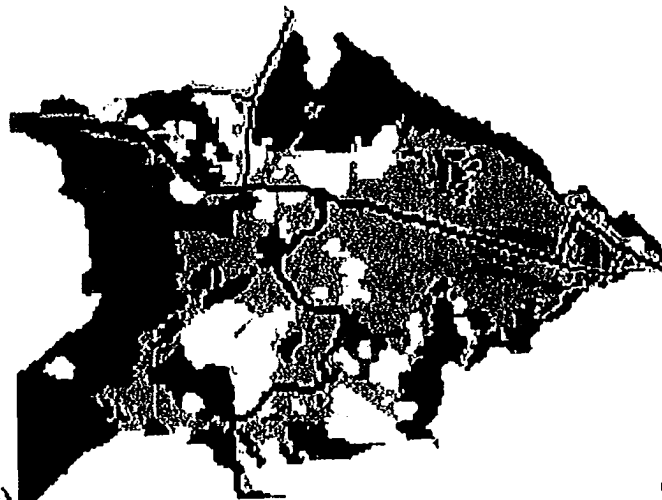


Figure 6.12. Drakes Island scenarios, plant cover results. A: Current conditions (2002), B: Prediction for 2022 if no changes made, C: Prediction for 2022 if hydrologic restoration (second 3' culvert added).

# Little River

A: Current Conditions



B: No Changes (20 yrs)

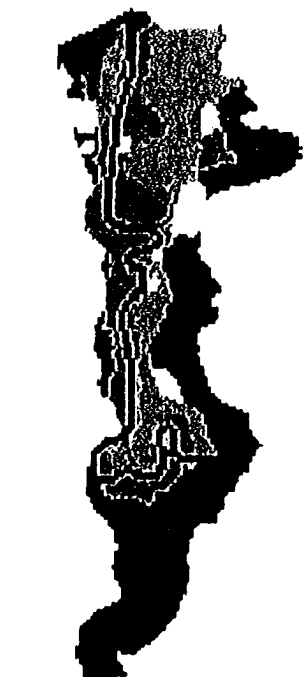


C: Restriction (20 yrs)



Figure 6.13. Little River scenarios, plant cover results. A: Current conditions (2002), B: Prediction for 2022 if no changes made, C: Prediction for 2022 if return to tidal restriction conditions with undersized culvert.

# Mill Brook



A: Current Conditions

B: No Changes 2022



C: Flap gate 2022

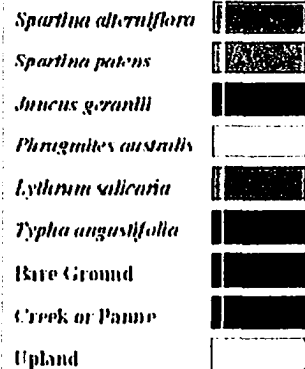


Figure 6.14. Mill Brook scenarios, plant cover results. A: Current conditions (2002), B: Prediction for 2022 if no changes made, C: Prediction for 2022 if return to tidal restriction conditions with original flap gate.

# Oak Knoll

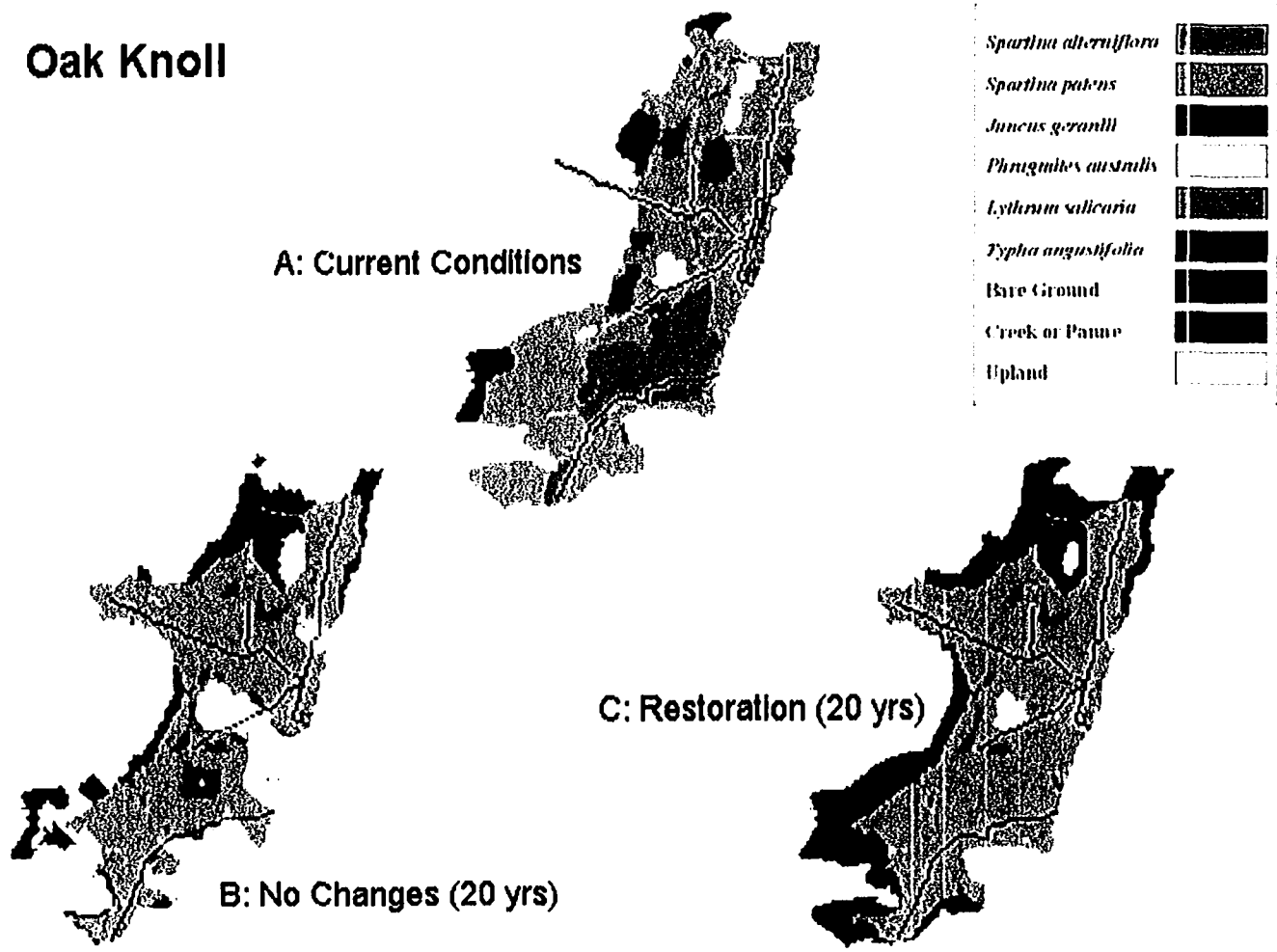


Figure 6.15. Drakes Island scenarios, plant cover results. A: Current conditions (2002), B: Prediction for 2022 if no changes made, C: Prediction for 2022 if hydrologic restoration (north culvert expanded to 4').

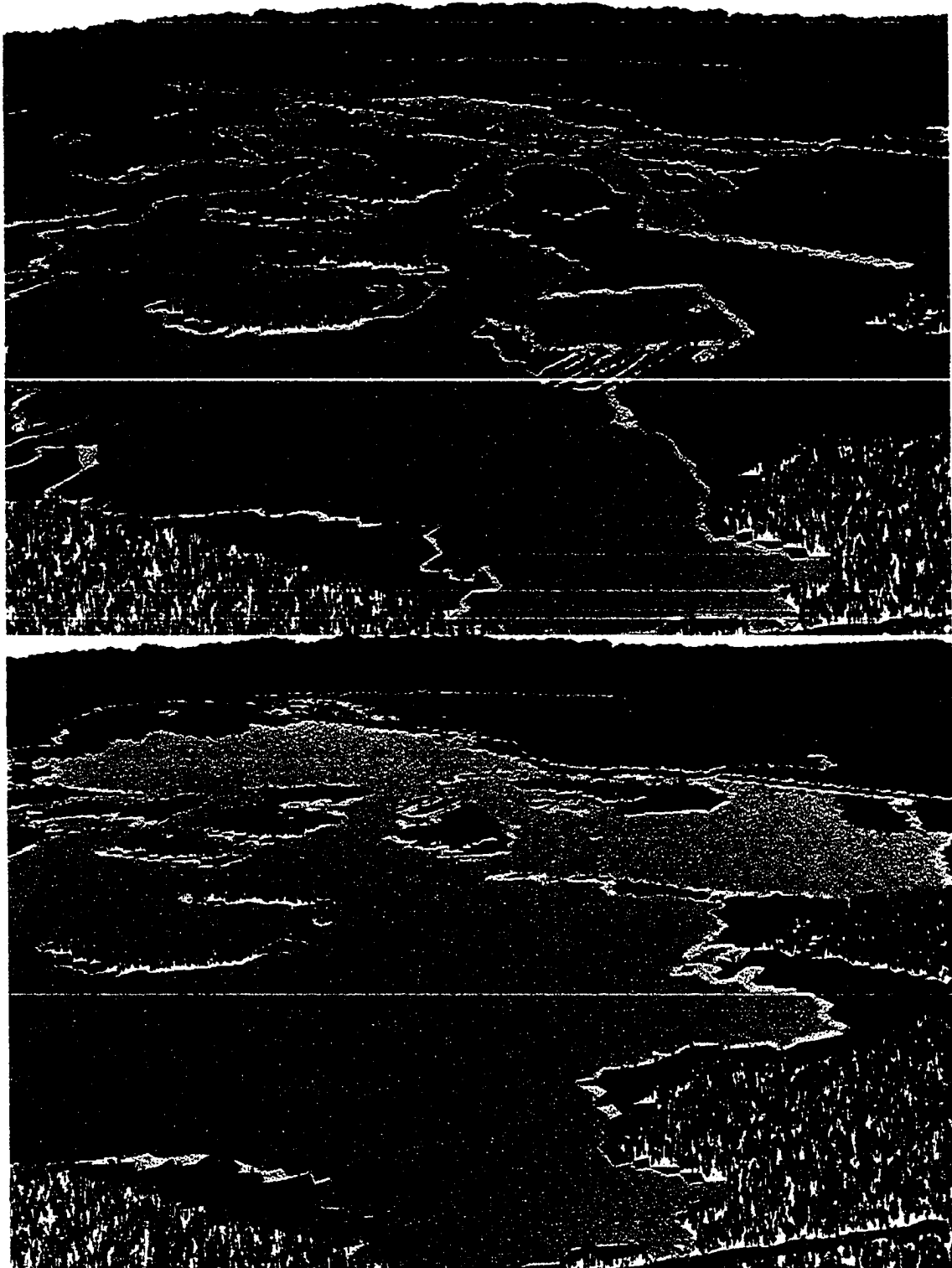
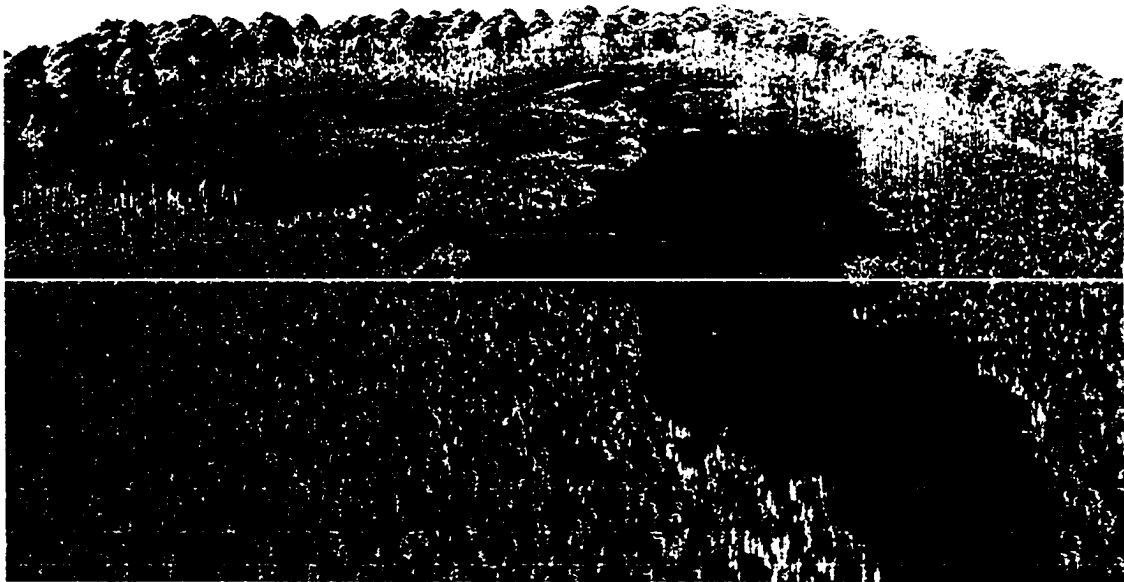


Figure 6.16. Drakes Island scenario visualizations. Top: View of marsh during spring tide under current conditions; Bottom: View of marsh during spring tide with proposed additional culvert (0.91 m diameter).



**Figure 6.17. Little River scenario visualizations. Top: View of marsh at high tide under current restoration conditions; Bottom: Marsh at high tide under pre-restoration conditions (1.22 m diameter culvert).**

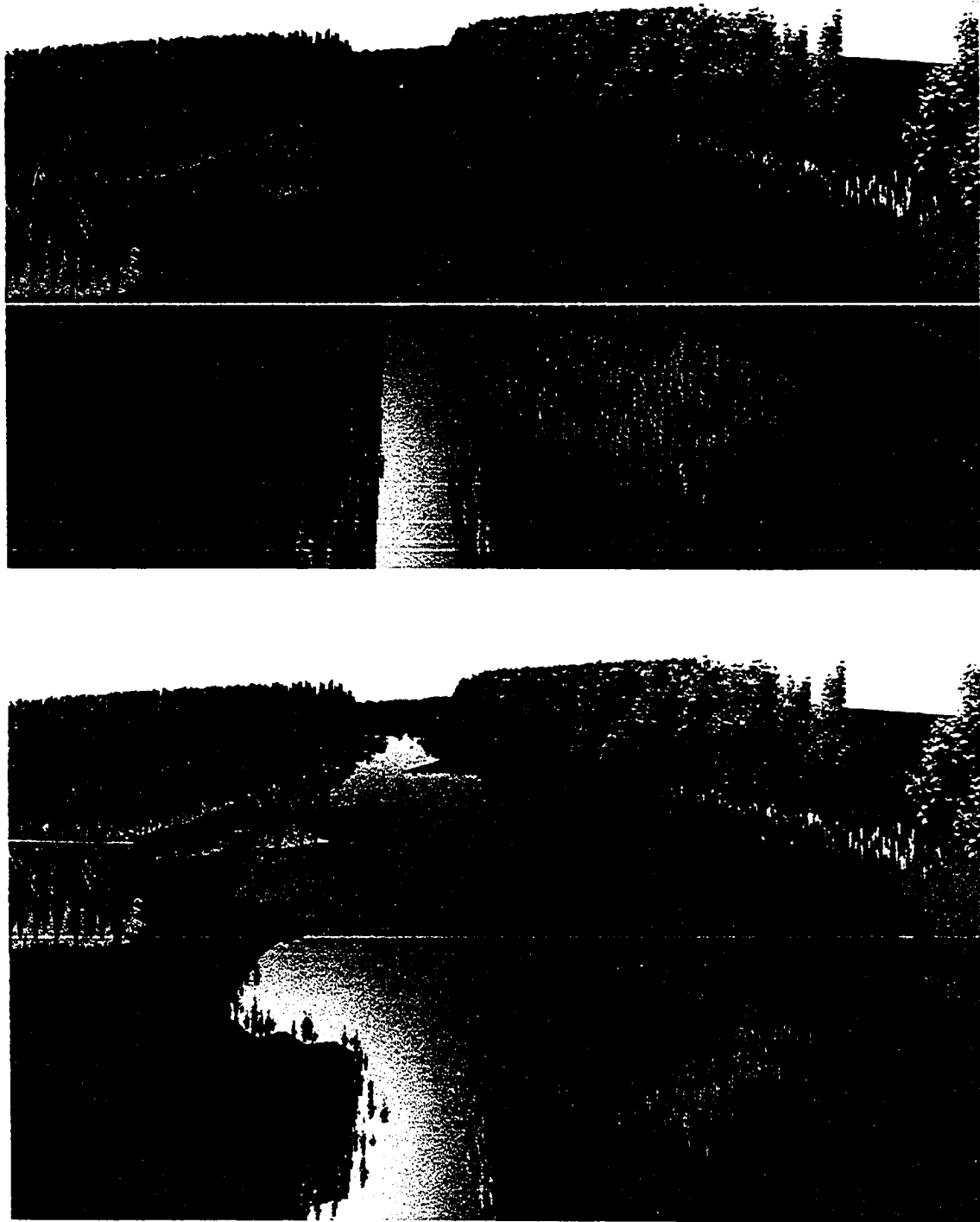


Figure 6.18. Mill Brook scenario visualizations. Top: View of marsh creek pre-restoration (tide gate); Bottom: Marsh under current restoration conditions at high tide.

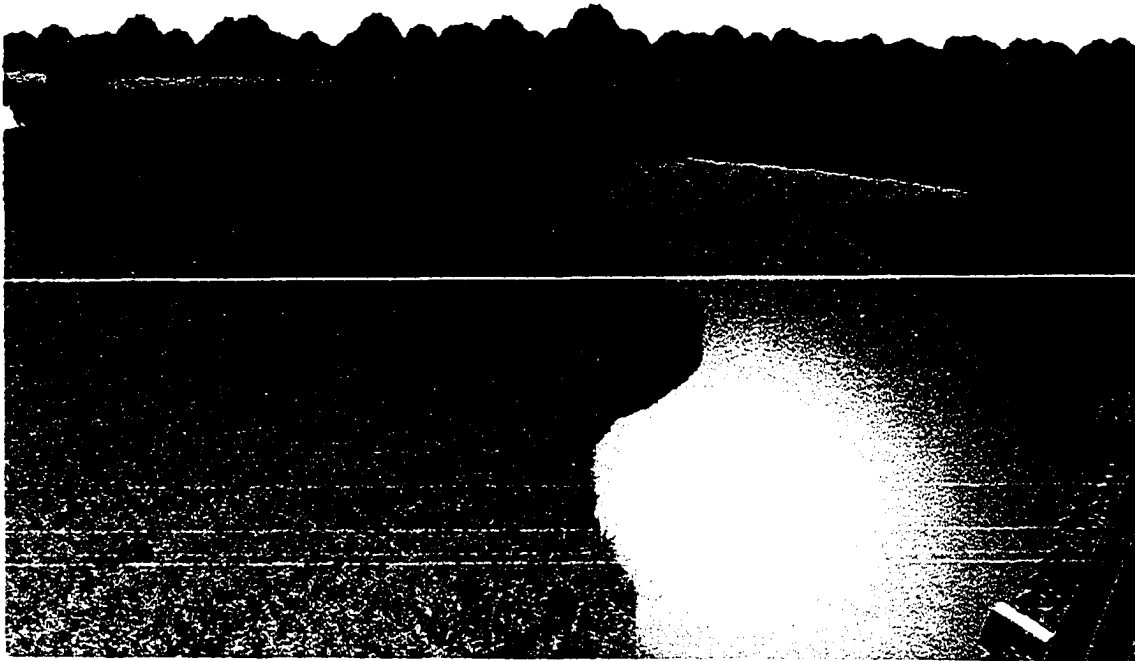


Figure 6.19. Oak Knoll scenario visualization. Top: View of marsh at high tide under current conditions; Bottom: Marsh at high tide with expanded culvert (1.22 m diameter).



## LIST OF REFERENCES

- Aber, J.D., Ollinger, S.V., Federer, C.A., Reich, P.B., Goulden, M.L., Kicklighter, D.W., Melillo, J.M., and Lathrop, R.G. 1995. Predicting the effects of climate change on water yield and forest production in the northeastern United States. *Climate Research* 5:207-222.
- Aber, J.D., Reich, P.B., and Goulden, M.L. 1996. Extrapolating leaf CO<sub>2</sub> exchange to the canopy: a generalized model of forest photosynthesis compared with measurements by eddy correlation. *Oecologia* 106:257-265.
- Anisfeld, S.C., Tobin, M.J., and Benoit, G. 1999. Sedimentation rates in flow-restricted and restored salt marshes in Long Island Sound. *Estuaries* 22:231-244.
- ATTAR Engineering, Inc. 1996. Hydrologic investigation of Drakes Island culvert and marsh. Eliot, Maine. 63 pp.
- Ayers Jr., F. 1962. Theories and Problems of Matrices. McGraw-Hill Book Co., New York.
- Bart, D. and Hartman, J.M. 2000. Environmental determinants of *Phragmites australis* expansion in a New Jersey salt marsh: an experimental approach. *Oikos* 89:59-69.
- Beare, P.A. and Zedler, J.B. 1987. Cattail invasion and persistence in a coastal salt marsh: The role of salinity reduction. *Estuaries* 10:165-170.
- Bertness, M.D. 1988. Peat accumulation and the success of marsh plants. *Ecology* 69:703-713.
- Bertness, M.D. 1991a. Interspecific interactions among high marsh perennials in a New England salt marsh. *Ecology* 72: 125-137
- Bertness, M.D. 1991b. Zonation of *Spartina patens* and *Spartina alterniflora* in a New England salt marsh. *Ecology* 72: 138-148
- Bertness, M.D. 1992. The ecology of a New England salt marsh. *American Scientist* 80:260-268.
- Bertness, M.D. and Ellison, A.M. 1987. Determinants of pattern in a New England salt marsh plant community. *Ecological Monographs* 57:129-147.
- Bertness, M.D. and Hacker, S.D. 1994. Physical stress and positive interactions among marsh plants. *American Naturalist* 144:363-372.

- Bertness, M.D. and Yeh, S.M. 1994. Cooperative and competitive interactions in the recruitment of marsh elders. *Ecology* 75:2416-2429.
- Boumans, R.M.J., Burdick, D.M., and Dionne, M. 2002. Modeling habitat change in salt marshes after tidal restoration. *Restoration Ecology* 10:543-555.
- Boumans, R.M.J., and Day, J.W. 1994. Effects of two marsh management plans on water and material flux and short term sedimentation in the Mississippi Delta. *Wetlands* 14:247-261.
- Brewer, J.S., Rand, T., Levine, J.M., and Bertness, M.D. 1998. Biomass allocation, clonal dispersal, and competitive success in three salt marsh plants. *Oikos* 82:347-353.
- Burdick, D.M. 2002. Evaluation of pre-restoration conditions including impacts from tidal restriction in Little River Marsh, New Hampshire. New Hampshire Coastal Program, Concord, New Hampshire. 26 pp.
- Burdick, D. M., Boumans, R.M., Dionne, M., and Short, F. T. 1999. Impacts to salt marshes from tidal restrictions and ecological responses to tidal restoration. Final Report to NOAA, Grant #NA570R0343.
- Burdick, D.M., Buchsbaum, R., Holt, E. 2001. Variation in soil salinity associated with expansion of *Phragmites australis* in salt marshes. *Environmental and Experimental Botany* 46:247-261.
- Burdick, D.M., Dionne, M., Boumans, R.M, and Short, F.T. 1997. Ecological responses to tidal restoration of two New England salt marshes. *Wetlands Ecology and Management* 4:129-144.
- Burdick, D.M., Mendelssohn, I.A., and McKee, K.L. 1989. Live standing crop and metabolism of the marsh grass *Spartina patens* as related to edaphic factors in a brackish, mixed marsh community in Louisiana. *Estuaries* 12:195-204.
- Cahoon, D.R. and Turner, R.E. 1989. Accretion and canal impacts in a rapidly subsiding wetland. II: Feldspar marker horizon technique. *Estuaries* 12:260-268.
- Chalmers, A.G., Wiegert, R.G., and Wolf, P.L. 1985. Carbon balance in a salt marsh: interactions of diffusive export, tidal deposition and rainfall-caused erosion. *Estuarine Coastal Shelf Science* 21:757-771.
- Chambers, R.M. 1997. Porewater chemistry associated with *Phragmites* and *Spartina* in a Connecticut tidal marsh. *Wetlands* 17:360-367.

Chambers, R.M., Mozdzer, T.J., Ambrose, J.C. 1998. Effects of salinity and sulfide distribution on *Phragmites australis* and *Spartina alterniflora* in a tidal saltmarsh. *Aquatic Botany* 62:161-169.

Chambers, R.M., L.A. Meyerson, and K. Saltonstall. 1999. Expansion of *Phragmites australis* into tidal wetlands of North America. *Aquatic Botany* 64:261-273.

Chanson, H. 1999. The Hydraulics of Open Channel Flow: An Introduction. John Wiley & Sons, New York.

Cook, R.A., Lindley-Stone, A.J., and Amman, A.P. 1993. Method for the evaluation and inventory of vegetated tidal marshes in New Hampshire. Audubon Society of New Hampshire, Concord, New Hampshire.

Connell, J.H., and Slayter, R.O. 1977. Mechanisms of succession in natural communities and their role in community stability and organization. *American Naturalist* 111:1119-1144.

Costanza, R., and Sklar, F.H. 1985. Articulation, accuracy, and effectiveness of mathematical models: a review of freshwater wetland applications, *Ecological Modelling* 27:45-68.

Dai, T. and Wiegert, R.G. 1996. Estimation of the primary productivity of *Spartina alterniflora* using a canopy model. *Ecography* 19:410-423.

Day, J.W., Rybczyk, J.M., Scarton, F., Rismondo, A., Are, D., and Cecconi, G. 1999. Soil accretion dynamics, sea level rise, and the survival of wetlands in a Venice lagoon: A field and modeling approach. *Estuarine, Coastal, and Shelf Science* 49:607-628.

DeLaune, R.D., Baumann, R.H., and Gosselink, J.G. 1983. Relationship among vertical accretion, coastal submergence, and erosion in a Louisiana Gulf Coast marsh. *Journal of Sedimentary Petrology* 53:147-157.

Dionne, M., Short, F.T., and Burdick, D.M. 1999. Fish utilization of restored, created, and reference salt-marsh habitat in the Gulf of Maine. *American Fisheries Society Symposium* 22:384-404.

Donnelly, J.P., and Bertness, M.D. 2001. Rapid shoreward encroachment of salt marsh cordgrass in response to accelerated sea-level rise. *PNAS* 98:14218-14223.

Dormann C.F., Van Der Wal, R., Bakker, J.P. 2000. Competition and herbivory during salt marsh succession: The importance of forb growth strategy. *Journal of Ecology* 88:571-583.

- Dzierzeski, M.J. 1991. Factors controlling the invasion of *Lythrum salicaria* (purple loosestrife) in a hydrologically altered salt marsh. Masters Thesis. University of New Hampshire, Durham, New Hampshire.
- Eleuterius, L.N., and Eleuterius, C.K. 1979. Tide levels and marsh zonation. *Bulletin of Marine Sciences* 29:394-400.
- Ellison, A. E. 1987. Effects of competition, disturbance, and herbivory on *Salicornia europaea*. *Ecology* 68:576-586.
- Ellison, A. M., Bertness, M.D., and Miller, T. 1986. Seasonal patterns in the belowground biomass of *Spartina alterniflora* (Gramineae) across a tidal gradient. *American Journal of Botany* 73:1546-1554.
- Emery, N.C., Ewanchuk, P.J., and Bertness, M.D. 2001. Competition and salt-marsh plant zonation: Stress tolerators may be dominant competitors. *Ecology* 82:2471-2485.
- Fitz, C., DeBellevue, E., Costanza, R., Boumans, R.M.J., Maxwell, T., Wainger, L. and Sklar, F.H. 1996. Development of a generic transforming ecological model (GEM) for a range of scales and ecosystems. *Ecological Modeling* 88:263-295.
- Frankic, A. 1999. Technology and information needs of the coastal estuarine management community. National Oceanic and Atmospheric Administration, Office of Ocean and Coastal Resource Management.
- Frenkel, R.E. and Moran, J.C. 1991. Can we restore our salt marshes? Lessons from the Salmon River, Oregon. *Northwest Environmental Journal* 7:119-135.
- Gallagher, J.L. 1983. Seasonal patterns of recoverable underground reserves in *Spartina alterniflora* Loisel. *American Journal of Botany* 70:212-215.
- Gallagher, J.L. and Howarth, R.W. 1987. Seasonal differences in *Spartina* recoverable underground reserves in the Great Sippewissett Marsh in Massachusetts. *Estuarine, Coastal and Shelf Science* 25:313-319.
- Gallagher, J.L. and Plumley, F.G. 1979. Underground biomass profiles and productivity in Atlantic Coastal Marshes. *American Journal of Botany* 66:156-161.
- Gardner, L.R., Reeves, H.W., and Thibodeau, P.M. 2002. Groundwater dynamics along forest-marsh transects in a southeastern salt marsh, USA: Description, interpretation and challenges for numerical modeling. *Wetlands Ecology and Management* 10:145-159.
- Garver, E.G., Dubbe, D.R., and Pratt, D.C. 1988. Seasonal patterns in accumulation and partitioning of biomass and macronutrients in *Typha* spp. *Aquatic Botany* 32:115-127.

- Hartman, J.M. 1988. Recolonization of small disturbance patches in a New England salt marsh. *American Journal of Botany* 75:1625-1631.
- Gornitz, V. 1995. Sea level rise: a review of recent past and near-future trends. *Earth Surf. Landf.* 18:63-81.
- Gosselink, J.G. and Hatton, R.S. 1984. Relationship of organic carbon and mineral content to bulk density in Louisiana soils. *Soil Science* 137:177-180.
- Grace, J.B. 1987. The impact of preemption on the zonation of two *Typha* species along lakeshores. *Ecological Monographs*. 57:283-303.
- Grime, J.P. 1979. Plant Strategies and Vegetation Processes. Wiley, Chichester, UK.
- Gross, M.F., Hardisky, M.A., and Klemas, V. 1990. Inter-annual spatial variability in response to *Spartina alterniflora* biomass to amount of precipitation. *Journal of Coastal Research* 6:949-960.
- Hacker, S.D. and Bertness, M.D. 1999. Experimental evidence for factors maintaining plant species diversity in a New England salt marsh. *Ecology* 80:2064-2073.
- Hartman, J.M. 1988. Recolonization of small disturbance patches in a New England salt marsh. *American Journal of Botany* 75:1625-1631.
- Harvey, J.W., Germann, P.F., and Odum, W.E. 1987. Geomorphological control of subsurface hydrology in the creekbank zone of tidal marshes. *Estuarine, Coastal, and Shelf Science* 25:677-691.
- Hatton, R.S., DeLaune, R.D., Patrick, W.H. 1983. Sedimentation, accretion and subsidence in marshes of Barataria Basin, Louisiana. *Limnol. Oceanogr.* 28:494-502.
- Hellings, S.E. and Gallagher, J.L. 1992. The effects of salinity and flooding on *Phragmites australis*. *Journal of Applied Ecology* 29:41-49.
- Helsel, D.R., and Hirsch, R.M. 1997. Statistical methods in water resources. Elsevier, Amsterdam, Netherlands.
- Hemminga, M.A. and Buth, G.J.C. 1991. Decomposition in salt marsh ecosystems of the S.W. Netherlands: the effects of biotic and abiotic factors. *Vegetatio* 92:73-83.
- Hill, B.H. 1987. *Typha* productivity in a Texas USA pond: implications for energy and nutrient dynamics in freshwater wetlands. *Aquatic Botany* 27:385-394

- Hopkinson, C.S. and Schubauer, J.P. 1984. Static and dynamic aspects of nitrogen cycling in the salt marsh grass *Spartina alterniflora*. *Ecology* 65:961-969.
- Horn, H.S. 1975. Forest succession. *Scientific American* 232:90-98.
- Huckle, J.M., Potter, J.A., and Marrs, R.H. 2000. Influence of environmental factors on the growth and interactions between salt marsh plants: effects of salinity, sediment and waterlogging. *Journal of Ecology* 88:492-505.
- Huston, M.A. 1979. A general hypothesis of species diversity. *American Naturalist* 113:81-101.
- Isaaks, E.H. and Srivastava, R.M. 1989. Applied Geostatistics. Oxford University Press, New York.
- Jaworski, N.A., Howarth, R.W., and Hetling, L.J. 1997. Atmospheric deposition of nitrogen oxides onto the landscape contributes to coastal eutrophication in the northeast United States. *Environmental Science and Technology* 31:1995-2004.
- Kaswadji, R.F., Gosselink, J.G., and Turner, R.E. 1990. Estimation of primary production using five different methods in a *Spartina alterniflora* salt marsh. *Wetlands Ecology and Management* 1:57-64.
- Keddy, P.A. 1989. Competition. Chapman & Hall, London, United Kingdom.
- Keddy, P.A., Twolan-Strutt, L., and Wisheu, I.C. 1994. Competitive effect and response rankings in 20 wetland plants: are they consistent across three environments? *Journal of Ecology* 82:635-643.
- Kelley, J.T., Gehrels, W.R., and Belnap, D.F. 1995. Late Holocene relative sea level rise and the geological development of tidal marshes at Wells, Maine, USA. *Journal of Coastal Research* 11:136-153.
- Kneib, R.T. 1997. The role of tidal marshes in the ecology of estuarine nekton. *Oceanography and Marine Biology* 35:163-220.
- Lana, P.C., Guiss, C., and Disaro, S.T. 1991. Seasonal variation of biomass and production dynamics for above and below ground components of a *Spartina alterniflora* marsh in the euhaline sector of Paranagua Bay (SE Brazil). *Estuarine, Coastal and Shelf Science* 32:231-241.
- Levine, J.M., Brewer, J.S., and Bertness, M.D. 1998. Nutrients, competition and plant zonation in a New England salt marsh. *Journal of Ecology* 86:285-292.

Little, L.S., Edwards, D., and Porter, D.E. 1997. Kriging in estuaries: as the crow flies, or as the fish swims? *Journal of Experimental Marine Biology and Ecology* 213:1-11.

Maxwell, T. and Constanza, R. 1997. An open geographic modeling environment. *Simulation Journal* 68:175-185.

McGuire, D.A., Melillo, J.M., Kicklighter, D.W., Pan, Y., Xiao, X., Helfrich, J., Moore, B., Vorosmarty, C.J., and Schloss, A.L. 1997. Equilibrium responses of global net primary production and carbon storage to doubled atmospheric carbon dioxide: Sensitivity to changes in vegetation nitrogen concentration. *Global Biogeochemical Cycles* 11:173-189.

McKee, K.L. and Patrick, W.H. 1988. The relationship of smooth cordgrass (*Spartina alterniflora*) to tidal datums: A review. *Estuaries* 22:143-151.

Melillo, J.M., McGuire, A.D., Kicklighter, D.W., Moore III, B., Vorosmarty, C.J., and Schloss, A.L. 1993. Global climate change and terrestrial net primary production. *Nature* 363: 234-240.

Mendelssohn, I.A. and Morris, J.M. 2000. Eco-physiological controls on the productivity of *Spartina alterniflora* Loisel. From: Concepts and Controversies in Tidal Marsh Ecology. Editors M.P. Weinstein and D. A. Kreeger, Kluwer Academic Publishers, Dordrecht, Netherlands, pp. 59-80.

Meyerson, L.A., Saltonstall, K., Windham, L., Kiviat, E., and Findlay, S. 2000. A comparison of *Phragmites australis* in freshwater and brackish marsh environments in North America. *Wetlands Ecology and Management* 8:89-103.

Minello, T.J. and Webb Jr., J.W. 1997. Use of natural and created *Spartina alterniflora* salt marshes by fishery species and other aquatic fauna in Galveston Bay, Texas, USA. *Marine Ecology Progress Series* 151:165-179.

Mitsch, W.J. and Gosselink, J.G. 1993. Wetlands. Wiley, New York, US.

Moy, L.D. and Levin, L.A. 1991. Are *Spartina* marshes a replaceable resource? A functional approach to evaluation of marsh creation efforts. *Estuaries* 14:1-16.

Morgan, P.A. and Short, F.T. 2002. Using functional trajectories to track constructed salt marsh development in the Great Bay Estuary, Maine/New Hampshire, USA. *Restoration Ecology* 10:461-473.

Neckles, H.A. and Dionne, M. (Editors). 2000. Regional standards to identify and evaluate tidal wetland restoration in the Gulf of Maine. Wells National Estuarine Research Reserve Technical Report, Wells, Maine. 21 pp.

- Nerem, R.S. 1999. Measuring very low frequency sea level variations using satellite altimeter data. *Global and Planetary Change* 20:157-171.
- Nestler, J. 1977. Interstitial salinity as a cause of ecophenic variation in *Spartina alterniflora*. *Estuarine Coastal Marine Sciences* 16:103-109.
- New Hampshire Office of State Planning. 1996. Restoring New Hampshire's salt marshes. NOAA Report 470ZO237. 8 pp.
- Niering, W.A. and Bowers, R.M. 1966. Our disappearing tidal marshes. *Connecticut Aboreal Bulletin*. 12:1-36.
- Niering, W.A. and Warren, R.S. 1980. Vegetation patterns and processes of New England salt marshes. *Bioscience* 30:301-307.
- Nixon, S. W. 1982. The ecology of New England high salt marshes: a community profile. United States Department of the Interior, Washington, DC. USA.
- Odum, W.E., Smith III, T.J., Hoover, J.K., and McIvor, C.C. 1984, The ecology of tidal freshwater marshes of the United States East Coast: A community profile. U.S. Fish and Wildlife Service, FWS/OBS-87/17, Washington, D.C. 177 pp.
- Parton, W.J., Scurlock, M.O., Ojima, D.S., Gilmanov, T.G., Scholes, R.J., Schmiel, D.S., Kirchner, T., Menaut, J-C., Seastedt, T., Moya, E.G., Kamnalrut, A., and Kinyamario, J.I. 1993. Observations and modeling of biomass and soil organic matter dynamics for the grassland biome worldwide. *Global Biogeochemical Cycles*, 7:785-809.
- Pearlstine, L.G., Kitchens, W.M., Latham, P.J., and Bartleson, R.D. 1993. Tide gate influences on a tidal marsh. *Proceedings from Symposium on Geographic Information Systems and Water Resource*, American Water Resources Association, Mobile, Alabama, pp. 433-440.
- Peltier, W.R. 1998. Postglacial variations in the level of the Sea: implications of climate dynamics and solid-earth geophysics. *Review of Geophysics* 36:603-689.
- Pennings, S.C. and Callaway, R.M. 1992. Salt marsh zonation: The relative importance of competition and physical factors. *Ecology* 73:681-690.
- Porter, D.E., Edwards, D. Scott, G., Jones, B., and Street, W.S. 1997. Assessing the impacts of anthropogenic and physiographic influences on grass shrimp in localized salt-marsh estuaries. *Aquatic Botany* 68:289-306.
- Portnoy, J.W. 1991. Summer oxygen depletion in a diked New England estuary. *Estuaries* 14:122-129.



Portnoy, J.W. and Giblin, A.E. 1997. Effects of historic tidal restrictions on salt marsh sediment chemistry. *Biogeochemistry* 36:275-303.

Race, M.S. 1985. Critique of present wetlands mitigation policies in the United States based on an analysis of past restoration projects in San Francisco Bay. *Environmental Management*. 9:71-82.

Raich, J.W., Rastetter, E.B., Melillo, J.M., Kicklighter, D.W., Steudler, P.A., Peterson, B.J., Grace, A.L., Moore III, B., and Vorosmarty, C.J. 1991. Potential net primary productivity in South America: application of a global model. *Ecological Applications* 1:399-429.

Rand, T.A. 2000. Seed dispersal, habitat suitability and the distribution of halophytes across a salt marsh tidal gradient. *Journal of Ecology* 88:608-621.

Redfield, A.C. 1972. Development of a New England salt marsh. *Ecological Monographs* 42:201-237.

Reinert, S.E. and Mello, M.J. 1995. Avian community structure and habitat use in a southern New England estuary. *Wetlands* 15:9-19.

Richardson, J.L. 1980. The organismic community: resilience of an embattled ecological concept. *Bioscience* 30:465-471.

Roman, C.T., Niering, W.A., and Warren, R.S. 1984. Salt marsh vegetation change in response to tidal restrictions. *Environmental Management* 8:141-149.

Roman, C.T., Garvine, R.W., and Portnoy, J.W. 1995. Hydrologic modeling as a predictive basis for the ecological restoration of salt marshes. *Environmental Management* 19: 559-566.

Roman, C.T., Raposa, K.B., Adamowicz, S.C., James-Pirri, M., and Catena, J.G. 2002. Quantifying vegetation and nekton response to tidal restoration of a New England salt marsh. *Restoration Ecology* 10:450-461.

Rozsa, R. 1995. Tidal restoration in Connecticut. In: G.D. Dreyer and W.A. Niering (eds.) Tidal Marshes of Long Island Sound: Ecology, History and Restoration, The Connecticut College Arboretum Bulletin 34, New London, Connecticut, pp: 51-65.

Running, S.W. and Coughlan, J.C. 1988. A general model of forest ecosystem processes for regional applications 1. Hydrologic balance, canopy gas exchange, and primary production processes. *Ecological Modelling* 42:125-154.

- Rybczyk, J.M., Callaway J.C., and Day, J.W. 1998. A relative elevation model for a subsiding coastal forested wetland receiving wastewater effluent. *Ecological Modeling* 112:23-44.
- SAS Institute. 1997. JMP statistics software version 3.1. SAS Institute, Inc., Cary, North Carolina, USA.
- Save the Sound. 1998. The Long Island Sound Conservation Blueprint. V. Pyle III editor. Stamford, CT. 200 pp.
- Schat, M. 1984. A comparative ecophysiological study of the effects of waterlogging and submergence on dune slack plants: growth, survival and mineral nutrition in sand culture experiments. *Oecologia (Berlin)* 62:279-286.
- Short, F.T., Boumans, R.M., Celikkol, B., and Costanza, R. 1998. Spatial modeling of eelgrass habitat change in Great Bay National Estuarine Research Reserve. Cooperative Institute for Coastal and Estuarine Environmental Technology (CICEET).
- Short, F.T., Burdick, D.M., Short, C.A., Davis, R.C., and Morgan, P.A. 2000. Developing success criteria for restored eelgrass, salt marsh, and mudflat habitats. *Ecological Engineering* 15:283-302.
- Shugart, H.H., Crow, T.R., and Hett, J.M. 1973. Forest succession models: A rationale and methodology for modeling forest succession over large regions. *Forest Science* 19:203-212.
- Shugart, H.H., and West, D.C. 1976. Development of an Appalachian deciduous forest succession model and its application to assessment of the impact of the chestnut blight. *Journal of Environmental Management* 5:161-179.
- Silliman, B.R. and Zieman, J.C. 2001. Top-down control of *Spartina alterniflora* production by periwinkle grazing in a Virginia salt marsh. *Ecology* 82:2830-2845.
- Sinicrope, T.L., Hine, P.G., Warren, R.S. and Niering, W.A. 1990. Restoration of an impounded salt marsh in New England. *Estuaries* 13:25-30.
- Simenstad, C.A and Thom, R.M. 1996. Functional equivalency trajectories of the restored Gog Le Hi Te estuarine wetland. *Ecological Applications* 6:38-56.
- Simon, A.L. 1976. Practical Hydraulics. John Wiley & Sons, New York.
- Sklar, F.H., Costanza, R. and Day Jr., J.W. 1985. Dynamic spatial simulation modeling of coastal wetland habitat succession. *Ecological Modeling* 29:261-281.

Streever, W.J. and Genders, A.J. 1997. Effect of tidal flushing and competitive interactions at the boundary between salt marsh and pasture. *Estuaries* 20:807-818.

Stumpf, R.P. 1983. The process of sedimentation on the surface of a salt marsh. *Estuarine, Coastal, and Shelf Science* 17:495-508.

Teal, J.M. 1962. Energy flow in the salt marsh ecosystem of Georgia. *Ecology* 43:614-624.

Tilman, D. 1982. Resource competition and community structure. Princeton University Press, Princeton, New Jersey, USA.

Tilman, D. 1988. Plant strategies and the dynamics and structure of plant communities. Princeton University Press, Princeton, New Jersey, USA.

Turner, M.G., Costanza, R., and Sklar, F.H. 1989. Methods to evaluate the performance of spatial simulation models. *Ecological Modelling* 48:1-18.

Turner, R.E. 1991. Tide gauge records, water level rise, and subsidence in the northern Gulf of Mexico. *Estuaries* 14:139-147.

Turner, R.E., Swenson, E.M., and Milan, C.S. 2000. Organic and inorganic contributions to vertical accretion in salt marsh sediments. From: Concepts and Controversies in Tidal Marsh Ecology. Editors M.P. Weinstein and D. A. Kreeger, Kluwer Academic Publishers, Dordrecht, Netherlands, pp. 583-595.

Underwood, A.J. 1997. Experiments in ecology. Cambridge University Press, New York, New York, USA.

US Army Corps of Engineers. 1999. Section 22, Planning assistance to state programs Little River Marsh study, North Hampton and Hampton, NH. New England District, Concord, MA. 19 pp.

USDA SCS (U.S. Department of Agriculture Soil Conservation Service). 1994. Evaluation of restorable salt marshes in New Hampshire. U.S. Department of Agriculture, Durham, New Hampshire.

Valiela, I., and Teal, J.M. 1974. Nutrient limitation in salt marsh vegetation. In: Ecology of Halophytes, R.J. Reimold and W.H. Queen, editors, Academic Press, New York, New York, USA.

Valiela, I., Teal, J.M., and Persson, N.Y. 1976. Production and dynamics of experimentally enriched salt marsh vegetation: belowground biomass. *Limnol. Oceanogr.* 21:245-252.

Valiela, I., Teal, J.M., Allen, S.D., Van Etten, R. Goehring, D., and Volkman, S. 1985. Decomposition in salt marsh ecosystems: The phases and major factors affecting disappearance of above-ground organic matter. *Journal of Experimental Biology and Ecology* 89:29-54.

Van Der Wal, R., Egas, M., Van Der Veen, A., and Bakker, J. 2000. Effects of resource competition and herbivory on plant performance along a natural productivity gradient. *Journal of Ecology* 88:317-330.

Voinov, A.A., Fitz, H.C., and Constanza, R. 1998. Surface water flow in landscape models: 1. Everglades case study. *Ecological Modelling* 108:131-144.

Voinov, A.A., Voinov, H. and Costanza, R. 1999. Surface water flow in landscape models: 2. Patuxent watershed case study. *Ecological Modelling* 119:211-230.

Ward, L.W., Kearney, M.S., and Stevenson, J.C. 1998. Variations in sedimentary environments and accretionary patterns in estuarine marshes undergoing rapid submergence, Chesapeake Bay. *Marine Geology* 151:111-134.

Warren, R.S., Fell, P.E., Grimsby, J.L., Buck, E.L., Rilling, C.G., and Fertek, R.A. 2001. Rates, patterns, and impacts of *Phragmites australis* expansion and effects of experimental *Phragmites* control on vegetation, macroinvertebrates, and fish within tidelands of the lower Connecticut River. *Estuaries* 24:90-107.

Warren, R.S., Fell, P.E., Rozsa, R., Brawley, A. H., Orsted, A.C., Olson, E.T., Swamy, V., and Niering, W.A. 2002. Salt marsh restoration in Connecticut: 20 years of science and management. *Restoration Ecology* 10:497-514.

Webb, J.W. 1983. Soil water salinity variations and their effects on *Spartina alterniflora*. *Contributions of Marine Science* 26:1-13.

Whigham, D.F., McCormick, J., Good, R.E., and Simpson, R.L. 1978. Biomass and primary production in freshwater tidal wetlands of the middle Atlantic coast. Freshwater wetlands: ecological processes and management potential. New York, Academic Press. pp 3-20.

Williams, P.B. and Orr, M.K. 2002. Physical evolution of restored breached levee salt marshes in the San Francisco Bay Estuary. *Restoration Ecology* 10:527-543.

Williams, P.B., Orr, M.K., and Garrity, N.J. 2002. Hydraulic geometry: A geomorphic design tool for tidal marsh channel evolution in wetland restoration projects. *Restoration Ecology* 10:577-591.

Windham, L., and Lathrop, R.G. 1999. Effects of *Phragmites australis* (common reed) invasion on aboveground biomass and soil properties in brackish tidal marsh of the Mullica River, New Jersey. *Estuaries* 22:927-935.

Wood, M.E., Kelley, J.T., and Belknap, D.F. 1989. Patterns of sediment accumulation in the tidal marshes of Maine. *Estuaries* 12:237-246.

Yang, S.L. 1998. The role of *Scirpus* marsh in attenuation of hydrodynamics and retention of fine sediment in the Yangtze estuary. *Estuarine Coastal and Shelf Science* 47:227-233.

Zedler, J.B. 2000. Progress in wetland restoration ecology. *TREE* 15:402-407.

## **APPENDICES**

Table A.1. Transplant experiment salinity measurements for three salinity regimes (high, mid, and low), with three elevation locations (high, mid, low) within each regime.

DATE	SALINITY (ppt)		
	High Elevation	Mid Elevation	Low Elevation
<b>High Salinity</b>			
5/31/2000	14	18	20
6/2/2000	17	19	22
6/15/2000	18	15	16
6/29/2000	19	16	12
7/13/2000	22	26	28
7/26/2000	25	26	29
8/9/2000	25	24	25
8/23/2000	26	24	23
9/5/2000	30	30	30
9/20/2000	18	28	30
<b>Mid Salinity</b>			
4/29/2001	6	6	8
5/7/2001	11	9	9
5/21/2001	16	18	11
5/30/2001	18	17	13
6/15/2001	18	16	12
7/3/2001	18	20	18
7/12/2001	22	23	17
7/25/2001	24	24	18
8/8/2001	24	23	23
8/22/2001	28	27	26
9/1/2001	24	20	20
<b>Low Salinity</b>			
4/29/2001	5	2	2
5/7/2001	9	9	9
5/21/2001	10	10	8
5/30/2001	16	12	12
6/15/2001	14	12	12
7/3/2001	8	9	8
7/12/2001	17	19	19
7/25/2001	23	20	20
8/8/2001	20	22	22
8/22/2001	27	25	24
9/1/2001	18	17	17

Table A.2. Final above and belowground biomass (grams dry weight) for experimental transplants.

Salinity Regime	Elevation Regime	Species	Competitor	Aboveground Biomass (g dw)	Belowground Biomass (g dw)
HI	HI	<i>Spartina alterniflora</i>	<i>Phragmites australis</i>	5.285	10.51
HI	HI	<i>Spartina alterniflora</i>	<i>Spartina alterniflora</i>	0.09	0.665
HI	HI	<i>Spartina alterniflora</i>	<i>Spartina alterniflora</i>	0.1	0.72
HI	HI	<i>Spartina alterniflora</i>	<i>Phragmites australis</i>	3.12	7.445
HI	HI	<i>Spartina alterniflora</i>	<i>Spartina alterniflora</i>	2.37	4.545
HI	HI	<i>Spartina alterniflora</i>	<i>Spartina alterniflora</i>	1.68	3.6
HI	MID	<i>Spartina alterniflora</i>	<i>Spartina patens</i>	1.02	3.31
HI	MID	<i>Spartina alterniflora</i>	<i>Juncus gerardii</i>	4.04	14.5
HI	LO	<i>Spartina alterniflora</i>	<i>Spartina patens</i>	10.725	16.42
HI	LO	<i>Spartina alterniflora</i>	<i>Juncus gerardii</i>	2.415	8.8
HI	LO	<i>Spartina alterniflora</i>	<i>Typha angustifolia</i>	15.04	23.5
HI	LO	<i>Spartina alterniflora</i>	<i>Spartina alterniflora</i>	5.26	10.7
HI	LO	<i>Spartina alterniflora</i>	<i>Spartina alterniflora</i>	3.51	9.65
HI	LO	<i>Spartina alterniflora</i>	<i>Spartina patens</i>	4.645	8.465
HI	LO	<i>Spartina alterniflora</i>	<i>Juncus gerardii</i>	10.83	17.505
HI	LO	<i>Spartina alterniflora</i>	<i>Phragmites australis</i>	7.8	15.9
HI	LO	<i>Spartina alterniflora</i>	<i>Lythrum salicaria</i>	8.96	30.08
HI	LO	<i>Spartina alterniflora</i>	<i>Typha angustifolia</i>	5.815	10.145
HI	LO	<i>Spartina alterniflora</i>	<i>Spartina alterniflora</i>	5.92	18.025
HI	LO	<i>Spartina alterniflora</i>	<i>Spartina alterniflora</i>	10.22	21.1
HI	HI	<i>Spartina patens</i>	<i>Spartina alterniflora</i>	2.48	2.88
HI	HI	<i>Spartina patens</i>	<i>Juncus gerardii</i>	1.765	2.12
HI	HI	<i>Spartina patens</i>	<i>Phragmites australis</i>	1.225	1.015
HI	HI	<i>Spartina patens</i>	<i>Lythrum salicaria</i>	3.35	3.5
HI	HI	<i>Spartina patens</i>	<i>Typha angustifolia</i>	3.29	3.82
HI	HI	<i>Spartina patens</i>	<i>Spartina patens</i>	1.785	2.965
HI	HI	<i>Spartina patens</i>	<i>Spartina patens</i>	2.085	2.68
HI	HI	<i>Spartina patens</i>	<i>Spartina alterniflora</i>	6.995	12.15
HI	HI	<i>Spartina patens</i>	<i>Juncus gerardii</i>	1.73	2.335
HI	HI	<i>Spartina patens</i>	<i>Phragmites australis</i>	1.47	2.85
HI	HI	<i>Spartina patens</i>	<i>Lythrum salicaria</i>	4.62	10.48
HI	HI	<i>Spartina patens</i>	<i>Typha angustifolia</i>	4.68	5.92
HI	HI	<i>Spartina patens</i>	<i>Spartina patens</i>	2.45	5.5
HI	HI	<i>Spartina patens</i>	<i>Spartina patens</i>	1.795	4.255
HI	MID	<i>Spartina patens</i>	<i>Spartina alterniflora</i>	5.85	7.865
HI	MID	<i>Spartina patens</i>	<i>Juncus gerardii</i>	4.42	7.535
HI	MID	<i>Spartina patens</i>	<i>Phragmites australis</i>	5.45	14.4
HI	MID	<i>Spartina patens</i>	<i>Lythrum salicaria</i>	5.18	10.125
HI	MID	<i>Spartina patens</i>	<i>Typha angustifolia</i>	1.81	7.71
HI	MID	<i>Spartina patens</i>	<i>Spartina patens</i>	3.28	9.19
HI	MID	<i>Spartina patens</i>	<i>Spartina patens</i>	3.9	6.805
HI	MID	<i>Spartina patens</i>	<i>Spartina alterniflora</i>	2.89	5.77
HI	MID	<i>Spartina patens</i>	<i>Juncus gerardii</i>	4.04	11.6



Table A.2 (continued). Final above and belowground biomass (grams dry weight) for experimental transplants.

Salinity Regime	Elevation Regime	Species	Competitor	Aboveground Biomass (g dw)	Belowground Biomass (g dw)
HI	MID	<i>Spartina patens</i>	<i>Phragmites australis</i>	6.65	9.38
HI	MID	<i>Spartina patens</i>	<i>Lythrum salicaria</i>	5.47	8.28
HI	MID	<i>Spartina patens</i>	<i>Typha angustifolia</i>	4.41	10.14
HI	MID	<i>Spartina patens</i>	<i>Spartina patens</i>	2.785	4.76
HI	MID	<i>Spartina patens</i>	<i>Spartina patens</i>	3.345	5.25
HI	LO	<i>Spartina patens</i>	<i>Spartina alterniflor</i>	1.69	3
HI	LO	<i>Spartina patens</i>	<i>Juncus gerardii</i>	3.35	4.755
HI	LO	<i>Spartina patens</i>	<i>Typha angustifolia</i>	4.445	6.9
HI	LO	<i>Spartina patens</i>	<i>Spartina patens</i>	0.74	1.375
HI	LO	<i>Spartina patens</i>	<i>Spartina patens</i>	2.86	4.35
HI	LO	<i>Spartina patens</i>	<i>Spartina alterniflor</i>	4.27	6.4
HI	LO	<i>Spartina patens</i>	<i>Juncus gerardii</i>	2.87	3.645
HI	LO	<i>Spartina patens</i>	<i>Typha angustifolia</i>	4.81	5.705
HI	LO	<i>Spartina patens</i>	<i>Spartina patens</i>	1.51	3.16
HI	LO	<i>Spartina patens</i>	<i>Spartina patens</i>	1.535	4.21
HI	HI	<i>Juncus gerardii</i>	<i>Spartina alterniflor</i>	0.68	1.73
HI	HI	<i>Juncus gerardii</i>	<i>Spartina patens</i>	0.505	1.135
HI	HI	<i>Juncus gerardii</i>	<i>Phragmites australis</i>	0.41	1.82
HI	HI	<i>Juncus gerardii</i>	<i>Lythrum salicaria</i>	0.165	1.62
HI	HI	<i>Juncus gerardii</i>	<i>Typha angustifolia</i>	0.375	0.91
HI	HI	<i>Juncus gerardii</i>	<i>Juncus gerardii</i>	0.42	0.77
HI	HI	<i>Juncus gerardii</i>	<i>Juncus gerardii</i>	0.245	0.775
HI	HI	<i>Juncus gerardii</i>	<i>Spartina alterniflor</i>	0.045	0.555
HI	HI	<i>Juncus gerardii</i>	<i>Spartina patens</i>	0.66	3.165
HI	HI	<i>Juncus gerardii</i>	<i>Phragmites australis</i>	1.8	2.78
HI	HI	<i>Juncus gerardii</i>	<i>Lythrum salicaria</i>	2.31	5
HI	HI	<i>Juncus gerardii</i>	<i>Typha angustifolia</i>	0.79	2.36
HI	HI	<i>Juncus gerardii</i>	<i>Juncus gerardii</i>	1.53	4.04
HI	HI	<i>Juncus gerardii</i>	<i>Juncus gerardii</i>	1.44	2.88
HI	MID	<i>Juncus gerardii</i>	<i>Spartina alterniflor</i>	0.12	0.91
HI	MID	<i>Juncus gerardii</i>	<i>Spartina patens</i>	0.195	3.44
HI	MID	<i>Juncus gerardii</i>	<i>Phragmites australis</i>	0.48	2.43
HI	MID	<i>Juncus gerardii</i>	<i>Lythrum salicaria</i>	0.085	0.905
HI	MID	<i>Juncus gerardii</i>	<i>Typha angustifolia</i>	1.015	3.515
HI	MID	<i>Juncus gerardii</i>	<i>Juncus gerardii</i>	0.395	1.21
HI	MID	<i>Juncus gerardii</i>	<i>Juncus gerardii</i>	0.185	2.375
HI	MID	<i>Juncus gerardii</i>	<i>Spartina alterniflor</i>	0.95	4.52
HI	MID	<i>Juncus gerardii</i>	<i>Spartina patens</i>	0.15	0.66
HI	MID	<i>Juncus gerardii</i>	<i>Phragmites australis</i>	0.99	2.805
HI	MID	<i>Juncus gerardii</i>	<i>Lythrum salicaria</i>	3.58	8.03
HI	MID	<i>Juncus gerardii</i>	<i>Typha angustifolia</i>	0.28	1.1
HI	MID	<i>Juncus gerardii</i>	<i>Juncus gerardii</i>	1.155	2.38
HI	MID	<i>Juncus gerardii</i>	<i>Juncus gerardii</i>	1.49	2.845

Table A.2 (continued). Final above and belowground biomass (grams dry weight) for experimental transplants.

Salinity Regime	Elevation Regime	Species	Competitor	Aboveground Biomass (g dw)	Belowground Biomass (g dw)
HI	LO	<i>Juncus gerardii</i>	<i>Spartina alterniflor</i>	0.36	0.765
HI	LO	<i>Juncus gerardii</i>	<i>Spartina patens</i>	0.19	0.41
HI	LO	<i>Juncus gerardii</i>	<i>Phragmites australis</i>	0.145	0.85
HI	LO	<i>Juncus gerardii</i>	<i>Lythrum salicaria</i>	0.04	0.21
HI	LO	<i>Juncus gerardii</i>	<i>Typha angustifolia</i>	0.39	0.905
HI	LO	<i>Juncus gerardii</i>	<i>Juncus gerardii</i>	0.615	0.825
HI	LO	<i>Juncus gerardii</i>	<i>Juncus gerardii</i>	0.13	0.185
HI	LO	<i>Juncus gerardii</i>	<i>Spartina alterniflor</i>	0.035	0.84
HI	LO	<i>Juncus gerardii</i>	<i>Spartina patens</i>	0.195	0.42
HI	LO	<i>Juncus gerardii</i>	<i>Lythrum salicaria</i>	0.355	2.04
HI	LO	<i>Juncus gerardii</i>	<i>Typha angustifolia</i>	0.175	0.445
HI	LO	<i>Juncus gerardii</i>	<i>Juncus gerardii</i>	0.375	0.79
HI	LO	<i>Juncus gerardii</i>	<i>Juncus gerardii</i>	0.585	1.245
HI	HI	<i>Phragmites australis</i>	<i>Phragmites australis</i>	0.02	1.725
HI	HI	<i>Phragmites australis</i>	<i>Juncus gerardii</i>	2.005	8.15
HI	MID	<i>Phragmites australis</i>	<i>Juncus gerardii</i>	2.72	7.335
HI	MID	<i>Phragmites australis</i>	<i>Phragmites australis</i>	3.84	3.6
HI	MID	<i>Phragmites australis</i>	<i>Phragmites australis</i>	1.165	3.41
HI	LO	<i>Phragmites australis</i>	<i>Phragmites australis</i>	0.74	0.69
HI	LO	<i>Phragmites australis</i>	<i>Phragmites australis</i>	2.905	2
HI	LO	<i>Phragmites australis</i>	<i>Juncus gerardii</i>	5	4.82
HI	LO	<i>Phragmites australis</i>	<i>Lythrum salicaria</i>	4.04	5.265
HI	LO	<i>Phragmites australis</i>	<i>Phragmites australis</i>	6.15	9.16
HI	LO	<i>Phragmites australis</i>	<i>Phragmites australis</i>	5.5	4.555
HI	HI	<i>Lythrum salicaria</i>	<i>Lythrum salicaria</i>	0.31	3.555
HI	HI	<i>Lythrum salicaria</i>	<i>Lythrum salicaria</i>	0.27	2.245
HI	HI	<i>Typha angustifolia</i>	<i>Phragmites australis</i>	0.165	2.19
HI	HI	<i>Typha angustifolia</i>	<i>Typha angustifolia</i>	0.05	0.855
HI	HI	<i>Typha angustifolia</i>	<i>Typha angustifolia</i>	0.105	1.01
HI	HI	<i>Typha angustifolia</i>	<i>Juncus gerardii</i>	0.3	2.79
HI	HI	<i>Typha angustifolia</i>	<i>Typha angustifolia</i>	0.185	2.49
HI	HI	<i>Typha angustifolia</i>	<i>Typha angustifolia</i>	0.145	2.3
MID	HI	<i>Spartina alterniflor</i>	<i>Spartina patens</i>	1.63	10.95
MID	HI	<i>Spartina alterniflor</i>	<i>Juncus gerardii</i>	5.94	19.51
MID	HI	<i>Spartina alterniflor</i>	<i>Phragmites australis</i>	4.47	23.05
MID	HI	<i>Spartina alterniflor</i>	<i>Lythrum salicaria</i>	5.22	18.17
MID	HI	<i>Spartina alterniflor</i>	<i>Typha angustifolia</i>	5.5	27.64
MID	HI	<i>Spartina alterniflor</i>	<i>Spartina alterniflor</i>	1.94	10.595
MID	HI	<i>Spartina alterniflor</i>	<i>Spartina alterniflor</i>	1.94	10.595
MID	HI	<i>Spartina alterniflor</i>	<i>Spartina patens</i>	3.97	13.51
MID	HI	<i>Spartina alterniflor</i>	<i>Juncus gerardii</i>	3.34	7.52
MID	HI	<i>Spartina alterniflor</i>	<i>Phragmites australis</i>	6.76	19.09
MID	HI	<i>Spartina alterniflor</i>	<i>Lythrum salicaria</i>	4.98	14.52

Table A.2 (continued). Final above and belowground biomass (grams dry weight) for experimental transplants.

Salinity Regime	Elevation Regime	Species	Competitor	Aboveground Biomass (g dw)	Belowground Biomass (g dw)
MID	HI	<i>Spartina alterniflora</i>	<i>Typha angustifolia</i>	2.84	7.29
MID	HI	<i>Spartina alterniflora</i>	<i>Spartina alterniflora</i>	4.48	10.22
MID	HI	<i>Spartina alterniflora</i>	<i>Spartina alterniflora</i>	4.48	10.22
MID	MID	<i>Spartina alterniflora</i>	<i>Spartina patens</i>	22.38	96.66
MID	MID	<i>Spartina alterniflora</i>	<i>Juncus gerardii</i>	15.37	73.21
MID	MID	<i>Spartina alterniflora</i>	<i>Phragmites australis</i>	17.44	88.07
MID	MID	<i>Spartina alterniflora</i>	<i>Lythrum salicaria</i>	15.88	77.91
MID	MID	<i>Spartina alterniflora</i>	<i>Typha angustifolia</i>	22.37	98.76
MID	MID	<i>Spartina alterniflora</i>	<i>Spartina alterniflora</i>	9.97	41.705
MID	MID	<i>Spartina alterniflora</i>	<i>Spartina alterniflora</i>	9.97	41.705
MID	MID	<i>Spartina alterniflora</i>	<i>Spartina patens</i>	6.82	27.43
MID	MID	<i>Spartina alterniflora</i>	<i>Juncus gerardii</i>	9.7	46
MID	MID	<i>Spartina alterniflora</i>	<i>Phragmites australis</i>	14.69	80.78
MID	MID	<i>Spartina alterniflora</i>	<i>Lythrum salicaria</i>	9.94	32.77
MID	MID	<i>Spartina alterniflora</i>	<i>Typha angustifolia</i>	13.3	54.3
MID	MID	<i>Spartina alterniflora</i>	<i>Spartina alterniflora</i>	12.79	45.325
MID	MID	<i>Spartina alterniflora</i>	<i>Spartina alterniflora</i>	12.79	45.325
MID	LO	<i>Spartina alterniflora</i>	<i>Spartina patens</i>	25.51	43.93
MID	LO	<i>Spartina alterniflora</i>	<i>Juncus gerardii</i>	21.8	93.84
MID	LO	<i>Spartina alterniflora</i>	<i>Lythrum salicaria</i>	26.53	86.11
MID	LO	<i>Spartina alterniflora</i>	<i>Typha angustifolia</i>	21.56	92.04
MID	LO	<i>Spartina alterniflora</i>	<i>Spartina alterniflora</i>	19.54	61.24
MID	LO	<i>Spartina alterniflora</i>	<i>Spartina alterniflora</i>	19.54	61.24
MID	LO	<i>Spartina alterniflora</i>	<i>Spartina patens</i>	18.9	49.19
MID	LO	<i>Spartina alterniflora</i>	<i>Juncus gerardii</i>	7.27	45.55
MID	LO	<i>Spartina alterniflora</i>	<i>Phragmites australis</i>	17.95	49.89
MID	LO	<i>Spartina alterniflora</i>	<i>Lythrum salicaria</i>	12.28	29.82
MID	LO	<i>Spartina alterniflora</i>	<i>Typha angustifolia</i>	25.96	98.67
MID	LO	<i>Spartina alterniflora</i>	<i>Spartina alterniflora</i>	15.365	44.37
MID	LO	<i>Spartina alterniflora</i>	<i>Spartina alterniflora</i>	15.365	44.37
MID	HI	<i>Spartina patens</i>	<i>Spartina alterniflora</i>	7.8	19.01
MID	HI	<i>Spartina patens</i>	<i>Juncus gerardii</i>	5.23	10.26
MID	HI	<i>Spartina patens</i>	<i>Phragmites australis</i>	6.26	10.13
MID	HI	<i>Spartina patens</i>	<i>Lythrum salicaria</i>	9.58	23.59
MID	HI	<i>Spartina patens</i>	<i>Typha angustifolia</i>	4.88	9.42
MID	HI	<i>Spartina patens</i>	<i>Spartina patens</i>	5.615	14.465
MID	HI	<i>Spartina patens</i>	<i>Spartina patens</i>	5.615	14.465
MID	HI	<i>Spartina patens</i>	<i>Spartina alterniflora</i>	5.13	22
MID	HI	<i>Spartina patens</i>	<i>Juncus gerardii</i>	8.25	16.23
MID	HI	<i>Spartina patens</i>	<i>Phragmites australis</i>	6.1	20.57
MID	HI	<i>Spartina patens</i>	<i>Lythrum salicaria</i>	6.82	24.35
MID	HI	<i>Spartina patens</i>	<i>Typha angustifolia</i>	6.42	23.45
MID	HI	<i>Spartina patens</i>	<i>Spartina patens</i>	3.29	10.885

Table A.2 (continued). Final above and belowground biomass (grams dry weight) for experimental transplants.

Salinity Regime	Elevation Regime	Species	Competitor	Aboveground Biomass (g dw)	Belowground Biomass (g dw)
MID	HI	<i>Spartina patens</i>	<i>Spartina patens</i>	3.29	10.885
MID	MID	<i>Spartina patens</i>	<i>Spartina alterniflor</i>	4.31	11.55
MID	MID	<i>Spartina patens</i>	<i>Juncus gerardii</i>	4.61	8.14
MID	MID	<i>Spartina patens</i>	<i>Phragmites australis</i>	7.59	11.98
MID	MID	<i>Spartina patens</i>	<i>Lythrum salicaria</i>	6.2	6.93
MID	MID	<i>Spartina patens</i>	<i>Typha angustifolia</i>	8.45	9.18
MID	MID	<i>Spartina patens</i>	<i>Spartina patens</i>	4.77	10.17
MID	MID	<i>Spartina patens</i>	<i>Spartina patens</i>	4.77	10.17
MID	MID	<i>Spartina patens</i>	<i>Spartina alterniflor</i>	4.53	8.54
MID	MID	<i>Spartina patens</i>	<i>Juncus gerardii</i>	1.65	4.22
MID	MID	<i>Spartina patens</i>	<i>Phragmites australis</i>	3.33	7.3
MID	MID	<i>Spartina patens</i>	<i>Lythrum salicaria</i>	4.6	8.67
MID	MID	<i>Spartina patens</i>	<i>Typha angustifolia</i>	7.46	14.57
MID	MID	<i>Spartina patens</i>	<i>Spartina patens</i>	2.135	4.55
MID	MID	<i>Spartina patens</i>	<i>Spartina patens</i>	2.135	4.55
MID	LO	<i>Spartina patens</i>	<i>Spartina alterniflor</i>	0.84	2.17
MID	LO	<i>Spartina patens</i>	<i>Juncus gerardii</i>	0.19	1.53
MID	LO	<i>Spartina patens</i>	<i>Phragmites australis</i>	0.1	0.8
MID	LO	<i>Spartina patens</i>	<i>Spartina patens</i>	0.11	1.48
MID	LO	<i>Spartina patens</i>	<i>Spartina patens</i>	0.11	1.48
MID	LO	<i>Spartina patens</i>	<i>Spartina alterniflor</i>	0.18	1.11
MID	LO	<i>Spartina patens</i>	<i>Juncus gerardii</i>	0.57	1.01
MID	LO	<i>Spartina patens</i>	<i>Phragmites australis</i>	0.26	0.79
MID	LO	<i>Spartina patens</i>	<i>Lythrum salicaria</i>	0.28	1.35
MID	LO	<i>Spartina patens</i>	<i>Typha angustifolia</i>	0.35	0.53
MID	LO	<i>Spartina patens</i>	<i>Spartina patens</i>	0.15	0.22
MID	LO	<i>Spartina patens</i>	<i>Spartina patens</i>	0.15	0.22
MID	HI	<i>Juncus gerardii</i>	<i>Spartina alterniflor</i>	1.21	1.41
MID	HI	<i>Juncus gerardii</i>	<i>Spartina patens</i>	1.87	8.38
MID	HI	<i>Juncus gerardii</i>	<i>Phragmites australis</i>	0.82	2.78
MID	HI	<i>Juncus gerardii</i>	<i>Lythrum salicaria</i>	0.81	2.09
MID	HI	<i>Juncus gerardii</i>	<i>Typha angustifolia</i>	0.96	2.01
MID	HI	<i>Juncus gerardii</i>	<i>Juncus gerardii</i>	1.025	2.61
MID	HI	<i>Juncus gerardii</i>	<i>Juncus gerardii</i>	1.025	2.61
MID	HI	<i>Juncus gerardii</i>	<i>Spartina alterniflor</i>	1.21	3.23
MID	HI	<i>Juncus gerardii</i>	<i>Spartina patens</i>	1.67	9.4
MID	HI	<i>Juncus gerardii</i>	<i>Phragmites australis</i>	3.14	10.99
MID	HI	<i>Juncus gerardii</i>	<i>Lythrum salicaria</i>	1.76	6.87
MID	HI	<i>Juncus gerardii</i>	<i>Typha angustifolia</i>	1.23	6.82
MID	HI	<i>Juncus gerardii</i>	<i>Juncus gerardii</i>	1.46	6.895
MID	HI	<i>Juncus gerardii</i>	<i>Juncus gerardii</i>	1.46	6.895
MID	MID	<i>Juncus gerardii</i>	<i>Spartina alterniflor</i>	0.12	0.91
MID	MID	<i>Juncus gerardii</i>	<i>Spartina patens</i>	0.7	2.37

Table A.2 (continued). Final above and belowground biomass (grams dry weight) for experimental transplants.

Salinity Regime	Elevation Regime	Species	Competitor	Aboveground Biomass (g dw)	Belowground Biomass (g dw)
MID	MID	<i>Juncus gerardii</i>	<i>Phragmites australis</i>	0.28	1.99
MID	MID	<i>Juncus gerardii</i>	<i>Lythrum salicaria</i>	1.17	1.71
MID	MID	<i>Juncus gerardii</i>	<i>Juncus gerardii</i>	0.91	1.435
MID	MID	<i>Juncus gerardii</i>	<i>Juncus gerardii</i>	0.91	1.435
MID	MID	<i>Juncus gerardii</i>	<i>Spartina alterniflor</i>	0.44	1.43
MID	MID	<i>Juncus gerardii</i>	<i>Spartina patens</i>	0.69	1.94
MID	MID	<i>Juncus gerardii</i>	<i>Phragmites australis</i>	0.23	0.58
MID	MID	<i>Juncus gerardii</i>	<i>Lythrum salicaria</i>	0.43	0.82
MID	MID	<i>Juncus gerardii</i>	<i>Juncus gerardii</i>	0.93	1.095
MID	MID	<i>Juncus gerardii</i>	<i>Juncus gerardii</i>	0.93	1.095
MID	HI	<i>Phragmites australis</i>	<i>Spartina alterniflor</i>	1.73	2.51
MID	HI	<i>Phragmites australis</i>	<i>Spartina patens</i>	3.48	1.28
MID	HI	<i>Phragmites australis</i>	<i>Spartina patens</i>	2.97	6.71
MID	HI	<i>Phragmites australis</i>	<i>Juncus gerardii</i>	3.76	10.11
MID	HI	<i>Phragmites australis</i>	<i>Phragmites australis</i>	1.085	3.02
MID	HI	<i>Phragmites australis</i>	<i>Phragmites australis</i>	1.085	3.02
MID	MID	<i>Phragmites australis</i>	<i>Juncus gerardii</i>	19.39	33.67
MID	MID	<i>Phragmites australis</i>	<i>Phragmites australis</i>	2.195	10.095
MID	MID	<i>Phragmites australis</i>	<i>Phragmites australis</i>	2.195	10.095
MID	MID	<i>Phragmites australis</i>	<i>Spartina patens</i>	2.26	5.9
MID	MID	<i>Phragmites australis</i>	<i>Lythrum salicaria</i>	4.63	11.33
MID	MID	<i>Phragmites australis</i>	<i>Phragmites australis</i>	1.675	2.755
MID	MID	<i>Phragmites australis</i>	<i>Phragmites australis</i>	1.675	2.755
MID	LO	<i>Phragmites australis</i>	<i>Spartina alterniflor</i>	1.85	2.14
MID	LO	<i>Phragmites australis</i>	<i>Phragmites australis</i>	5.11	12.67
MID	LO	<i>Phragmites australis</i>	<i>Phragmites australis</i>	5.11	12.67
MID	LO	<i>Phragmites australis</i>	<i>Spartina alterniflor</i>	4.3	5.06
MID	LO	<i>Phragmites australis</i>	<i>Phragmites australis</i>	3.11	5.22
MID	LO	<i>Phragmites australis</i>	<i>Phragmites australis</i>	3.11	5.22
MID	HI	<i>Lythrum salicaria</i>	<i>Spartina patens</i>	0.34	1.01
MID	HI	<i>Lythrum salicaria</i>	<i>Juncus gerardii</i>	3.15	23.44
MID	HI	<i>Lythrum salicaria</i>	<i>Phragmites australis</i>	2.43	7.13
MID	HI	<i>Lythrum salicaria</i>	<i>Spartina patens</i>	0.88	8.06
MID	HI	<i>Lythrum salicaria</i>	<i>Juncus gerardii</i>	3.92	21.3
MID	HI	<i>Lythrum salicaria</i>	<i>Phragmites australis</i>	1.39	7.72
MID	HI	<i>Lythrum salicaria</i>	<i>Lythrum salicaria</i>	1.225	20.495
MID	HI	<i>Lythrum salicaria</i>	<i>Lythrum salicaria</i>	1.225	20.495
MID	HI	<i>Typha angustifolia</i>	<i>Spartina alterniflor</i>	0.23	0.91
MID	HI	<i>Typha angustifolia</i>	<i>Spartina patens</i>	1.54	2.76
MID	HI	<i>Typha angustifolia</i>	<i>Juncus gerardii</i>	1.91	6
MID	HI	<i>Typha angustifolia</i>	<i>Phragmites australis</i>	1.08	6.52
MID	HI	<i>Typha angustifolia</i>	<i>Lythrum salicaria</i>	1.47	3.53
MID	HI	<i>Typha angustifolia</i>	<i>Typha angustifolia</i>	0.455	3.54

Table A.2 (continued). Final above and belowground biomass (grams dry weight) for experimental transplants.

Salinity Regime	Elevation Regime	Species	Competitor	Aboveground Biomass (g dw)	Belowground Biomass (g dw)
MID	HI	<i>Typha angustifolia</i>	<i>Typha angustifolia</i>	0.455	3.54
MID	HI	<i>Typha angustifolia</i>	<i>Spartina alterniflor</i>	0.63	4.19
MID	HI	<i>Typha angustifolia</i>	<i>Spartina patens</i>	0.41	0.93
MID	HI	<i>Typha angustifolia</i>	<i>Juncus gerardii</i>	0.9	11.37
MID	HI	<i>Typha angustifolia</i>	<i>Phragmites australis</i>	0.68	6.41
MID	HI	<i>Typha angustifolia</i>	<i>Lythrum salicaria</i>	0.42	3.49
MID	HI	<i>Typha angustifolia</i>	<i>Typha angustifolia</i>	1.2	8.02
MID	HI	<i>Typha angustifolia</i>	<i>Typha angustifolia</i>	1.2	8.02
MID	MID	<i>Typha angustifolia</i>	<i>Spartina alterniflor</i>	2.78	8.93
MID	MID	<i>Typha angustifolia</i>	<i>Spartina patens</i>	1.11	11.01
MID	MID	<i>Typha angustifolia</i>	<i>Phragmites australis</i>	3.88	15.77
MID	MID	<i>Typha angustifolia</i>	<i>Lythrum salicaria</i>	3.99	8.71
MID	MID	<i>Typha angustifolia</i>	<i>Typha angustifolia</i>	5.205	33.405
MID	MID	<i>Typha angustifolia</i>	<i>Typha angustifolia</i>	5.205	33.405
MID	MID	<i>Typha angustifolia</i>	<i>Spartina alterniflor</i>	2.47	3.73
MID	MID	<i>Typha angustifolia</i>	<i>Juncus gerardii</i>	5.62	9.6
MID	MID	<i>Typha angustifolia</i>	<i>Phragmites australis</i>	2.77	15.46
MID	MID	<i>Typha angustifolia</i>	<i>Lythrum salicaria</i>	2.84	18.68
MID	MID	<i>Typha angustifolia</i>	<i>Typha angustifolia</i>	5.005	25.03
MID	MID	<i>Typha angustifolia</i>	<i>Typha angustifolia</i>	5.005	25.03
MID	LO	<i>Typha angustifolia</i>	<i>Spartina patens</i>	1.43	30.53
MID	LO	<i>Typha angustifolia</i>	<i>Phragmites australis</i>	6.4	12.73
MID	LO	<i>Typha angustifolia</i>	<i>Typha angustifolia</i>	3.805	17.2
MID	LO	<i>Typha angustifolia</i>	<i>Typha angustifolia</i>	3.805	17.2
MID	LO	<i>Typha angustifolia</i>	<i>Spartina alterniflor</i>	0.99	2.4
MID	LO	<i>Typha angustifolia</i>	<i>Typha angustifolia</i>	3.725	21.69
MID	LO	<i>Typha angustifolia</i>	<i>Typha angustifolia</i>	3.725	21.69
LO	HI	<i>Spartina alterniflor</i>	<i>Spartina patens</i>	3.66	20.13
LO	HI	<i>Spartina alterniflor</i>	<i>Juncus gerardii</i>	12.58	40.98
LO	HI	<i>Spartina alterniflor</i>	<i>Phragmites australis</i>	13.42	21.49
LO	HI	<i>Spartina alterniflor</i>	<i>Lythrum salicaria</i>	6.61	24.55
LO	HI	<i>Spartina alterniflor</i>	<i>Typha angustifolia</i>	2.48	12.39
LO	HI	<i>Spartina alterniflor</i>	<i>Spartina alterniflor</i>	9.635	42.74
LO	HI	<i>Spartina alterniflor</i>	<i>Spartina alterniflor</i>	9.635	42.74
LO	HI	<i>Spartina alterniflor</i>	<i>Spartina patens</i>	2.45	10.42
LO	HI	<i>Spartina alterniflor</i>	<i>Juncus gerardii</i>	15.39	97.14
LO	HI	<i>Spartina alterniflor</i>	<i>Phragmites australis</i>	1.91	11.03
LO	HI	<i>Spartina alterniflor</i>	<i>Lythrum salicaria</i>	6.8	8.1
LO	HI	<i>Spartina alterniflor</i>	<i>Typha angustifolia</i>	12.85	85.47
LO	MID	<i>Spartina alterniflor</i>	<i>Spartina patens</i>	16.12	40.43
LO	MID	<i>Spartina alterniflor</i>	<i>Juncus gerardii</i>	23.34	76.75
LO	MID	<i>Spartina alterniflor</i>	<i>Phragmites australis</i>	20.53	98.87
LO	MID	<i>Spartina alterniflor</i>	<i>Lythrum salicaria</i>	17.66	85.02

Table A.2 (continued). Final above and belowground biomass (grams dry weight) for experimental transplants.

Salinity Regime	Elevation Regime	Species	Competitor	Aboveground Biomass (g dw)	Belowground Biomass (g dw)
LO	MID	<i>Spartina alterniflora</i>	<i>Typha angustifolia</i>	20.77	89.88
LO	MID	<i>Spartina alterniflora</i>	<i>Spartina alterniflora</i>	3.985	18.315
LO	MID	<i>Spartina alterniflora</i>	<i>Spartina alterniflora</i>	3.985	18.315
LO	MID	<i>Spartina alterniflora</i>	<i>Spartina patens</i>	13.3	92.09
LO	MID	<i>Spartina alterniflora</i>	<i>Juncus gerardii</i>	34.72	98.66
LO	MID	<i>Spartina alterniflora</i>	<i>Phragmites australis</i>	11.2	96.2
LO	MID	<i>Spartina alterniflora</i>	<i>Lythrum salicaria</i>	19.18	95.48
LO	MID	<i>Spartina alterniflora</i>	<i>Typha angustifolia</i>	13.67	96.41
LO	MID	<i>Spartina alterniflora</i>	<i>Spartina alterniflora</i>	4.94	31.085
LO	MID	<i>Spartina alterniflora</i>	<i>Spartina alterniflora</i>	4.94	31.085
LO	LO	<i>Spartina alterniflora</i>	<i>Spartina patens</i>	5.37	17.91
LO	LO	<i>Spartina alterniflora</i>	<i>Juncus gerardii</i>	5.44	19.9
LO	LO	<i>Spartina alterniflora</i>	<i>Phragmites australis</i>	22.42	58.8
LO	LO	<i>Spartina alterniflora</i>	<i>Lythrum salicaria</i>	10.79	50.73
LO	LO	<i>Spartina alterniflora</i>	<i>Typha angustifolia</i>	10.36	26.6
LO	LO	<i>Spartina alterniflora</i>	<i>Spartina alterniflora</i>	17.415	49.56
LO	LO	<i>Spartina alterniflora</i>	<i>Spartina alterniflora</i>	17.415	49.56
LO	LO	<i>Spartina alterniflora</i>	<i>Spartina patens</i>	3.7	19.68
LO	LO	<i>Spartina alterniflora</i>	<i>Juncus gerardii</i>	22.99	54.08
LO	LO	<i>Spartina alterniflora</i>	<i>Phragmites australis</i>	11.27	62.29
LO	LO	<i>Spartina alterniflora</i>	<i>Lythrum salicaria</i>	40.04	99.44
LO	LO	<i>Spartina alterniflora</i>	<i>Spartina alterniflora</i>	10.955	40.005
LO	LO	<i>Spartina alterniflora</i>	<i>Spartina alterniflora</i>	10.955	40.005
LO	HI	<i>Spartina patens</i>	<i>Spartina alterniflora</i>	2.62	6.45
LO	HI	<i>Spartina patens</i>	<i>Juncus gerardii</i>	5.43	8.13
LO	HI	<i>Spartina patens</i>	<i>Phragmites australis</i>	5.95	12.74
LO	HI	<i>Spartina patens</i>	<i>Lythrum salicaria</i>	5.53	8.98
LO	HI	<i>Spartina patens</i>	<i>Typha angustifolia</i>	5.04	11.42
LO	HI	<i>Spartina patens</i>	<i>Spartina patens</i>	3.245	13.86
LO	HI	<i>Spartina patens</i>	<i>Spartina patens</i>	3.245	13.86
LO	HI	<i>Spartina patens</i>	<i>Spartina alterniflora</i>	3.88	29.34
LO	HI	<i>Spartina patens</i>	<i>Juncus gerardii</i>	1.51	13.5
LO	HI	<i>Spartina patens</i>	<i>Phragmites australis</i>	2.47	28.27
LO	HI	<i>Spartina patens</i>	<i>Lythrum salicaria</i>	1.11	15.49
LO	HI	<i>Spartina patens</i>	<i>Typha angustifolia</i>	2.97	20.63
LO	HI	<i>Spartina patens</i>	<i>Spartina patens</i>	2.685	13.69
LO	HI	<i>Spartina patens</i>	<i>Spartina patens</i>	2.685	13.69
LO	MID	<i>Spartina patens</i>	<i>Spartina alterniflora</i>	1.61	12.85
LO	MID	<i>Spartina patens</i>	<i>Juncus gerardii</i>	4.71	10.18
LO	MID	<i>Spartina patens</i>	<i>Phragmites australis</i>	0.61	10.03
LO	MID	<i>Spartina patens</i>	<i>Lythrum salicaria</i>	1.56	4.54
LO	MID	<i>Spartina patens</i>	<i>Typha angustifolia</i>	1.36	1.94
LO	MID	<i>Spartina patens</i>	<i>Spartina patens</i>	2.85	4.26

Table A.2 (continued). Final above and belowground biomass (grams dry weight) for experimental transplants.

Salinity Regime	Elevation Regime	Species	Competitor	Aboveground Biomass (g dw)	Belowground Biomass (g dw)
LO	MID	<i>Spartina patens</i>	<i>Spartina patens</i>	2.85	4.26
LO	MID	<i>Spartina patens</i>	<i>Spartina alterniflor</i>	2.42	9.32
LO	MID	<i>Spartina patens</i>	<i>Juncus gerardii</i>	4.68	20.25
LO	MID	<i>Spartina patens</i>	<i>Phragmites australis</i>	0.46	2.91
LO	MID	<i>Spartina patens</i>	<i>Lythrum salicaria</i>	2.72	6.39
LO	MID	<i>Spartina patens</i>	<i>Typha angustifolia</i>	1.26	5.9
LO	MID	<i>Spartina patens</i>	<i>Spartina patens</i>	1.91	5.52
LO	MID	<i>Spartina patens</i>	<i>Spartina patens</i>	1.91	5.52
LO	LO	<i>Spartina patens</i>	<i>Spartina patens</i>	0.915	1.48
LO	LO	<i>Spartina patens</i>	<i>Spartina patens</i>	0.915	1.48
LO	LO	<i>Spartina patens</i>	<i>Spartina alterniflor</i>	0.65	2.18
LO	LO	<i>Spartina patens</i>	<i>Juncus gerardii</i>	1.01	2.06
LO	LO	<i>Spartina patens</i>	<i>Lythrum salicaria</i>	0.26	2.14
LO	LO	<i>Spartina patens</i>	<i>Spartina patens</i>	0.385	5.245
LO	LO	<i>Spartina patens</i>	<i>Spartina patens</i>	0.385	5.245
LO	HI	<i>Juncus gerardii</i>	<i>Spartina alterniflor</i>	1.96	3.2
LO	HI	<i>Juncus gerardii</i>	<i>Spartina patens</i>	3.85	8.28
LO	HI	<i>Juncus gerardii</i>	<i>Phragmites australis</i>	1.68	10.7
LO	HI	<i>Juncus gerardii</i>	<i>Lythrum salicaria</i>	10.76	14.75
LO	HI	<i>Juncus gerardii</i>	<i>Typha angustifolia</i>	5.25	20.22
LO	HI	<i>Juncus gerardii</i>	<i>Juncus gerardii</i>	1.005	3.825
LO	HI	<i>Juncus gerardii</i>	<i>Juncus gerardii</i>	1.005	3.825
LO	HI	<i>Juncus gerardii</i>	<i>Spartina alterniflor</i>	4.33	6.05
LO	HI	<i>Juncus gerardii</i>	<i>Spartina patens</i>	8.01	9.49
LO	HI	<i>Juncus gerardii</i>	<i>Phragmites australis</i>	2.63	5.42
LO	HI	<i>Juncus gerardii</i>	<i>Lythrum salicaria</i>	2.35	10.75
LO	HI	<i>Juncus gerardii</i>	<i>Typha angustifolia</i>	5.04	30.85
LO	HI	<i>Juncus gerardii</i>	<i>Juncus gerardii</i>	3.095	5.885
LO	HI	<i>Juncus gerardii</i>	<i>Juncus gerardii</i>	3.095	5.885
LO	MID	<i>Juncus gerardii</i>	<i>Spartina alterniflor</i>	1.34	5.01
LO	MID	<i>Juncus gerardii</i>	<i>Spartina patens</i>	1.64	5.48
LO	MID	<i>Juncus gerardii</i>	<i>Phragmites australis</i>	0.21	0.39
LO	MID	<i>Juncus gerardii</i>	<i>Typha angustifolia</i>	0.85	1.73
LO	MID	<i>Juncus gerardii</i>	<i>Juncus gerardii</i>	1.035	3.585
LO	MID	<i>Juncus gerardii</i>	<i>Juncus gerardii</i>	1.035	3.585
LO	MID	<i>Juncus gerardii</i>	<i>Spartina alterniflor</i>	0.11	0.2
LO	MID	<i>Juncus gerardii</i>	<i>Spartina patens</i>	1.14	8.5
LO	MID	<i>Juncus gerardii</i>	<i>Phragmites australis</i>	1.09	3.04
LO	MID	<i>Juncus gerardii</i>	<i>Lythrum salicaria</i>	0.37	5.2
LO	MID	<i>Juncus gerardii</i>	<i>Typha angustifolia</i>	0.56	1.27
LO	MID	<i>Juncus gerardii</i>	<i>Juncus gerardii</i>	0.415	3.365
LO	MID	<i>Juncus gerardii</i>	<i>Juncus gerardii</i>	0.415	3.365
LO	HI	<i>Phragmites australis</i>	<i>Spartina alterniflor</i>	6.55	8.2



Table A.2 (continued). Final above and belowground biomass (grams dry weight) for experimental transplants.

Salinity Regime	Elevation Regime	Species	Competitor	Aboveground Biomass (g dw)	Belowground Biomass (g dw)
LO	HI	<i>Phragmites australis</i>	<i>Spartina patens</i>	9.53	14.23
LO	HI	<i>Phragmites australis</i>	<i>Juncus gerardii</i>	8.77	5.63
LO	HI	<i>Phragmites australis</i>	<i>Lythrum salicaria</i>	17.01	38.78
LO	HI	<i>Phragmites australis</i>	<i>Typha angustifolia</i>	9.08	13.76
LO	HI	<i>Phragmites australis</i>	<i>Phragmites australis</i>	10.505	16.93
LO	HI	<i>Phragmites australis</i>	<i>Phragmites australis</i>	10.505	16.93
LO	HI	<i>Phragmites australis</i>	<i>Spartina alterniflor</i>	11.54	27
LO	HI	<i>Phragmites australis</i>	<i>Spartina patens</i>	5.68	12.74
LO	HI	<i>Phragmites australis</i>	<i>Juncus gerardii</i>	2.09	1.92
LO	HI	<i>Phragmites australis</i>	<i>Lythrum salicaria</i>	8.3	15.87
LO	HI	<i>Phragmites australis</i>	<i>Phragmites australis</i>	6.785	32.825
LO	HI	<i>Phragmites australis</i>	<i>Phragmites australis</i>	6.785	32.825
LO	MID	<i>Phragmites australis</i>	<i>Juncus gerardii</i>	3.85	6.56
LO	MID	<i>Phragmites australis</i>	<i>Typha angustifolia</i>	3.16	22.62
LO	MID	<i>Phragmites australis</i>	<i>Phragmites australis</i>	5.9	12.865
LO	MID	<i>Phragmites australis</i>	<i>Phragmites australis</i>	5.9	12.865
LO	MID	<i>Phragmites australis</i>	<i>Spartina patens</i>	10.39	9.8
LO	MID	<i>Phragmites australis</i>	<i>Typha angustifolia</i>	8.54	14.53
LO	MID	<i>Phragmites australis</i>	<i>Phragmites australis</i>	3.71	2.845
LO	MID	<i>Phragmites australis</i>	<i>Phragmites australis</i>	3.71	2.845
LO	LO	<i>Phragmites australis</i>	<i>Phragmites australis</i>	5.015	7.56
LO	LO	<i>Phragmites australis</i>	<i>Phragmites australis</i>	5.015	7.56
LO	LO	<i>Phragmites australis</i>	<i>Spartina patens</i>	8	7.29
LO	LO	<i>Phragmites australis</i>	<i>Juncus gerardii</i>	1.16	9.35
LO	LO	<i>Phragmites australis</i>	<i>Typha angustifolia</i>	0.66	10.67
LO	HI	<i>Lythrum salicaria</i>	<i>Phragmites australis</i>	2.86	19.25
LO	HI	<i>Lythrum salicaria</i>	<i>Lythrum salicaria</i>	5.41	33.95
LO	HI	<i>Lythrum salicaria</i>	<i>Lythrum salicaria</i>	5.41	33.95
LO	HI	<i>Typha angustifolia</i>	<i>Spartina alterniflor</i>	9.41	20.41
LO	HI	<i>Typha angustifolia</i>	<i>Spartina patens</i>	9.82	32.12
LO	HI	<i>Typha angustifolia</i>	<i>Phragmites australis</i>	24.17	38.09
LO	HI	<i>Typha angustifolia</i>	<i>Lythrum salicaria</i>	12.1	32.91
LO	HI	<i>Typha angustifolia</i>	<i>Typha angustifolia</i>	14.93	31.1
LO	HI	<i>Typha angustifolia</i>	<i>Typha angustifolia</i>	14.93	31.1
LO	HI	<i>Typha angustifolia</i>	<i>Spartina alterniflor</i>	4.56	6.27
LO	HI	<i>Typha angustifolia</i>	<i>Spartina patens</i>	8.32	91.19
LO	HI	<i>Typha angustifolia</i>	<i>Juncus gerardii</i>	3.11	11.59
LO	HI	<i>Typha angustifolia</i>	<i>Phragmites australis</i>	7.98	11.44
LO	HI	<i>Typha angustifolia</i>	<i>Lythrum salicaria</i>	18.31	98.32
LO	HI	<i>Typha angustifolia</i>	<i>Typha angustifolia</i>	13.44	15.2
LO	HI	<i>Typha angustifolia</i>	<i>Typha angustifolia</i>	13.44	15.2
LO	MID	<i>Typha angustifolia</i>	<i>Spartina alterniflor</i>	2.37	13.61
LO	MID	<i>Typha angustifolia</i>	<i>Spartina patens</i>	6.76	22.85

Table A.2 (continued). Final above and belowground biomass (grams dry weight) for experimental transplants.

Salinity Regime	Elevation Regime	Species	Competitor	Aboveground Biomass (g dw)	Belowground Biomass (g dw)
LO	MID	<i>Typha angustifolia</i>	<i>Juncus gerardii</i>	29.28	45.68
LO	MID	<i>Typha angustifolia</i>	<i>Phragmites australis</i>	7.84	29.22
LO	MID	<i>Typha angustifolia</i>	<i>Lythrum salicaria</i>	4.14	7.88
LO	MID	<i>Typha angustifolia</i>	<i>Spartina patens</i>	9.05	11.14
LO	MID	<i>Typha angustifolia</i>	<i>Lythrum salicaria</i>	36.31	94.22
LO	MID	<i>Typha angustifolia</i>	<i>Typha angustifolia</i>	24.295	32.21
LO	MID	<i>Typha angustifolia</i>	<i>Typha angustifolia</i>	24.295	32.21
LO	LO	<i>Typha angustifolia</i>	<i>Spartina alterniflor</i>	9.35	19.1
LO	LO	<i>Typha angustifolia</i>	<i>Lythrum salicaria</i>	3.21	8.03
LO	LO	<i>Typha angustifolia</i>	<i>Spartina alterniflor</i>	11.48	38.4
LO	LO	<i>Typha angustifolia</i>	<i>Juncus gerardii</i>	15.59	25.18
LO	LO	<i>Typha angustifolia</i>	<i>Phragmites australis</i>	11.64	30.17
LO	LO	<i>Typha angustifolia</i>	<i>Typha angustifolia</i>	4.295	18.76
LO	LO	<i>Typha angustifolia</i>	<i>Typha angustifolia</i>	4.295	18.76